

AD-A031 171

ARMY ENGINEER WATERWAYS EXPERIMENT STATION VICKSBURG MISS F/G 8/3
LONG BEACH HARBOR NUMERICAL ANALYSIS OF HARBOR OSCILLATIONS. RE--ETC(U)
SEP 76 J R HOUSTON

UNCLASSIFIED

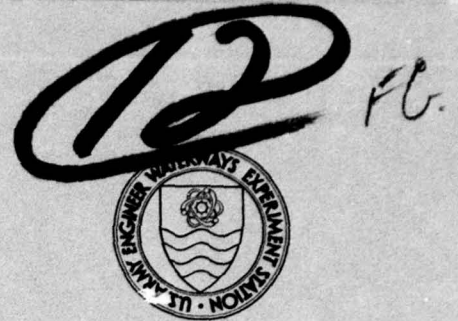
WES-MP-H-76-20-1

NL

1 OF 3
AD
A031171



AD A031171



MISCELLANEOUS PAPER H-76-20

LONG BEACH HARBOR NUMERICAL ANALYSIS OF HARBOR OSCILLATIONS

Report I

EXISTING CONDITIONS AND PROPOSED IMPROVEMENTS

by

James R. Houston

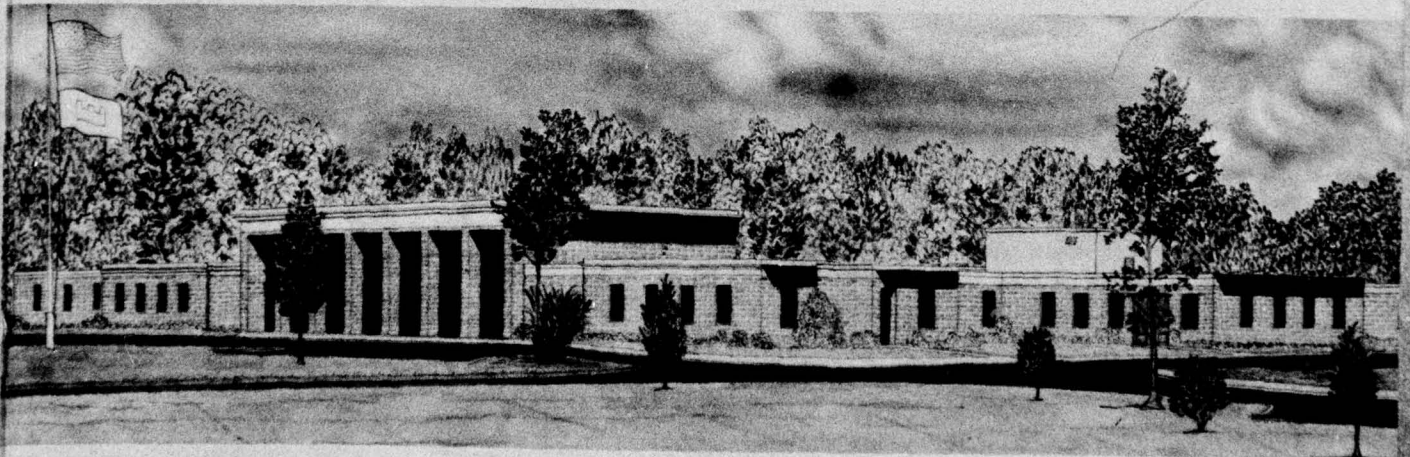
Hydraulics Laboratory

U. S. Army Engineer Waterways Experiment Station
P. O. Box 631, Vicksburg, Miss. 39180

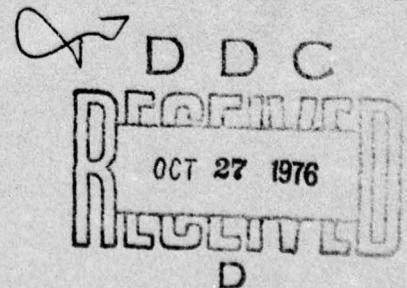
September 1976

Report I of a Series

Approved For Public Release; Distribution Unlimited



Prepared for Port of Long Beach
Long Beach, California 90801



Destroy this report when no longer needed. Do not return
it to the originator.

Unclassified

SECURITY CLASSIFICATION OF THIS PAGE (When Data Entered)

REPORT DOCUMENTATION PAGE		READ INSTRUCTIONS BEFORE COMPLETING FORM
1. REPORT NUMBER Miscellaneous Paper H-76-20	2. GOVT ACCESSION NO.	3. RECIPIENT'S CATALOG NUMBER
4. TITLE (and Subtitle) LONG BEACH HARBOR NUMERICAL ANALYSIS OF HARBOR OSCILLATIONS; Report 1. EXISTING CONDITIONS AND PROPOSED IMPROVEMENTS.	5. TYPE OF REPORT & PERIOD COVERED Report 1 of a series	6. PERFORMING ORG. REPORT NUMBER
7. AUTHOR(s) James R. Houston	8. CONTRACT OR GRANT NUMBER(s) WES-76-4	9. PERFORMING ORGANIZATION NAME AND ADDRESS U. S. Army Engineer Waterways Experiment Station Hydraulics Laboratory P. O. Box 631, Vicksburg, Mississippi 39180
10. CONTROLLING OFFICE NAME AND ADDRESS Port of Long Beach Long Beach, California 90801	11. REPORT DATE Sept 1976	12. NUMBER OF PAGES 194
13. MONITORING AGENCY NAME & ADDRESS (if different from Controlling Office)	14. SECURITY CLASS. (of this report) Unclassified	15a. DECLASSIFICATION/DOWNGRADING SCHEDULE
16. DISTRIBUTION STATEMENT (of this Report) Approved for public release; distribution unlimited.		
17. DISTRIBUTION STATEMENT (of the abstract entered in Block 20, if different from Report)		
18. SUPPLEMENTARY NOTES		
19. KEY WORDS (Continue on reverse side if necessary and identify by block number) Finite element method Harbor oscillations Long Beach Harbor Numerical analysis		
20. ABSTRACT (Continue on reverse side if necessary and identify by block number) A hybrid finite element numerical model was used to calculate harbor resonance for existing conditions and proposed improvements of Los Angeles and Long Beach Harbors. The numerical model calculates harbor oscillation for harbors of arbitrary shape and variable depth. Ten finite element numerical grids were used to calculate the response of the harbors complex for incident waves with periods from 1 to 10 min.		

(Continued)

Unclassified

SECURITY CLASSIFICATION OF THIS PAGE (When Data Entered)

038100

Y/P

Unclassified

SECURITY CLASSIFICATION OF THIS PAGE(When Data Entered)

20. ABSTRACT (Continued).

→ Calculations of the model for existing conditions of the harbors were shown to be in good agreement with prototype measurements. The numerical model calculations indicate that resonant oscillations in existing harbor facilities will not be radically altered by the proposed modifications of the harbors complex. The resonant oscillations are, in general, somewhat smaller for the modified conditions of the harbors complex than for existing conditions.

ACCESSION for	
NTIS	White Section <input checked="" type="checkbox"/>
DDC	Buff Section <input type="checkbox"/>
UNANNOUNCED	<input type="checkbox"/>
JUSTIFICATION	
BY	
DISTRIBUTION/AVAILABILITY CODES	
Dist. ANAL. and/or SPECIAL	
A	

Unclassified

SECURITY CLASSIFICATION OF THIS PAGE(When Data Entered)

PREFACE

The investigation reported herein was authorized by the Long Beach Port Authority under a contract, Agreement No. WES 76-4, dated 12 September 1975.

This study was conducted during the period September 1975 to April 1976 in the Hydraulics Laboratory of the U. S. Army Engineer Waterways Experiment Station (WES), under the direction of Mr. H. B. Simmons, Chief of the Hydraulics Laboratory, Dr. R. W. Whalin, Chief of the Wave Dynamics Division (WDD), Mr. D. D. Davidson, Chief of the Wave Research Branch, and Mr. C. E. Chatham, Chief of the Harbor Wave Action Branch. Mr. J. R. Houston conducted the study and prepared this report.

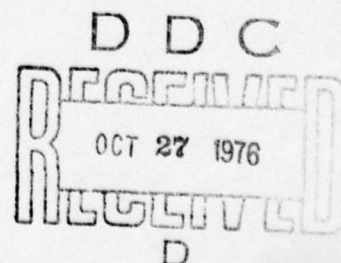
Messrs. R. R. Bottin, C. Bryant, and A. W. Garcia (WDD) prepared the finite element numerical grids. Mr. D. G. Outlaw (WDD) developed the computer plotting programs and aided in eliminating errors in the finite element grids; Mr. Bottin plotted the frequency response curves.

Mr. H. L. Butler (WDD) rewrote the matrix solving subroutine of the hybrid finite element computer program, thus reducing significantly the running time of the program.

Drs. H. S. Chen and C. C. Mei of the Massachusetts Institute of Technology provided documentation of the hybrid finite element computer program they developed and materials to aid in its utilization.

A significant proportion of the numerical computations were performed on a CDC-7600 computer at the Los Alamos Scientific Laboratory (LASL), Los Alamos, New Mexico. Mr. P. Johnson and Mrs. Margaret McCormick of LASL assisted significantly in coordinating visits to Los Alamos and scheduling computer time on the LASL system.

Directors of WES during the conduct of the study and the preparation and publication of this report were COL G. H. Hilt, CE, and COL John L. Cannon, CE. Technical Director was Mr. F. R. Brown.



CONTENTS

	<u>Page</u>
PREFACE	1
CONVERSION FACTORS, U. S. CUSTOMARY TO METRIC (SI)	
UNITS OF MEASUREMENT	3
PART I: INTRODUCTION	4
Harbor Oscillation Problem	4
Purpose of Study	5
PART II: NUMERICAL MODEL	7
PART III: APPLICATION OF NUMERICAL MODEL	13
Boundary Conditions	13
Numerical Grids	15
PART IV: RESULTS	17
Comparison of Prototype Data and Numerical Calculations for Existing Conditions	17
Comparison of Harbor Response for Existing and Revised Conditions	20
PART V: CONCLUSIONS	24
REFERENCES	26
TABLES 1-5	
PLATES 1-161	
APPENDIX A: NOTATION	

CONVERSION FACTORS, U. S. CUSTOMARY TO METRIC (SI)
UNITS OF MEASUREMENT

U. S. customary units of measurement used in this report can be converted to metric (SI) units as follows:

<u>Multiply</u>	<u>By</u>	<u>To Obtain</u>
feet	0.3048	metres
feet per second	0.3048	metres per second
feet per second per second	0.3048	metres per second per second
square feet per second	0.09290304	square metres per second

LONG BEACH HARBOR NUMERICAL ANALYSIS OF HARBOR OSCILLATIONS

EXISTING CONDITIONS AND PROPOSED IMPROVEMENTS

PART I: INTRODUCTION

Harbor Oscillation Problem

1. A harbor excited by long waves with a period close to the natural oscillation period of the harbor experiences a resonant reaction that may produce wave heights in the harbor far greater than the incident wave heights. Generally, the vertical movement of water in the harbor is still only a few tenths of a foot due to the very small heights of the incident long waves. However, the horizontal movement of water may cover a distance greater than 10 ft* as a result of the long wavelength of the incident waves. Such horizontal water movements cause surge and sway motion of moored ships that may hamper unloading operations and damage mooring facilities.

2. A number of harbors on the west coast of the United States have histories of ship motion problems resulting from harbor resonant oscillations. It is likely that the long-period waves responsible for exciting harbor oscillations permeate the Pacific Basin. Lack of modern harbor development may prevent the occurrence of any problem for most coastal areas of the Pacific. Many places that have a problem may merely tolerate it through ignorance of possible remedial measures with the result that the problem goes unreported.

3. The generating mechanism of the very small amplitude long waves that excite harbors is still unknown. However, Munk's surf-beat theory¹ suggested an attractive explanation of the origin of these waves. Surf beats result from the superposition of two trains of waves of slightly different period. The beats are an amplitude modulation of

* A table of factors for converting U. S. customary units of measurement to metric (SI) units is presented on page 3.

a shorter period wave train. Swell, for example, almost always exhibits an irregular beating up to several minutes in period.

4. Carr² argued that local surf beat could not cause the long-period waves known to excite harbors. Although the surf-beat process produces a long-period vertical water motion, the really important factor of long-period horizontal water motion is lacking in surf beats. Severe harbor surging also is known to occur during otherwise calm seas with identical long-period wave activity reported along hundreds of miles of a coastline. Carr maintained that such activity is not compatible with long-period wave generation by local surf beat.

5. True long-period wave trains may be generated from surf beats through nonlinear processes in the surf zone. Munk¹ estimated that beaches reflected 1 percent of the energy incident upon them in the form of these long-period waves. It is perhaps these waves reflected from distant shores of the Pacific which cause oscillation problems in harbors on the west coast of the United States. Long-period wave activity would then increase after distant storms of the south or west Pacific Ocean created large swell conditions and the resulting surf beat generated long-period wave trains in the surf zone which reflected off shorelines. Wilson³ has noted that harbor oscillation in Los Angeles and Long Beach Harbors has a seasonal fluctuation of frequency and intensity which is greatest during the summer months and least during the winter. He noted that such a pattern is almost identical with that found for Table Bay Harbour, Cape Town, South Africa, and suggests that the storms in the Southern Hemisphere are responsible for the long-period waves.

6. Further evidence that long-period wave trains exist from time to time as a general ocean condition and are not generated by local surf beats comes from a harbor study for San Nicholas Bay, Peru.⁴ It was concluded from horizontal water velocity measurements that long-period waves affecting San Nicholas Harbor were progressive waves unassociated with the concurrent swell waves.

Purpose of Study

7. The purpose of this study was to investigate harbor

oscillations excited by long waves with periods from 1 to 10 min using a finite element numerical model. Existing conditions of Los Angeles and Long Beach Harbors and conditions of a proposed harbor expansion were considered to ensure that the expansion would not cause undesirable oscillations in existing basins or characteristic oscillations of its own that were undesirable.

8. The amplification peaks predicted by the numerical model may be much larger than the peaks which actually occur in nature, since the model neglects all dissipative processes except radiation of energy by a harbor. However, the model adequately predicts the relative severity of various modes of oscillation, and the results can be used to compare oscillation characteristics of the existing Los Angeles and Long Beach Harbors complex and proposed harbor expansions. Information about periods of resonant peaks and the spatial patterns of wave heights and currents when areas of the harbor are excited also will be used to determine both the incident wave period ranges which need to be tested and the optimum gage placement during future wave tests in the Los Angeles and Long Beach Harbors hydraulic model.

PART II: NUMERICAL MODEL

9. Response of the Los Angeles and Long Beach Harbors complex to long wave excitation was determined by using a hybrid finite element numerical model developed recently by Chen and Mei at Massachusetts Institute of Technology.⁵ The model solves the following generalized Helmholtz equation:

$$\nabla \cdot [h(x,y) \nabla \phi(x,y)] + \frac{w^2}{g} \phi(x,y) = 0 \quad (1)$$

where $\phi(x,y)^*$ is the velocity potential defined by $U(x,y) = -\nabla \phi(x,y)$, with $U(x,y)$ being a two-dimensional velocity vector and w an angular frequency, $h(x,y)$ is the water depth, and g is the acceleration due to gravity. Equation 1 governs small amplitude undamped oscillations of water in a basin of arbitrary shape and variable depth forced by periodic long waves. It has been further assumed that the flow is irrotational.

10. The Helmholtz equation:

$$\nabla^2 \phi(x,y) + \frac{w^2}{gh} \phi(x,y) = 0 \quad (2)$$

is the governing equation for a constant-depth ocean region outside the basin.

11. For a harbor in a semi-infinite ocean with a straight coastline there is an incident, reflected, and scattered wave. The scattered wave has a velocity potential ϕ_s given by

$$\phi_s = \sum_{n=0}^{\infty} \alpha_n H_n(kr) \cos n\theta \quad (3)$$

where α_n are unknown coefficients and $H_n(kr)$ are Hankel functions of the first kind of order n .

* For convenience, symbols and unusual abbreviations are listed and defined in the Notation: Appendix A.

12. ϕ_s satisfies the radiation condition that the scattered wave must behave as an outgoing wave at infinity. This condition is known as the Sommerfeld radiation condition and may be expressed mathematically as follows:

$$\lim_{r \rightarrow \infty} \sqrt{r} \left(\frac{\partial}{\partial r} - ik \right) \phi_s = 0 \quad (4)$$

13. Chen and Mei used a calculus of variations approach and obtained a Euler-Lagrange formulation of the boundary value problem. The following functional with the property that it is stationary with respect to arbitrary first variations of $\phi(x,y)$ was constructed by Chen and Mei:

$$\begin{aligned} F(\phi) = & \iint 1/2 \{ h(\nabla\phi)^2 - \frac{w^2}{g} \phi^2 \} dA \\ & + 1/2 \oint \{ h(\phi_R - \phi_I) \frac{\partial(\phi_R - \phi_I)}{\partial n_a} \} da - \oint \{ h\phi_a \frac{\partial(\phi_R - \phi_I)}{\partial n_a} \} da \\ & - \oint \{ h\phi_a \frac{\partial\phi_I}{\partial n_a} \} da + \oint \{ h\phi_I \frac{\partial(\phi_R - \phi_I)}{\partial n_a} \} da \end{aligned} \quad (5)$$

where

A = the region inside the harbor

\oint = line integral

ϕ_R = far field velocity potential

ϕ_I = velocity potential of the incident wave

n_a = unit normal vector outward from region A

a = boundary of region A

ϕ_a = total velocity potential evaluated on boundary a

14. Proof was given by Chen and Mei that the stationarity of this functional is equivalent to the original boundary value problem.

15. The integral equation obtained from extremizing the functional is solved by utilizing the finite element method. This method is a technique of numerical approximation that involves dividing a

domain into a number of nonoverlapping subdomains which are called elements.

16. The solution of the problem is approximated within each element by suitable interpolation functions in terms of a finite number of unknown parameters. These unknown parameters are the values of the field variable $\phi(x,y)$ at a finite number of points which are called nodes. The relations for individual elements are combined into a system of equations for all unknown parameters.

17. In the region outside the basin, the velocity potentials are solved analytically in terms of unknown coefficients. The region is considered a single element with an "interpolation function" given by Equation 3. The infinite series is terminated at some finite value such that the addition of further terms does not significantly influence the calculated values of $\phi(x,y)$. The resulting equation is combined with the system of equations for unknown parameters at nodal points within the basin and this complete system is solved using Gaussian elimination matrix methods.

18. $\eta(x,y)$ is related to $\phi(x,y)$ through the linearized dynamic free surface boundary condition

$$\eta(x,y) = - \frac{1}{g} \frac{\partial \phi(x,y)}{\partial t} \quad (6)$$

19. The horizontal velocity components have the following form:

$$u(x,y) = - \frac{g}{w} \frac{\partial \eta(x,y)}{\partial x} ; v(x,y) = - \frac{g}{w} \frac{\partial \eta(x,y)}{\partial y} \quad (7)$$

20. The hybrid finite element method (so named by Chen and Mei because the method involves the combination of analytical and finite element numerical solutions) is a steady-state solution of the boundary value problem. The response of a harbor to an arbitrary forcing function can be easily determined within the framework of a linearized theory. For example, an arbitrary incident wave amplitude at the harbor mouth in the absence of the harbor can be Fourier decomposed as follows:

$$b_o(t) = \int_{-\infty}^{\infty} b(w)e^{-iwt} dw \quad (8)$$

If $\eta(x,y,w)$ is the response amplitude at any point (x,y) inside the harbor due to an incident plane wave of unit amplitude and frequency w , then the response of the harbor to the arbitrary incident wave amplitude $b_o(t)$ is given by

$$\xi(x,y,t) = R_e \left[\int_{-\infty}^{\infty} b(w)\eta(x,y,w)e^{-iwt} dw \right] \quad (9)$$

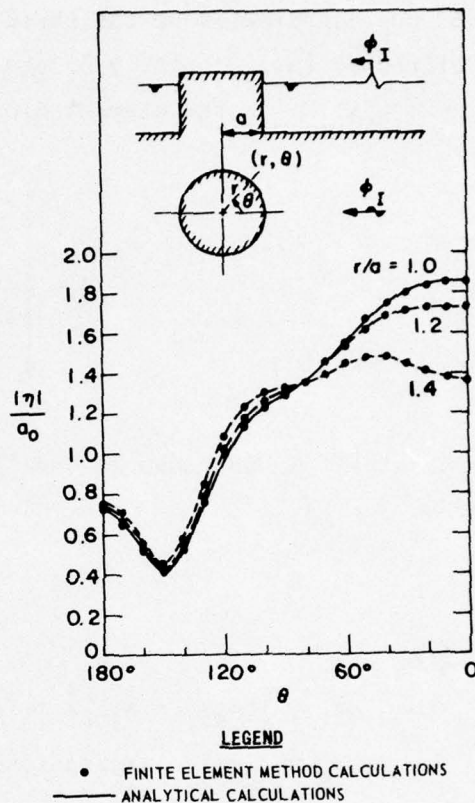
where the operation $R_e[\]$ takes the real part of the bracketed quantity.

21. Therefore, as soon as $\eta(x,y,w)$ is known for all w , the harbor response to an arbitrary incident wave can be calculated.

22. Chen and Mei⁵ verified their finite element numerical model by comparing the model's calculations with analytical and experimental results for simple wave problems. Figure 1 is a comparison of analytical and numerical results of wave diffraction by a vertical circular cylinder. Similar excellent agreement was obtained by comparing numerical calculations with an analytical solution for a semicircular harbor with two openings. Experimental data for the oscillation of a rectangular harbor also were compared with the finite element numerical calculations. Calculated periods of the resonant peaks agreed with experimental data; however, calculated amplitudes of the resonant peaks were larger since the numerical model did not consider frictional effects.

23. Several modifications were made to the numerical computer program of Reference 5 before calculations were made for Los Angeles and Long Beach Harbors. Slight modifications were made to allow the model to handle harbors with variable depths. Chen and Mei⁵ applied their numerical model only to constant depth problems. The subroutine which solves the large system of algebraic equations arising from finite elements was modified to be more efficient. This modification resulted in a decrease in the computational time of the numerical model

Figure 1. Comparison of numerical and analytical results for wave scattering off a vertical circular cylinder⁵



by a factor of between two and three.

24. Velocity calculations also were added to the numerical model.⁶ Velocities are calculated using the expressions in Equation 7. The slope of η may be obtained at any point (x,y) within an element through the matrix equation

$$\begin{bmatrix} \frac{\partial \eta}{\partial x} \\ \frac{\partial \eta}{\partial y} \end{bmatrix} = G\{\eta\}^e \quad (10)$$

where the matrix vector $\{\eta\}^e$ is defined as

$$\{\eta\}^e = \begin{bmatrix} \eta_i \\ \eta_j \\ \eta_k \end{bmatrix} \quad (11)$$

and the coordinates of the three nodes (i,j,k) forming the elements are defined as (x_i, y_i) , (x_j, y_j) , and (x_k, y_k) .

25. G is the element slope matrix defined as

$$G = \begin{bmatrix} \frac{\partial N_i}{\partial x} & \frac{\partial N_j}{\partial x} & \frac{\partial N_k}{\partial x} \\ \frac{\partial N_i}{\partial y} & \frac{\partial N_j}{\partial y} & \frac{\partial N_k}{\partial y} \end{bmatrix} \quad (12)$$

and matrix N is known as the "interpolation" function and is defined as

$$N = \{N_i, N_j, N_k\} \quad (13)$$

where

$$N_i = \{(x_k y_j - x_j y_k) + (y_k - y_j)x + (x_j - x_k)y\} / 2\Delta$$

N_j, N_k = similar expressions obtained by the cyclical permutation of i,j, and k

Δ = area of the element A^e

26. The $\{\eta\}^e$ matrix is known from the finite element computations. Together with the interpolation function N, the horizontal velocity at any point (x,y) within an element can be determined. Velocities presented in this report were calculated at element centers.

27. The finite element numerical model has several important advantages compared with other numerical harbor oscillation models such as that of Lee and Raichlen.⁷ First, the model allows a variable depth. Furthermore, the computational time requirement for the model is substantially less than computational times required by other numerical models.⁸ It is the only present numerical model for harbor oscillations which can feasibly calculate resonance effects in a harbor as large as the Los Angeles and Long Beach Harbors complex.

PART III: APPLICATION OF NUMERICAL MODEL

Boundary Conditions

28. The boundary condition used in the numerical model along the shoreline of the Los Angeles and Long Beach Harbors complex is that the normal component of the velocity be equal to zero. The same boundary condition was used for the detached breakwater surrounding the proposed oil tanker terminal at Pier J in Long Beach Harbor. The breakwater core extends above still water and is impermeable to incident wave energy and is therefore represented as a solid barrier in this study. The eastern entrance to the tanker terminal basin is 600 ft wide and the basin is dredged to a depth of 62 ft mllw.

29. The San Pedro breakwater (Plate 1) does not have a solid core. It is composed of class B rock with an average diameter of approximately 1.8 ft and has a crown at mllw of fitted concrete blocks. Keulegan⁹ gives the following formula for calculating wave transmission through rock structures:

$$\frac{a_i}{a_t} = 1 + \gamma \left(\frac{a_i}{h} \right) \frac{L}{\lambda} \quad (14)$$

where

$$\gamma = 2.11 \frac{\lambda}{d} \left(gh \frac{T^2}{\lambda^2} \right)^{4/3} \quad (15)$$

and

- a_i = incident wave amplitude
- a_t = transmitted wave amplitude
- h = water depth
- L = width of breakwater
- λ = wavelength of incident waves
- T = wave period

Using these parameters

$h = 50$ ft

$$L = 125 \text{ ft}$$

$$T = 180 \text{ sec}$$

$$\lambda = 7222 \text{ ft}$$

$$d = 1.8 \text{ ft}$$

$$a_i = 0.05 \text{ ft}$$

yields

$$\frac{a_t}{a_i} = 0.87$$

30. This figure is a lower bound for the transmission through the San Pedro breakwater for a 3-min wave since $a_i = 0.05 \text{ ft}$ is probably the upperbound wave amplitude for a 3-min wave at the San Pedro breakwater. This upper bound can be deduced from prototype measurements taken in Los Angeles and Long Beach Harbors by WES.¹⁰ Long-period wave activity cannot be discerned in wave gage measurements at the San Pedro breakwater because of the large wave heights in the swell regime. However, a gage off Reservation Point in Los Angeles Harbor was sufficiently protected from swell that visual inspections could be made of long-period wave activity. A total of 107 visual inspections of 4-hr analog charts taken during ship motion occurrences from a year's prototype recording reveal only a single instance of a wave height as great as 0.1 ft for waves with periods of 1 to 10 min. The single recording was of a 6-min wave and probably results from the large 6-min resonant oscillation that occurs in the East Channel of Los Angeles Harbor.

31. A 3-min wave was considered in the above calculations since longer period waves of the same amplitude would more readily be transmitted through the breakwater and the finite element grids for 1- to 3-min waves (paragraphs 34-36) do not extend as far as this breakwater.

32. Since the San Pedro breakwater is very pervious to 3- to 10-min incident waves, it is not represented in the finite element grids. Although the breakwater looks impervious from the water as a result of the fitted concrete blocks extending up from the waterline, Wilson³ noted that this breakwater has long been considered an ineffective

filter against long waves because of its 43 percent voids; this is indeed the case.

33. The Middle breakwater (Plate 1) of Los Angeles and Long Beach Harbors has a solid core to -26 ft mllw which is covered with a layer of class B rock and a layer of class A rock (approximately 3 ft in diameter). The rock covering of the solid core is at least as permeable to long waves as the San Pedro breakwater, since it consists of rock the same size or larger. Therefore, the Middle breakwater is represented by a depth change with the core impermeable, and small finite element triangles are placed along the breakwater in the numerical grid to properly represent it.

Numerical Grids

34. The numerical grids used in the numerical model computations are shown in Plates 3-12. The elements are all triangular and often equilateral. The lengths of the triangle sides were in general selected so that they were one-eighth of the local wavelength or less. Chen and Mei⁵ compared the finite element solution of diffraction by a vertical cylinder with an exact analytical solution and found a global error of 0.7 percent when they used an element length of one-tenth the incident wavelength. They defined a global error as $\frac{1}{n} \sum \frac{\eta - \eta_t}{\eta_t}$ (local error), where the summation is performed over n finite element nodes. The local error is defined as

$$\text{Local error} = \frac{\eta - \eta_t}{\eta_t} \quad (16)$$

where η is the magnitude calculated by the finite element method at a nodal point and η_t is the theoretical value. In the present study, it was judged that element lengths equal to one-eighth of the local wavelength or less would provide sufficient accuracy. Element lengths vary in the grids in relation to local depths. Element lengths near harbor entrances are made much smaller than may be strictly necessary in order to ensure proper propagation of waves into inner basins.

35. Five finite element grids were used for each case tested and are tabulated below. It was not feasible to use a single grid to calculate harbor response for incident waves with periods from 1 to 10 min. For example, 1- to 3-min grids could not be constructed to cover the entire harbor complex because of computer memory and running time limitations. Separate grids were used for 3- to 4-, 4- to 6-, and 6- to 10-min calculations to reduce the cost of operating the model. The computational time of the model is approximately proportional to the number of nodes in the grid times the bandwidth squared. The bandwidth is the greater of either the maximum difference for all elements between two adjacent node numbers in an element of the grid or the sum of the number of nodes on the grid semicircle plus the number of terms retained in truncating the infinite series of Equation 3. In general, the bandwidth increases approximately linearly with a decrease in the lengths of the triangular element sides. The number of nodes increases approximately as the inverse square of the triangle side lengths. Thus, a grid for 3-min waves (eight nodes per wavelength) requires approximately 16 times more computational time than one for 6-min waves (eight nodes per wavelength).

<u>Existing Conditions</u>		<u>Revised Conditions</u>	
Grid 1	1 to 2 min	Grid 1A	1 to 2 min
Grid 2	2 to 3 min	Grid 2A	2 to 3 min
Grid 3	3 to 4 min	Grid 3A	3 to 4 min
Grid 4	4 to 6 min	Grid 4A	4 to 6 min
Grid 5	6 to 10 min	Grid 5A	6 to 10 min

36. Many of the numerical grids for existing conditions were designed so that they could be more readily modified to construct grids for the harbor expansion conditions. However, the design of the harbor was modified several times during the course of this study. Therefore, some element patterns in the grids may have no particular purpose. Grids also were constructed to minimize the bandwidth, and this requirement occasionally governed triangle shapes for areas of the grids.

PART IV: RESULTS

Comparison of Prototype Data and Numerical Calculations for Existing Conditions

37. Prototype wave gage recordings were collected at Los Angeles and Long Beach Harbors from 26 May 1971 to 29 June 1972 by the U. S. Army Engineer Waterways Experiment Station.¹⁰ Energy spectra were determined for 10 time periods of the year during which ship motion problems were reported. Spectral analyses were performed via Fast Fourier Transform (FFT) techniques. Variability of spectral estimates was decreased by smoothing over 10 adjacent frequency bands. Ten bands were chosen so that there would still be sufficient frequency resolution to define the long-period energy for wave periods as great as 10 min. The data record length analyzed for each spectral analysis was 24,576 sec (6.83 hr) and the lag time between successive record start times was chosen to be 3 hr. Further details of the analyses can be found in Reference 10.

38. Tables 1-5 give estimates of wave periods and spectral energy densities of peak energies for prototype wave gages 5, 6, 7, 8, and 14; Plate 1 shows the locations of these gages. The starting times in Tables 1-5 give the year, Julian day, and hour on a 24-hr clock. Each of the 10 time periods lasts approximately 2 days. Data do not exist for some time periods as a result of gage downtime. Gage 14 was in operation only during one time period.

39. Tables 1-5 give the wave period with the greatest spectral energy density within a range of periods. The range of periods is such that the spectral lines within the range cannot be resolved by the spectral analysis; for example, in the range 480-360 sec, the adjacent frequency lines corresponding to periods of 459.36 and 387.02 sec cannot be resolved by the spectral analysis and should be considered the same.

40. Plate 13 is a time-dependent spectral plot of gage 5 data for the time period of 1500 November 27-0300 November 29, 1971. The variability of energy levels in this plate illustrates the

nonstationarity of the variance in energy bands. Long-period waves are generally transient (time-dependent) phenomena, and some caution must be observed in the application of spectral analysis techniques to nonstationary processes. However, Tables 1-5 do give an indication of characteristic energy bands for each gage location.

41. It should be noted that the finite element nodal calculations provide only the response characteristics of Los Angeles and Long Beach Harbors. This response must be multiplied by the input spectrum of waves for a comparison with prototype data. However, the input wave spectrum is not known since long waves arriving from the deep ocean had heights too small to be measured by gages near the outer breakwaters during the prototype collection. Still, a correspondence exists between resonant peaks calculated by the numerical model and those measured in the prototype. Plates 14-38 are plots of the wave-height amplification factor calculated by the finite element numerical model for prototype gages 5, 6, 7, 8, and 14. The frequency response for the existing conditions of Los Angeles and Long Beach Harbors shown in Plate 1 is compared with the frequency response for the revised conditions shown in Plate 2. The wave-height amplification factor is defined at each point as the wave height at the point divided by twice the incident wave height. This definition of amplification factor is traditional and is a result of the fact that the standing wave height for a straight coast with no harbor would be twice the incident wave height due to the superposition of the incident and reflected waves.

42. Table 1 indicates that there is no resonant peak for gage 5 data between 8 and 10 min. The numerical calculations presented in Plate 18 also show no resonant peak for this period range. Table 1 shows that large peaks occur at 387 and 237 sec. Plates 16-18 show large peaks at 396 sec and 222 sec and no peaks from 240-360 sec. Neither the numerical computations in Plate 15 nor the prototype data of Table 1 indicate peaks from 120-210 sec. The prototype data have peaks at 100, 93, and 64 sec. The numerical model calculates peaks at 92, 89, and 63 sec as seen in Plate 14. Excellent agreement on the resonant peaks is apparent between prototype data and the numerical model calculations.

43. Table 2 shows a large resonant peak for gage 6 at 387 sec, small peaks at 237 and 160 sec, fairly large peaks at 93 and 86 sec, a moderate peak at 80 sec, and small peaks in the range 65-75 sec. Plates 19-23 show a large peak at 396 sec, small peaks at 222 sec and 158 sec, a fairly large peak at 88 sec, moderate peaks at 80 and 92 sec, and a small peak at 66 sec. Therefore, resonant peaks calculated by the numerical model and measured in the prototype are in excellent agreement for gage 6.

44. Gage 7 has large resonant peaks in Table 3 at 564 and 334 sec, fairly large peaks at 216 and 150 sec, and a small peak at 70 sec. Plates 24-28 show the frequency response calculated by the numerical model for gage 7. Plate 28 indicates a moderate peak at 518 sec and part of what may be a large peak beyond 600 sec. These peaks probably correspond to the 564-sec peak of Table 3, since the spectral lines adjacent to the 564-sec line are located at 733 and 459 sec; therefore, the 564-sec peak contains energy over a large range of periods. The numerical model calculates a large broad peak from 300 to 350 sec with a maximum at 338 sec (Plate 27); a large sharp peak at 280 sec is also shown in Plate 27. Such a sharp peak may not be important in the prototype since there would be little incident energy concentrated within such a small range of wave periods. Part of the energy in this resonant peak also may appear in the 334-sec spectral line in the prototype data analysis. The numerical model also predicts a moderate peak at 245 sec, a small peak at 216 sec (Plate 26), and a large peak at 177 sec (Plate 25) which probably corresponds to the 150-sec peak in the spectral analysis. Plate 24 shows a fairly large but sharp peak at 74 sec. This peak may correspond to the small peak at 70 sec in the spectral analysis. Again, the sharpness of the peak would limit the occurrence of the oscillation in the prototype data.

45. Gage 8 displays fairly large resonant peaks in Table 4 at 334 and 160 sec, moderate peaks at 564, 190, 120, and 85 to 100 sec, and a small peak at 76 sec. Plate 33 shows part of a peak which may occur beyond 600 sec and correspond to the 564-sec peak in the spectral analysis. Plate 32 shows a fairly large broad peak at 338 sec and a

very sharp peak at 280 sec, which again may not be important in the prototype as a result of the sharpness of the peak. There is a large peak in Plate 31 at 218 sec which corresponds to the 199-sec peak in the prototype data. Plate 29 shows peaks at 116, 90 to 105, 78 to 90, and 60 to 75 sec. These peaks are similar to those noted in Table 4. The very sharp peak at 108 sec is probably not important in the prototype.

46. Table 5 gives estimates of wave periods and spectral energy densities of peak energies for one time period for gage 14. Wave energies during this time period were fairly low (Tables 1-4). Resonant peaks in Table 5 occur at 387, 237, 160, 100, 90, 70, and 64 sec. Plates 34-38 show peaks at 396, 222, 160, 100, 92, and from 65 to 80 sec. The periods of resonant peaks calculated by the numerical model and measured in the prototype are in excellent agreement at gage 14.

Comparison of Harbor Response for Existing and Revised Conditions

47. Plates 14-38 show a comparison of plots of the wave-height amplification factor as a function of wave period at gages 5, 6, 7, 8, and 14 for existing and revised harbor conditions. Plates 1 and 2 show the existing harbor and the proposed modifications. The modifications include landfills, dredge cuts, and a small breakwater. Wave periods from 1 to 10 min are considered.

48. Plates 39-63 show a comparison of plots of the normalized maximum current velocity versus wave period at gages 5, 6, 7, 8, and 14 for existing and revised harbor conditions. The normalized maximum current velocity is a maximum velocity over one wave period, and it is normalized so that multiplication by the incident wave amplitude in feet gives velocity in units of feet per second.

49. Plates 64-76 show a comparison of plots of the wave-height amplification factor versus period for three sites in Long Beach Harbor, sta LB-1, LB-2, and LB-3 (Plate 1). Prototype wave gages are not located at these sites; however, the three sites may experience resonance problems. Plates 77-89 show a comparison of plots of the normalized

maximum current velocity versus period for these same three sites.

50. Plates 90-97 show plots of the wave-height amplification versus period for two sites (sta LB-4, LB-5) off Pier J in the area where the oil terminal is proposed (Plate 1). Plates 98-105 show plots of the normalized maximum current velocity versus period for the same two sites. These two sites were chosen to illustrate existing conditions in the area where the oil terminal is to be located. The plots indicate that there are no large resonant peaks between 2 and 10 min at these sites.

51. Plates 106-114 show plots of the wave-height amplification factor versus period for the three tanker terminals in the oil terminal of the revised Long Beach Harbor. Plates 115-123 show plots of the normalized maximum current velocity versus period for the same three tanker terminals. The main resonant peak for all three terminals occurs at a period of 220 sec. The wave-height amplification factor is similar for all three terminals at this period. This is an indication that at this period the basin between the detached breakwater and the Pier J landfill has an oscillation mode in which the water surface in the center part of the basin rises and falls fairly uniformly. This is indeed the case as can be seen in Plate 146. Plate 146 shows contours of the wave-height amplification factor over the entire grid area. The basin is experiencing a "pumping mode" type oscillation in which the water-surface level inside the basin rises and falls almost uniformly.

52. The resonant response of the oil terminal basin to long wave excitation shown in Plates 106-123 is very similar to the response calculated in a previous report¹¹ which used the same numerical model but a much finer numerical grid that only covered the basin and the immediate surrounding area. The numerical model predicts an amplification factor peak of approximately 4 at a 4-min period for both grids; the resonant response is smoother (fewer small peaks) for the finer grid, however. This difference probably results from the fact that the finer grid covers only a small region around the terminal area. There are no external influences for this case such as nearby resonances which may couple with the oil terminal basin response or reflected

waves from other parts of the harbor.

53. Plates 14-89 indicate that there is no radical difference between the resonant oscillations characteristic of the present and revised harbors. The amplification factor and normalized velocity plots have similar shapes with resonant peaks located at corresponding periods. The resonant peaks for the revised harbor conditions are in general shifted to slightly lower periods and have small amplitudes, for example, Plates 16, 18, and 23.

54. There are some very sharp resonant peaks, for example, the 108-sec resonant peak shown in Plate 29, which occur in response plots for one harbor configuration but not another. This difference is probably attributable to difficulties in locating the peaks and not differences in response. Response calculations were initially made every 2, 3, and 5 sec for incident waves with periods from 1 to 3, 3 to 7, and 7 to 10 min, respectively. Resonant peaks were then further defined by calculation intervals of 0.5 to 2 sec and sometimes 0.1 to 0.25 sec. If a resonant peak appeared for one harbor configuration and not another, there was a search for the missing peak. Occasionally it was difficult to locate a very sharp peak. These peaks are probably not important in the prototype since they are so sharp that only small amounts of energy in the incoming wave spectrum would be amplified.

55. Plates 124-161 are plots of contours of wave-height amplification and plots of normalized maximum current velocity for many of the resonant peaks shown in Plates 14-89. The velocities are represented by arrows whose centers lie at element centroids. Water particles move horizontally back and forth in a direction parallel to the arrows. The amplitude of the incident waves is assumed to be equal to 1 ft. The velocities are in units of feet per second for this amplitude incident wave. Incident waves in the prototype may have amplitude orders of magnitude smaller than 1 ft and the velocities they produce are correspondingly smaller.

56. Plates 124-161 basically illustrate patterns of wave-height amplification and current velocity and show how the harbor is oscillating. Quite often the resonances are localized. For example, the 4-min

oscillation shown in Plate 144 is localized in the gage 5 channel and does not extend throughout the Southeast Basin. This oscillation is the fundamental mode for the channel with an antinode forming at the end of the channel and a node at the mouth. It is interesting to note that a simple Merian's formula calculation also predicts a fundamental period of oscillation of the channel equal to 222 sec. The depth of the channel is assumed to be 58 ft and the length 2400 ft. This simple calculation works, of course, because this channel has a very simple shape.

57. Plate 156 is an illustration of a more complicated oscillation which involves all of Southeast Basin. A node cuts the basin in half. Antinodes which are out of phase develop at the ends of basin 6 and the gage 5 channel. Plate 156 indicates that the amplitude of the 396.5-sec oscillation should be approximately the same at prototype gages 5 and 6. The square root of the ratio of energies in the 360- to 480-sec period range for gages 5 and 6 (Tables 1 and 2) is very close to unity for the 10 time periods of the prototype data. The wave energy is proportioned to the square of the wave amplitude. This is an additional example of the close agreement between prototype data and calculations from the numerical model.

58. Plates 124-161 aid in understanding the resonant oscillations which develop in the Los Angeles and Long Beach Harbors complex. Knowledge of oscillation patterns would be helpful in determining remedial actions to limit oscillations, the proper location of wave gages in a hydraulic model of the harbors, and areas of low surge (antinodal locations).

PART V: CONCLUSIONS

59. The good agreement between prototype measurements in the Los Angeles and Long Beach Harbors complex and calculations of the hybrid finite element numerical model confirms the reliability of this numerical model as a viable engineering tool for studying resonant oscillations of complex harbors. Amplitudes of resonant peaks predicted by the numerical model will always be too large since the model does not include any dissipative effects other than radiation dissipation. However, the model can predict relative severities and is therefore extremely useful in comparing the oscillation characteristics for existing conditions with those for various proposed modifications. The rapid calculation time of the numerical model makes it feasible to apply the model to large harbors and broad incident wave period bands. This numerical model can be used as an aid to hydraulic model tests since it pinpoints the periods of resonant peaks and shows oscillation patterns which are useful in optimizing wave gage placement to measure extreme conditions.

60. The numerical model calculations indicate that resonant oscillations in existing harbor facilities will not be radically altered by the proposed modifications of the harbors complex. The resonant oscillations are, in general, somewhat smaller for the modified conditions of the harbor complex than for existing conditions. There are some peaks which are larger for the modified conditions; however, they are not drastically larger.

61. There is only one well-defined resonant peak from 1 to 10 min for the proposed oil terminal basin modification. The basin tested has a 600-ft eastern breakwater opening and a 62-ft depth. The resonant peak has a period of approximately 4 min and an amplification factor of approximately 4. This amplification factor is relatively small compared with amplification factors for many resonant peaks shown in Plates 14-89. Whether or not this peak could cause significant ship motion problems depends upon the natural resonant modes of the moored tankers berthing in the basin. There are no resonant peaks in the oil terminal basin of such a magnitude that they would obviously preclude

safe berthing at the terminals given proper mooring practices and adequate mooring equipment.

62. Detailed information on moored ship response as a function of incident wave amplitude and frequency, the incident wave spectrum, and the resonant response of the harbors complex to incident wave excitement must be known before definitive conclusions can be made on the precise degrees of ship motion in Los Angeles and Long Beach Harbors. Numerical model calculations presented in this report indicate that the resonant response of the harbors complex would probably not be changed enough to cause an increase in the severity of resonant oscillations. In general, the resonant oscillations for the proposed modifications are somewhat smaller than those for existing conditions. The few peaks which increased in magnitude were very sharp (narrow frequency band) and probably will not result in a significant problem due to their limited bandwidth.

REFERENCES

1. Munk, W. H., "Surf Beats," Transactions, American Geophysical Union, Vol 30, No. 6, Dec 1949, pp 849-854.
2. Carr, J. H., "Long Period Waves or Surges in Harbors," Transactions, American Society of Civil Engineers, Vol 118, 1953, pp 588-603.
3. Wilson, B. W. et al., "Wave and Surge-Action Study for Los Angeles-Long Beach Harbors," Vol II, Jul 1968, Science Engineering Associates, San Marino, Calif.
4. Keith, J. M. and Murphy, E. J., "Harbor Study for San Nicolas Bay, Peru," Journal, Waterways and Harbors Divison, American Society of Civil Engineers, Vol 96, No. WW2, May 1970, pp 251-273.
5. Chen, H. S. and Mei, C. C., "Oscillations and Wave Forces in an Off-shore Harbor (Applications of the Hybrid Finite Element Method to Water-Wave Scattering)," Report No. 190, 1974, Massachusetts Institute of Technology, Cambridge, Mass.
6. Crosby, L. G., Durham, D. L., and Chatham, C. E., Jr., "Expansion of Port Hueneme, California; Hydraulic Model Investigation," Technical Report H-75-8, Apr 1975, U. S. Army Engineer Waterways Experiment Station, CE, Vicksburg, Miss.
7. Lee, J.-J. and Raichlen, F., "Wave Induced Oscillations in Harbors with Connected Basins," Report No. KH-R-20, Dec 1969, W. M. Keck Laboratory of Hydraulics and Water Resources, California Institute of Technology, Pasadena, Calif.
8. Houston, J. R., "Comparison of Numerical Models for Harbor Resonant Oscillations" (In preparation), U. S. Army Engineer Waterways Experiment Station, CE, Vicksburg, Miss.
9. Keulegan, G. H., "Wave Transmission Through Rock Structures; Hydraulic Model Investigation," Research Report H-73-1, Feb 1973, U. S. Army Engineer Waterways Experiment Station, CE, Vicksburg, Miss.
10. Durham, D. L. et al., "Los Angeles and Long Beach Harbors Model Study; Analyses of Wave and Ship Motion Data," Technical Report H-75-4, Report 3, Jul 1976, U. S. Army Engineer Waterways Experiment Station, CE, Vicksburg, Miss.
11. Houston, J. R., "Long Beach Harbor Numerical Analysis of Harbor Oscillations; Alternate Plans for Pier J Completion and Tanker Terminal Project" (In preparation), Report 2, U. S. Army Engineer Waterways Experiment Station, CE, Vicksburg, Miss.

Table 1
Estimates of Wave Periods and Spectral Energy Densities
of Peak Energies for Gage 5

Starting Time of Time History	Ranges of Wave Periods			
	1800-480	480-360	270-210	110-100
71-166-1800	733.61*	459.36	262.85	109.97
	189.6**	210.1	1415.0	144.2
71-168-0300	733.61	459.36	262.85	109.97
	153.6	167.1	560.9	100.9
71-289-1600	733.61	387.02	237.45	105.25
	204.9	118.8	383.1	38.20
71-304-1200	733.61	387.02	237.45	100.93
	197.8	40.54	151.85	9.332
71-314-1500	733.61	387.02	237.45	105.25
	675.2	56.74	342.7	70.77
71-316-0900	733.61	387.02	237.45	105.25
	238.7	74.96	118.3	19.80
71-324-0000	733.61	387.02	237.45	100.93
	211.7	440.2	175.6	19.01
71-329-0300	733.61	387.02	237.45	105.25
	370.7	105.1	558.9	56.95
71-331-1500	733.61	387.02	237.45	100.93
	555.1	76.85	136.8	16.04
72-155-0600	733.61	387.02	237.45	100.93
	248.3	36.55	158.8	20.97
71-166-1800	95-85	70-60	55-45	45-35
	93.27	69.52	54.19	44.40
71-168-0300	11.80	35.41	33.58	18.91
	93.27	67.61	55.41	42.85
71-289-1600	110.74	35.61	25.84	13.55
	93.27	62.45	50.83	38.79
71-304-1200	58.08	30.48	8.900	8.456
	93.28	62.45	51.90	38.79
71-314-1500	11.84	19.20	4.345	3.723
	93.27	64.08	50.83	39.42
71-316-0900	70.35	56.34	9.781	11.36
	93.27	64.08	50.83	41.41
71-324-0000	26.91	22.06	5.045	5.696
	93.27	64.08	50.83	41.41
71-329-0300	19.85	28.77	6.284	5.110
	93.27	64.08	51.90	41.41
71-331-1500	55.97	40.26	10.15	9.978
	93.27	64.08	50.83	41.41
72-155-0600	7.381	15.74	4.401	4.157
	93.27	64.08	50.83	41.41
	45.39	45.55	13.34	8.966

* Wave periods in seconds.
** Spectral energy densities in 10^{-2} ft²-sec.

Table 2
Estimates of Wave Periods and Spectral Energy Densities
of Peak Energies for Gage 6

Starting Time of Time History	Ranges of Wave Periods				
	1800-480	480-360	270-210	170-150	95-75
71-166-1800	733.61*	459.36	262.85	171.27	93.27
	115.6**	117.7	32.42	26.74	90.86
71-168-0300	733.61	459.36	262.85	171.27	93.27
	92.91	138.6	15.84	15.92	92.79
71-289-1600	733.61	387.02	237.45	160.10	86.69
	149.3	135.4	137.6	23.46	124.4
71-304-1200	733.61	387.02	237.45	160.10	80.98
	149.6	37.85	4.673	5.29	31.26
71-314-1500	733.61	387.02	237.45	160.10	86.69
	497.5	41.36	10.52	40.68	140.3
71-316-0900	733.61	387.02	237.45	160.10	80.98
	172.7	67.92	5.491	10.75	58.36
71-324-0000	733.61	387.02	237.45	160.10	80.98
	145.5	405.6	6.132	13.36	40.11
71-329-0300	733.61	387.02	237.45	160.10	89.86
	265.1	106.9	15.05	41.55	151.9
71-331-1500	733.61	387.02	237.45	160.10	80.98
	465.0	93.32	5.133	9.459	30.29
72-155-0600	733.61	387.02	237.45	160.10	80.98
	169.0	29.05	5.526	12.17	76.92
	<u>75-65</u>	<u>50-40</u>	<u>40-35</u>	<u>35-30</u>	<u>30-25</u>
71-166-1800	71.55	46.95	37.61	32.62	25.51
	22.54	17.08	5.214	14.83	9.840
71-168-0300	71.54	46.95	37.61	31.77	25.51
	18.70	5.238	3.745	7.759	7.771
71-289-1600	65.80	44.40	35.96	30.97	26.33
	17.20	12.10	5.563	16.29	69.40
71-304-1200	65.80	44.40	35.96	30.97	25.51
	5.759	2.792	2.399	3.269	1.525
71-314-1500	65.80	45.22	36.49	30.97	25.77
	26.27	5.155	2.817	11.86	1.975
71-316-0900	65.80	45.22	35.96	30.97	25.51
	10.47	2.831	2.272	8.849	1.846
71-324-0000	69.52	45.22	36.49	30.97	25.77
	7.447	3.328	2.655	7.161	1.821
71-329-0300	69.52	45.22	36.49	31.37	26.05
	15.97	8.395	5.999	14.58	3.390
71-331-1500	65.80	45.22	36.49	30.97	25.77
	7.147	4.036	4.464	8.861	3.404
72-155-0600	65.80	45.22	36.49	30.97	25.25
	18.46	6.227	7.186	15.01	4.757
	<u>25-20</u>	<u>19-18</u>	<u>17-16</u>	<u>16-15</u>	
71-166-1800	22.27	18.71	16.68	15.82	
	4.836	156.6	21.64	551.4	
71-168-0300	21.87	18.57	16.68	15.82	
	7.626	226.7	926.1	520.5	
71-289-1600	21.49	18.57	16.46	15.14	
	10.08	74.49	645.6	744.3	
71-304-1200	21.87	18.57	16.35	15.23	
	3.684	9.856	54.19	63.49	
71-314-1500	21.49	18.57	16.68	15.14	
	13.91	104.0	96.87	38.75	
71-316-0900	21.12	18.57	16.46	15.14	
	6.251	176.8	394.7	48.23	
71-324-0000	21.49	18.43	16.68	<15.05	
	6.853	61.09	559.7	229.6	

* Wave periods in seconds.

** Spectral energy densities in 10^{-2} ft²-sec.

Table 3

Estimates of Wave Periods and Spectral Energy Densities
of Peak Energies for Gage 7

Starting Time of Time History	Ranges of Wave Periods			
	600-250	480-360	225-200	190-135
71-166-1800	564.97* 213.5**	334.37 339.9	216.53 100.4	150.31 154.7
71-168-0300	564.97 117.3	334.37 123.4	216.53 89.09	150.31 93.42
71-289-1600	564.97 153.7	334.37 121.2	216.53 112.2	150.31 51.60
71-304-1200	564.97 259.8	334.37 51.03	216.53 38.86	150.31 13.68
71-314-1500	564.97 387.8	334.37 361.2	216.53 187.1	150.31 55.30
71-316-0900	564.97 134.3	334.37 85.07	216.53 121.6	150.31 25.32
71-324-0000	+	+	+	+
71-329-0300	564.97 194.6	334.37 325.0	216.53 56.49	150.31 58.67
71-331-1500	564.97 252.0	334.37 127.1	216.53 30.35	150.31 10.50
72-155-0600	+	+	+	+
	<u>80-60</u>	<u>55-45</u>	<u>45-35</u>	
71-166-1800	69.52 14.23	50.83 18.63	38.79 3.914	
71-168-0300	69.52 14.88	50.83 11.01	40.06 2.307	
71-289-1600	69.52 10.85	50.83 6.148	41.41 2.409	
71-304-1200	69.52 3.694	49.80 2.190	39.42 1.186	
71-314-1500	69.52 18.82	50.83 8.291	40.72 3.503	
71-316-0900	69.52 7.049	50.83 4.039	40.72 1.711	
71-324-0000	+	+	+	
71-329-0300	69.52 12.77	50.83 4.506	40.72 1.517	
71-331-1500	69.52 2.905	51.90 2.303	40.72 0.9627	
72-155-0600	+	+	+	

* Wave periods in seconds.

** Spectral energy densities in 10^{-2} ft²-sec.

+ No data for this time period.

Table 4

Estimates of Wave Periods and Spectral Energy Densities
of Peak Energies for Gage 8

Starting Time of Time History	Ranges of Wave Periods			
	600-500	360-290	220-190	165-140
71-166-1800	*	*	*	*
71-168-0300	*	*	*	*
71-289-1600	564.97** 27.70†	334.37 66.37	199.00 44.77	160.10 121.1
71-304-1200	564.97 41.11	334.37 26.73	216.53 12.68	150.31 24.13
71-314-1500	564.97 66.54	334.37 188.7	199.00 64.04	150.31 90.77
71-316-0900	564.97 21.61	334.37 42.05	199.00 17.30	160.10 50.42
71-324-0000	*	*	*	*
71-329-0300	564.97 32.43	334.37 185.0	198.99 56.80	160.10 158.0
71-331-1500	564.97 44.00	334.37 69.60	199.00 11.54	160.10 23.17
72-155-0600	564.97 23.04	334.37 67.81	199.00 24.68	150.31 60.83
	<u>125-110</u>	<u>100-85</u>	<u>85-65</u>	
71-166-1800	*	*	*	
71-168-0300	*	*	*	
71-289-1600	120.77 87.86	96.94 52.82	75.97 26.32	
71-304-1200	120.77 13.10	89.86 10.53	75.97 5.727	
71-314-1500	120.77 75.90	93.27 47.52	78.39 21.46	
71-316-0900	120.77 33.84	93.27 27.55	75.97 16.24	
71-324-0000	*	*	*	
71-329-0300	120.77 113.1	100.93 48.12	75.97 18.77	
71-331-1500	120.77 17.90	93.27 11.70	75.97 4.722	
72-155-0600	120.77 45.00	93.27 29.76	78.39 20.62	

* Wave periods in seconds.

** Spectral energy densities in 10^{-2} ft²-sec.

† No data for this time period.

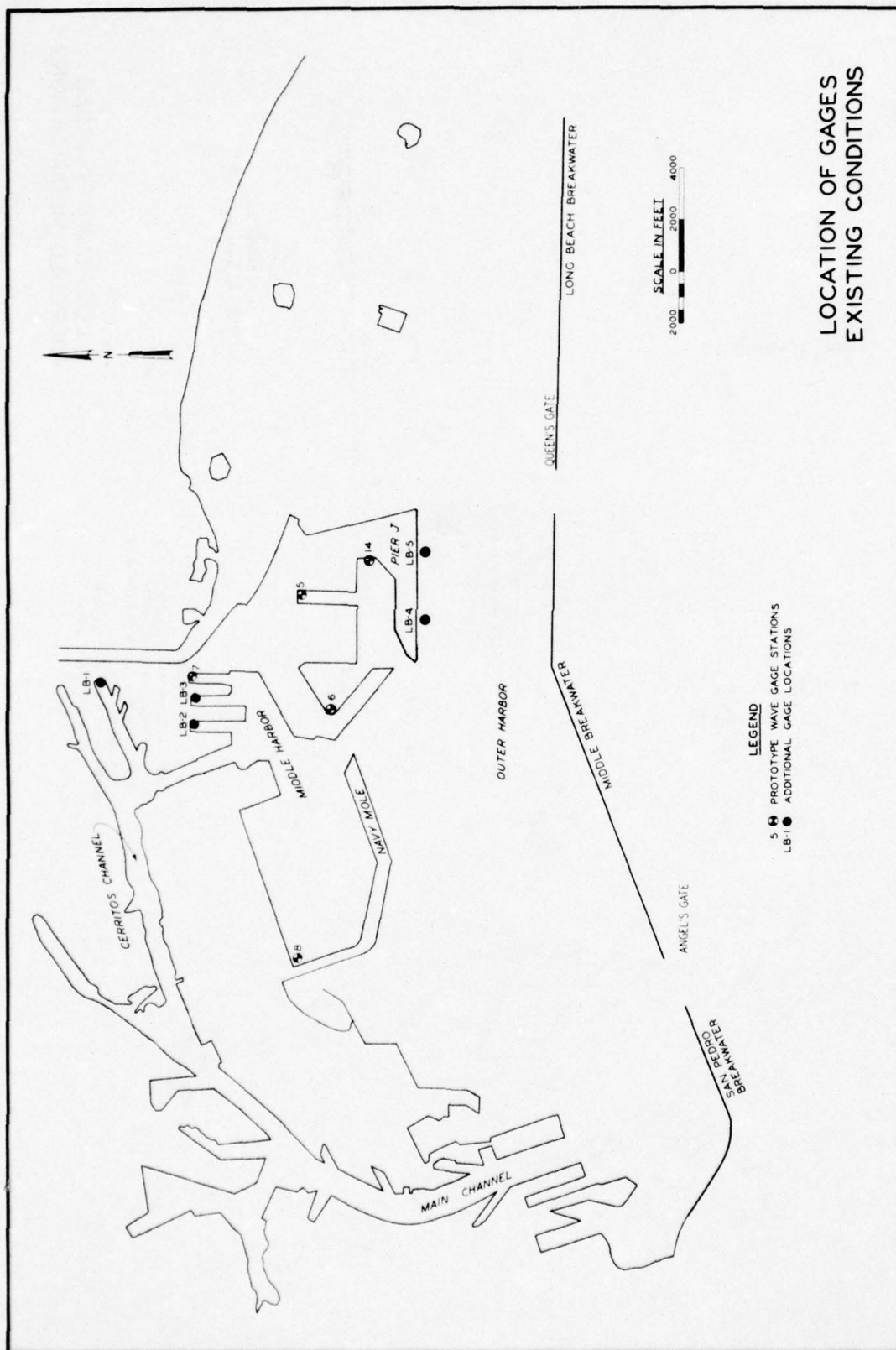
Table 5

Estimates of Wave Periods and Spectral Energy
Densities of Peak Energies for Gage 14

Starting Time of Time History	Ranges of Wave Periods				
	<u>1800-480</u>	<u>480-360</u>	<u>270-210</u>	<u>170-150</u>	<u>139-95</u>
72-155-0600	733.61*	387.02	237.45	160.01	100.93
	186.9**	13.59	22.28	91.33	46.85
72-155-0600	<u>90-80</u>	<u>80-65</u>	<u>65-60</u>	<u>51-46</u>	
	89.86	69.52	64.08	49.80	
	11.80	22.74	18.21	20.50	

* Wave periods in seconds.

** Spectral energy densities in 10^{-2} ft²-sec.



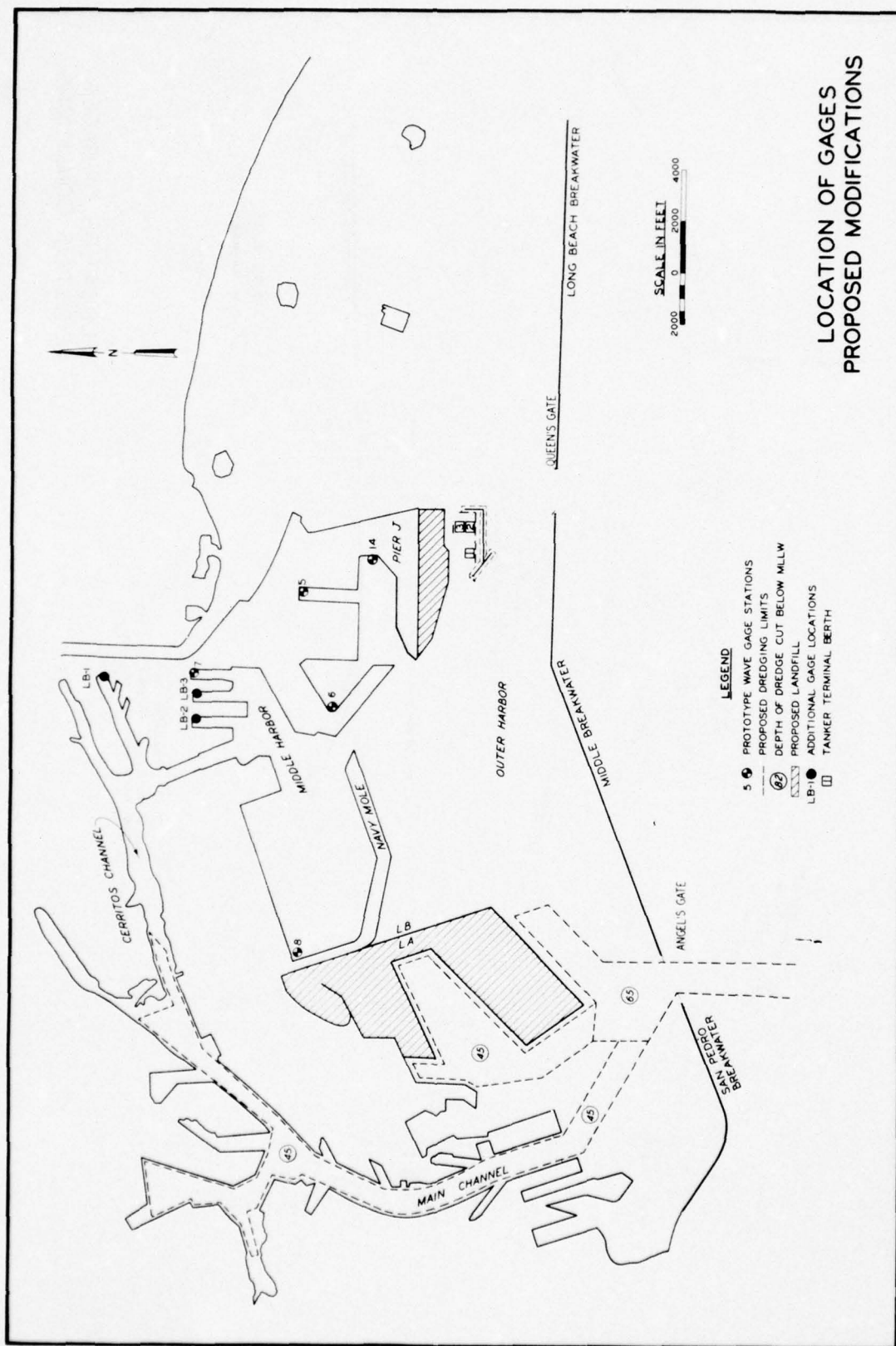
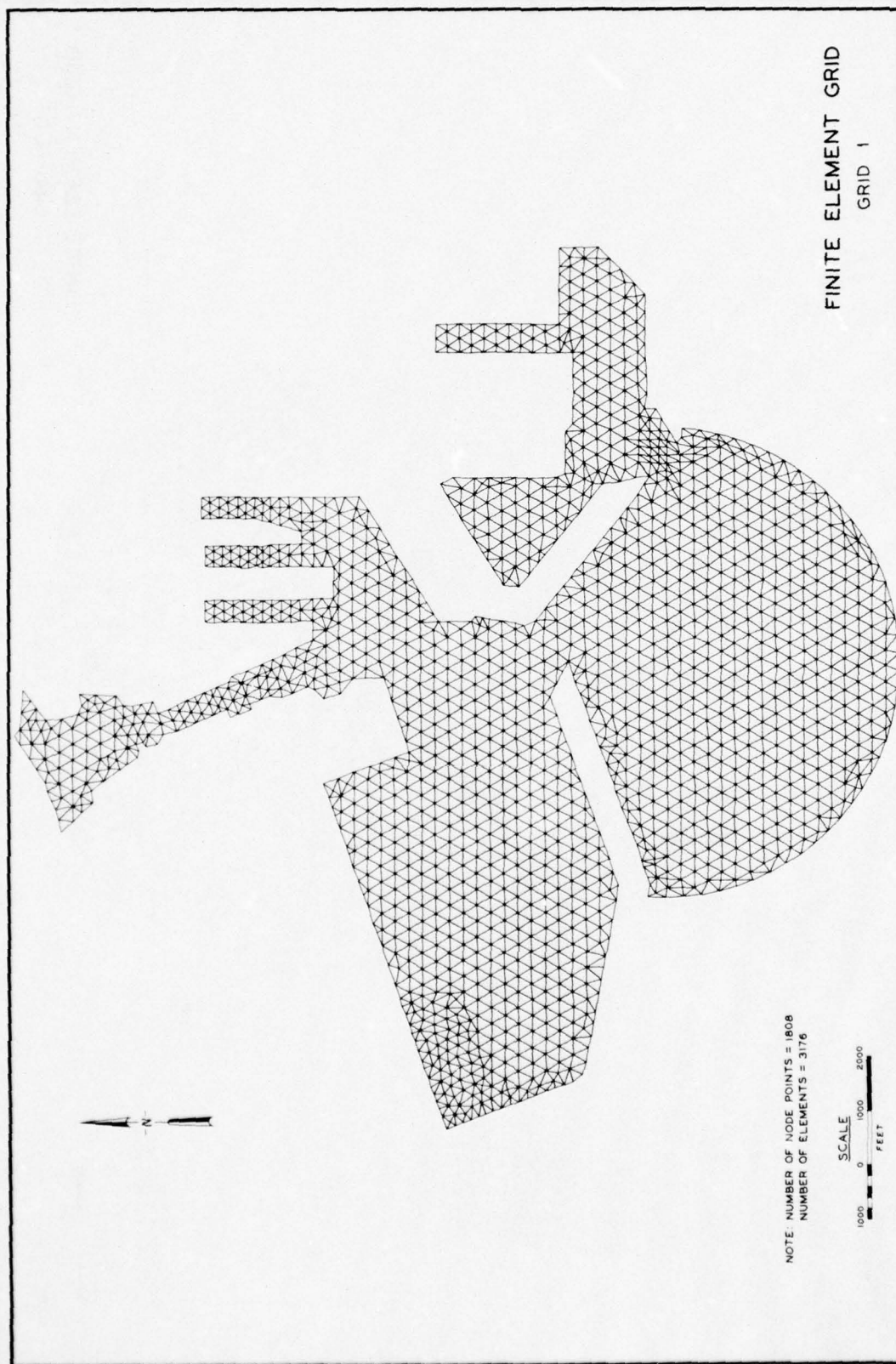


PLATE 2



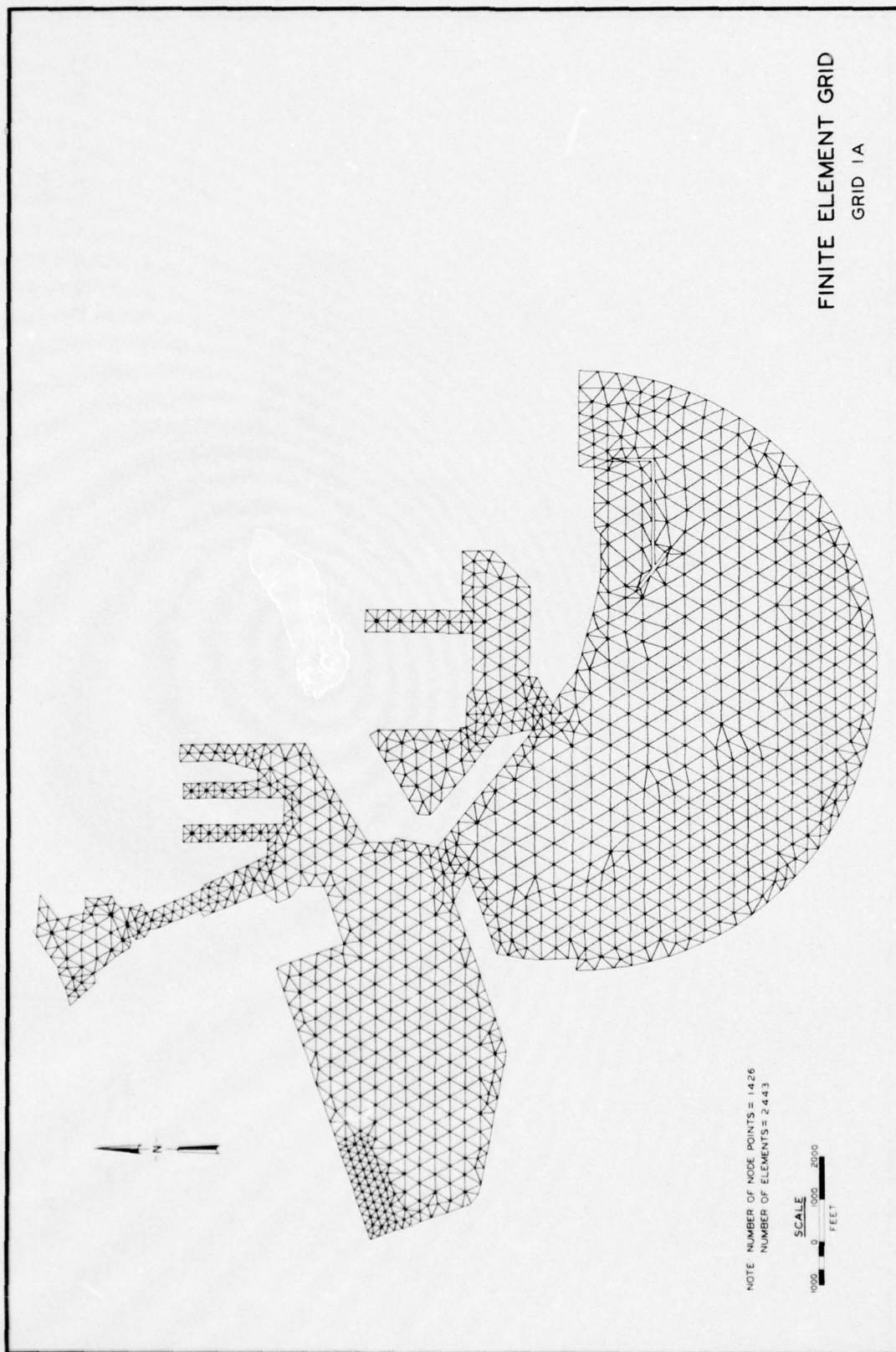
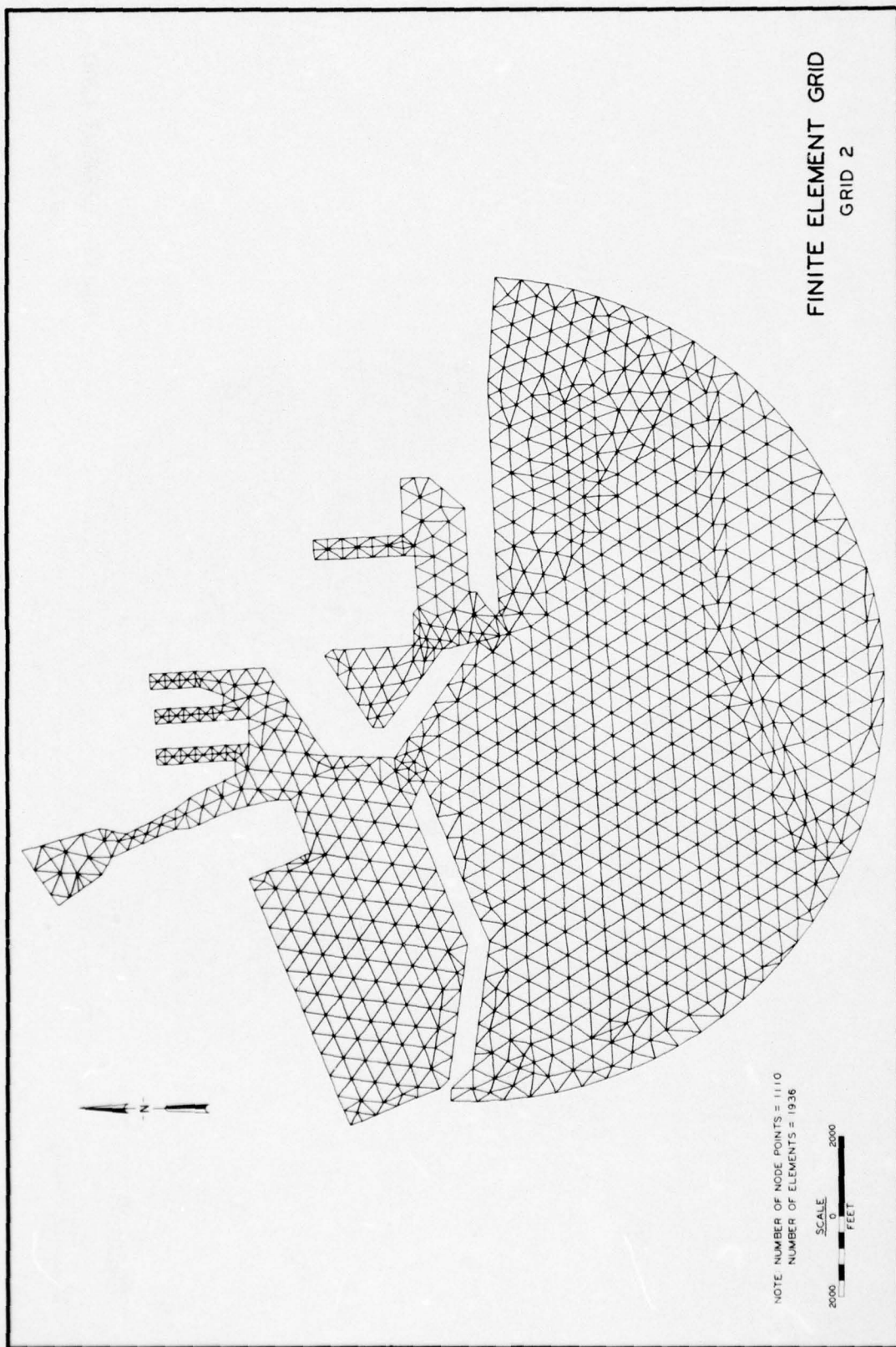


PLATE 4



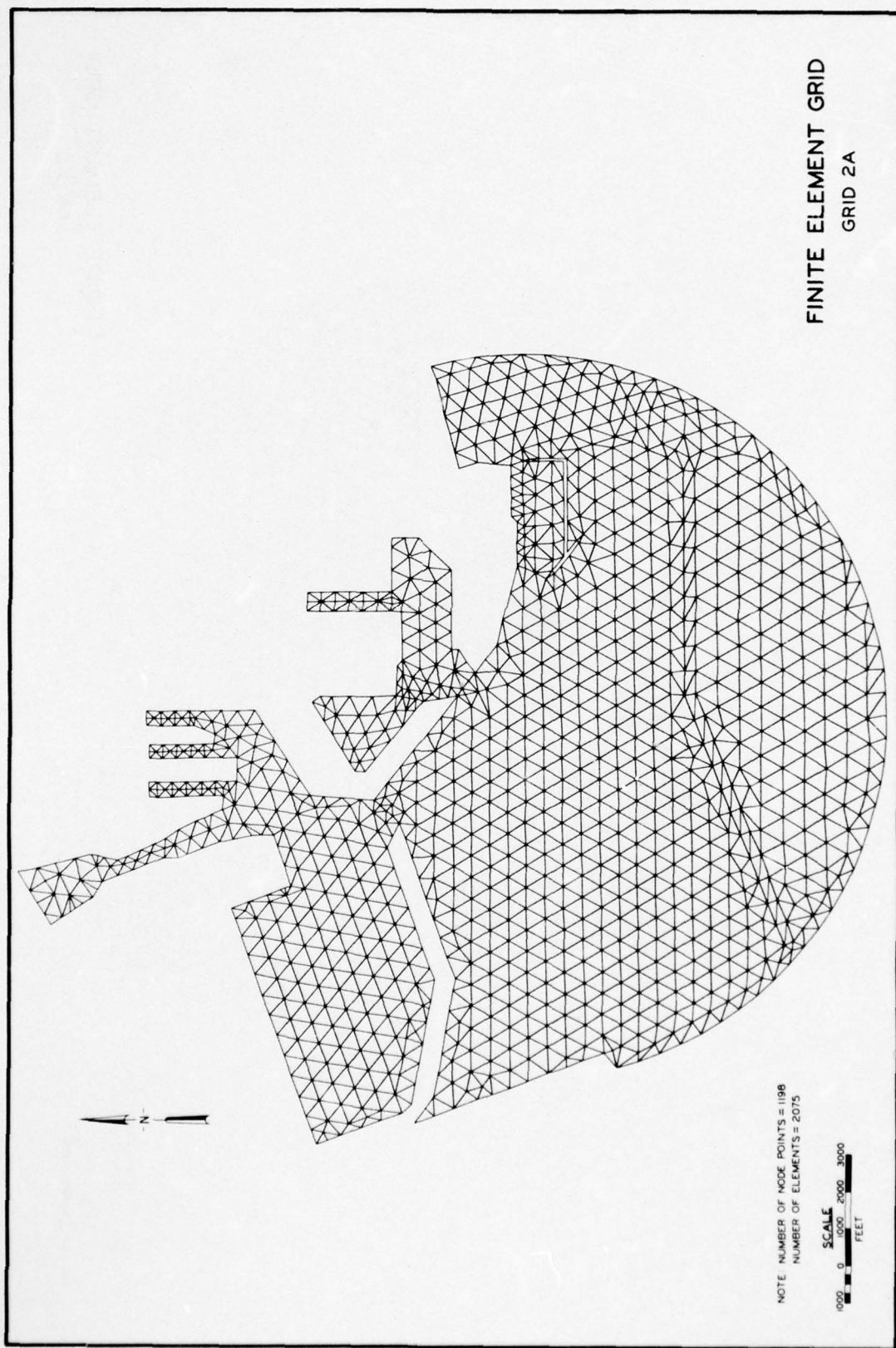
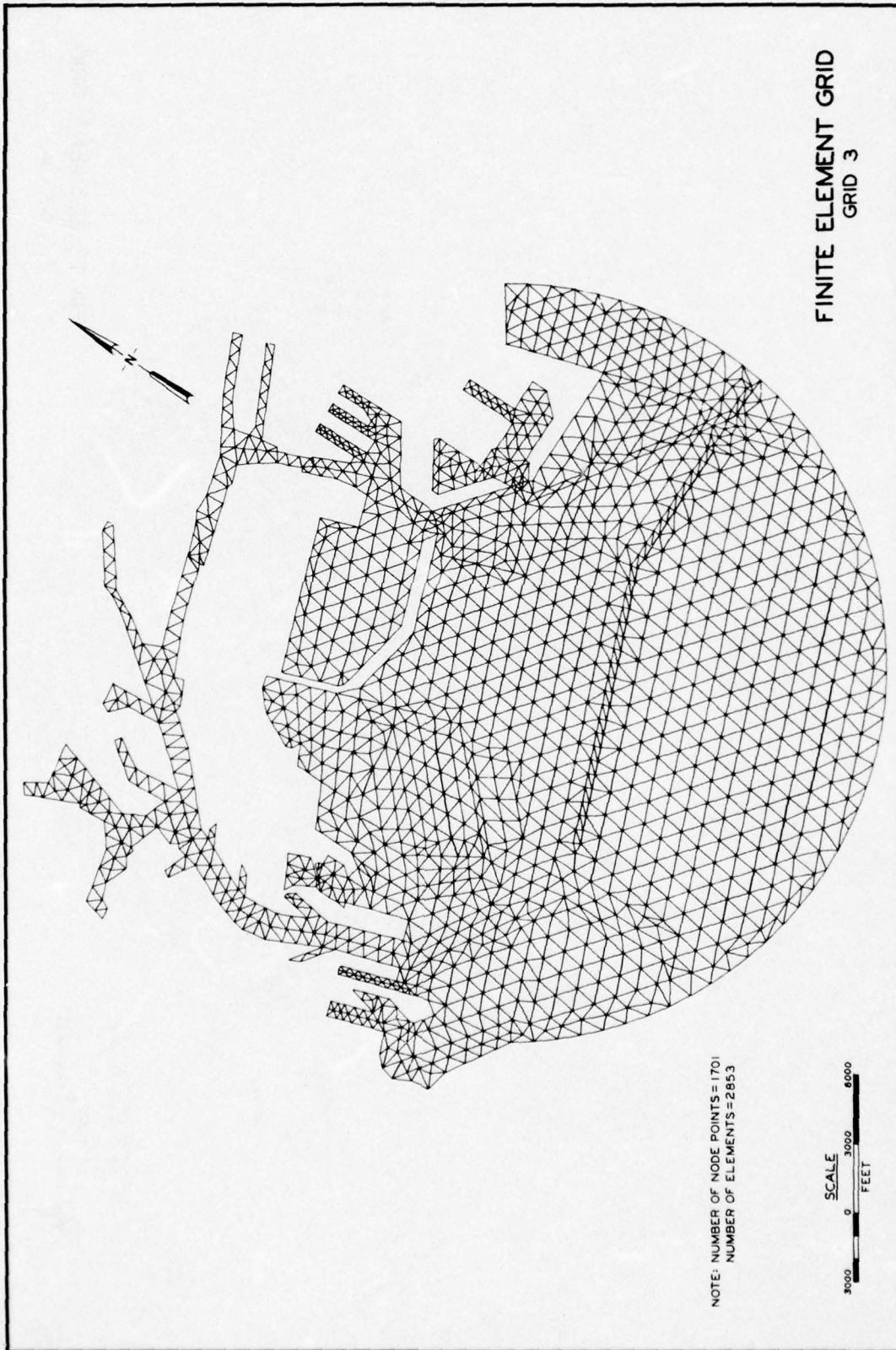


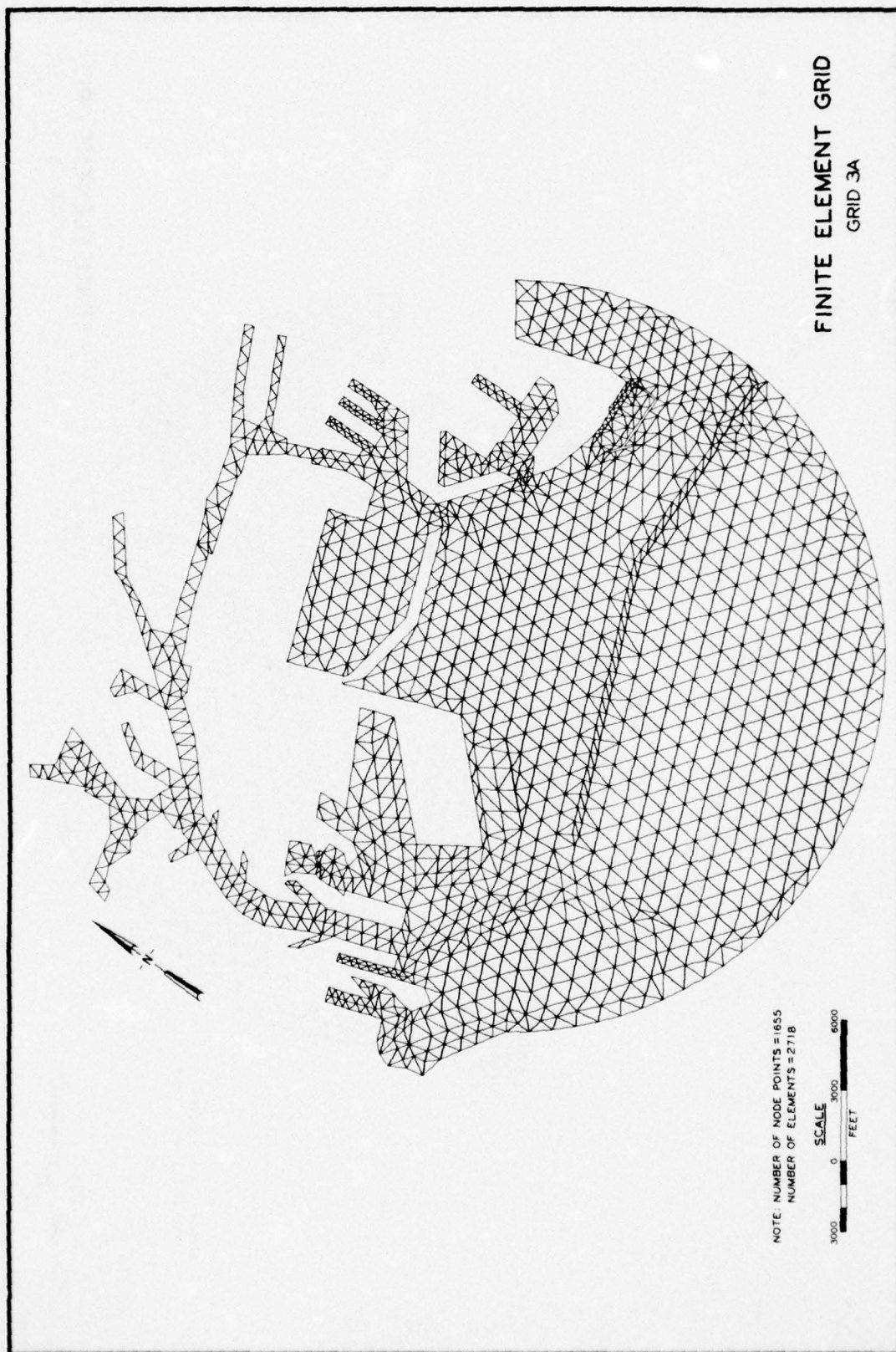
PLATE 6



NOTE: NUMBER OF NODE POINTS = 1701
NUMBER OF ELEMENTS = 2853

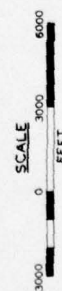
SCALE
0 3000 6000
FEET

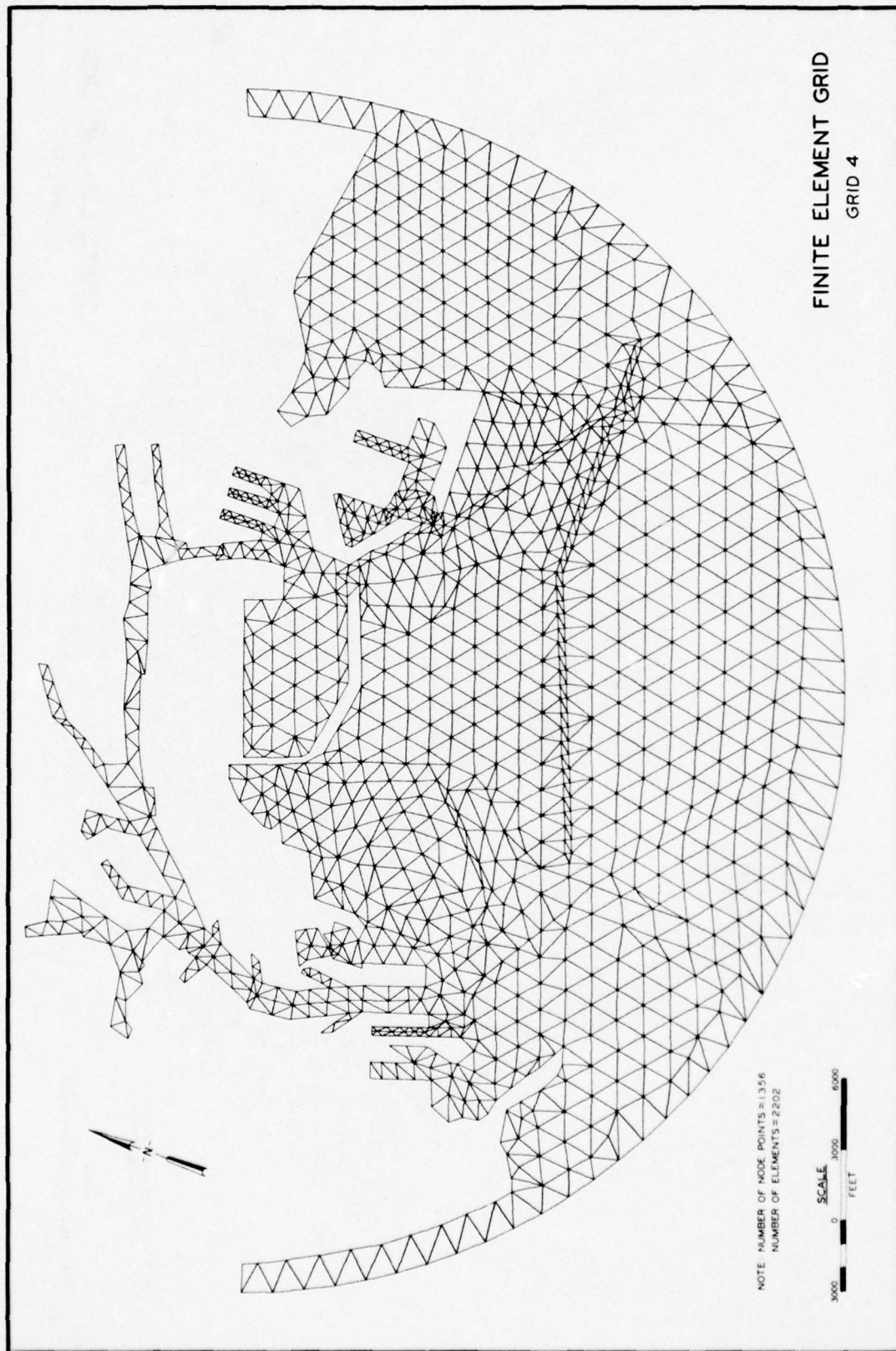
FINITE ELEMENT GRID
GRID 3



FINITE ELEMENT GRID
GRID 3A

NOTE: NUMBER OF NODE POINTS = 1655
NUMBER OF ELEMENTS = 2718

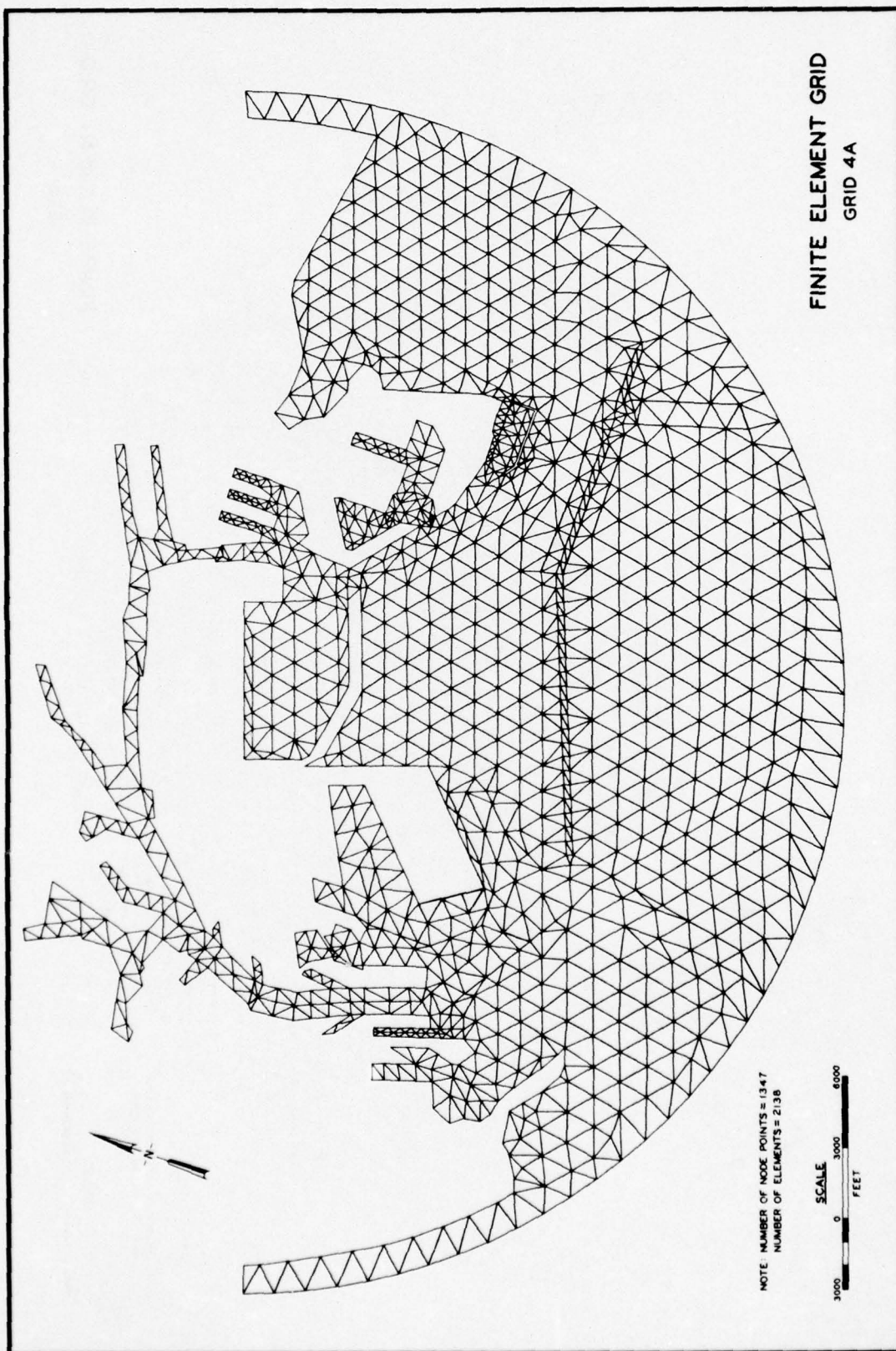


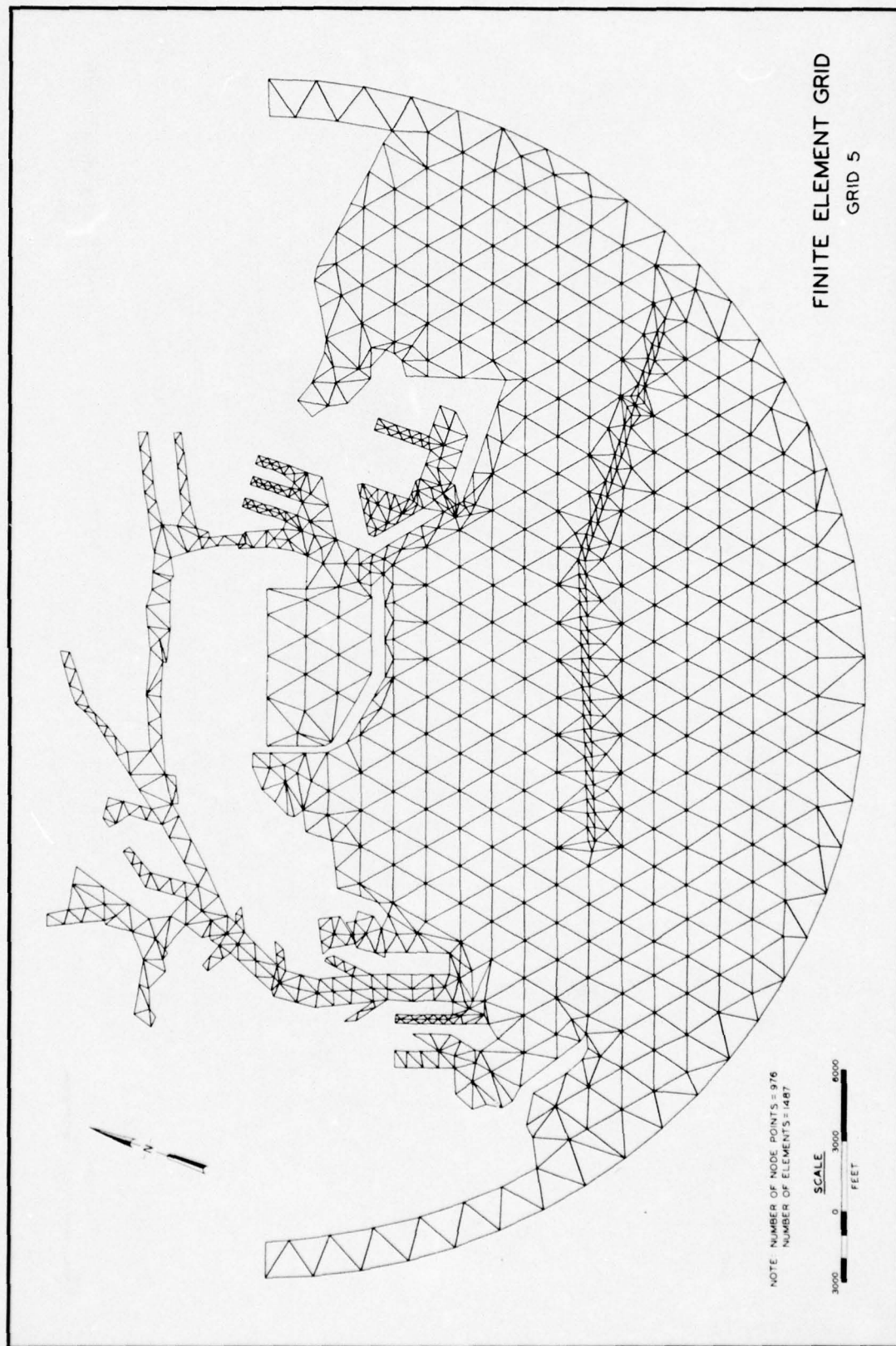


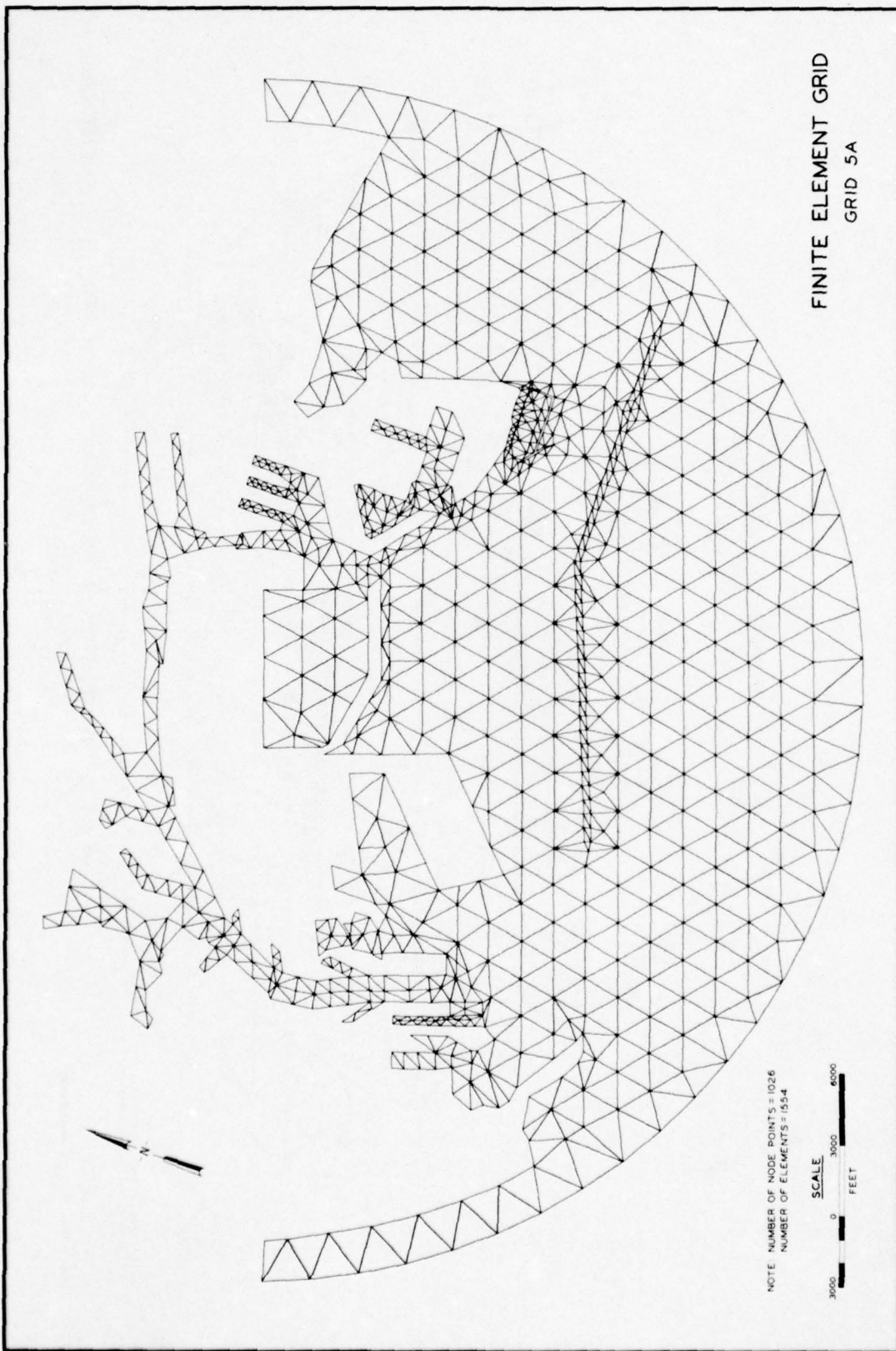
FINITE ELEMENT GRID
GRID 4

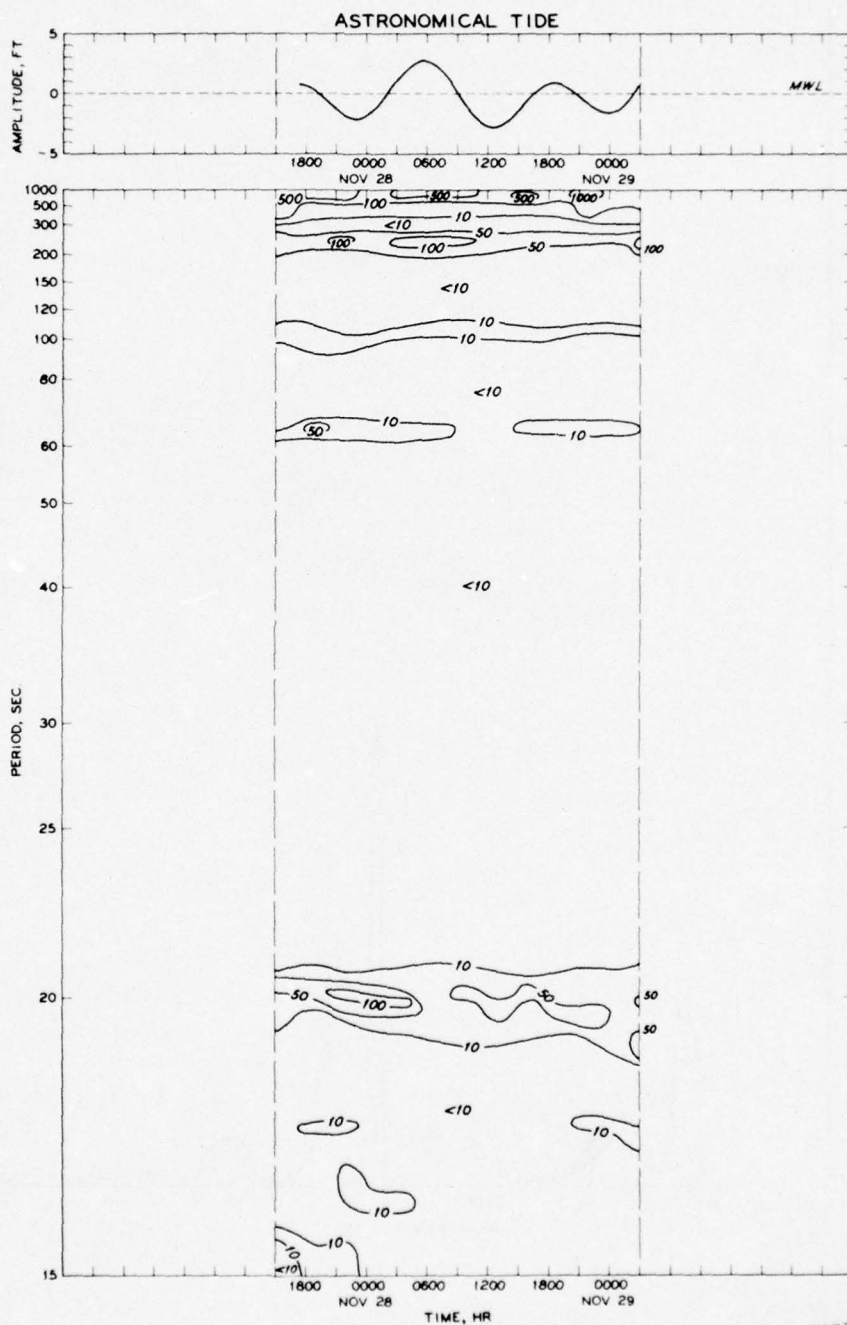
NOTE NUMBER OF NODE POINTS = 1356
NUMBER OF ELEMENTS = 2202

SCALE
0 3000 6000
FEET





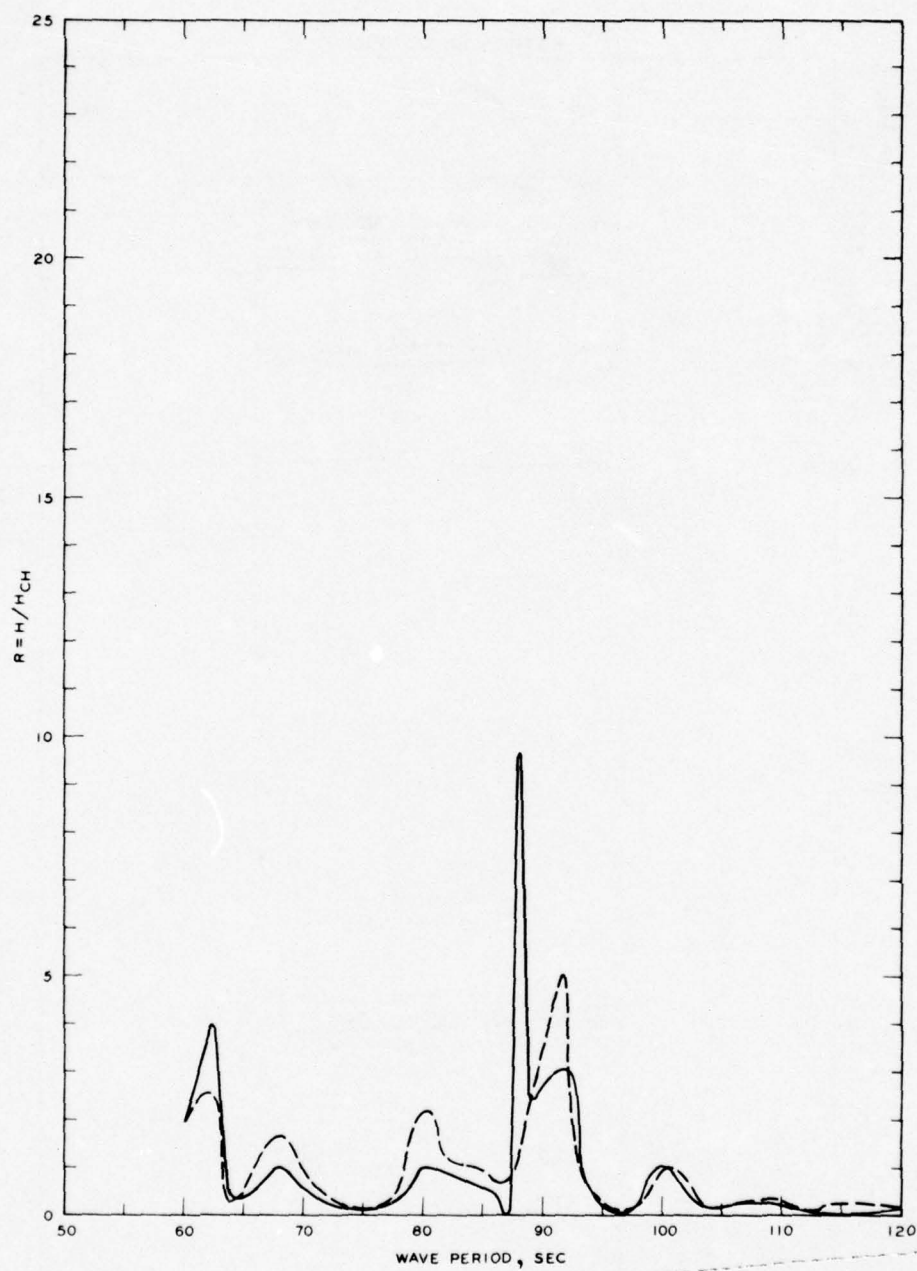




NOTE: ENERGY UNITS = 10^{-4} FT²/SEC
 MWL = MEAN WATER LEVEL

CONTOURS OF TIME-DEPENDENT ENERGY SPECTRUM

1500 NOVEMBER 27 - 0300 NOVEMBER 29, 1971
 GAGE 5 SOUTHEAST BASIN

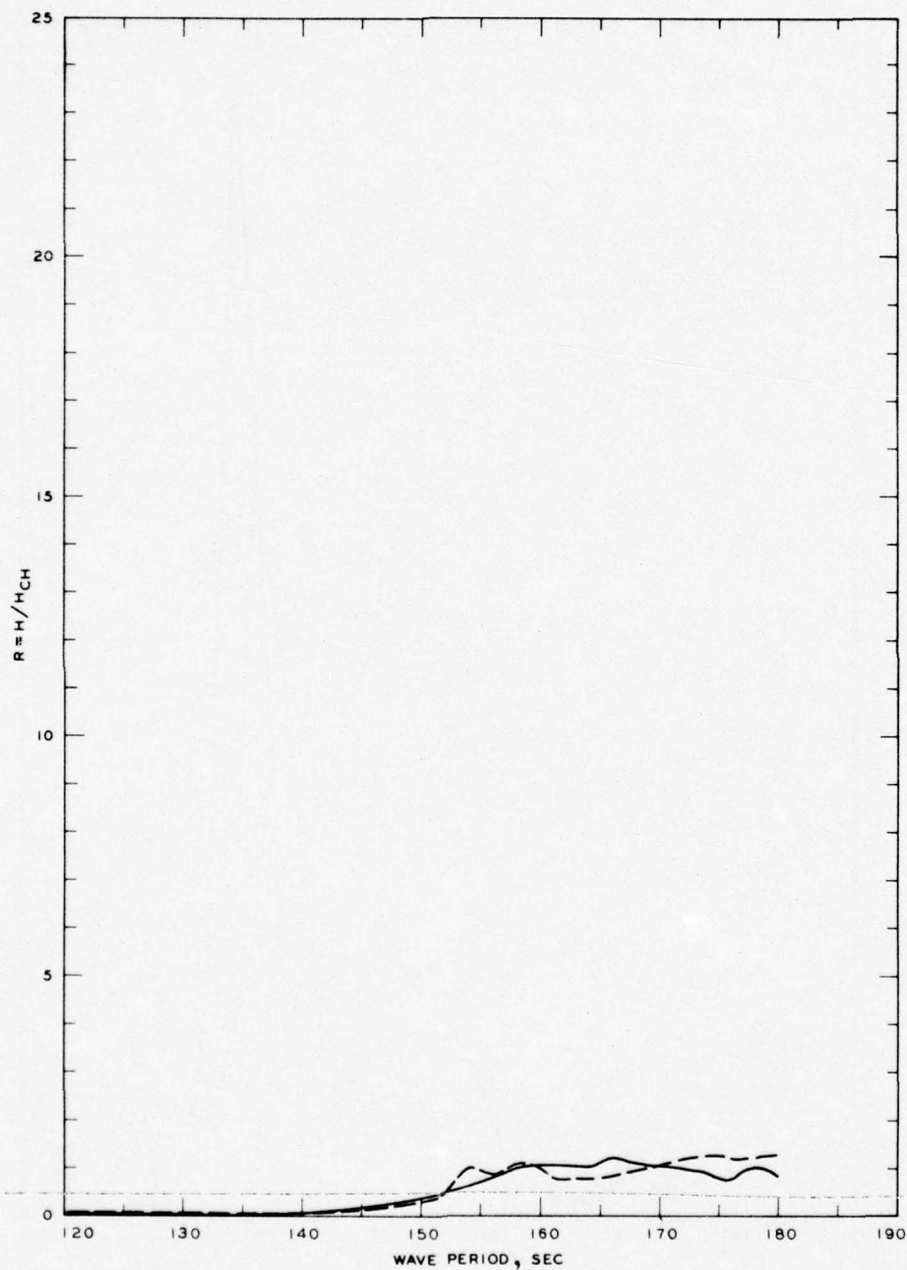


LEGEND

— GRID 1
 - - - GRID 1A

NOTE R = WAVE-HEIGHT AMPLIFICATION FACTOR
 H = WAVE HEIGHT, FT
 H_{CH} = WAVE HEIGHT FOR CLOSED HARBOR, FT

FREQUENCY RESPONSE
 WAVE-HEIGHT AMPLIFICATION FACTOR
 GAGE 5, GRIDS 1 AND 1A

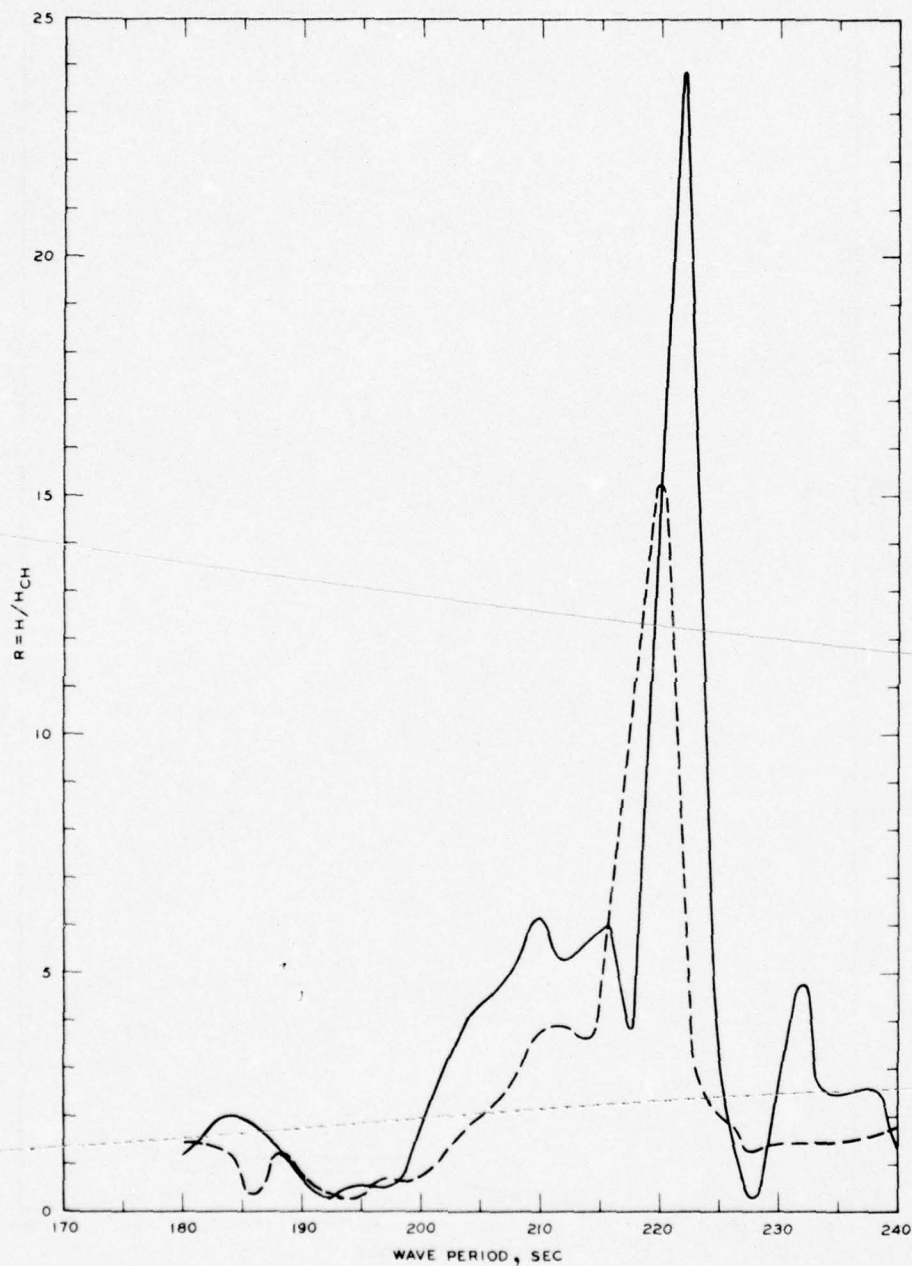


LEGEND

— GRID 2
 - - - GRID 2A

NOTE R = WAVE-HEIGHT AMPLIFICATION FACTOR
 H = WAVE HEIGHT, FT
 H_{CH} = WAVE HEIGHT FOR CLOSED HARBOR, FT

FREQUENCY RESPONSE
 WAVE-HEIGHT AMPLIFICATION FACTOR
 GAGE 5, GRIDS 2 AND 2A

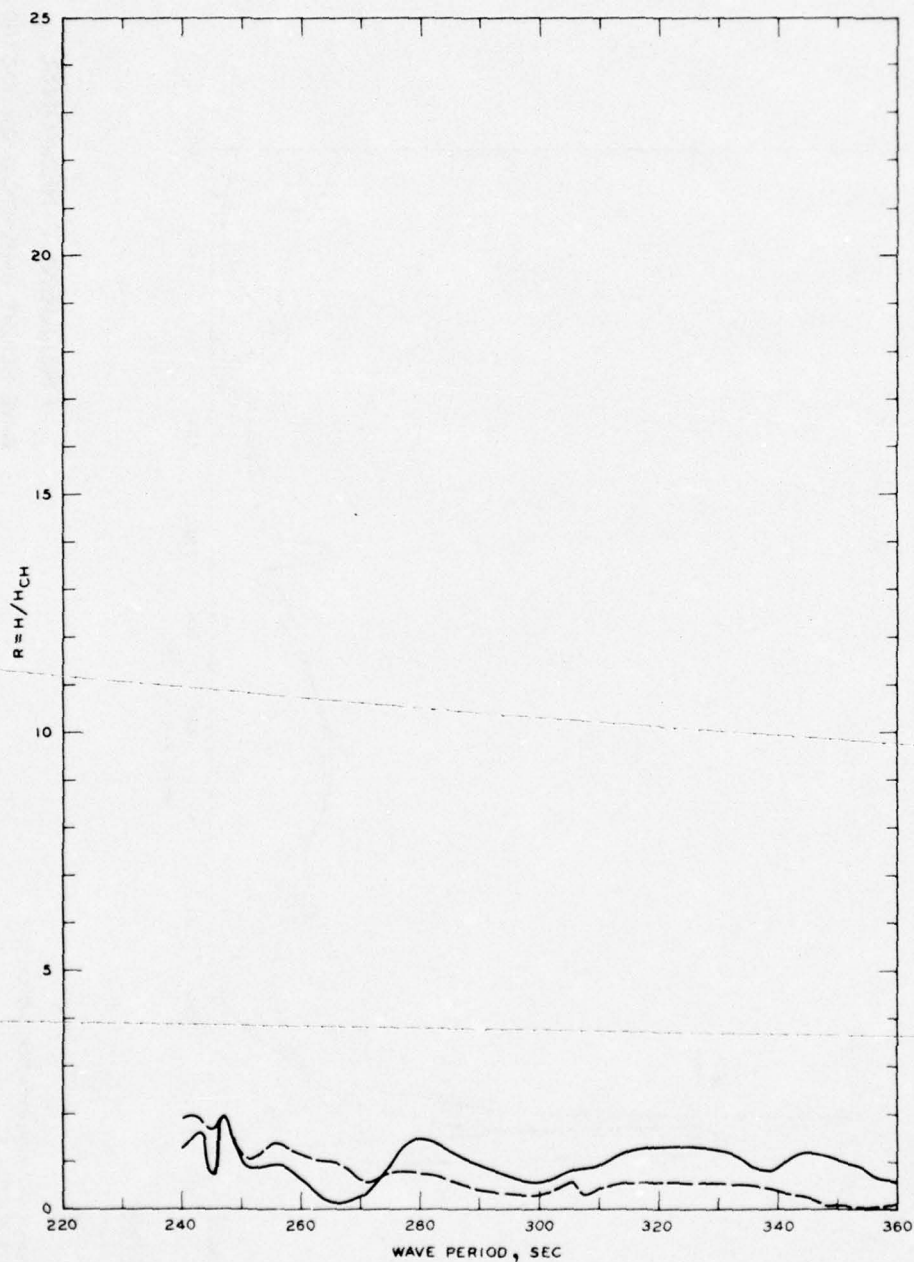


LEGEND

— GRID 3
 - - - GRID 3A

NOTE R = WAVE-HEIGHT AMPLIFICATION FACTOR
 H = WAVE HEIGHT, FT
 H_{CH} = WAVE HEIGHT FOR CLOSED HARBOR, FT

FREQUENCY RESPONSE
 WAVE-HEIGHT AMPLIFICATION FACTOR
 GAGE 5, GRIDS 3 AND 3A

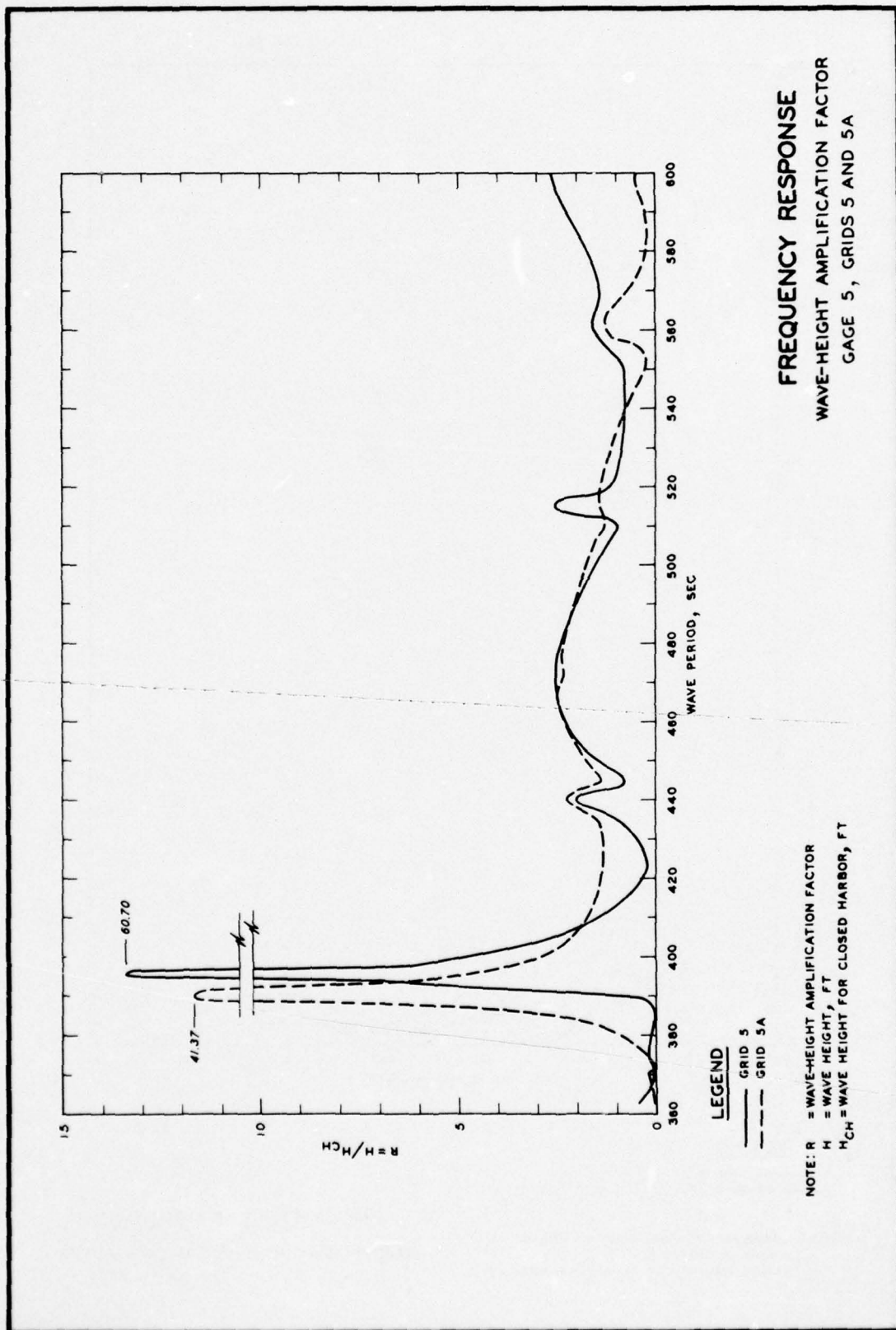


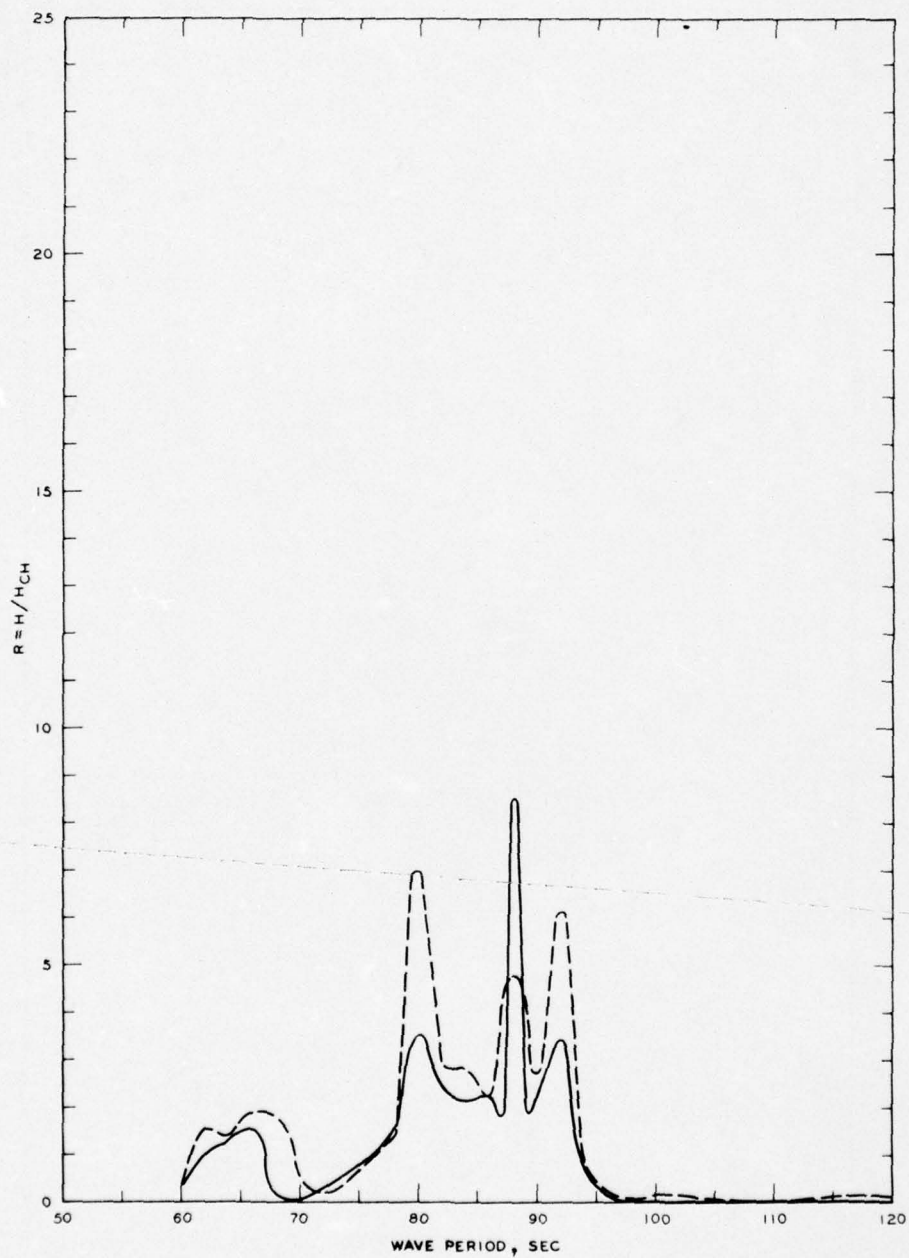
LEGEND

— GRID 4
 - - - GRID 4A

NOTE R = WAVE-HEIGHT AMPLIFICATION FACTOR
 H = WAVE HEIGHT, FT
 H_{CH} = WAVE HEIGHT FOR CLOSED HARBOR, FT

FREQUENCY RESPONSE
 WAVE-HEIGHT AMPLIFICATION FACTOR
 GAGE 5, GRIDS 4 AND 4A



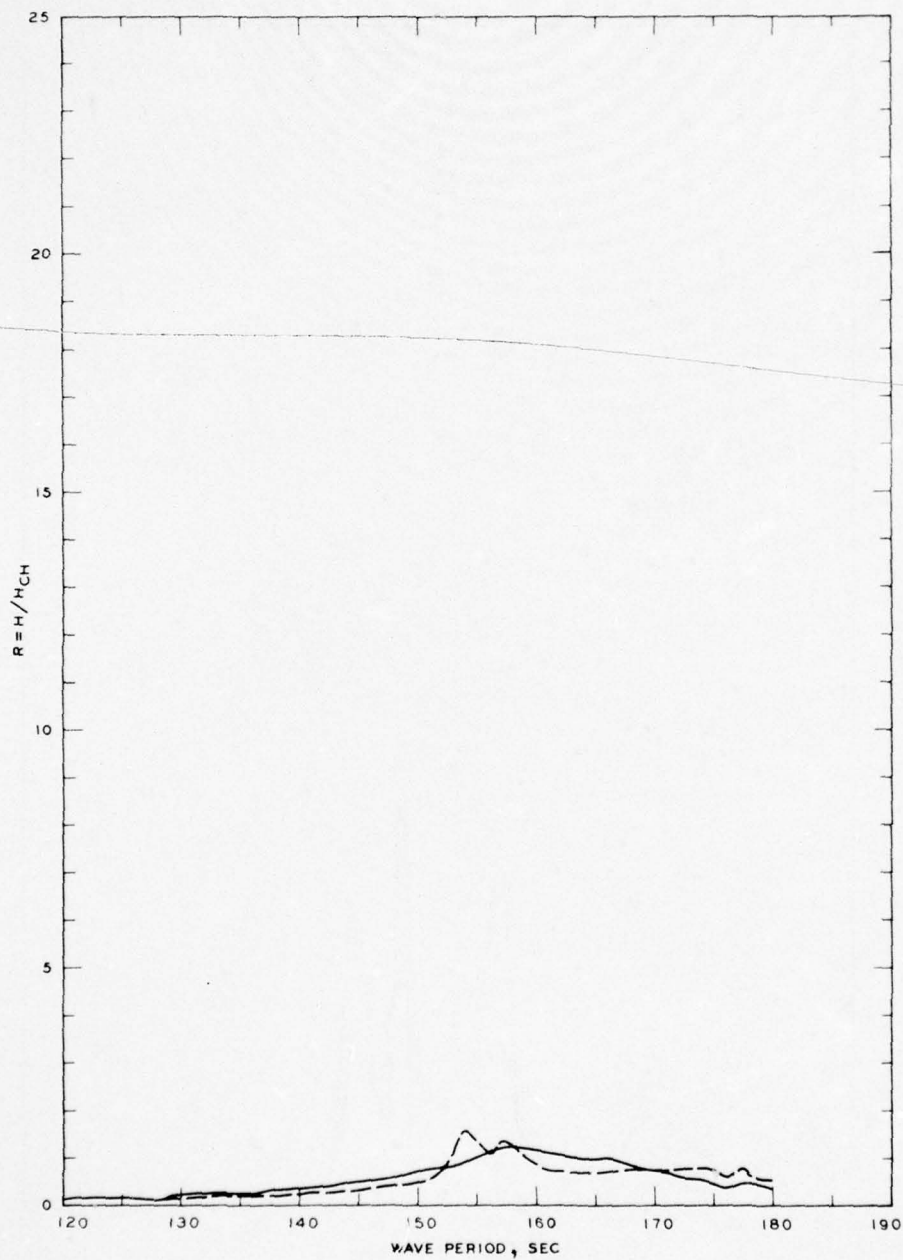


LEGEND

— GRID 1
 - - - GRID 1A

NOTE R = WAVE-HEIGHT AMPLIFICATION FACTOR
 H = WAVE HEIGHT, FT
 H_{CH} = WAVE HEIGHT FOR CLOSED HARBOR, FT

FREQUENCY RESPONSE
 WAVE-HEIGHT AMPLIFICATION FACTOR
 GAGE 6, GRIDS 1 AND 1A

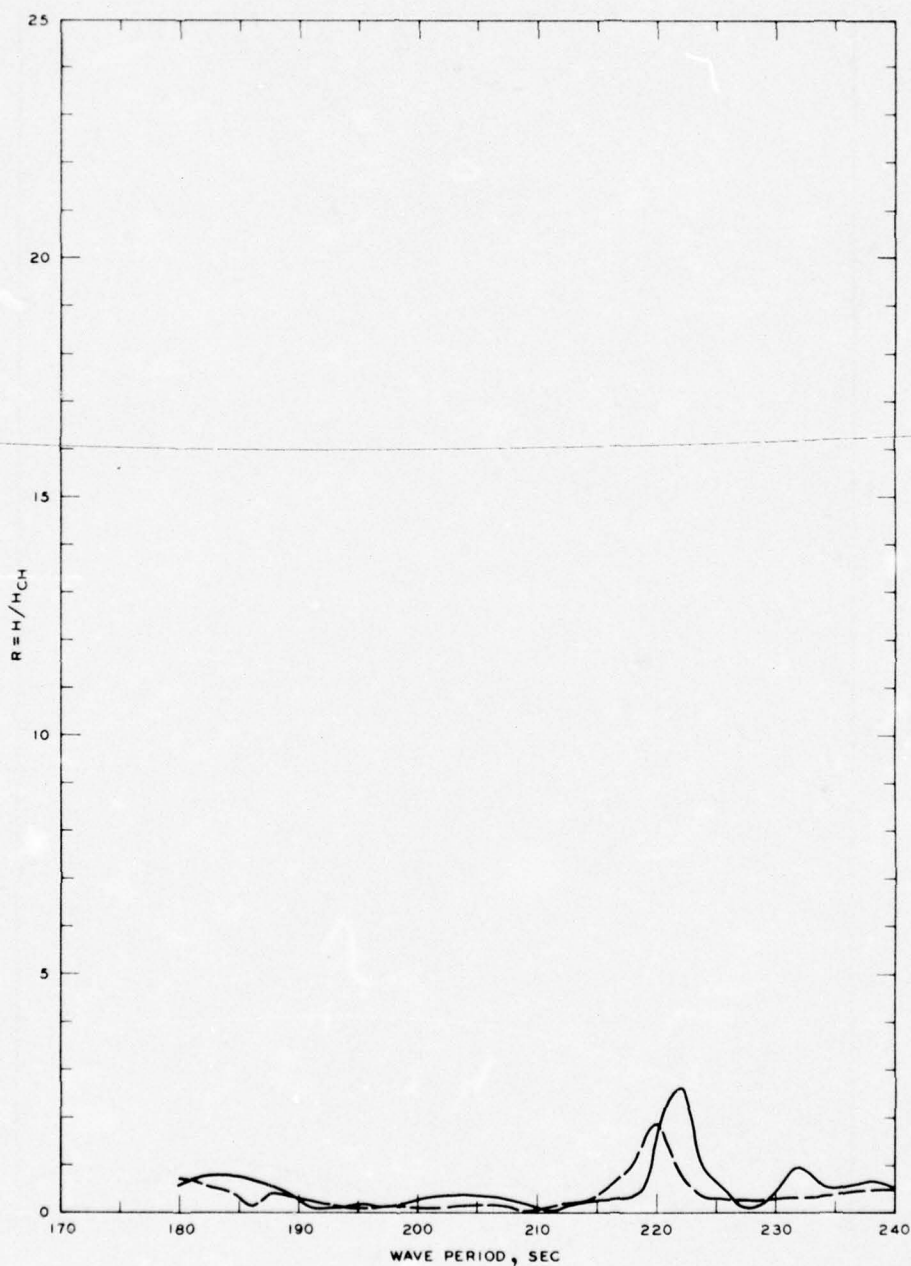


LEGEND

— GRID 2
 - - - GRID 2A

NOTE R = WAVE-HEIGHT AMPLIFICATION FACTOR
 H = WAVE HEIGHT, FT
 H_{CH} = WAVE HEIGHT FOR CLOSED HARBOR, FT

FREQUENCY RESPONSE
 WAVE-HEIGHT AMPLIFICATION FACTOR
 GAGE 6, GRIDS 2 AND 2A

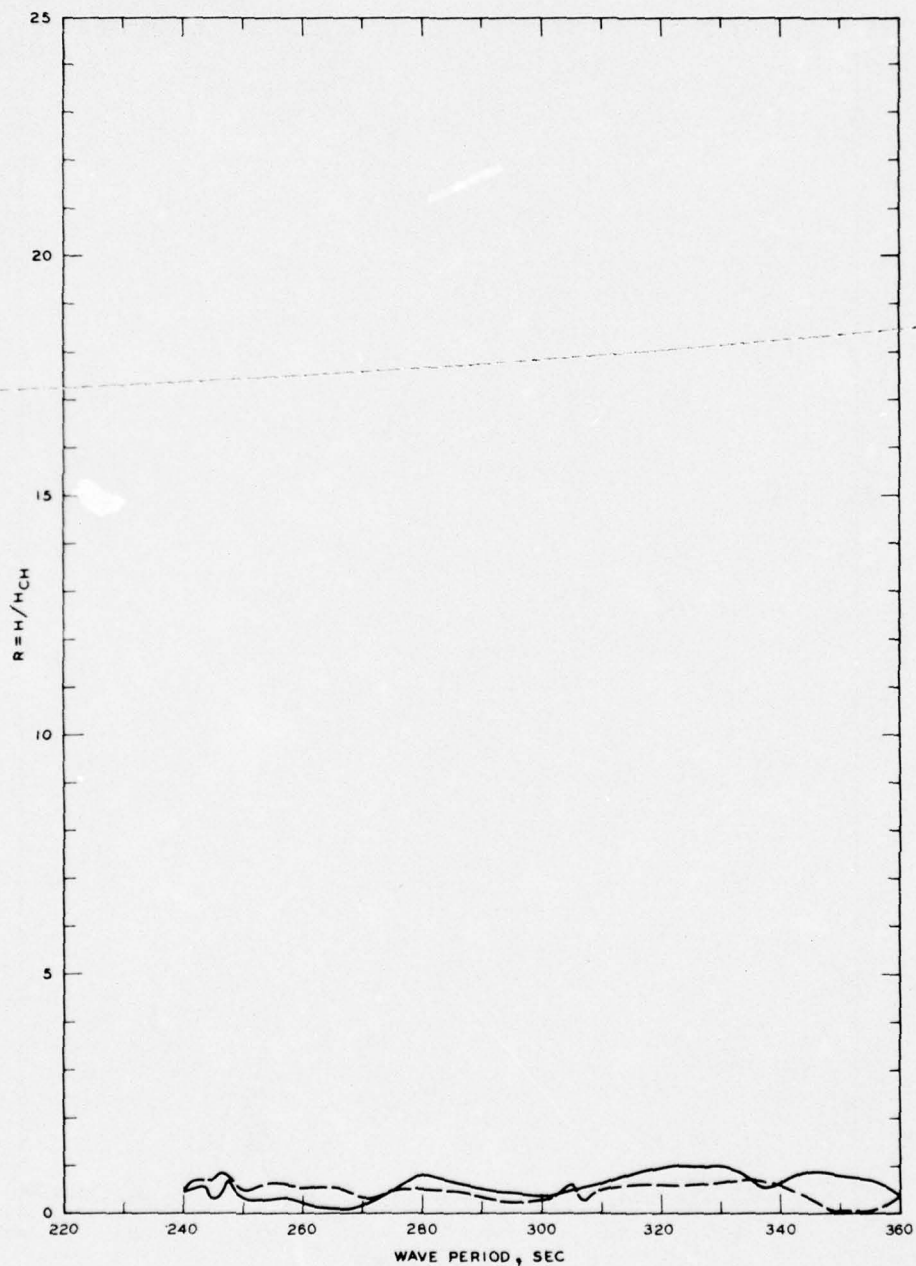


LEGEND

— GRID 3
 - - - GRID 3A

NOTE: R = WAVE-HEIGHT AMPLIFICATION FACTOR
 H = WAVE HEIGHT, FT
 H_{CH} = WAVE HEIGHT FOR CLOSED HARBOR, FT

FREQUENCY RESPONSE
 WAVE-HEIGHT AMPLIFICATION FACTOR
 GAGE 6, GRIDS 3 AND 3A



LEGEND

— GRID 4
 - - - GRID 4A

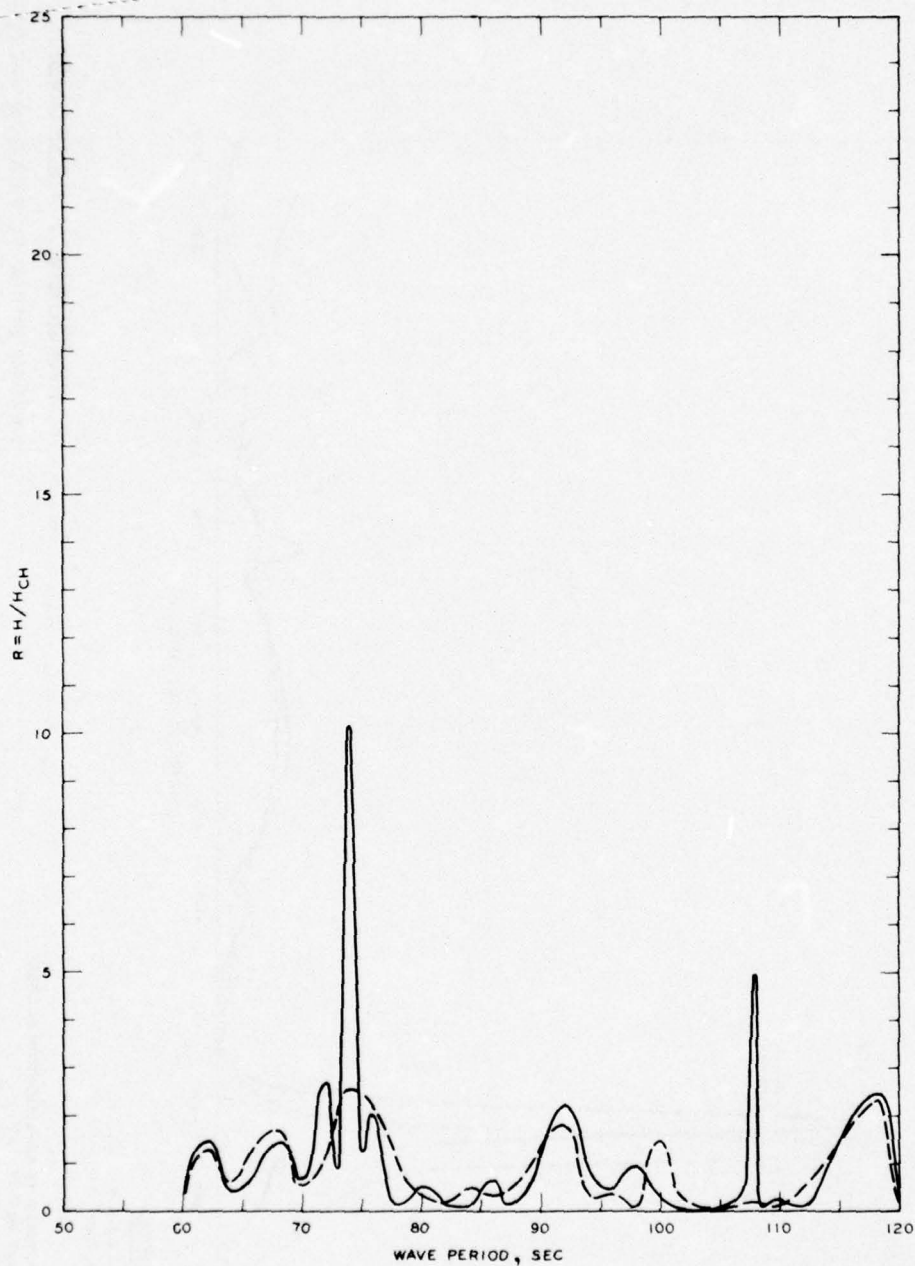
NOTE: R = WAVE-HEIGHT AMPLIFICATION FACTOR
 H = WAVE HEIGHT, FT
 H_{CH} = WAVE HEIGHT FOR CLOSED HARBOR, FT

FREQUENCY RESPONSE
 WAVE-HEIGHT AMPLIFICATION FACTOR
 GAGE 6, GRIDS 4 AND 4A



NOTE: R = WAVE-HEIGHT AMPLIFICATION FACTOR
H = WAVE HEIGHT, FT
H_{CH} = WAVE HEIGHT FOR CLOSED HARBOR, FT

FREQUENCY RESPONSE
WAVE-HEIGHT AMPLIFICATION FACTOR
GAGE 6, GRIDS 5 AND 5A

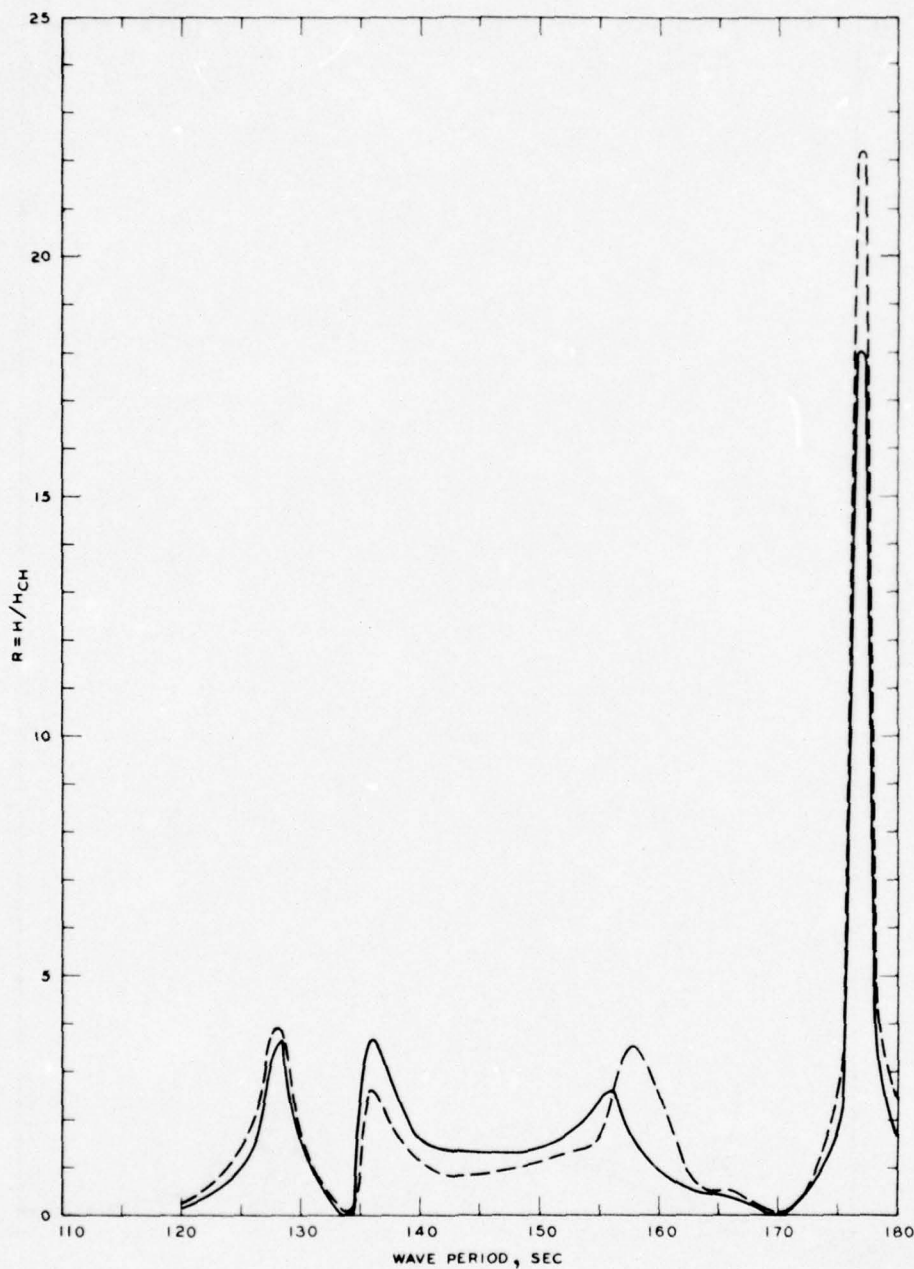


LEGEND

— GRID 1
 - - - GRID 1A

NOTE R = WAVE-HEIGHT AMPLIFICATION FACTOR
 H = WAVE HEIGHT, FT
 H_{CH} = WAVE HEIGHT FOR CLOSED HARBOR, FT

FREQUENCY RESPONSE
 WAVE-HEIGHT AMPLIFICATION FACTOR
 GAGE 7, GRIDS 1 AND 1A

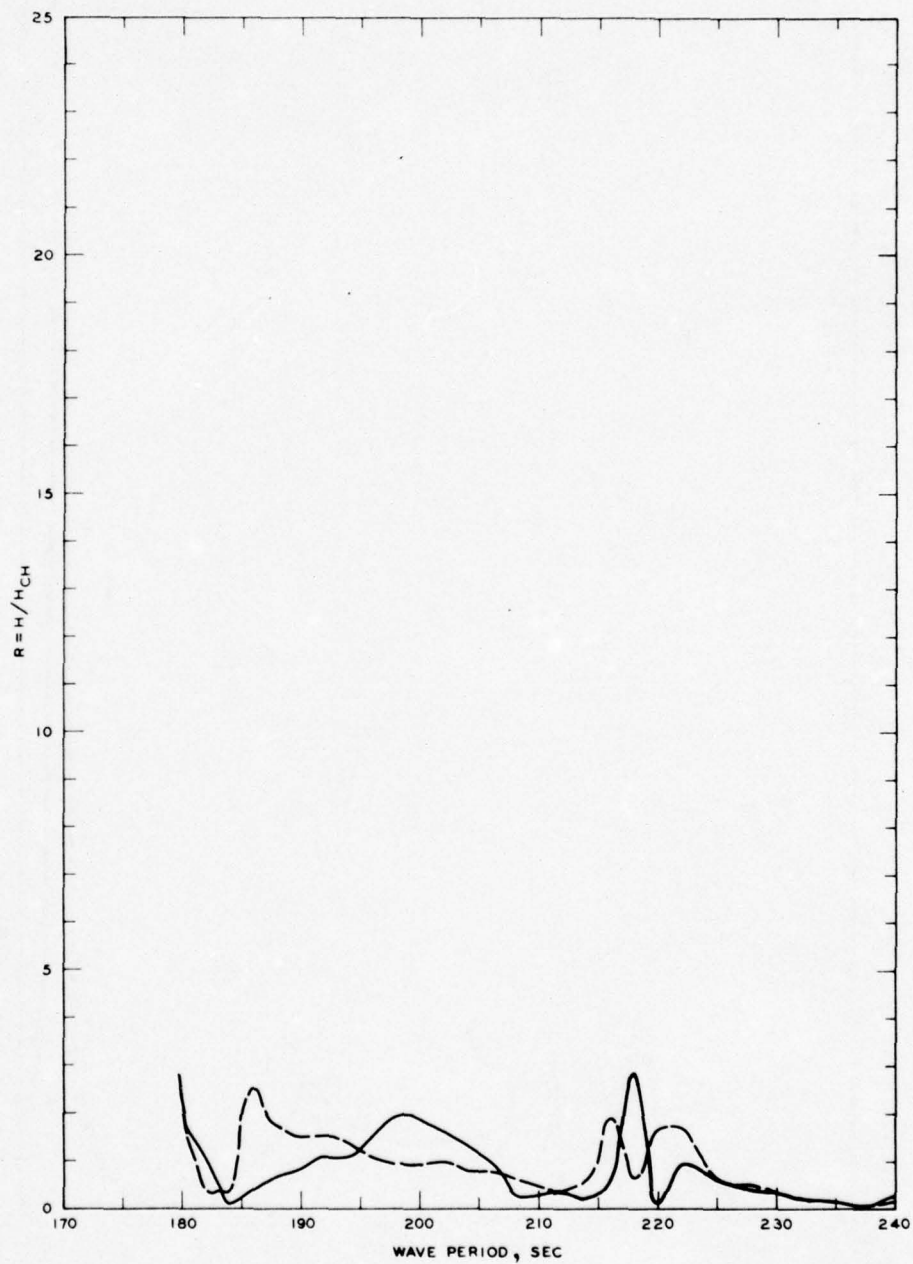


LEGEND

— GRID 2
 - - - GRID 2A

NOTE R = WAVE-HEIGHT AMPLIFICATION FACTOR
 H = WAVE HEIGHT, FT
 H_{CH} = WAVE HEIGHT FOR CLOSED HARBOR, FT

FREQUENCY RESPONSE
 WAVE-HEIGHT AMPLIFICATION FACTOR
 GAGE 7, GRIDS 2 AND 2A

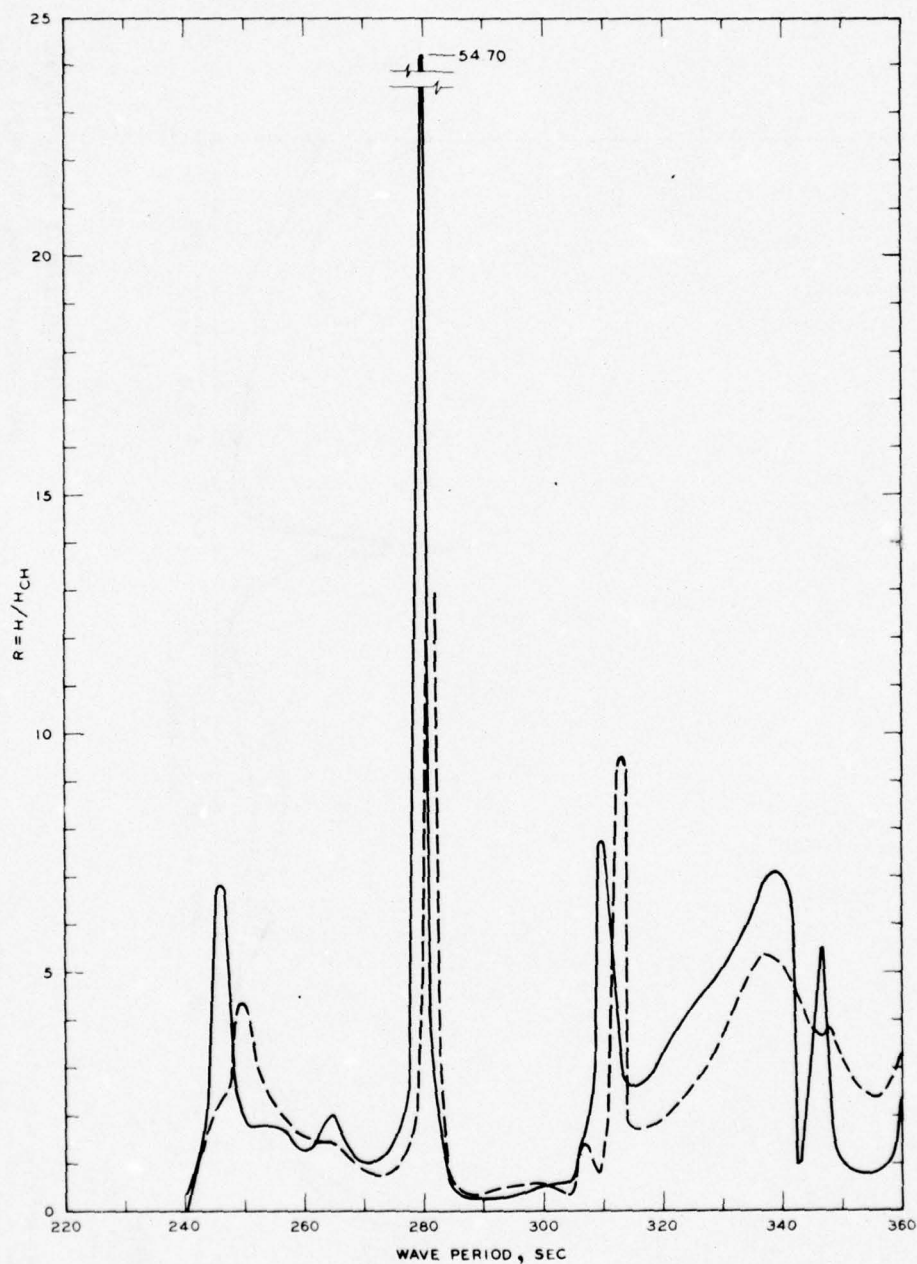


LEGEND

— GRID 3
 - - - GRID 3A

NOTE: R = WAVE-HEIGHT AMPLIFICATION FACTOR
 H = WAVE HEIGHT, FT
 H_{CH} = WAVE HEIGHT FOR CLOSED HARBOR, FT

FREQUENCY RESPONSE
 WAVE-HEIGHT AMPLIFICATION FACTOR
 GAGE 7, GRIDS 3 AND 3A

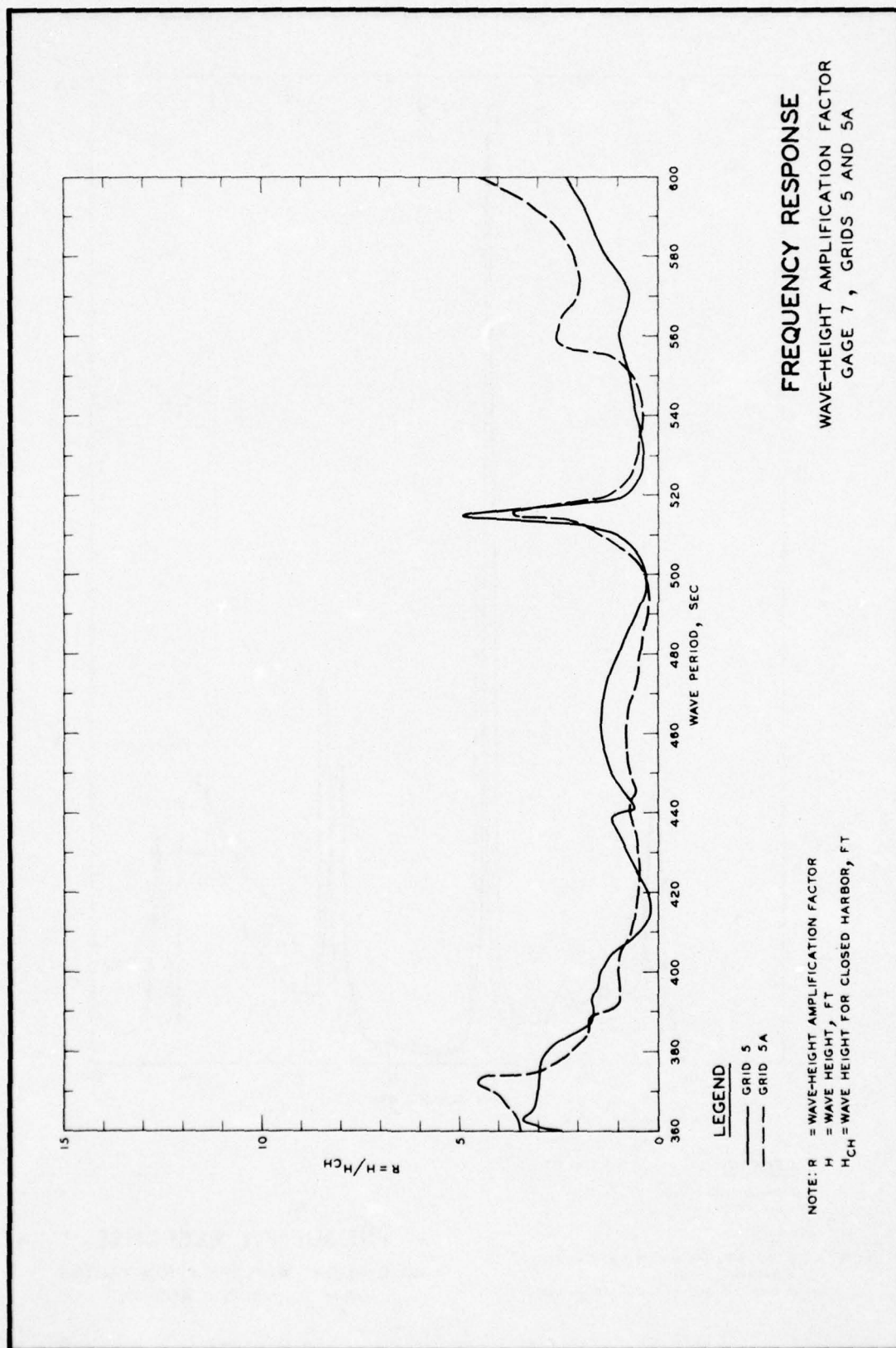


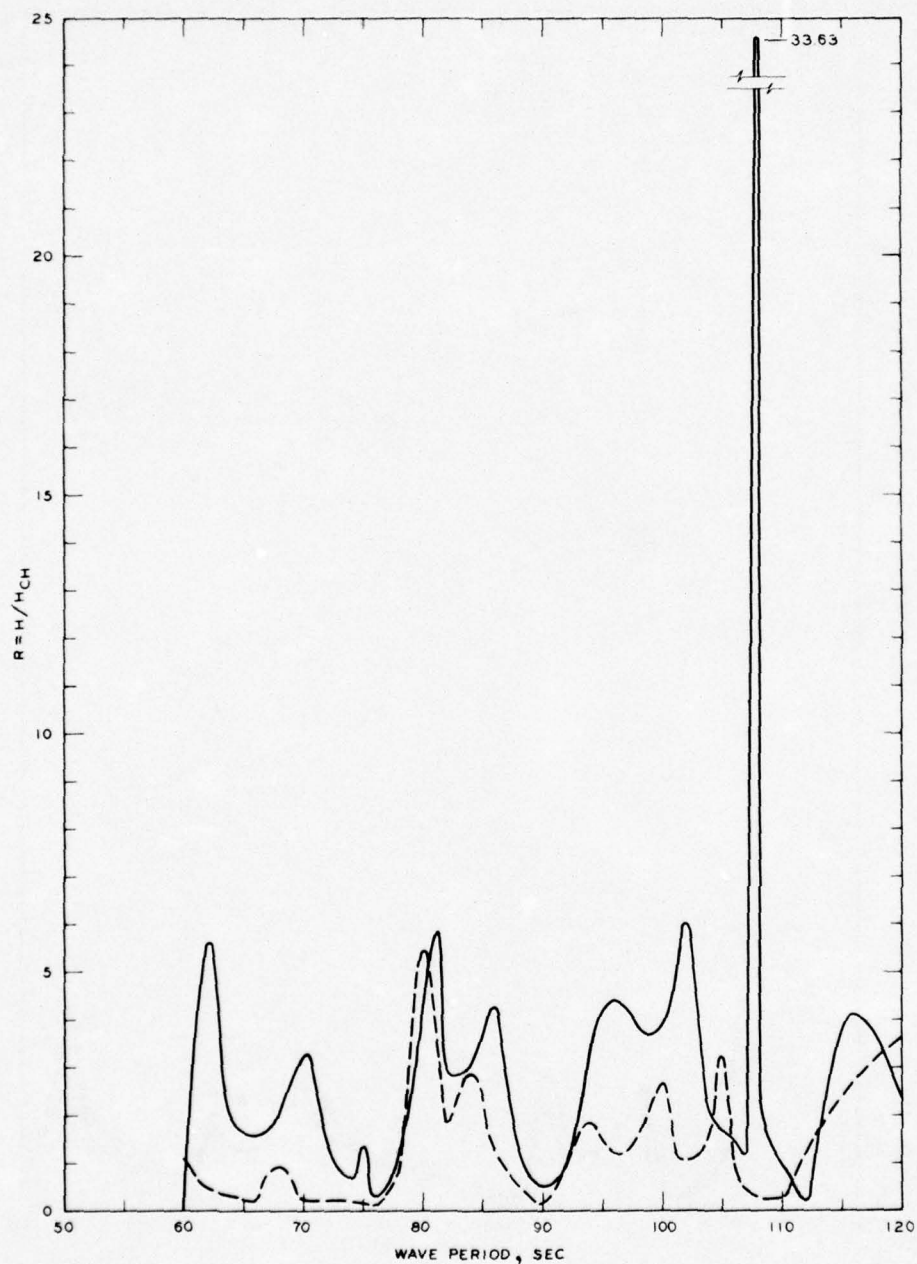
LEGEND

— GRID 4
 - - - GRID 4A

NOTE R = WAVE-HEIGHT AMPLIFICATION FACTOR
 H = WAVE HEIGHT, FT
 H_{CH} = WAVE HEIGHT FOR CLOSED HARBOR, FT

FREQUENCY RESPONSE
 WAVE-HEIGHT AMPLIFICATION FACTOR
 GAGE 7, GRIDS 4 AND 4A



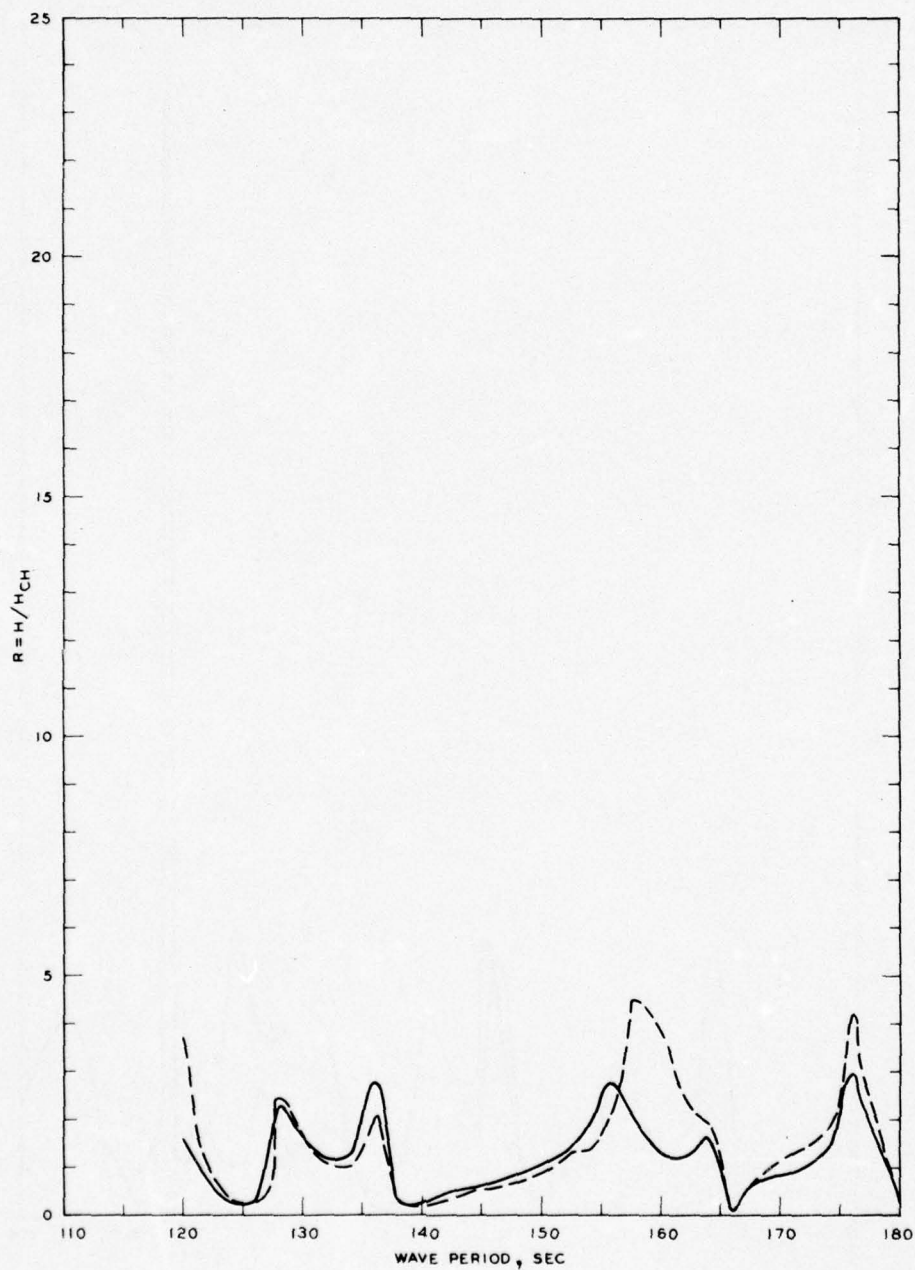


LEGEND

— GRID 1
 - - - GRID 1A

NOTE R = WAVE-HEIGHT AMPLIFICATION FACTOR
 H = WAVE HEIGHT, FT
 H_{CH} = WAVE HEIGHT FOR CLOSED HARBOR, FT

FREQUENCY RESPONSE
 WAVE-HEIGHT AMPLIFICATION FACTOR
 GAGE 8, GRIDS 1 AND 1A

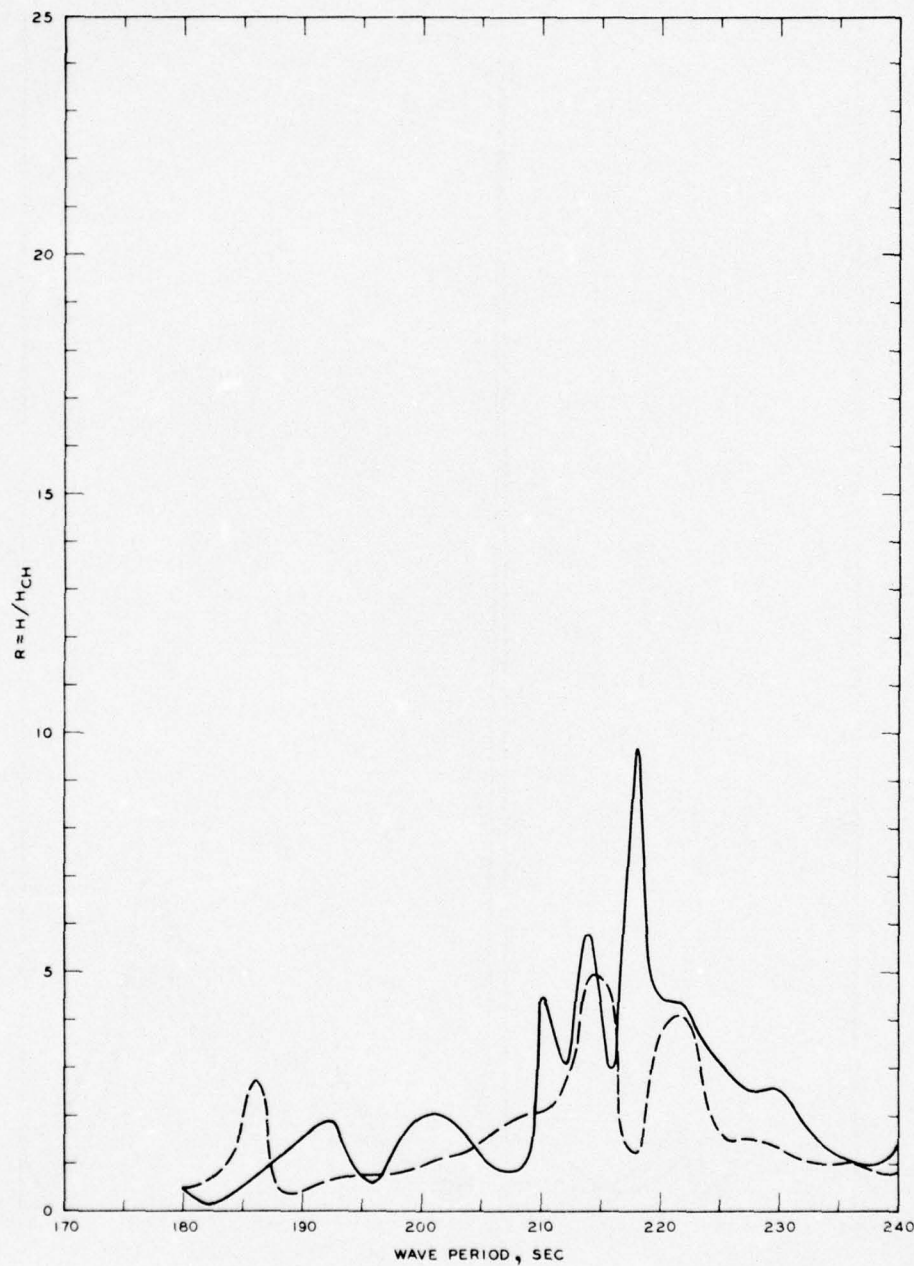


LEGEND

— GRID
 - - - GRID A

NOTE R = WAVE-HEIGHT AMPLIFICATION FACTOR
 H = WAVE HEIGHT, FT
 H_{CH} = WAVE HEIGHT FOR CLOSED HARBOR, FT

FREQUENCY RESPONSE
 WAVE-HEIGHT AMPLIFICATION FACTOR
 GAGE 8, GRIDS 2 AND 2A

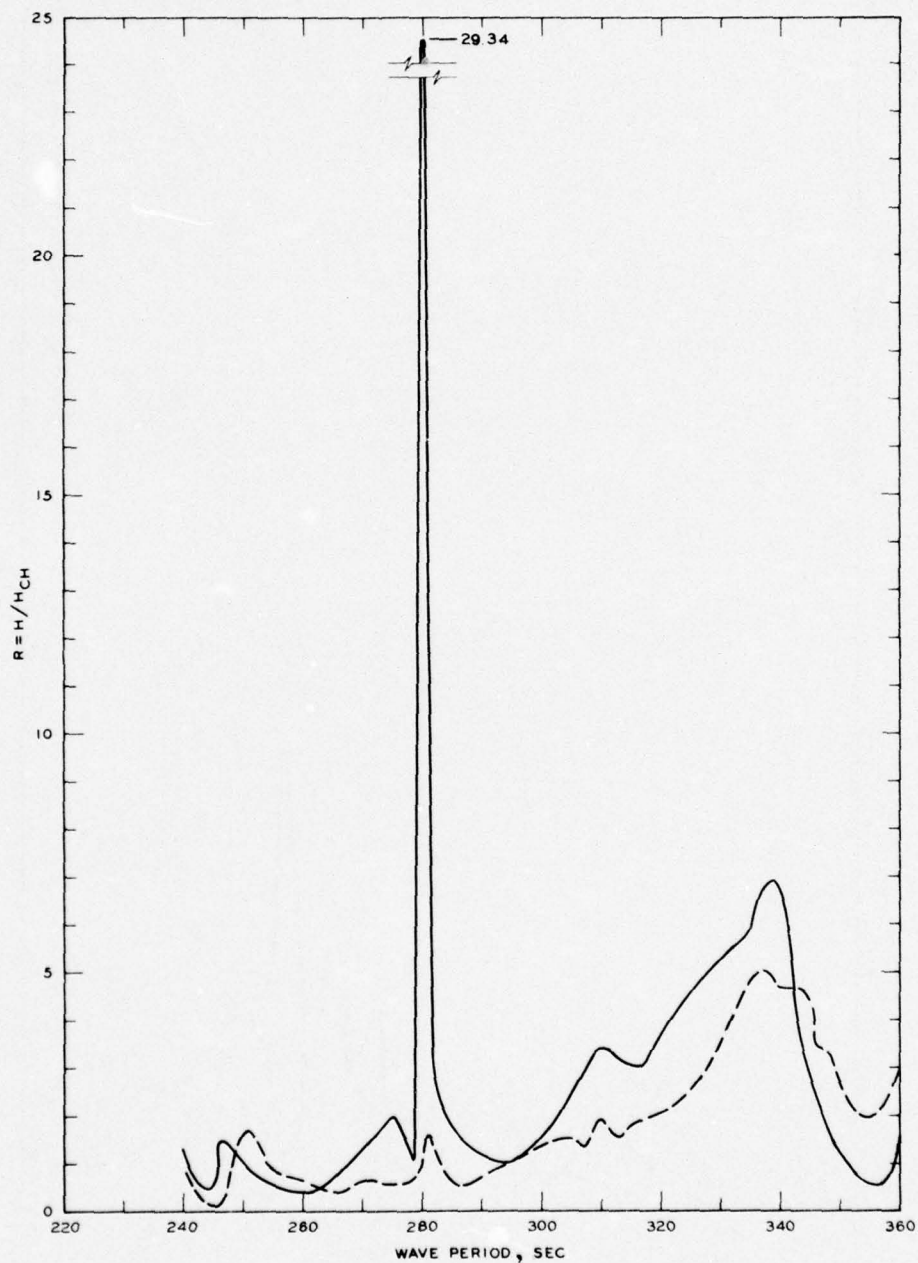


LEGEND

— GRID 3
 - - - GRID 3A

NOTE R = WAVE-HEIGHT AMPLIFICATION FACTOR
 H = WAVE HEIGHT, FT
 H_{CH} = WAVE HEIGHT FOR CLOSED HARBOR, FT

FREQUENCY RESPONSE
 WAVE-HEIGHT AMPLIFICATION FACTOR
 GAGE 8, GRIDS 3 AND 3A

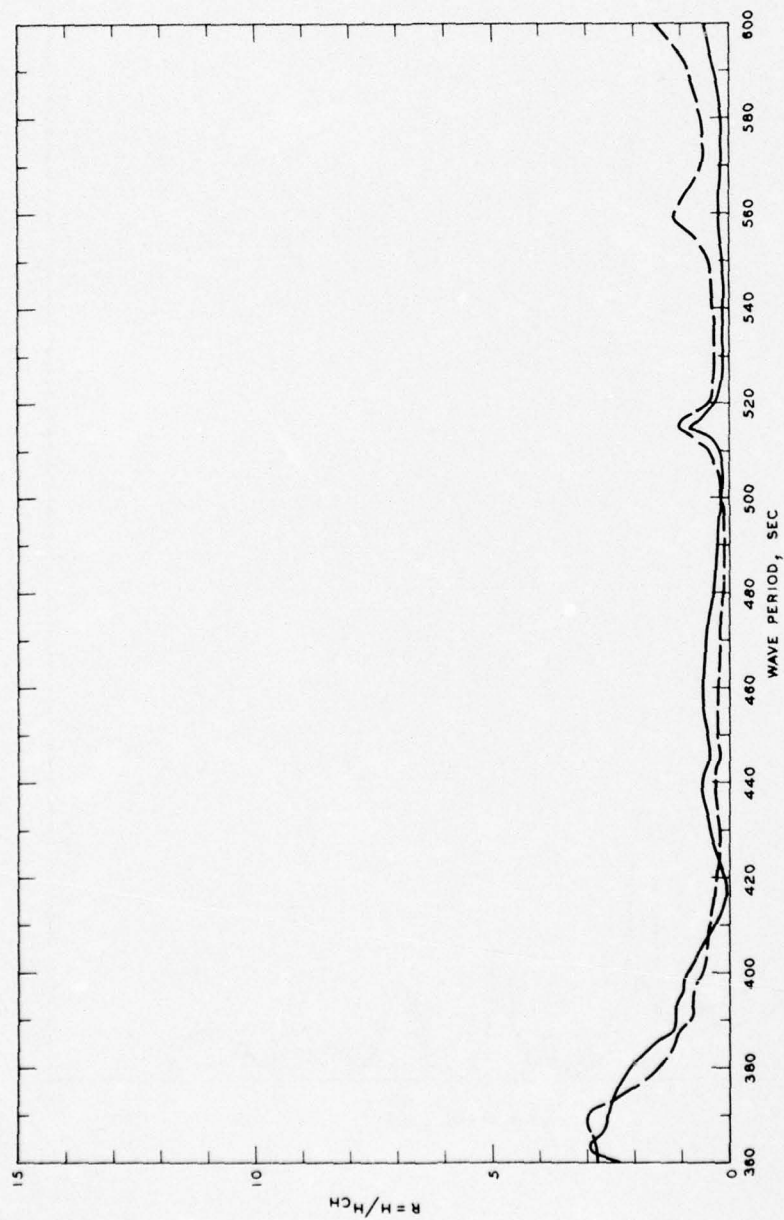


LEGEND

— GRID 4
 - - - GRID 4A

NOTE R = WAVE-HEIGHT AMPLIFICATION FACTOR
 H = WAVE HEIGHT, FT
 H_{CH} = WAVE HEIGHT FOR CLOSED HARBOR, FT

FREQUENCY RESPONSE
 WAVE-HEIGHT AMPLIFICATION FACTOR
 GAGE 8, GRIDS 4 AND 4A

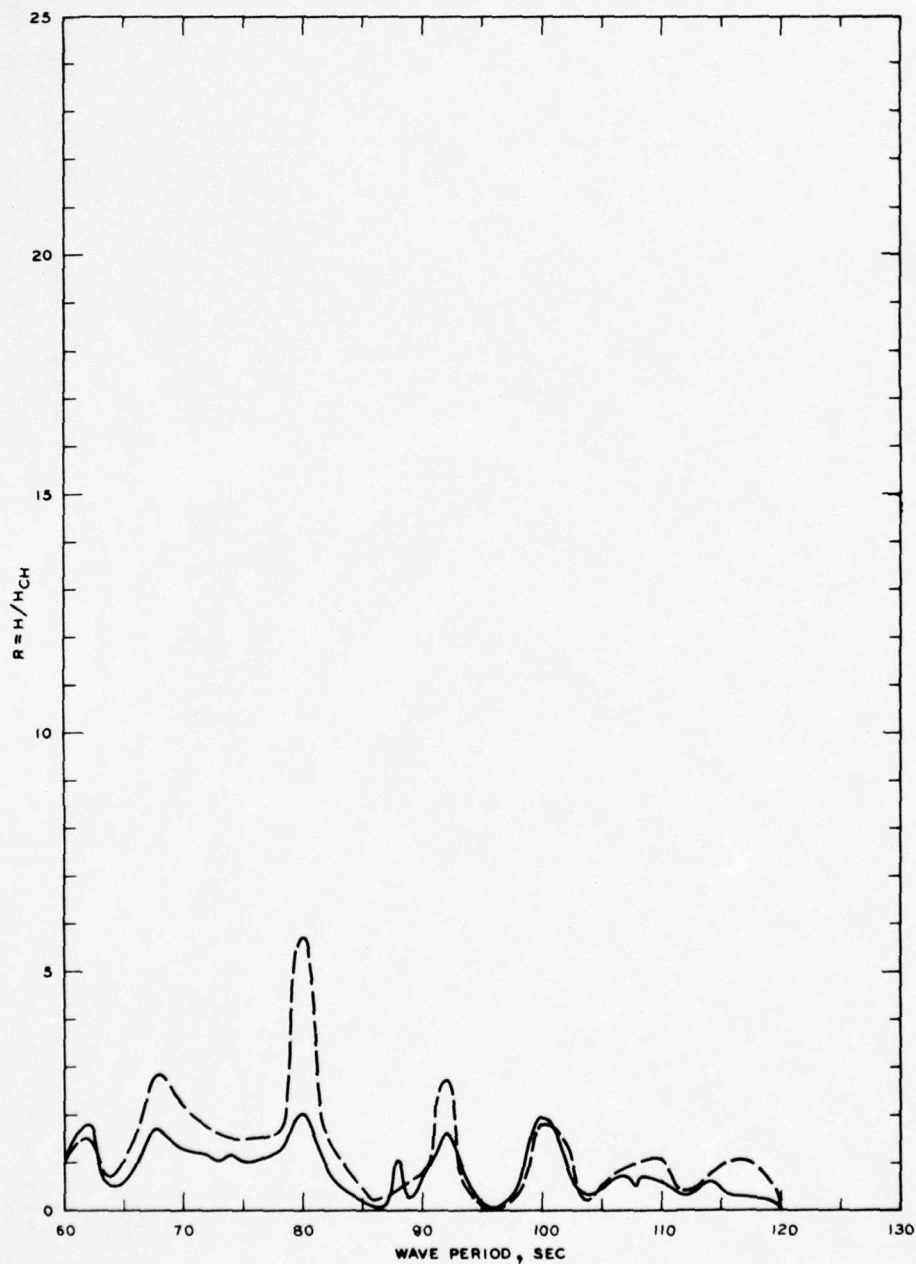


LEGEND

— GRID 5
 --- GRID 5A
 - · - GRID 8

NOTE: R = WAVE-HEIGHT AMPLIFICATION FACTOR
 H = WAVE HEIGHT, FT
 H_{CH} = WAVE HEIGHT FOR CLOSED HARBOR, FT

FREQUENCY RESPONSE
 WAVE-HEIGHT AMPLIFICATION FACTOR
 GAGE 8, GRIDS 5 AND 5A

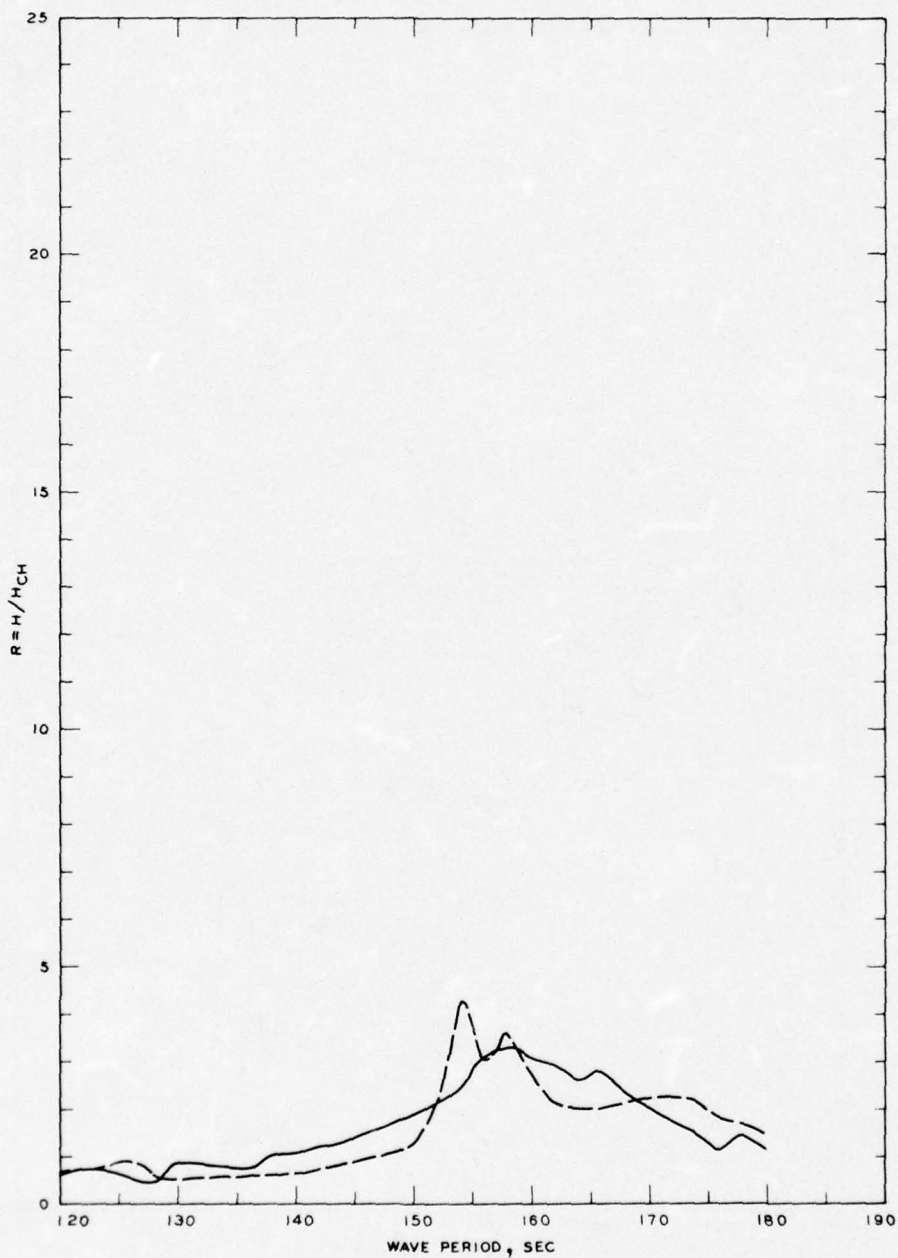


LEGEND

— GRID 1
 - - - GRID 1A

NOTE R = WAVE-HEIGHT AMPLIFICATION FACTOR
 H = WAVE HEIGHT, FT
 H_{CH} = WAVE HEIGHT FOR CLOSED HARBOR, FT

FREQUENCY RESPONSE
 WAVE-HEIGHT AMPLIFICATION FACTOR
 GAGE 14, GRIDS 1 AND 1A

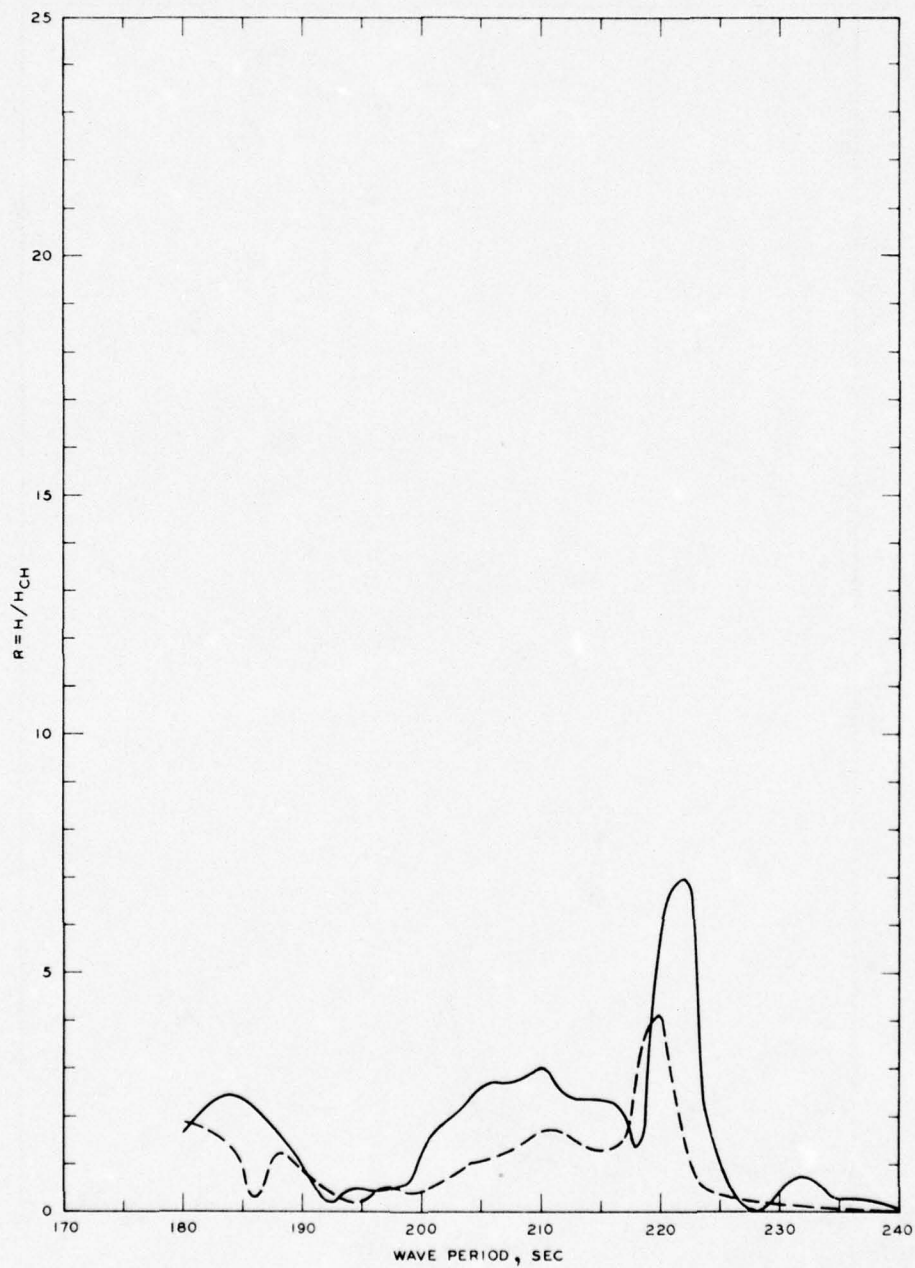


LEGEND

— GRID 2
 - - - GRID 2A

NOTE R = WAVE-HEIGHT AMPLIFICATION FACTOR
 H = WAVE HEIGHT, FT
 H_{CH} = WAVE HEIGHT FOR CLOSED HARBOR, FT

FREQUENCY RESPONSE
 WAVE-HEIGHT AMPLIFICATION FACTOR
 GAGE 14, GRIDS 2 AND 2A

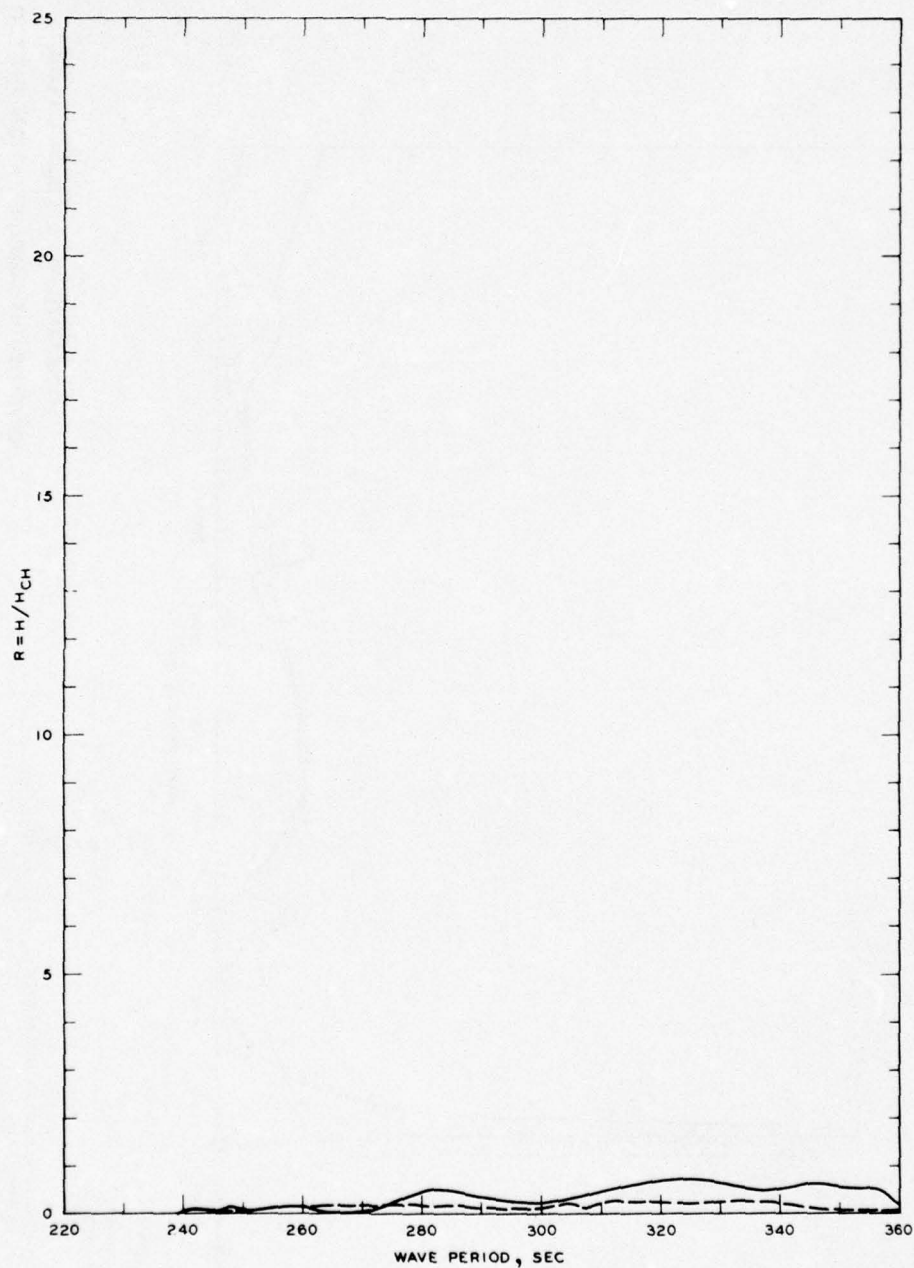


LEGEND

— GRID 3
 - - - GRID 3A

NOTE R = WAVE-HEIGHT AMPLIFICATION FACTOR
 H = WAVE HEIGHT, FT
 H_{CH} = WAVE HEIGHT FOR CLOSED HARBOR, FT

FREQUENCY RESPONSE
 WAVE-HEIGHT AMPLIFICATION FACTOR
 GAGE 14, GRIDS 3 AND 3A

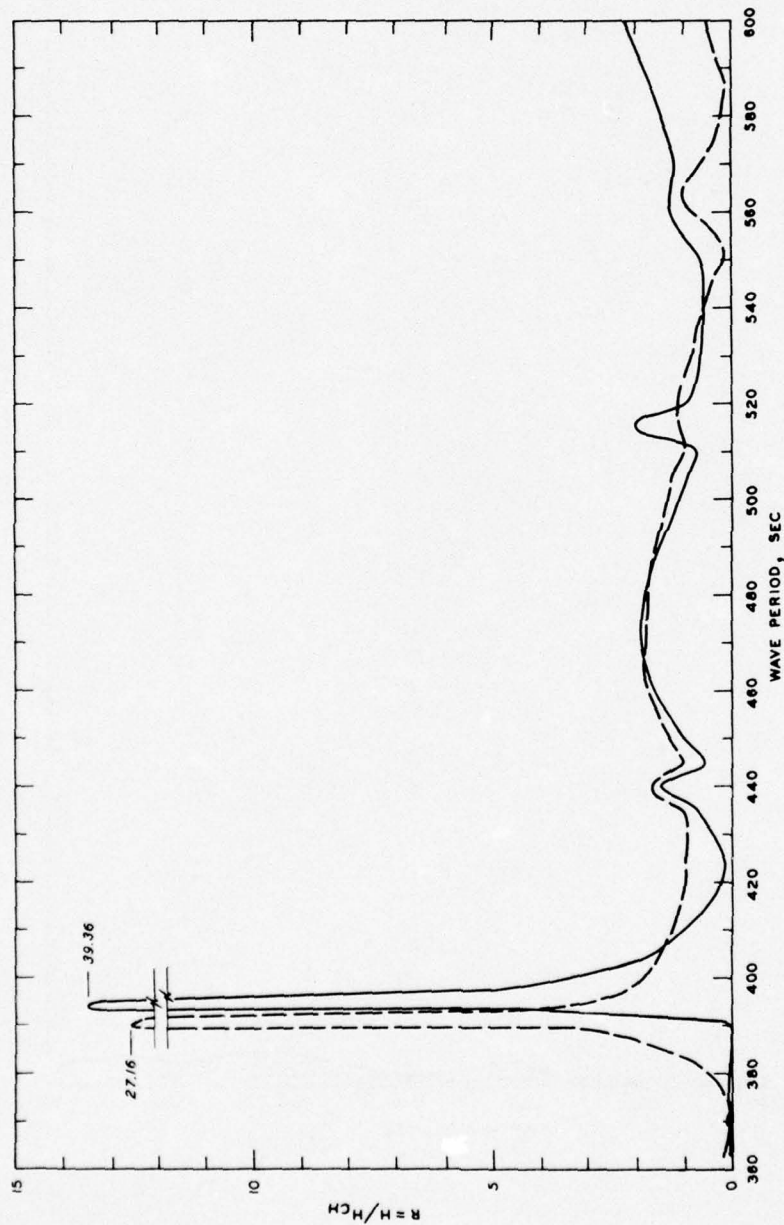


LEGEND

— GRID 4
 - - - GRID 4A

NOTE R = WAVE-HEIGHT AMPLIFICATION FACTOR
 H = WAVE HEIGHT, FT
 H_{CH} = WAVE HEIGHT FOR CLOSED HARBOR, FT

FREQUENCY RESPONSE
 WAVE-HEIGHT AMPLIFICATION FACTOR
 GAGE 14, GRIDS 4 AND 4A

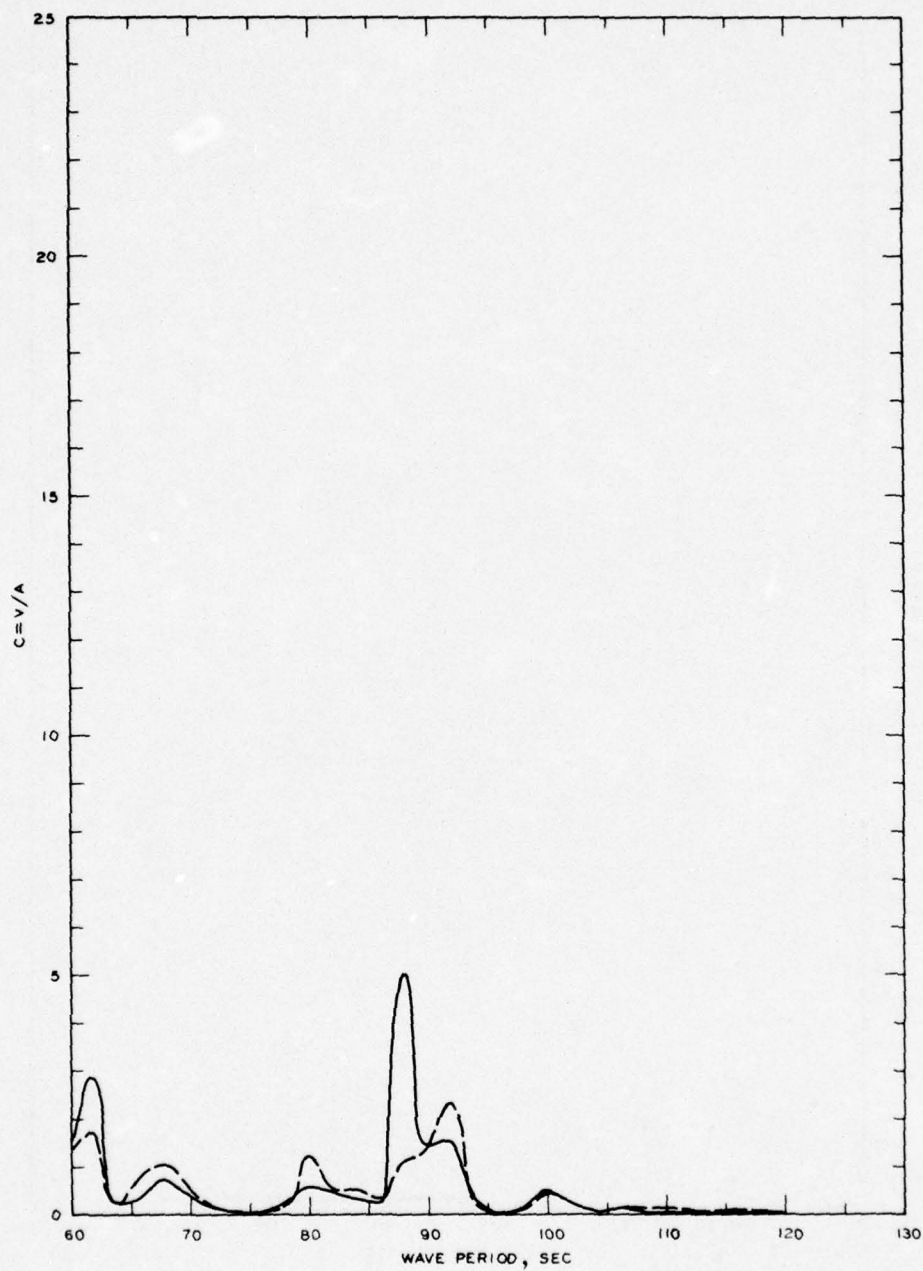


LEGEND

— GRID 5
 --- GRID 5A

NOTE: R = WAVE-HEIGHT AMPLIFICATION FACTOR
 H = WAVE HEIGHT, FT
 H_{CH} = WAVE HEIGHT FOR CLOSED HARBOR, FT

FREQUENCY RESPONSE
 WAVE-HEIGHT AMPLIFICATION FACTOR
 GAGE 14, GRIDS 5 AND 5A



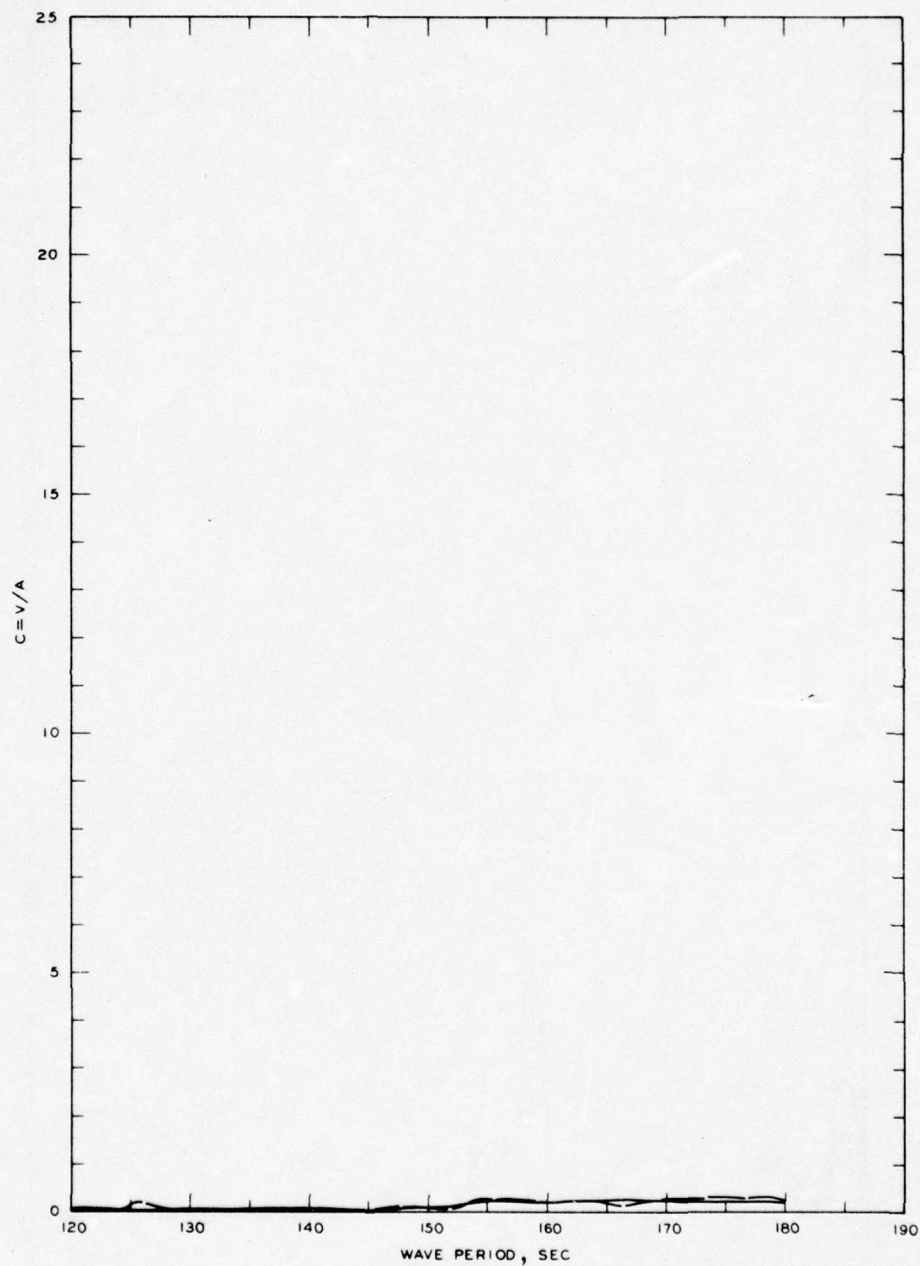
LEGEND

— GRID 1
 --- GRID 1A

NOTE: C = NORMALIZED MAXIMUM CURRENT
 VELOCITY
 V = CURRENT VELOCITY, FT/SEC
 A = INCIDENT WAVE AMPLITUDE

FREQUENCY RESPONSE

NORMALIZED MAXIMUM CURRENT VELOCITY
 GAGE 5, GRIDS 1 AND 1A

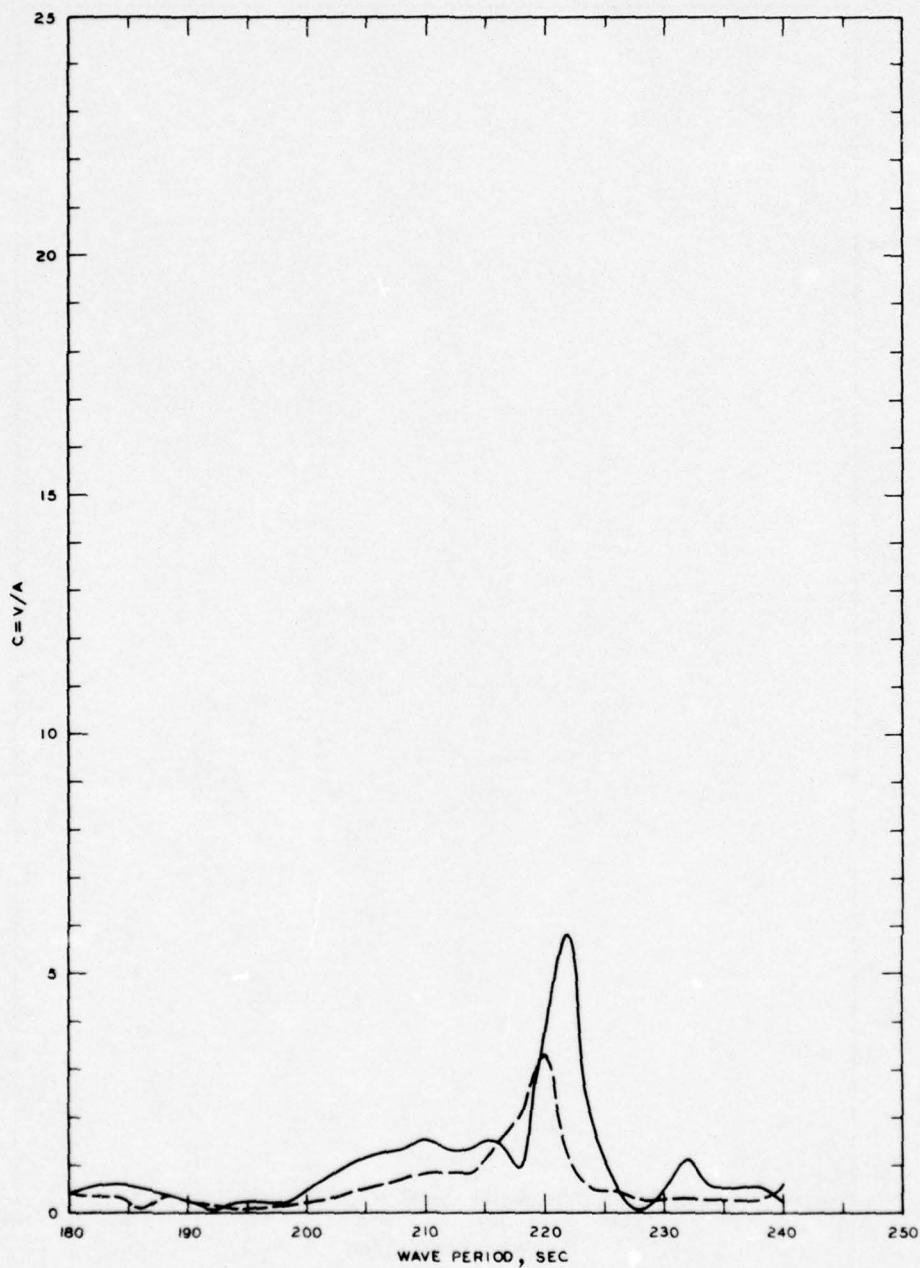


LEGEND

— GRID 2
 - - - GRID 2A

NOTE: C = NORMALIZED MAXIMUM CURRENT VELOCITY
 V = CURRENT VELOCITY, FT/SEC
 A = INCIDENT WAVE AMPLITUDE

FREQUENCY RESPONSE
 NORMALIZED MAXIMUM CURRENT VELOCITY
 GAGE 5, GRIDS 2 AND 2A

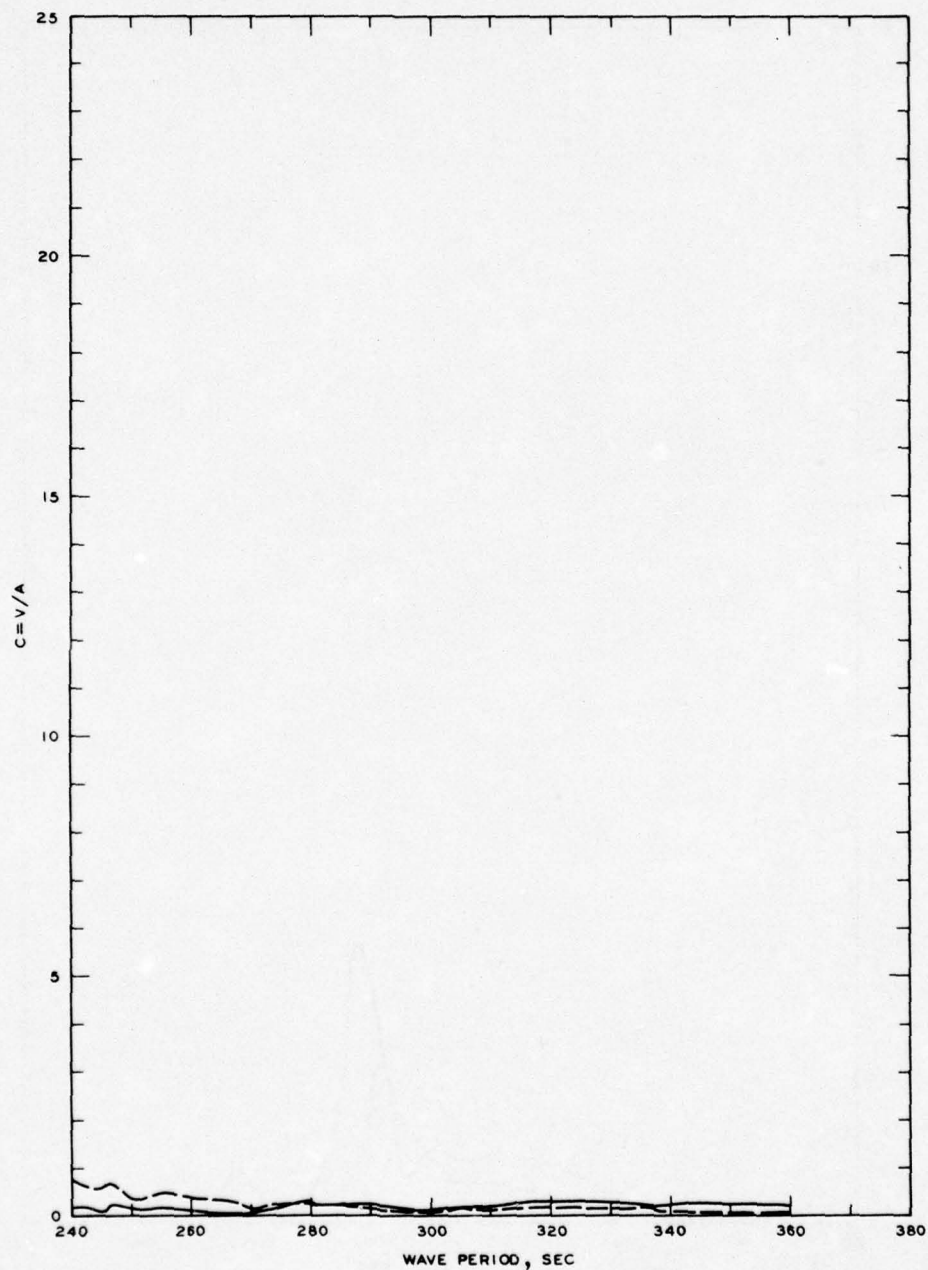


LEGEND

— GRID 3
 - - - GRID 3A

NOTE: C = NORMALIZED MAXIMUM CURRENT VELOCITY
 V = CURRENT VELOCITY, FT/SEC
 A = INCIDENT WAVE AMPLITUDE

FREQUENCY RESPONSE
 NORMALIZED MAXIMUM CURRENT VELOCITY
 GAGE 5, GRIDS 3 AND 3A

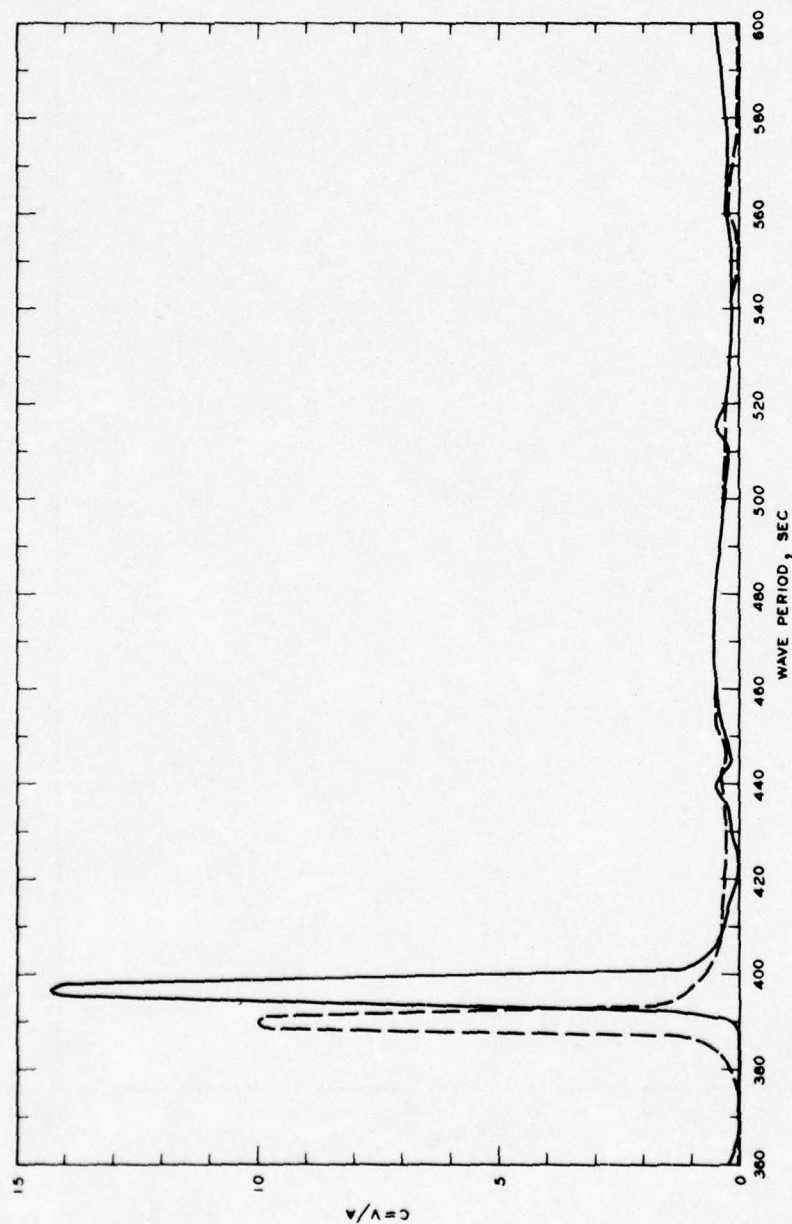


LEGEND

— GRID 4
 - - - GRID 4A

NOTE: C = NORMALIZED MAXIMUM CURRENT
 VELOCITY
 V = CURRENT VELOCITY, FT/SEC
 A = INCIDENT WAVE AMPLITUDE

FREQUENCY RESPONSE
 NORMALIZED MAXIMUM CURRENT VELOCITY
 GAGE 5, GRIDS 4 AND 4A

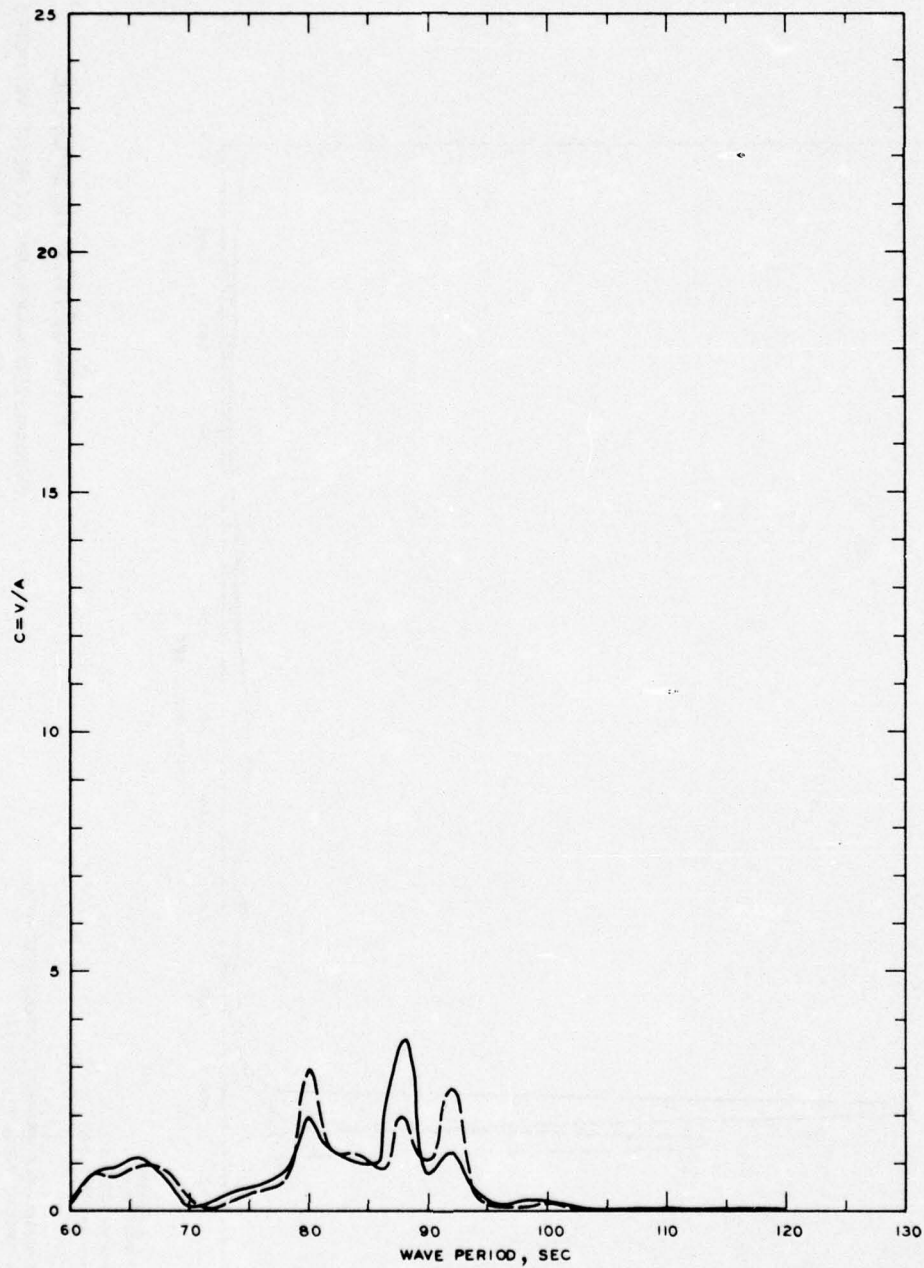


LEGEND

- GRID 5
- - - GRID 5A

NOTE: C = NORMALIZED MAXIMUM CURRENT VELOCITY
 V = CURRENT VELOCITY, FT/SEC
 A = INCIDENT WAVE AMPLITUDE

FREQUENCY RESPONSE
 NORMALIZED MAXIMUM CURRENT VELOCITY
 GAGE 5, GRIDS 5 AND 5A



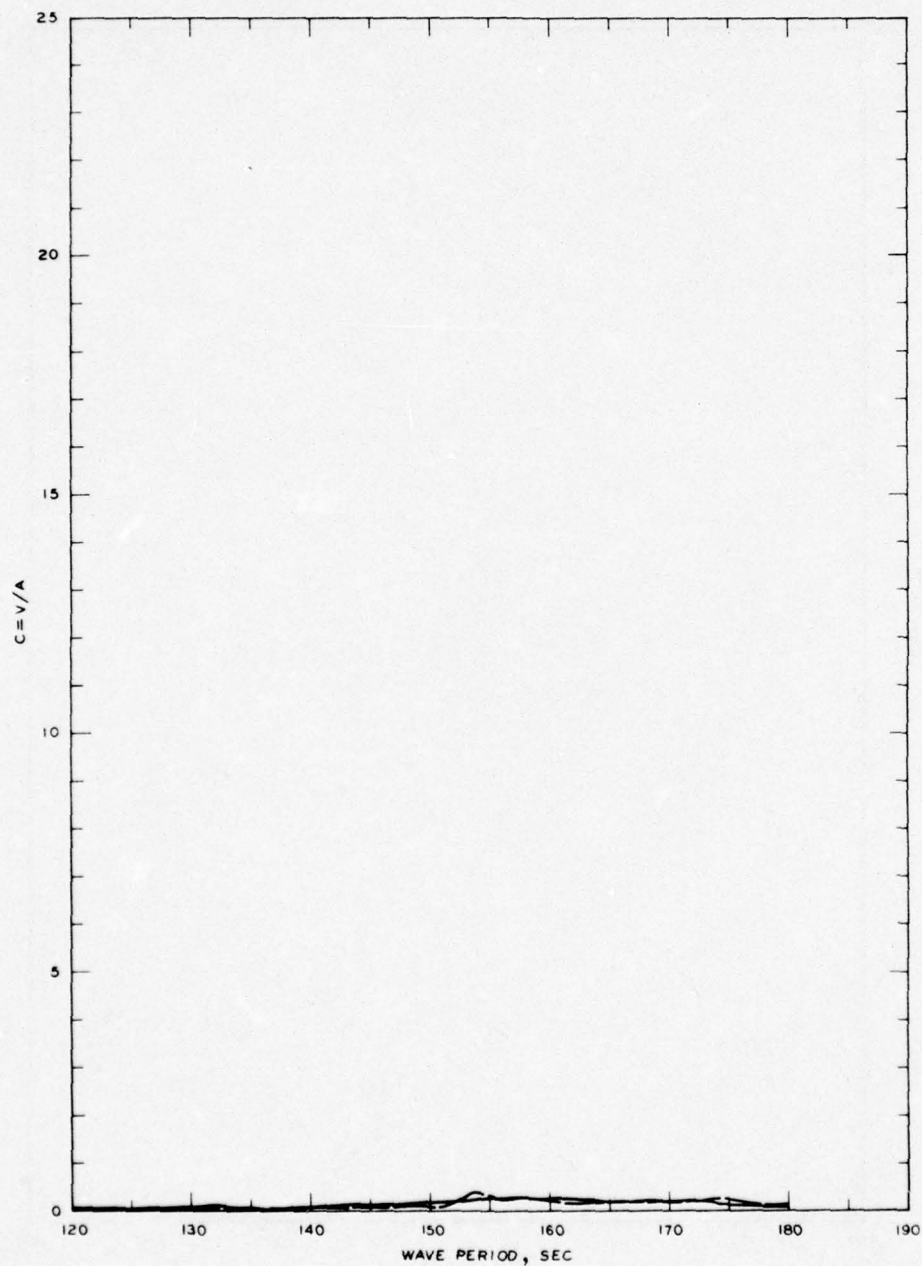
LEGEND

— GRID 1
 - - - GRID 1A

NOTE: C = NORMALIZED MAXIMUM CURRENT VELOCITY
 V = CURRENT VELOCITY, FT/SEC
 A = INCIDENT WAVE AMPLITUDE

FREQUENCY RESPONSE

NORMALIZED MAXIMUM CURRENT VELOCITY
 GAGE 6 , GRIDS 1 AND 1A



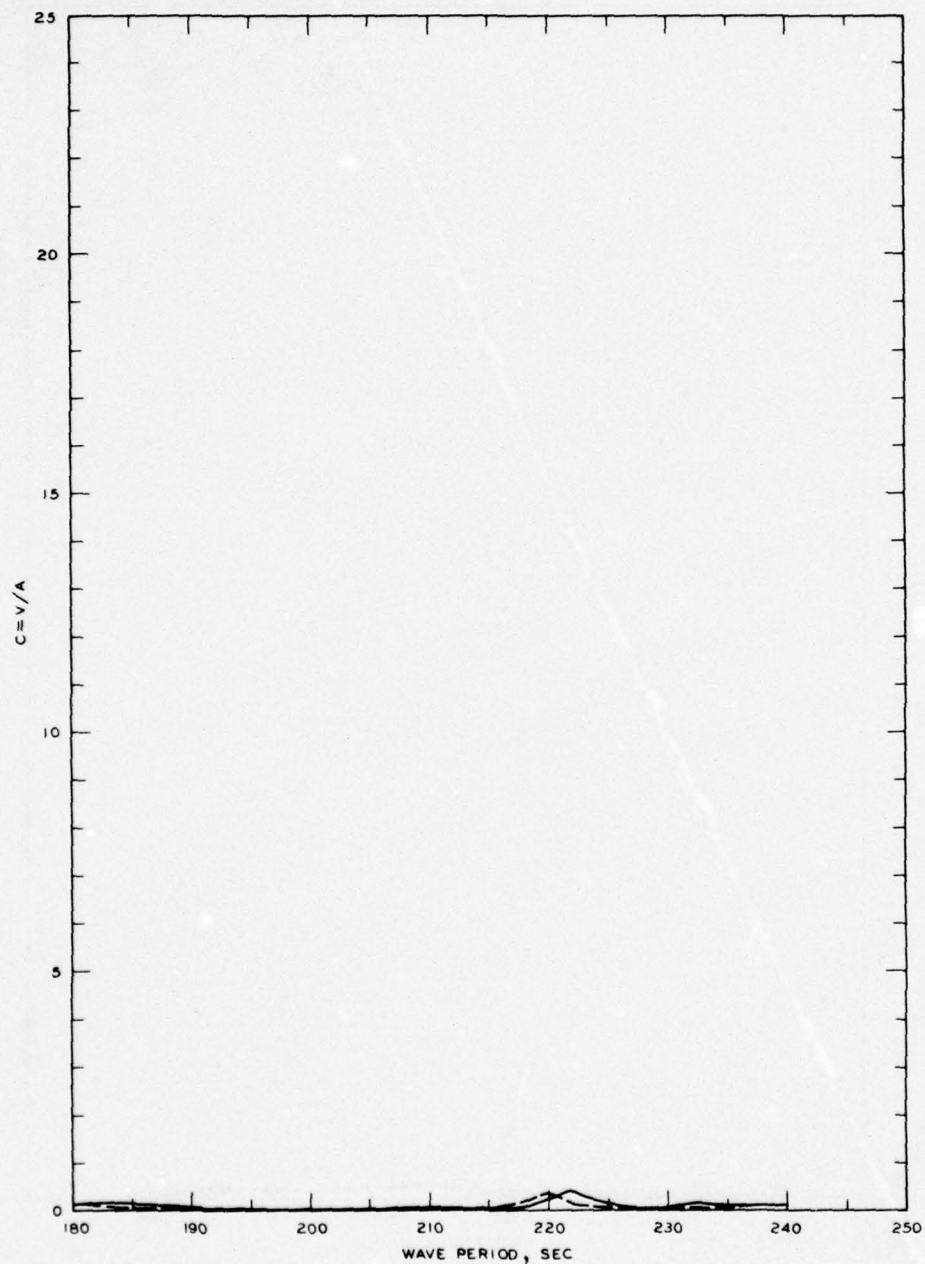
LEGEND

— GRID 2
 - - - GRID 2A

NOTE: C = NORMALIZED MAXIMUM CURRENT VELOCITY
 V = CURRENT VELOCITY, FT/SEC
 A = INCIDENT WAVE AMPLITUDE

FREQUENCY RESPONSE

NORMALIZED MAXIMUM CURRENT VELOCITY
 GAGE 6, GRIDS 2 AND 2A



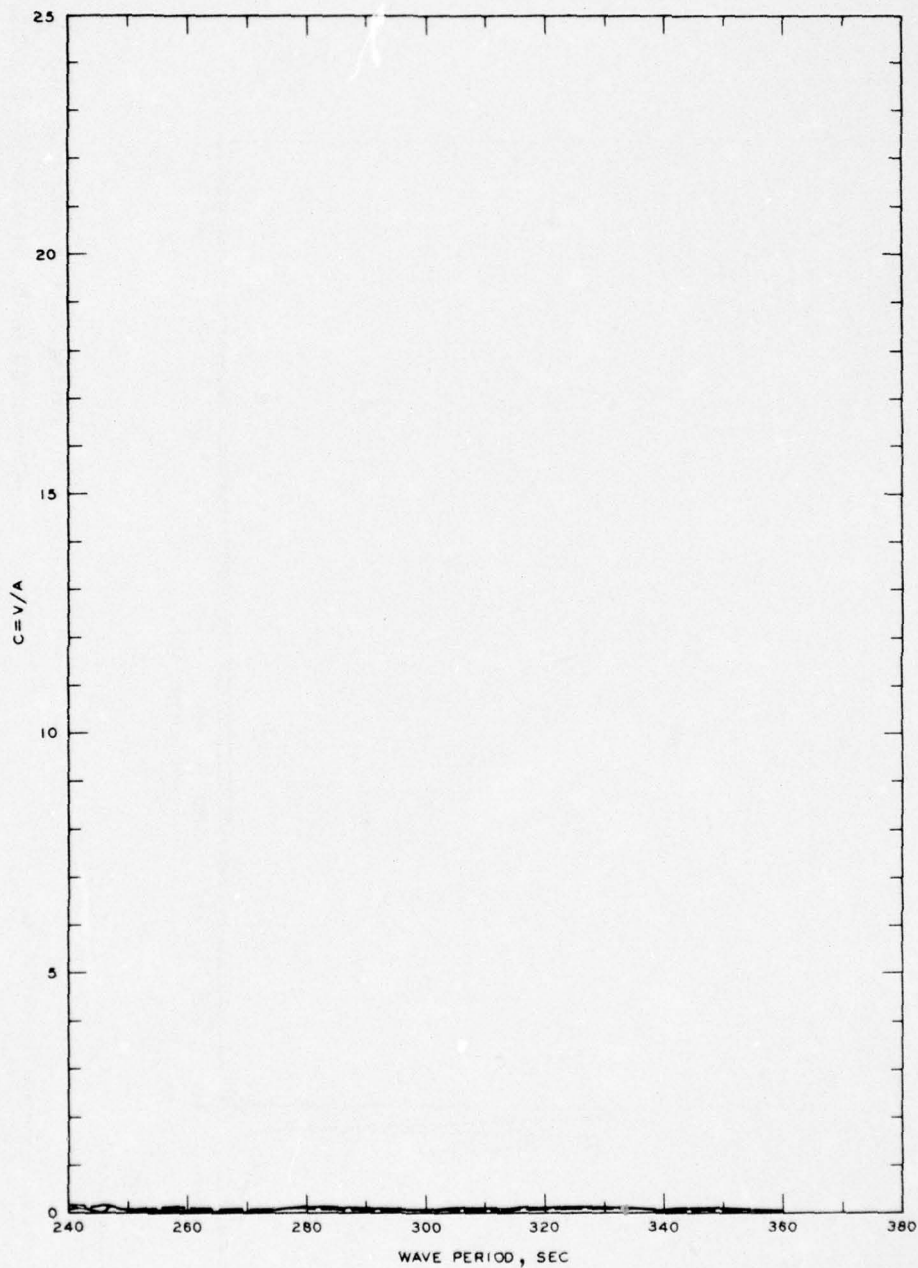
LEGEND

— GRID 3
 --- GRID 3 A

NOTE: C = NORMALIZED MAXIMUM CURRENT
 VELOCITY
 V = CURRENT VELOCITY, FT/SEC
 A = INCIDENT WAVE AMPLITUDE

FREQUENCY RESPONSE

NORMALIZED MAXIMUM CURRENT VELOCITY
 GAGE 6, GRIDS 3 AND 3A

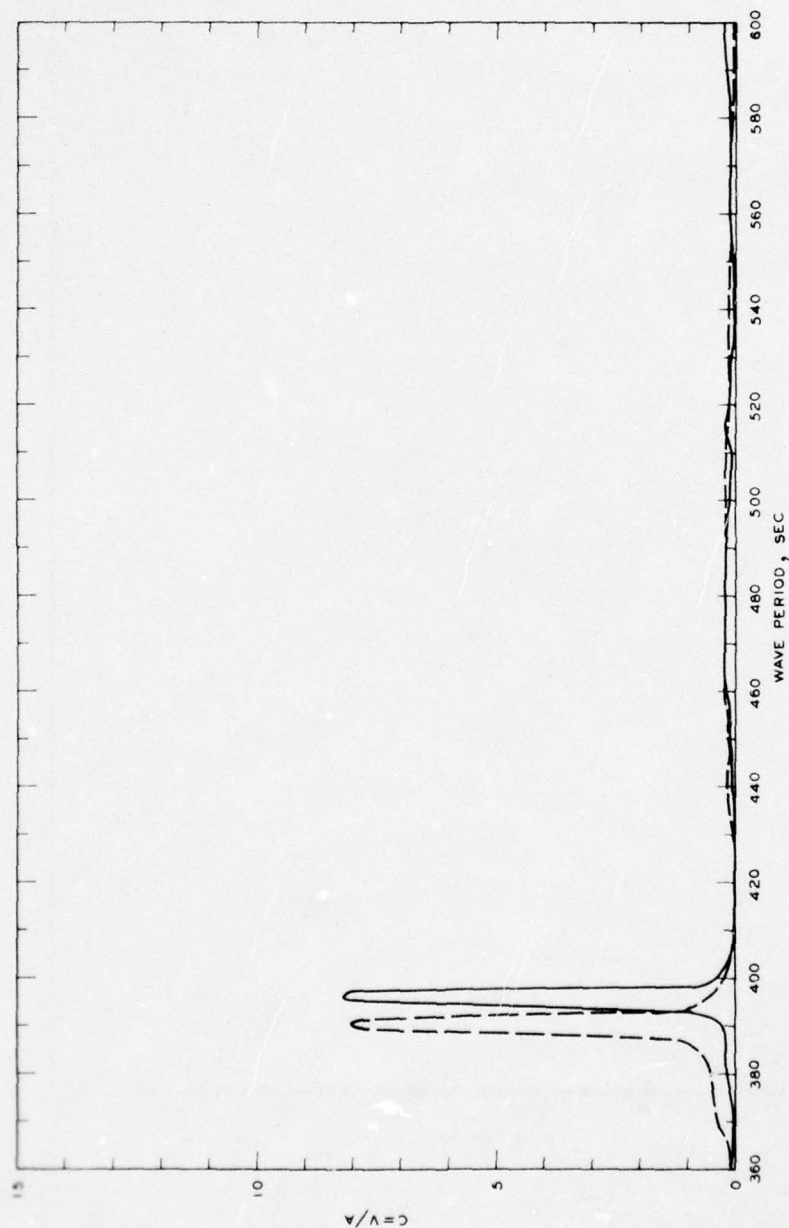


LEGEND

— GRID 4
 - - - GRID 4A

NOTE: C = NORMALIZED MAXIMUM CURRENT
 VELOCITY
 V = CURRENT VELOCITY, FT/SEC
 A = INCIDENT WAVE AMPLITUDE

FREQUENCY RESPONSE
 NORMALIZED MAXIMUM CURRENT VELOCITY
 GAGE 6, GRIDS 4 AND 4A

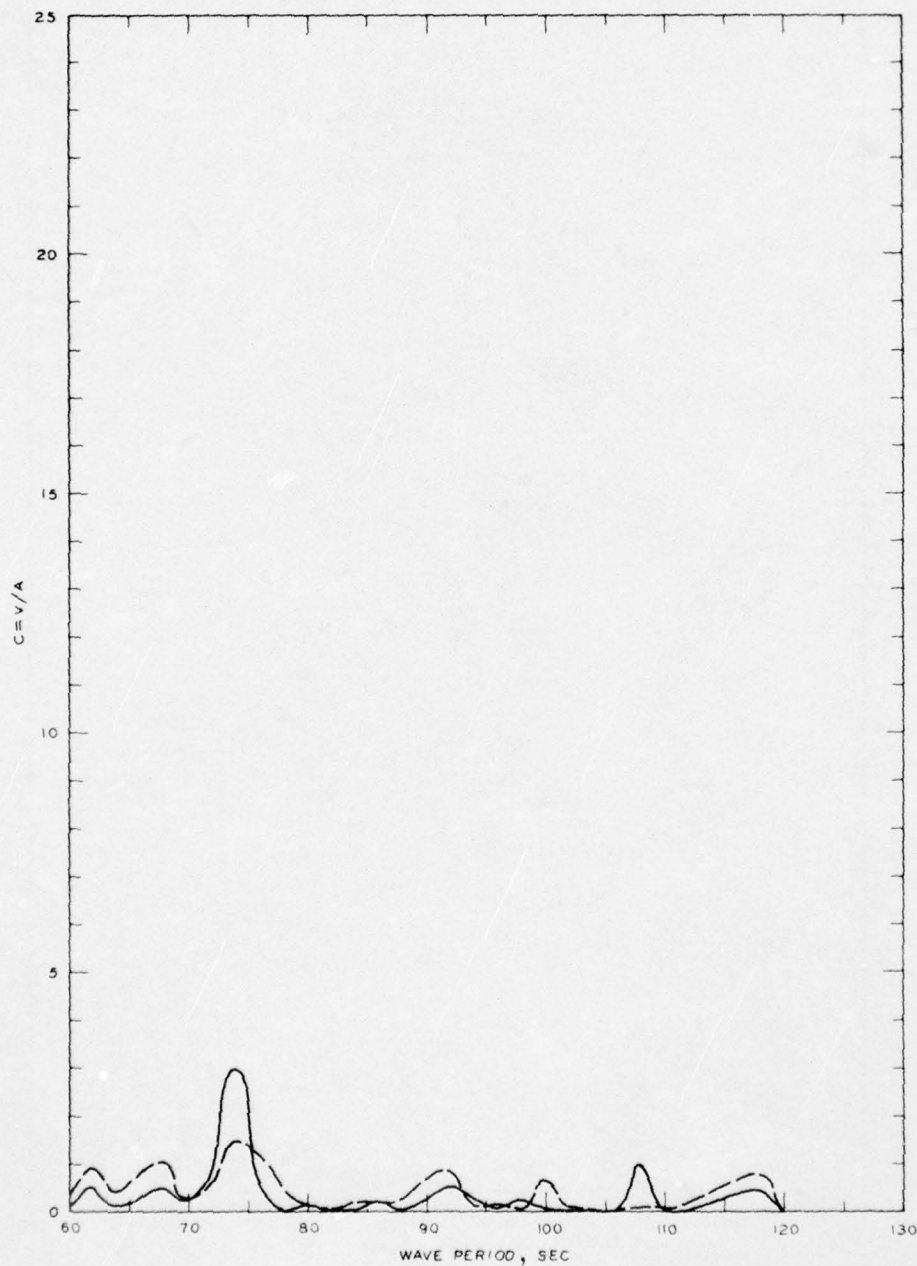


LEGEND

— GRID 5
- - - GRID 5A

NOTE: C = NORMALIZED MAXIMUM CURRENT VELOCITY
V = CURRENT VELOCITY, FT/SEC
A = INCIDENT WAVE AMPLITUDE

FREQUENCY RESPONSE
NORMALIZED MAXIMUM CURRENT VELOCITY
GAGE 6, GRIDS 5 AND 5A



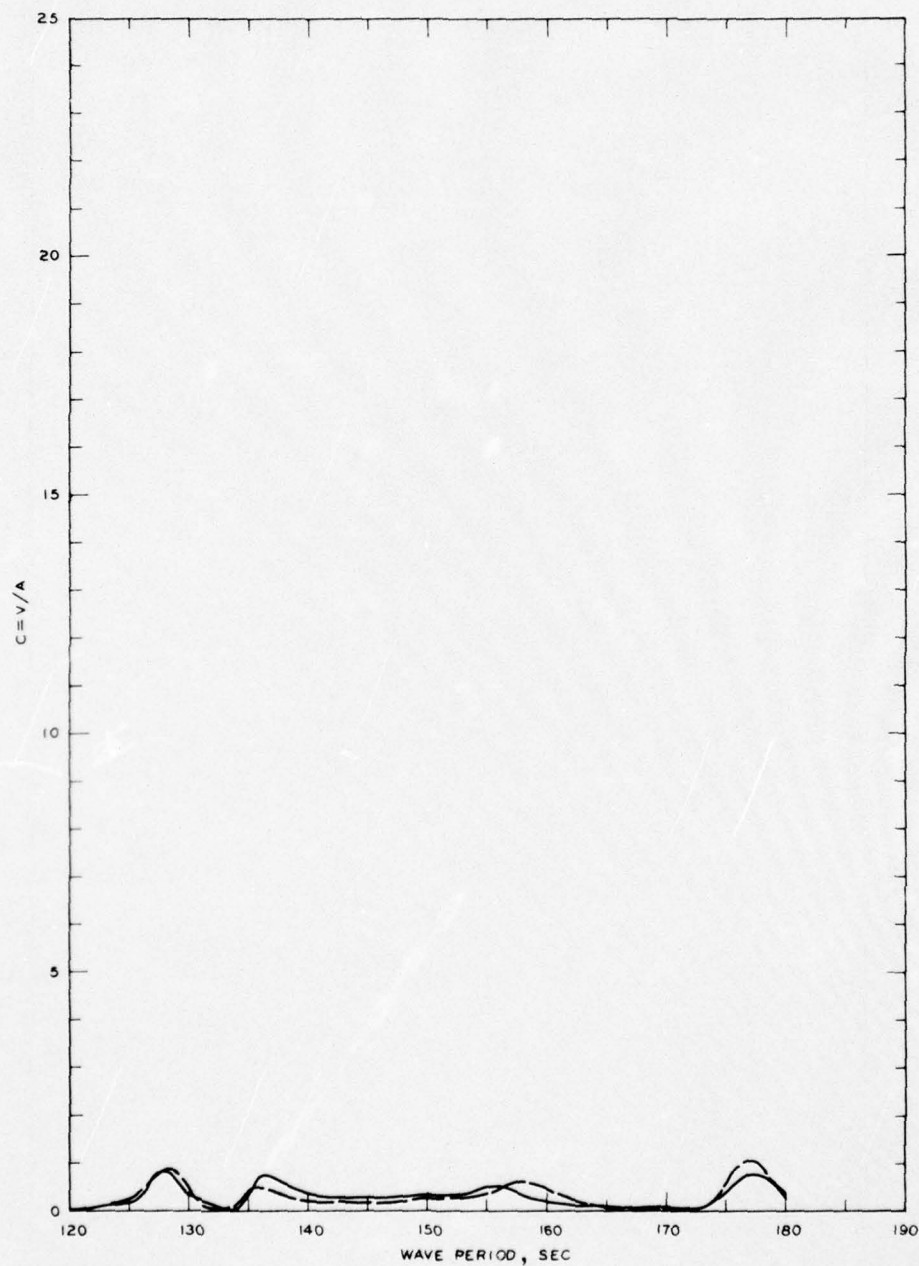
LEGEND

— GRID 1
 - - - GRID 1A

NOTE: C = NORMALIZED MAXIMUM CURRENT VELOCITY
 V = CURRENT VELOCITY, FT/SEC
 A = INCIDENT WAVE AMPLITUDE

FREQUENCY RESPONSE

NORMALIZED MAXIMUM CURRENT VELOCITY
 GAGE 7, GRIDS 1 AND 1A

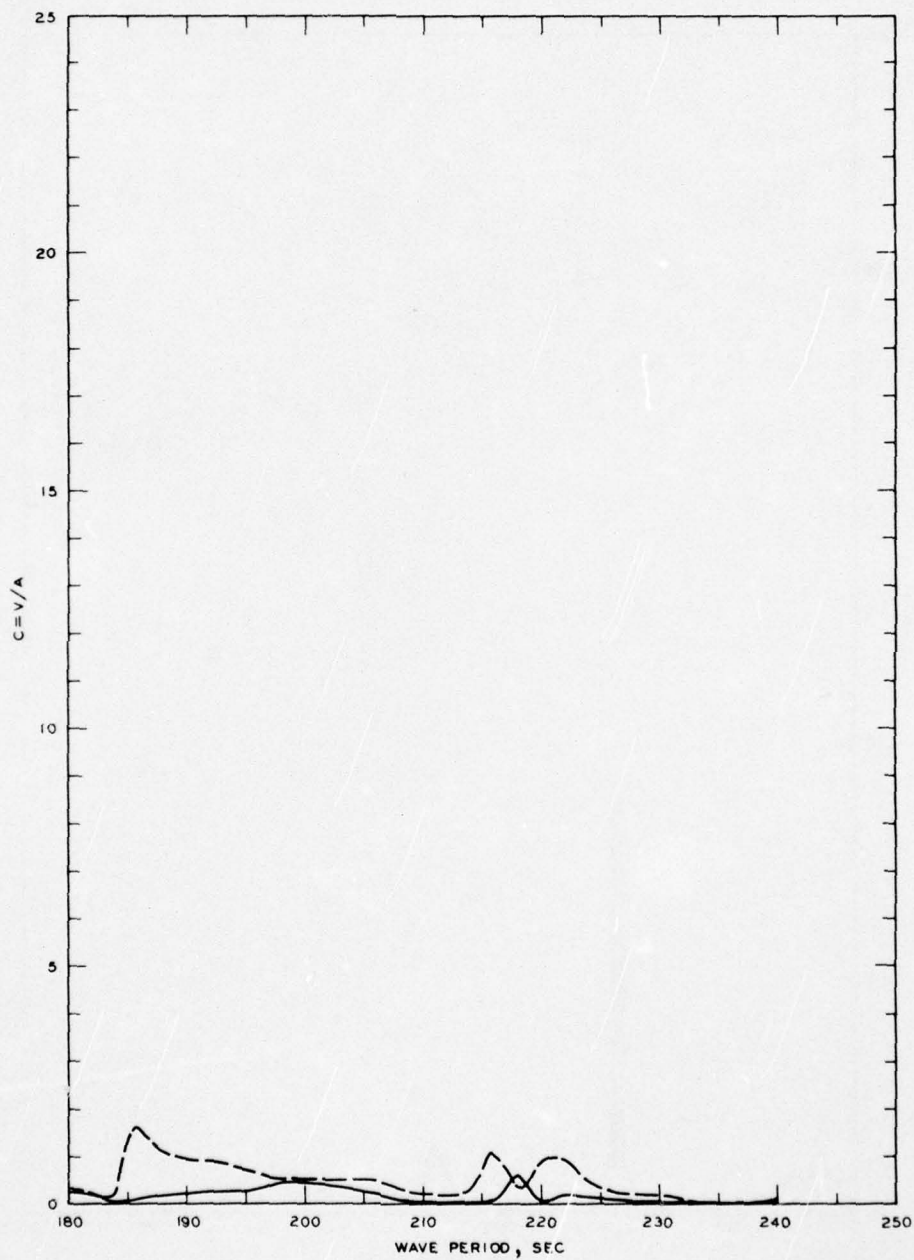


LEGEND

— GRID 2
 - - - GRID 2A

NOTE: C = NORMALIZED MAXIMUM CURRENT
 VELOCITY
 V = CURRENT VELOCITY, FT/SEC
 A = INCIDENT WAVE AMPLITUDE

FREQUENCY RESPONSE
 NORMALIZED MAXIMUM CURRENT VELOCITY
 GAGE 7, GRIDS 2 AND 2A



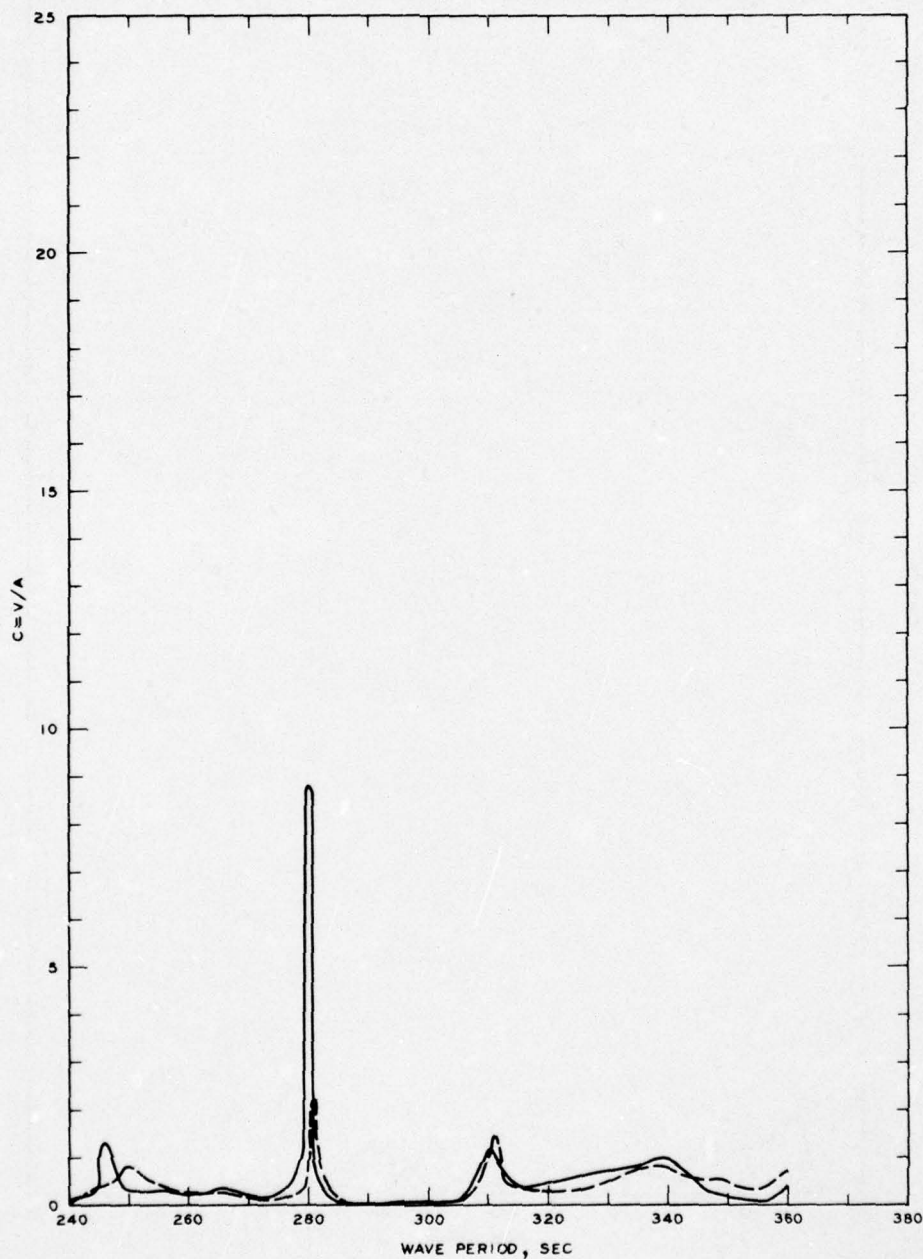
LEGEND

— GRID 3
 --- GRID 3A

NOTE: C = NORMALIZED MAXIMUM CURRENT VELOCITY
 V = CURRENT VELOCITY, FT/SEC
 A = INCIDENT WAVE AMPLITUDE

FREQUENCY RESPONSE

NORMALIZED MAXIMUM CURRENT VELOCITY
 GAGE 7, GRIDS 3 AND 3A



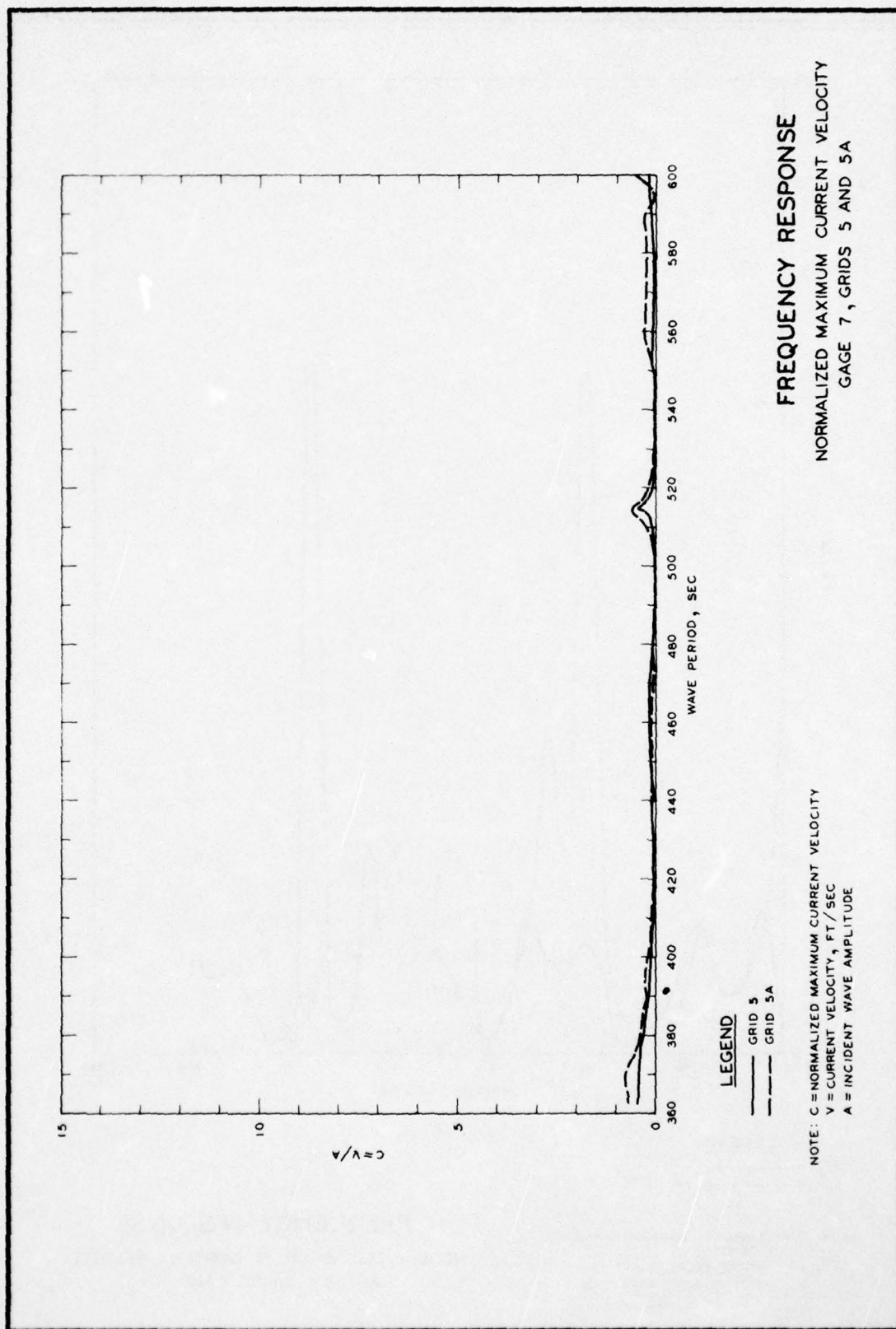
LEGEND

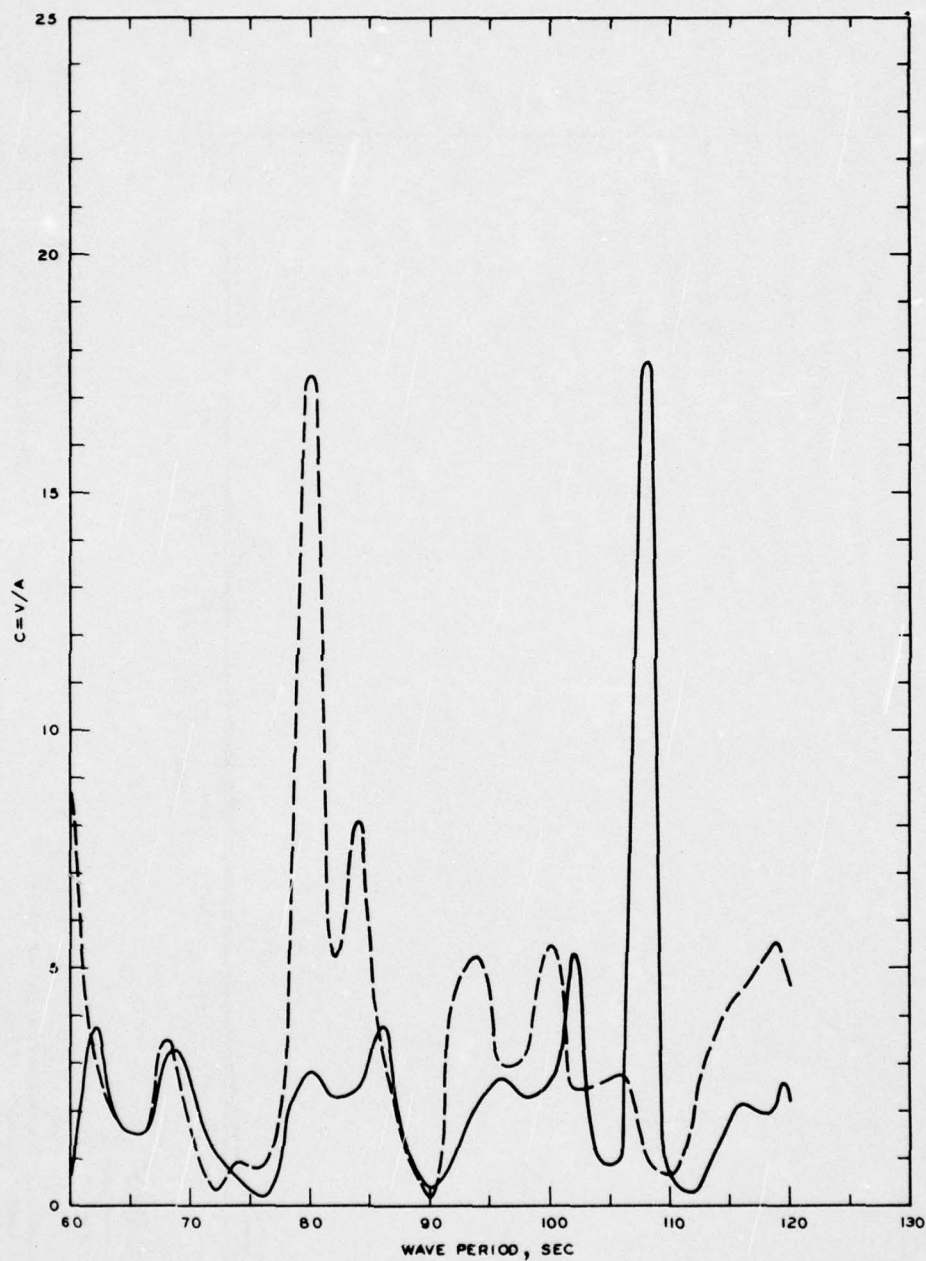
— GRID 4
 --- GRID 4A

NOTE: C = NORMALIZED MAXIMUM CURRENT
 VELOCITY
 V = CURRENT VELOCITY, FT/SEC
 A = INCIDENT WAVE AMPLITUDE

FREQUENCY RESPONSE

NORMALIZED MAXIMUM CURRENT VELOCITY
 GAGE 7, GRIDS 4 AND 4A



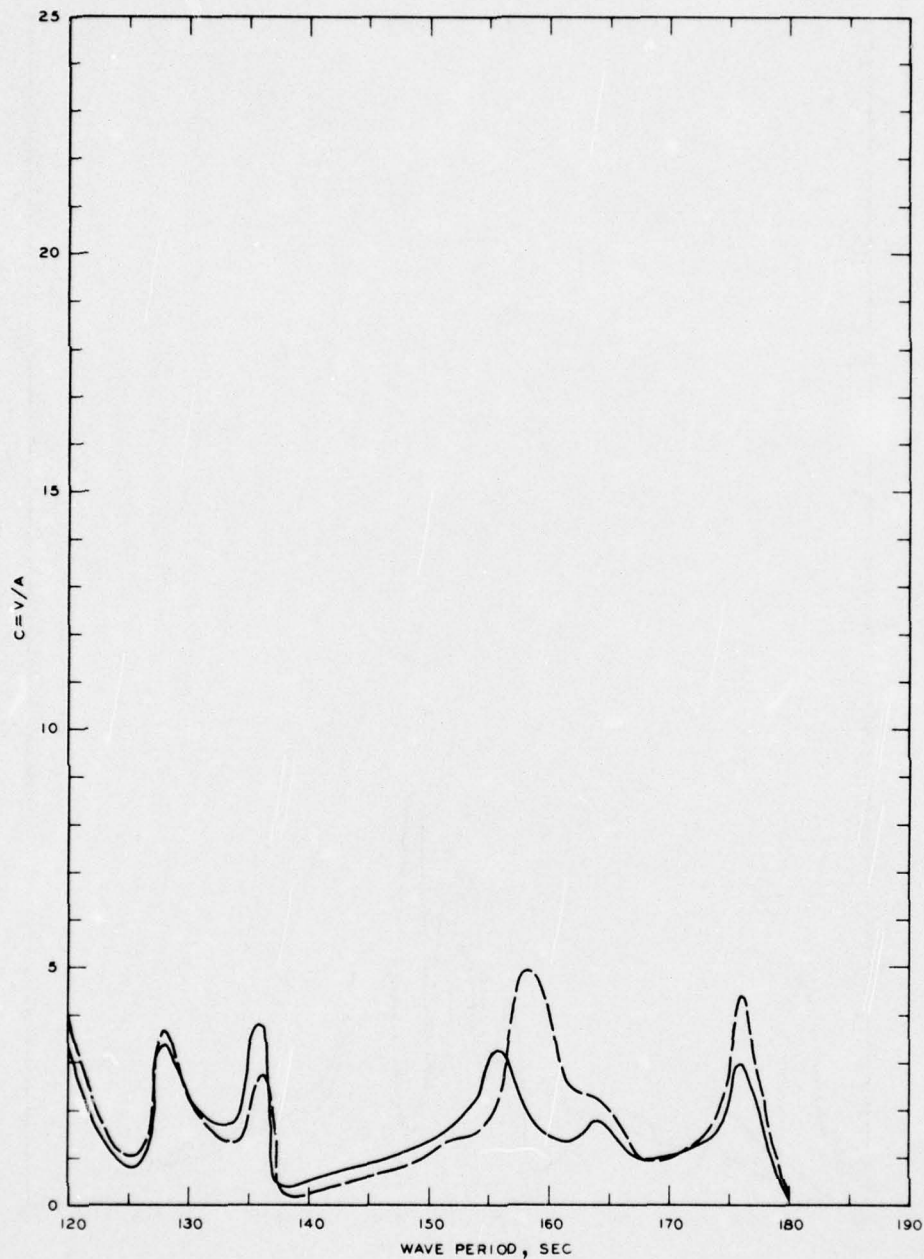


LEGEND

— GRID 1
 - - - GRID 1A

NOTE: C = NORMALIZED MAXIMUM CURRENT VELOCITY
 V = CURRENT VELOCITY, FT/SEC
 A = INCIDENT WAVE AMPLITUDE

FREQUENCY RESPONSE
 NORMALIZED MAXIMUM CURRENT VELOCITY
 GAGE 8, GRIDS 1 AND 1A



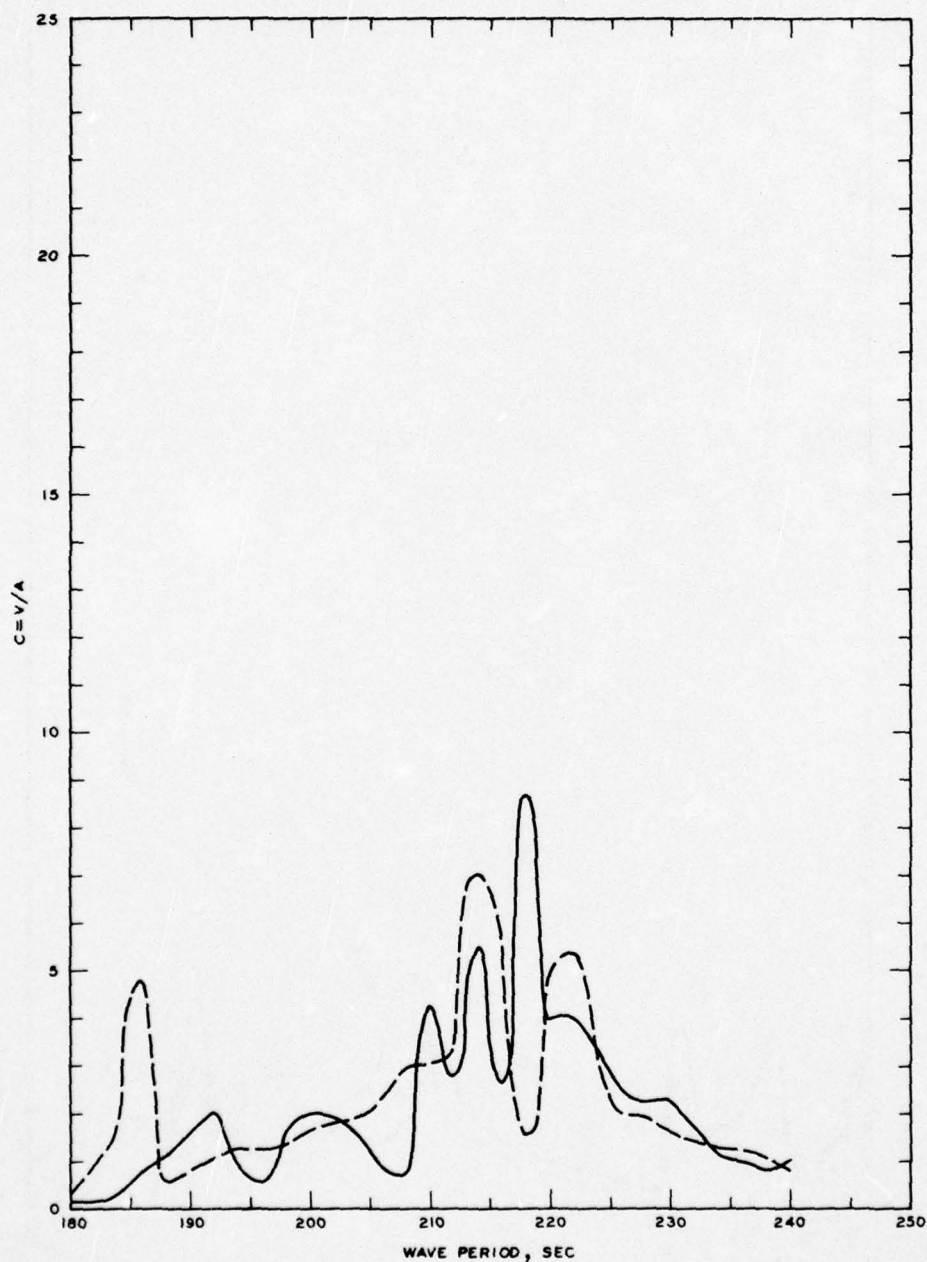
LEGEND

— GRID 2
 - - - GRID 2A

NOTE: C = NORMALIZED MAXIMUM CURRENT VELOCITY
 V = CURRENT VELOCITY, FT/SEC
 A = INCIDENT WAVE AMPLITUDE

FREQUENCY RESPONSE

NORMALIZED MAXIMUM CURRENT VELOCITY
 GAGE 8 , GRIDS 2 AND 2A

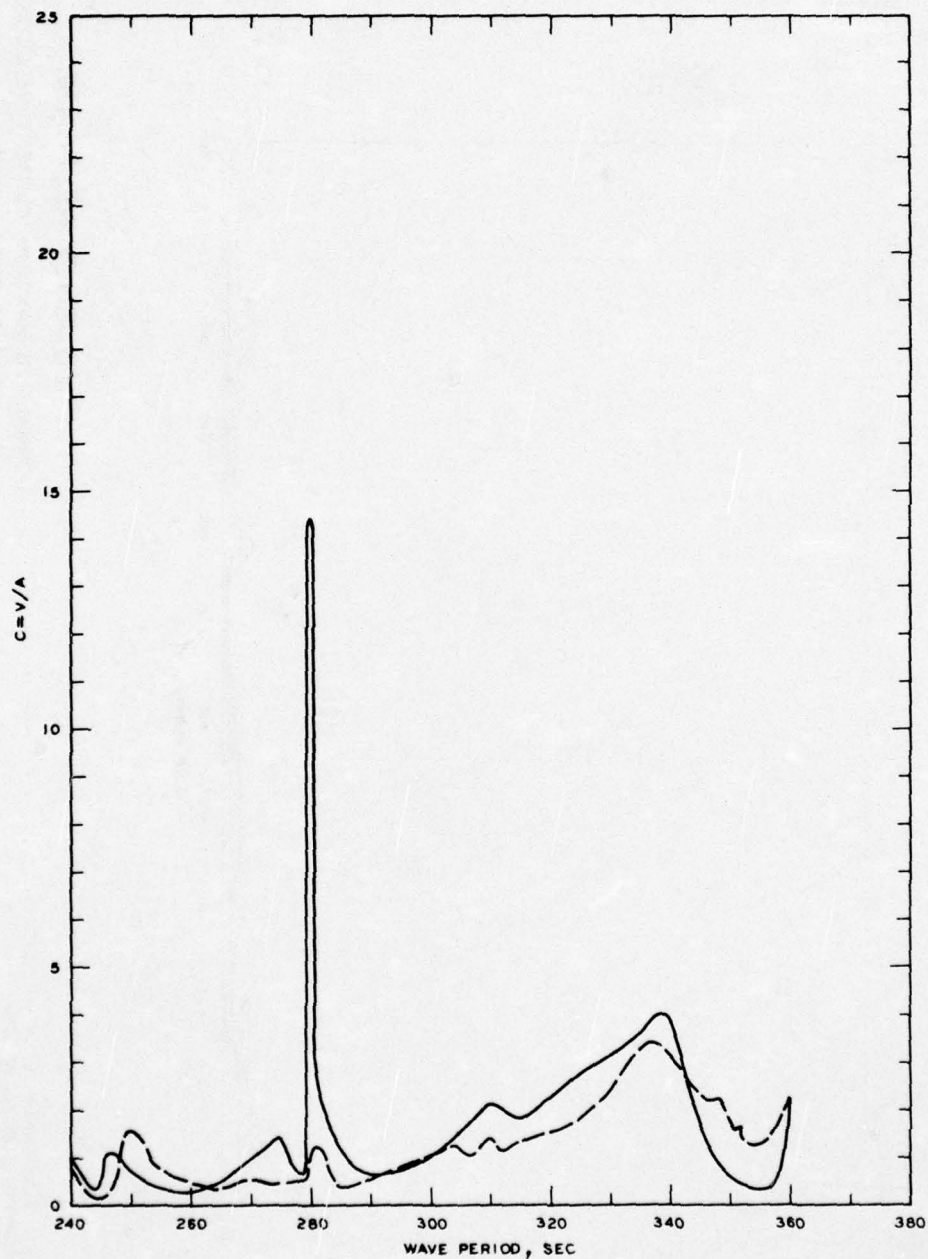


LEGEND

— GRID 3
 - - - GRID 3A

NOTE: C = NORMALIZED MAXIMUM CURRENT VELOCITY
 V = CURRENT VELOCITY, FT/SEC
 A = INCIDENT WAVE AMPLITUDE

FREQUENCY RESPONSE
 NORMALIZED MAXIMUM CURRENT VELOCITY
 GAGE 8, GRIDS 3 AND 3A

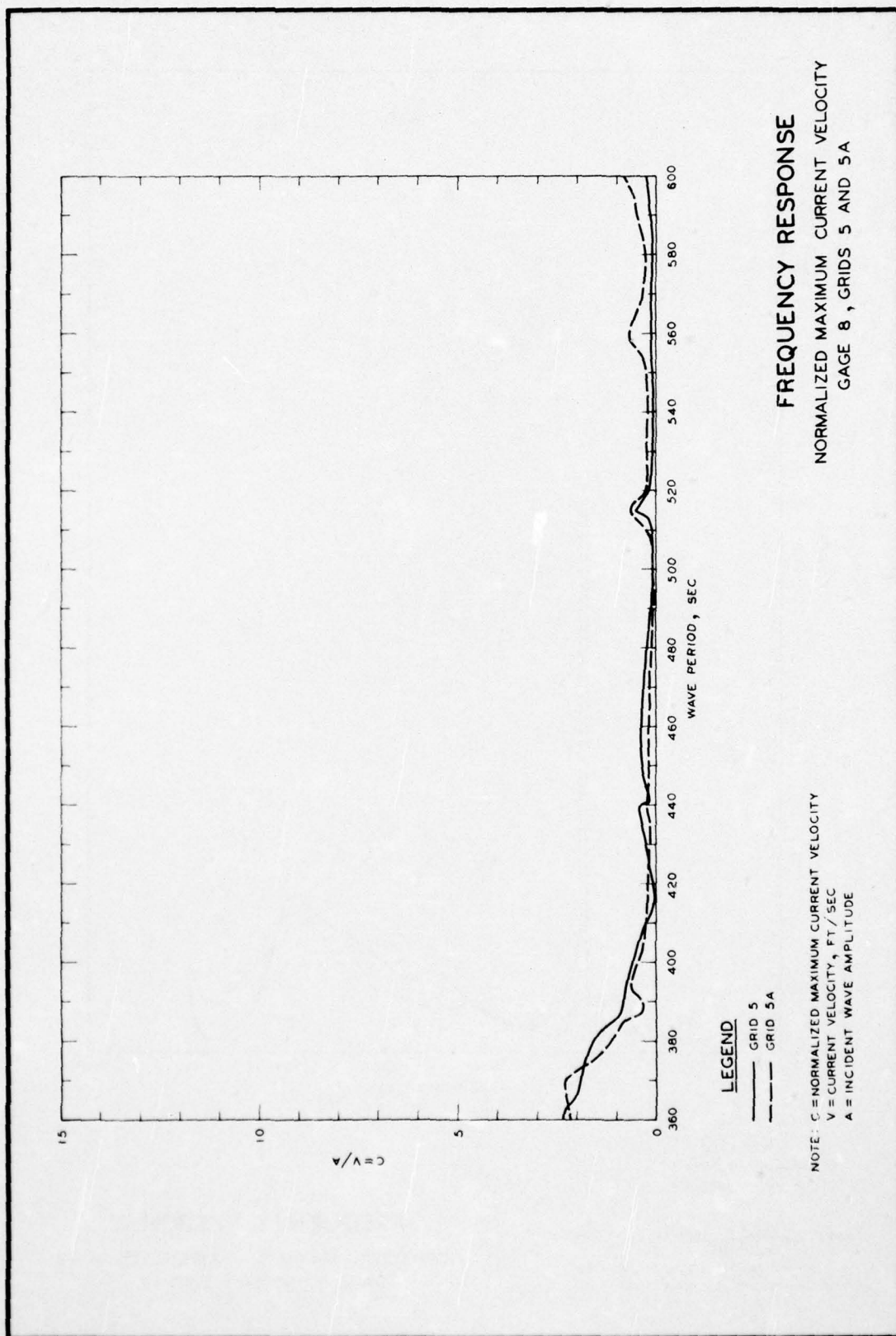


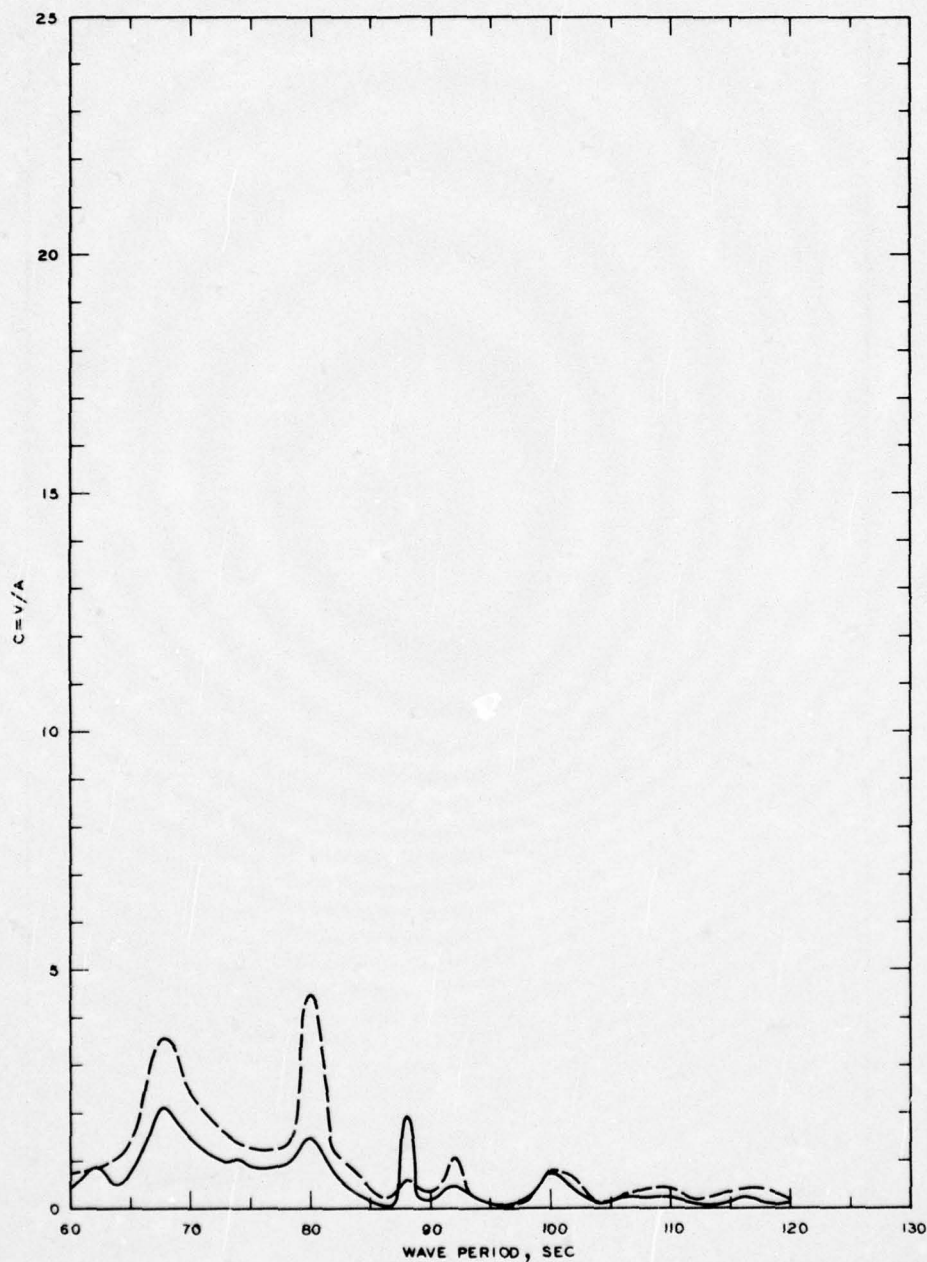
LEGEND

— GRID 4
 --- GRID 4 A

NOTE: C = NORMALIZED MAXIMUM CURRENT VELOCITY
 V = CURRENT VELOCITY, FT/SEC
 A = INCIDENT WAVE AMPLITUDE

FREQUENCY RESPONSE
 NORMALIZED MAXIMUM CURRENT VELOCITY
 GAGE 8 ,GRIDS 4 AND 4A





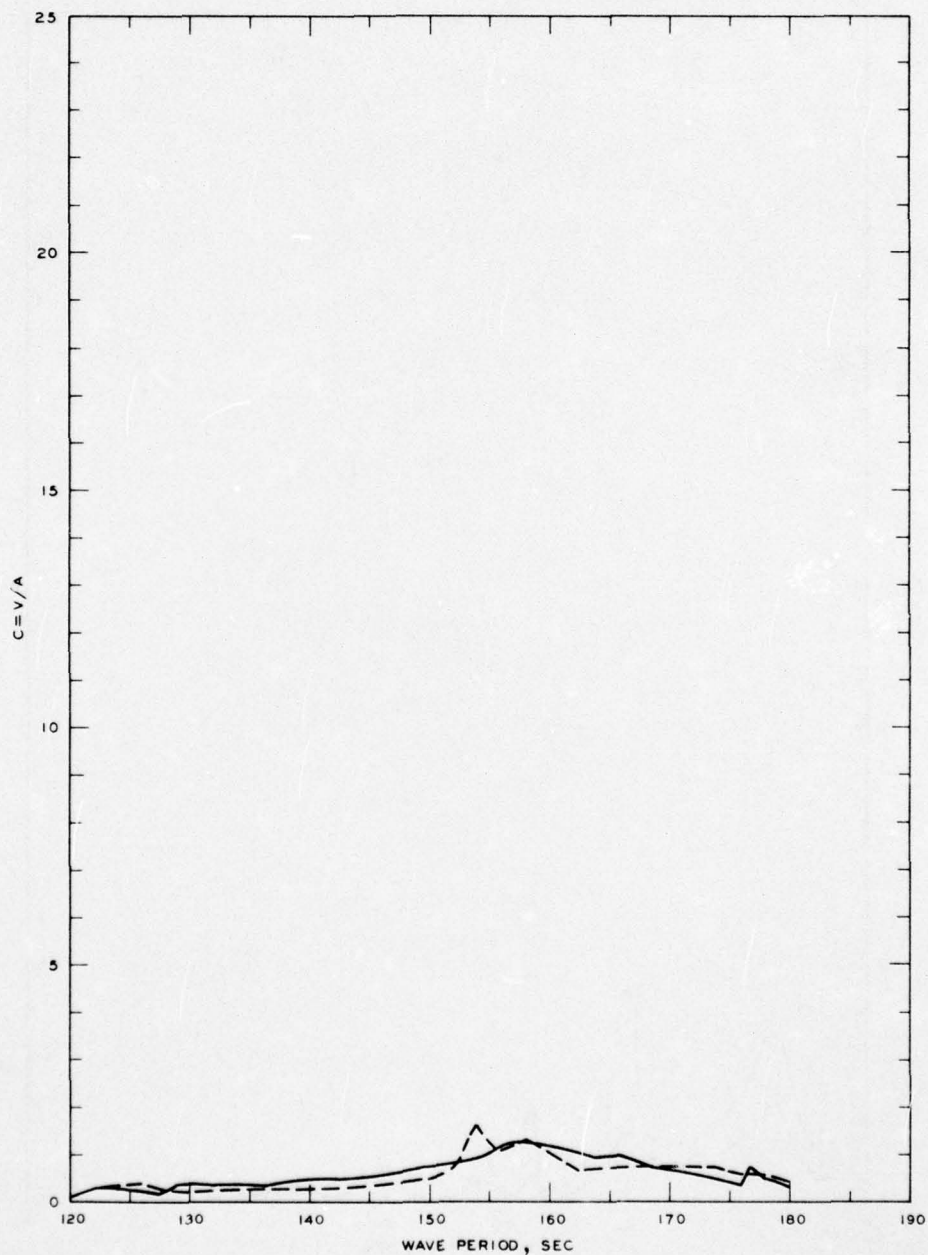
LEGEND

— GRID 1
 - - - GRID 1A

NOTE: C = NORMALIZED MAXIMUM CURRENT VELOCITY
 V = CURRENT VELOCITY, FT/SEC
 A = INCIDENT WAVE AMPLITUDE

FREQUENCY RESPONSE

NORMALIZED MAXIMUM CURRENT VELOCITY
 GAGE 14, GRIDS 1 AND 1A



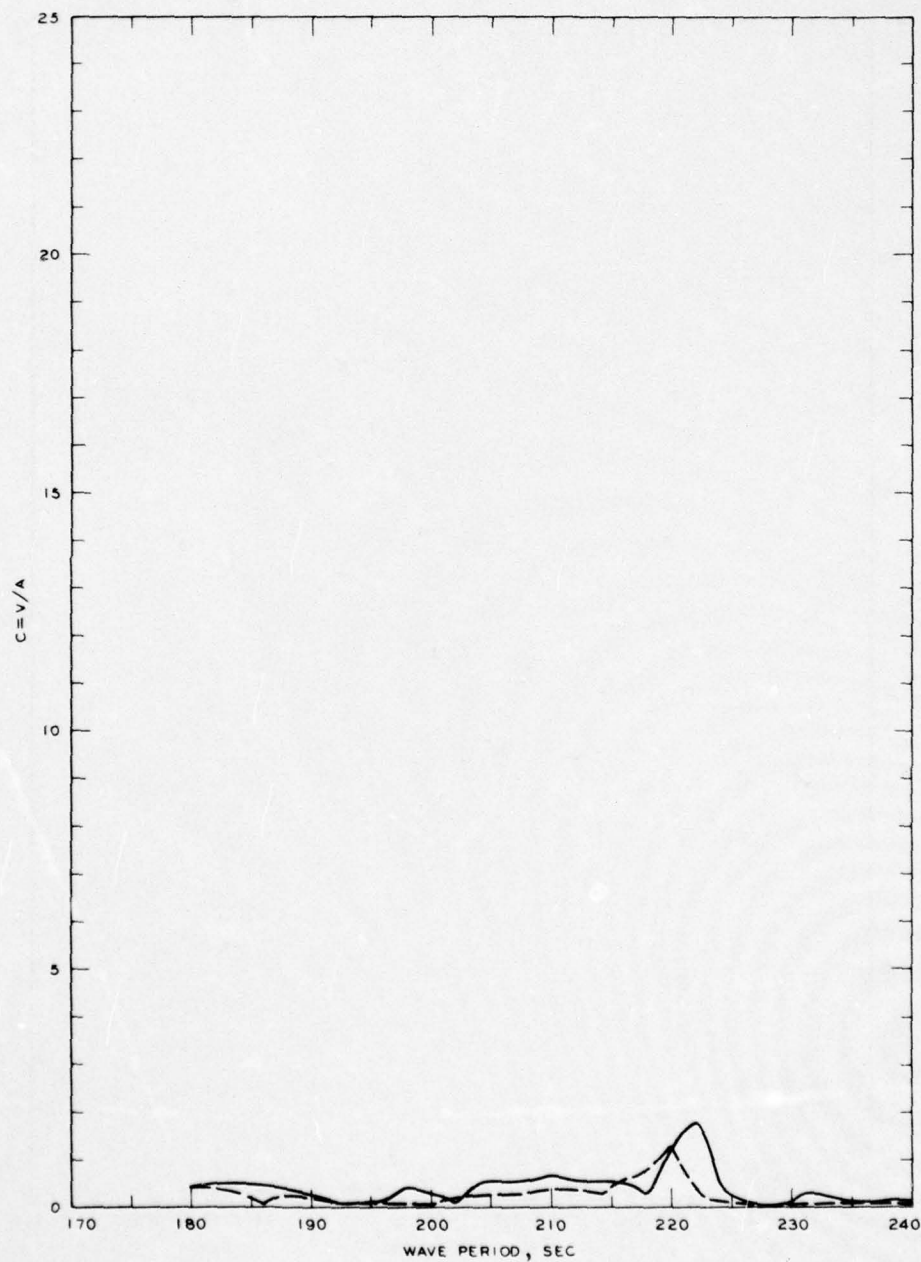
LEGEND

— GRID 2
 - - - GRID 2A

NOTE: C = NORMALIZED MAXIMUM CURRENT
 VELOCITY
 V = CURRENT VELOCITY, FT/SEC
 A = INCIDENT WAVE AMPLITUDE

FREQUENCY RESPONSE

NORMALIZED MAXIMUM CURRENT VELOCITY
 GAGE 14, GRIDS 2 AND 2A



LEGEND

— GRID 3
 - - - GRID 3A

NOTE: C = NORMALIZED MAXIMUM CURRENT VELOCITY
 V = CURRENT VELOCITY, FT/SEC
 A = INCIDENT WAVE AMPLITUDE

FREQUENCY RESPONSE
 NORMALIZED MAXIMUM CURRENT VELOCITY
 GAGE 14, GRIDS 3 AND 3A

AD-A031 171

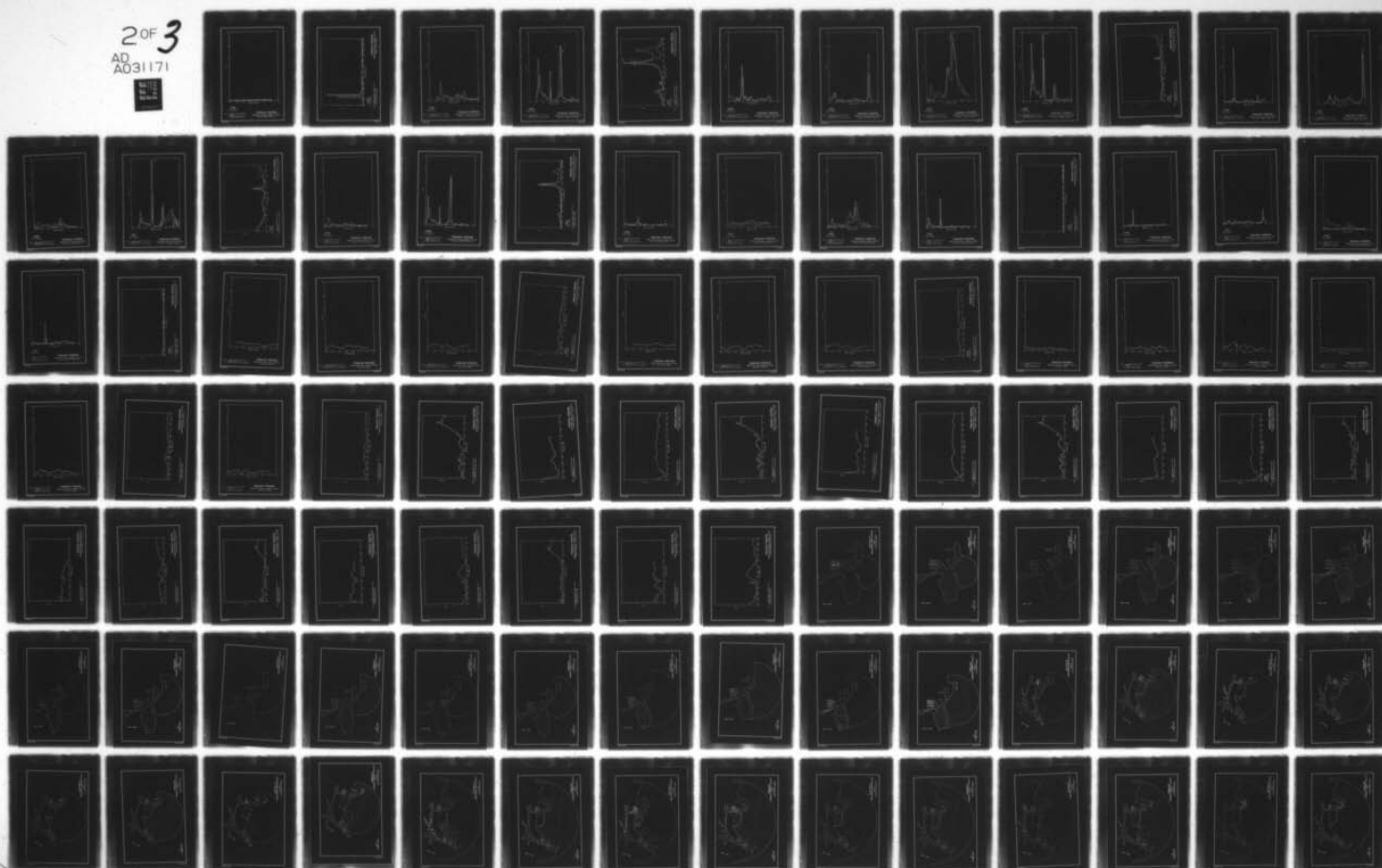
ARMY ENGINEER WATERWAYS EXPERIMENT STATION VICKSBURG MISS F/G 8/3
LONG BEACH HARBOR NUMERICAL ANALYSIS OF HARBOR OSCILLATIONS. RE--ETC(U)
SEP 76 J R HOUSTON

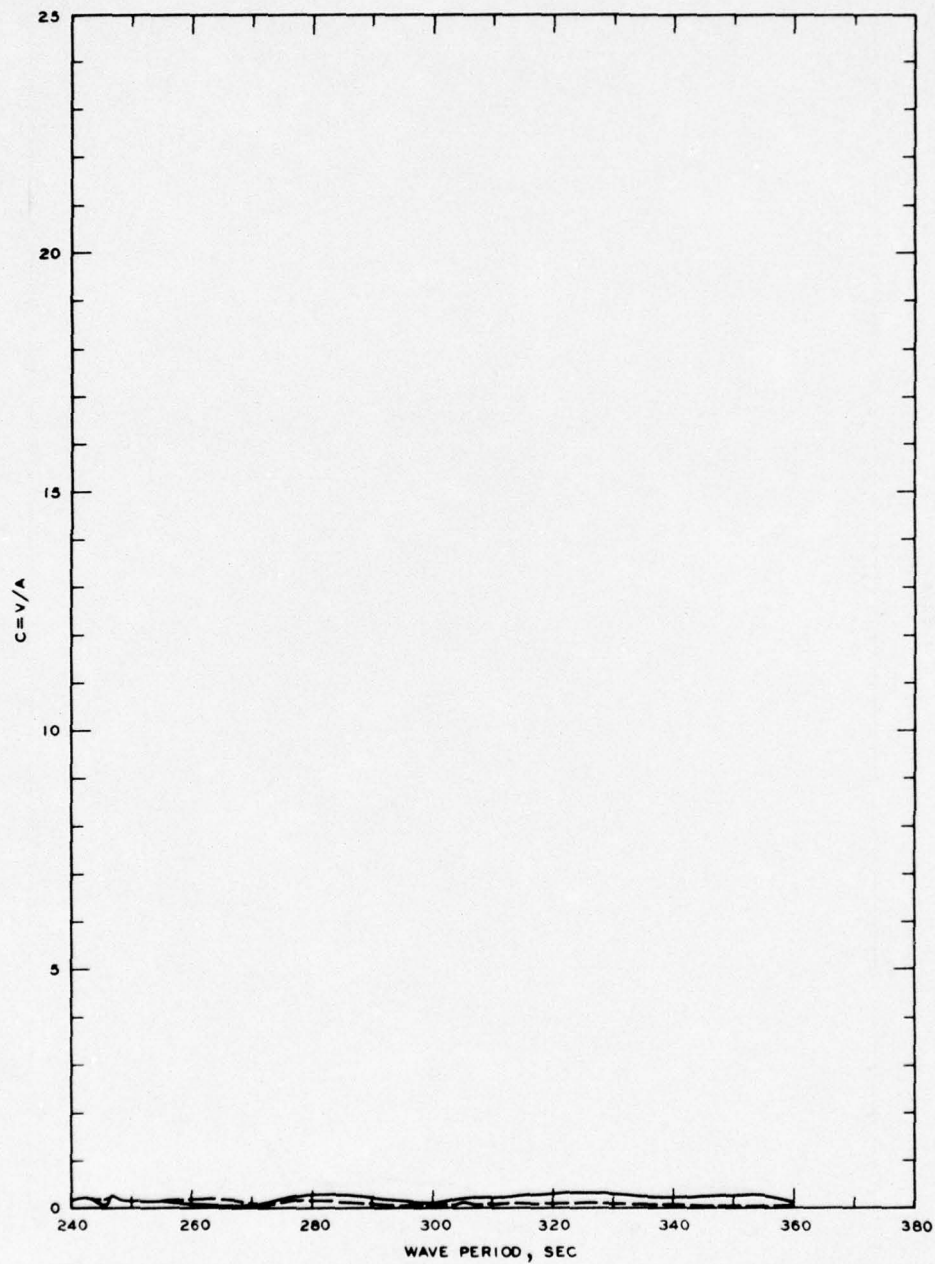
UNCLASSIFIED

WES-MP-H-76-20-1

NL

2 OF 3
AD
A031171



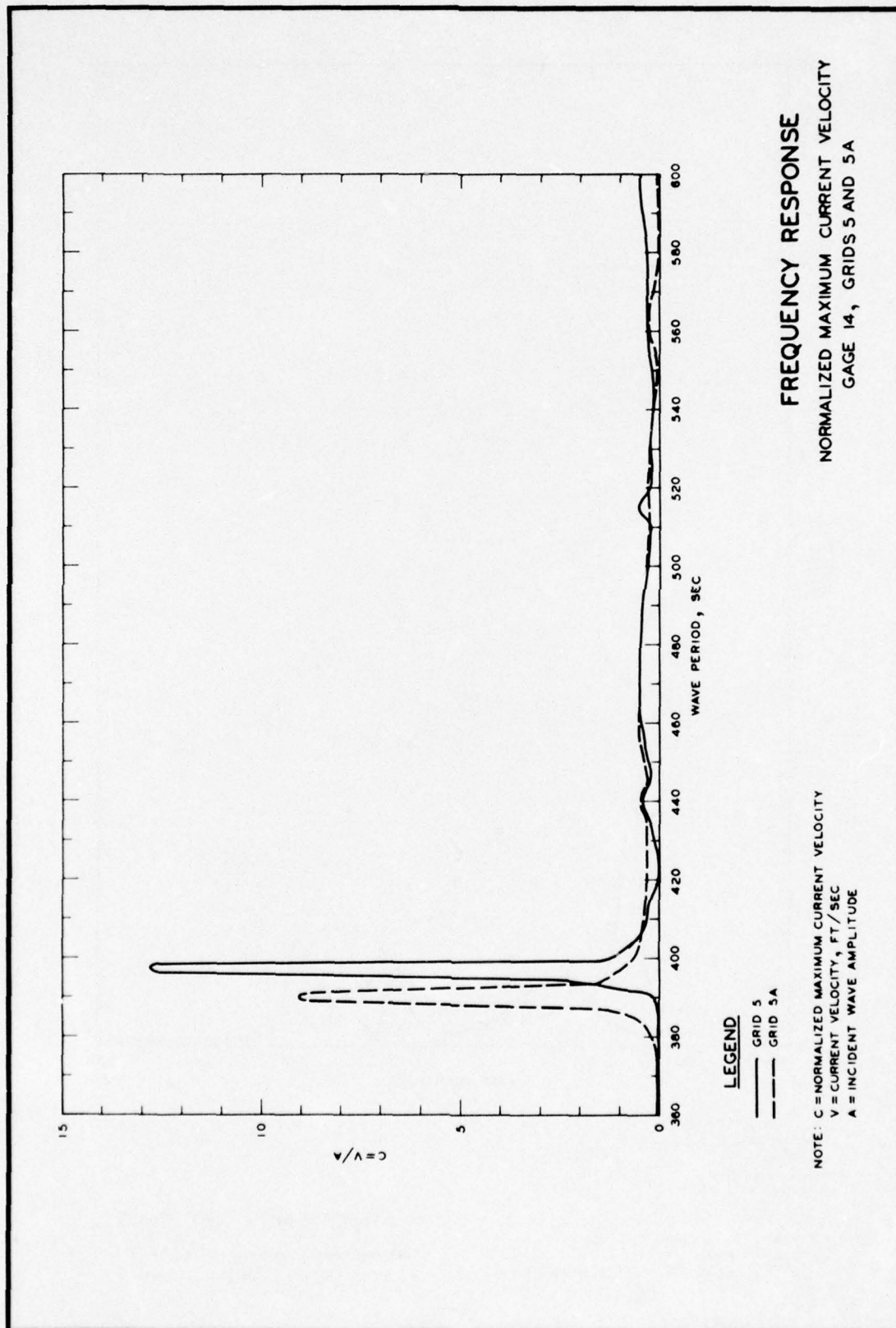


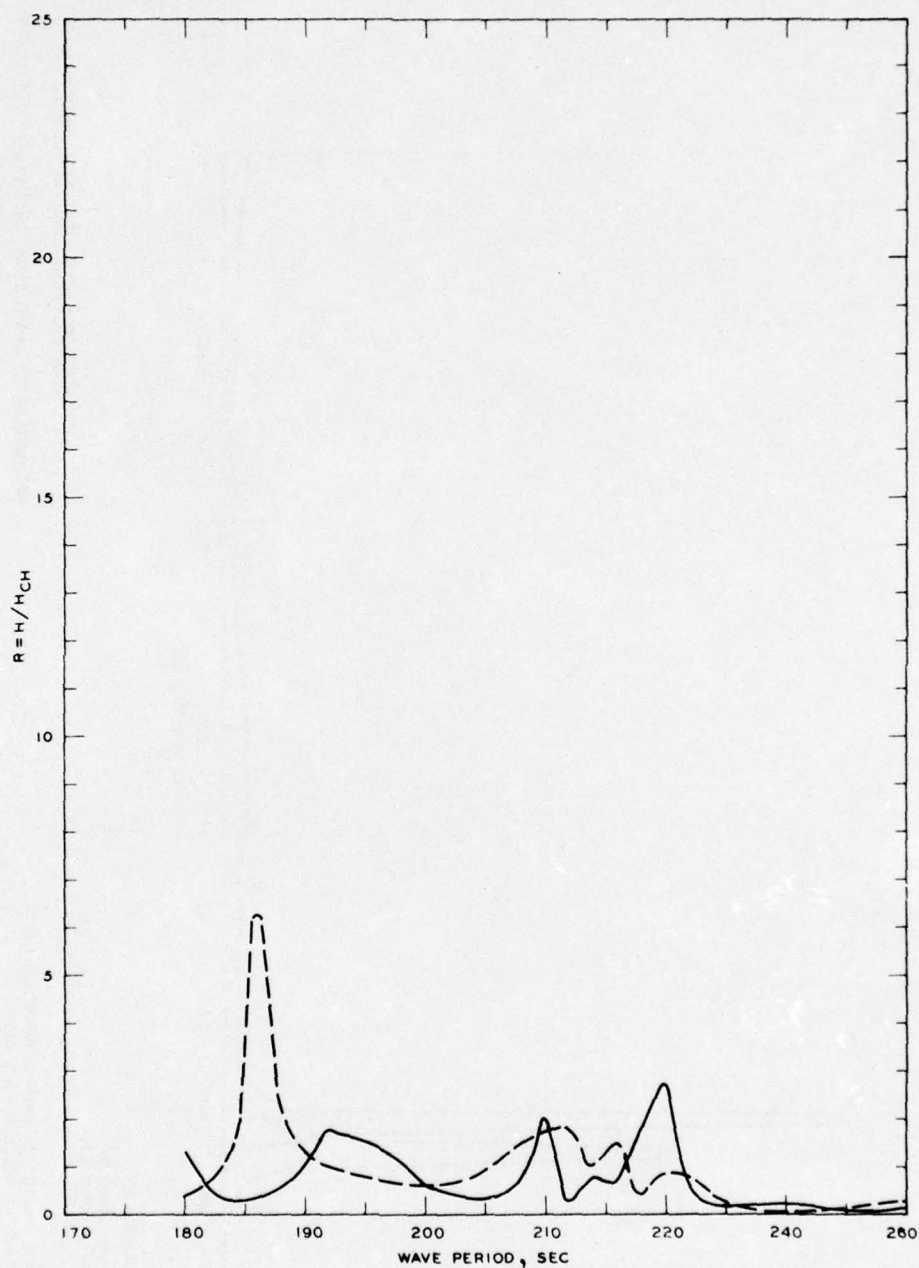
LEGEND

— GRID 4
 - - - GRID 4A

NOTE: C = NORMALIZED MAXIMUM CURRENT VELOCITY
 V = CURRENT VELOCITY, FT/SEC
 A = INCIDENT WAVE AMPLITUDE

FREQUENCY RESPONSE
 NORMALIZED MAXIMUM CURRENT VELOCITY
 GAGE 14, GRIDS 4 AND 4A



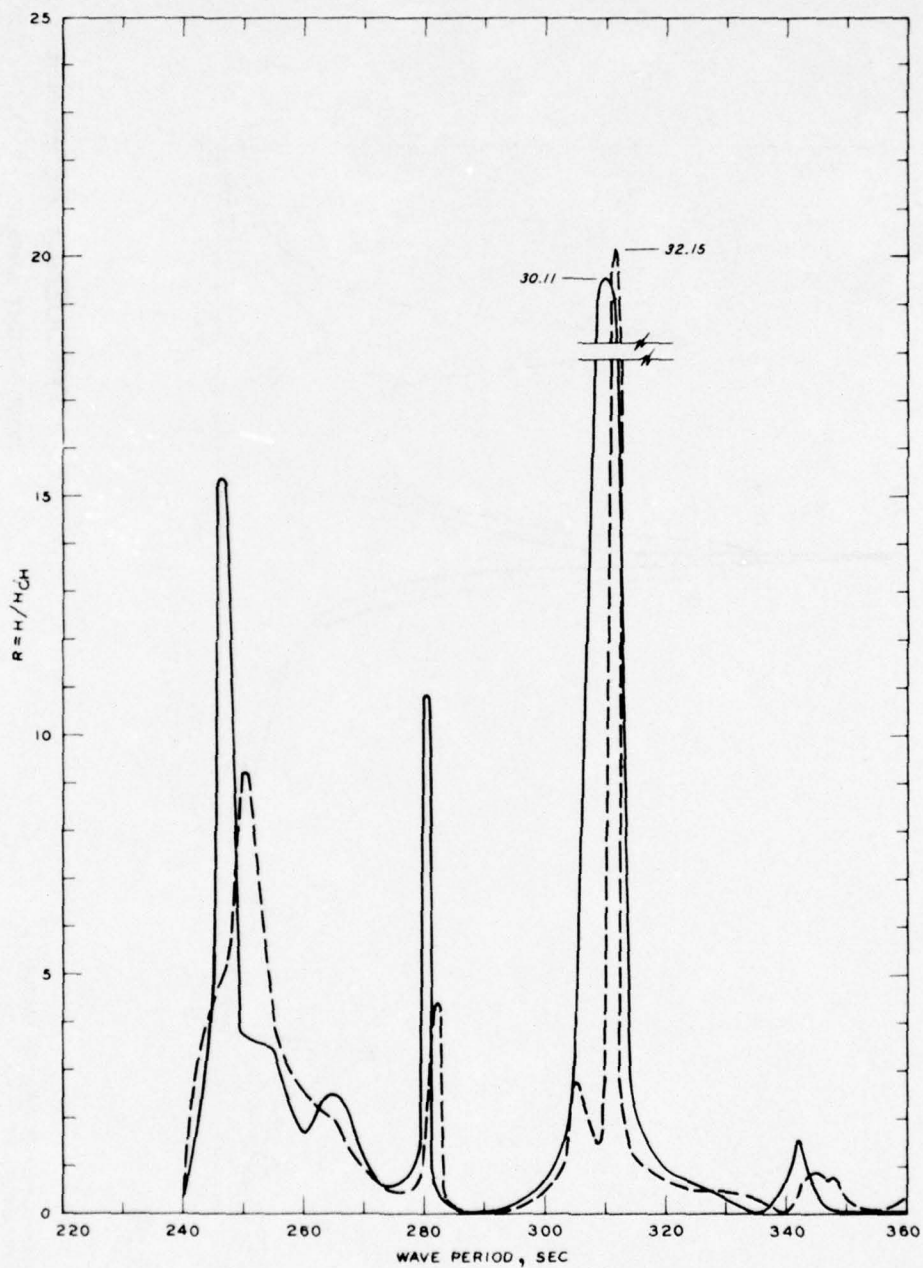


LEGEND

— GRID 3
 - - - GRID 3A

NOTE R = WAVE-HEIGHT AMPLIFICATION FACTOR
 H = WAVE HEIGHT, FT
 H_{CH} = WAVE HEIGHT FOR CLOSED HARBOR, FT

FREQUENCY RESPONSE
 WAVE-HEIGHT AMPLIFICATION FACTOR
 STA LB-1, GRIDS 3 AND 3A

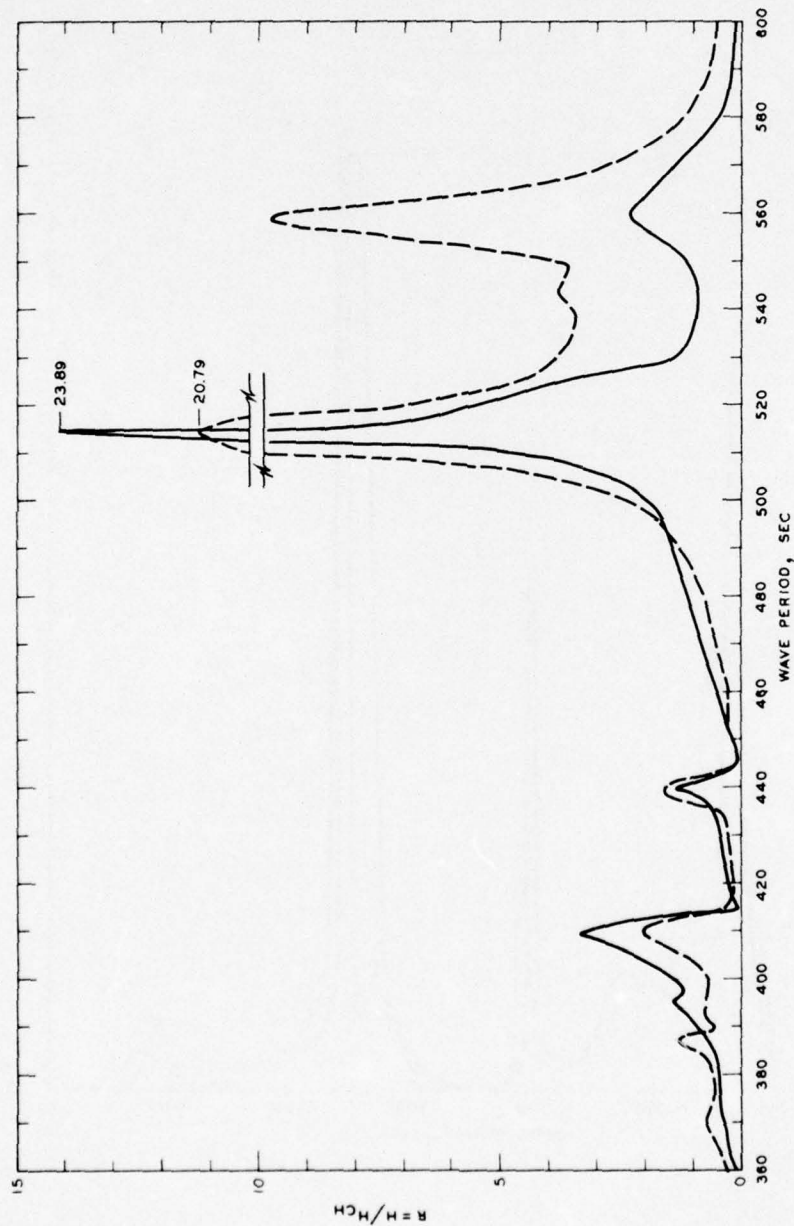


LEGEND

— GRID 4
 - - - GRID 4A

NOTE R = WAVE-HEIGHT AMPLIFICATION FACTOR
 H = WAVE HEIGHT, FT
 H_{CH} = WAVE HEIGHT FOR CLOSED HARBOR, FT

FREQUENCY RESPONSE
 WAVE-HEIGHT AMPLIFICATION FACTOR
 STA LB-1, GRIDS 4 AND 4A

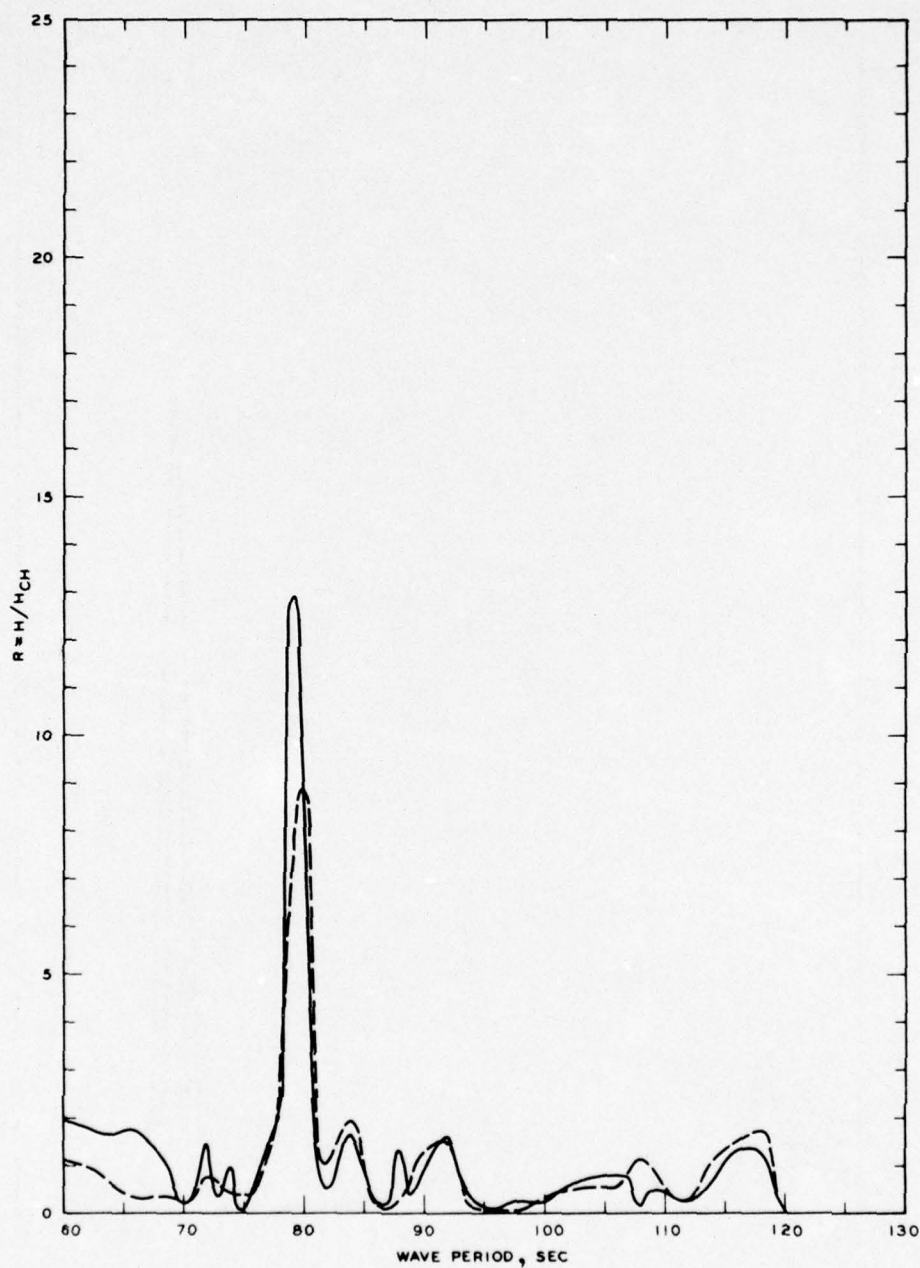


LEGEND

— GRID 5
 --- GRID 5A

NOTE: R = WAVE-HEIGHT AMPLIFICATION FACTOR
 H = WAVE HEIGHT, FT
 H_{CH} = WAVE HEIGHT FOR CLOSED HARBOR, FT

FREQUENCY RESPONSE
 WAVE-HEIGHT AMPLIFICATION FACTOR
 STA LB-1, GRIDS 5 AND 5A

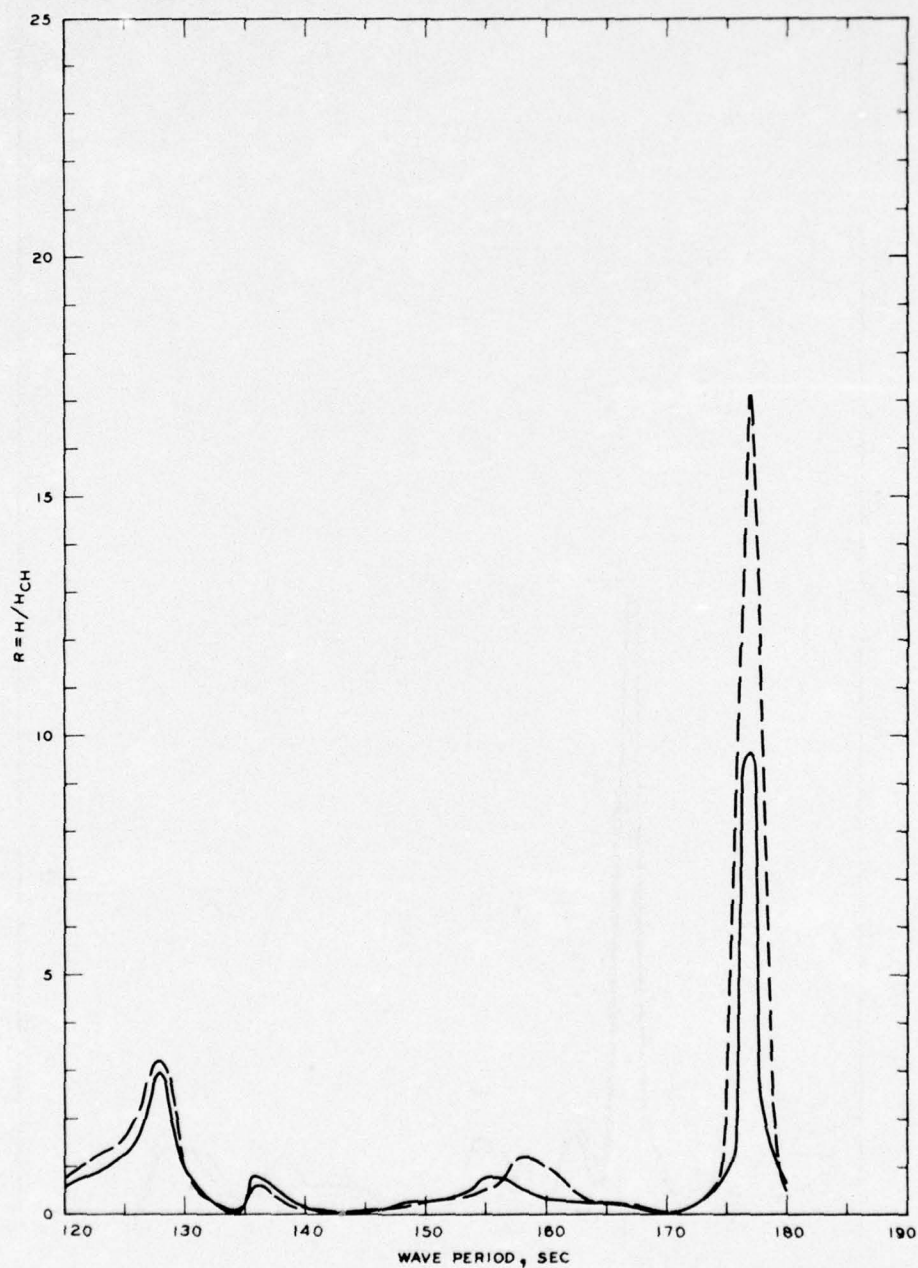


LEGEND

— GRID 1
 - - - GRID 1A

NOTE R = WAVE-HEIGHT AMPLIFICATION FACTOR
 H = WAVE HEIGHT, FT
 H_{CH} = WAVE HEIGHT FOR CLOSED HARBOR, FT

FREQUENCY RESPONSE
 WAVE-HEIGHT AMPLIFICATION FACTOR
 STA LB-2, GRIDS 1 AND 1A

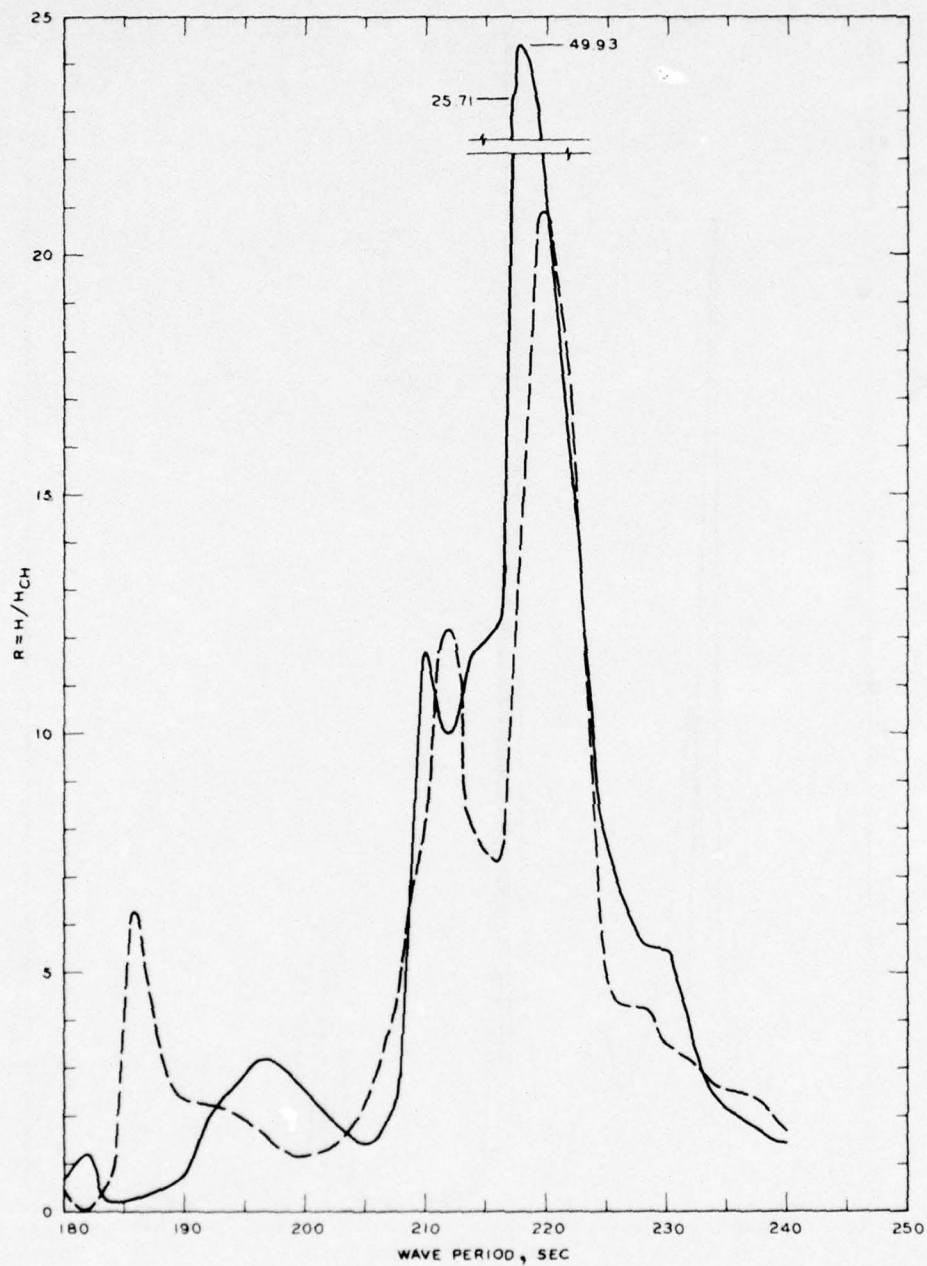


LEGEND

— GRID 2
 - - - GRID 2A

NOTE R = WAVE-HEIGHT AMPLIFICATION FACTOR
 H = WAVE HEIGHT, FT
 H_{CH} = WAVE HEIGHT FOR CLOSED HARBOR, FT

FREQUENCY RESPONSE
 WAVE-HEIGHT AMPLIFICATION FACTOR
 STA LB-2, GRIDS 2 AND 2A

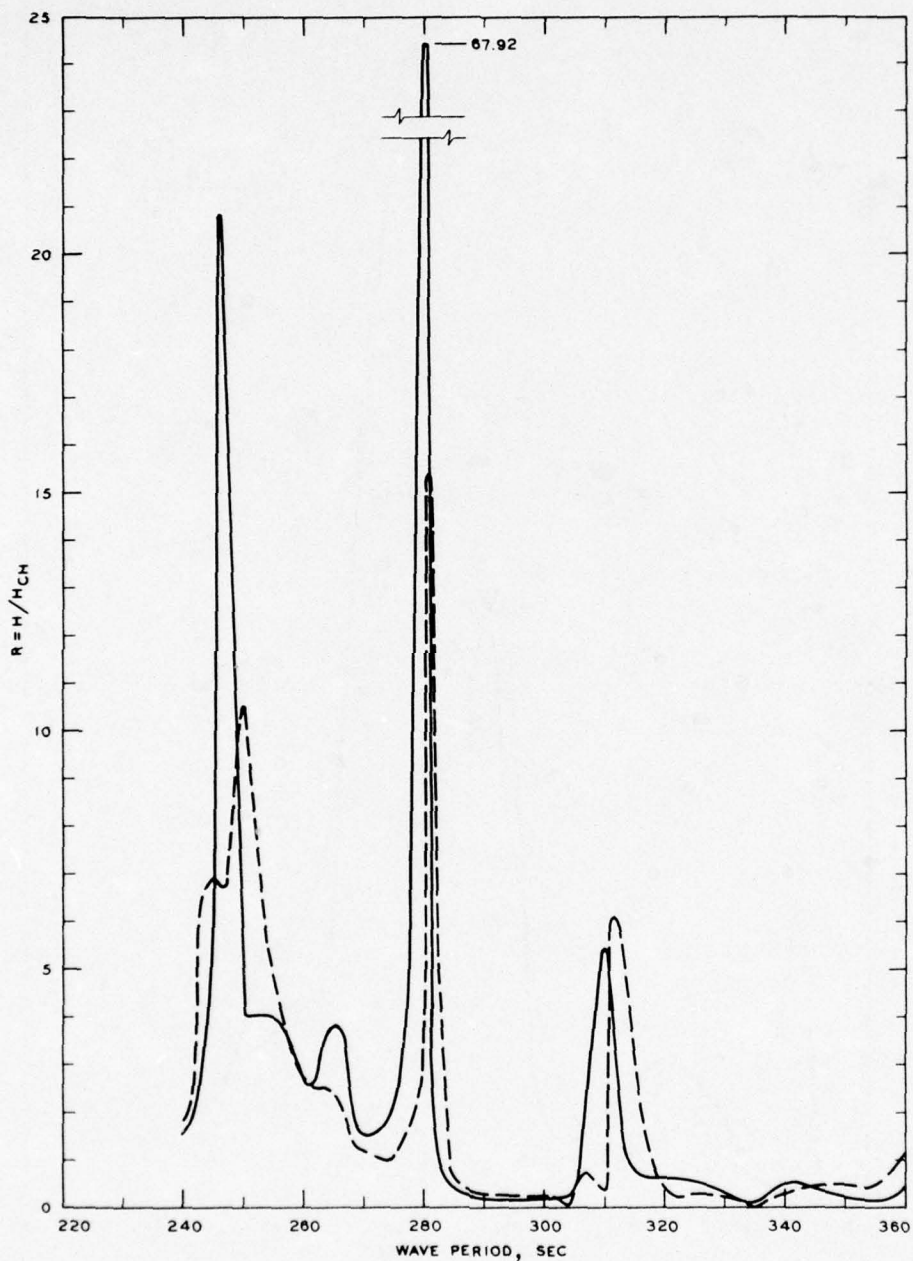


LEGEND

— GRID 3
 - - - GRID 3 A

NOTE R = WAVE-HEIGHT AMPLIFICATION FACTOR
 H = WAVE HEIGHT, FT
 H_{CH} = WAVE HEIGHT FOR CLOSED HARBOR, FT

FREQUENCY RESPONSE
 WAVE-HEIGHT AMPLIFICATION FACTOR
 STA LB-2, GRIDS 3 AND 3A



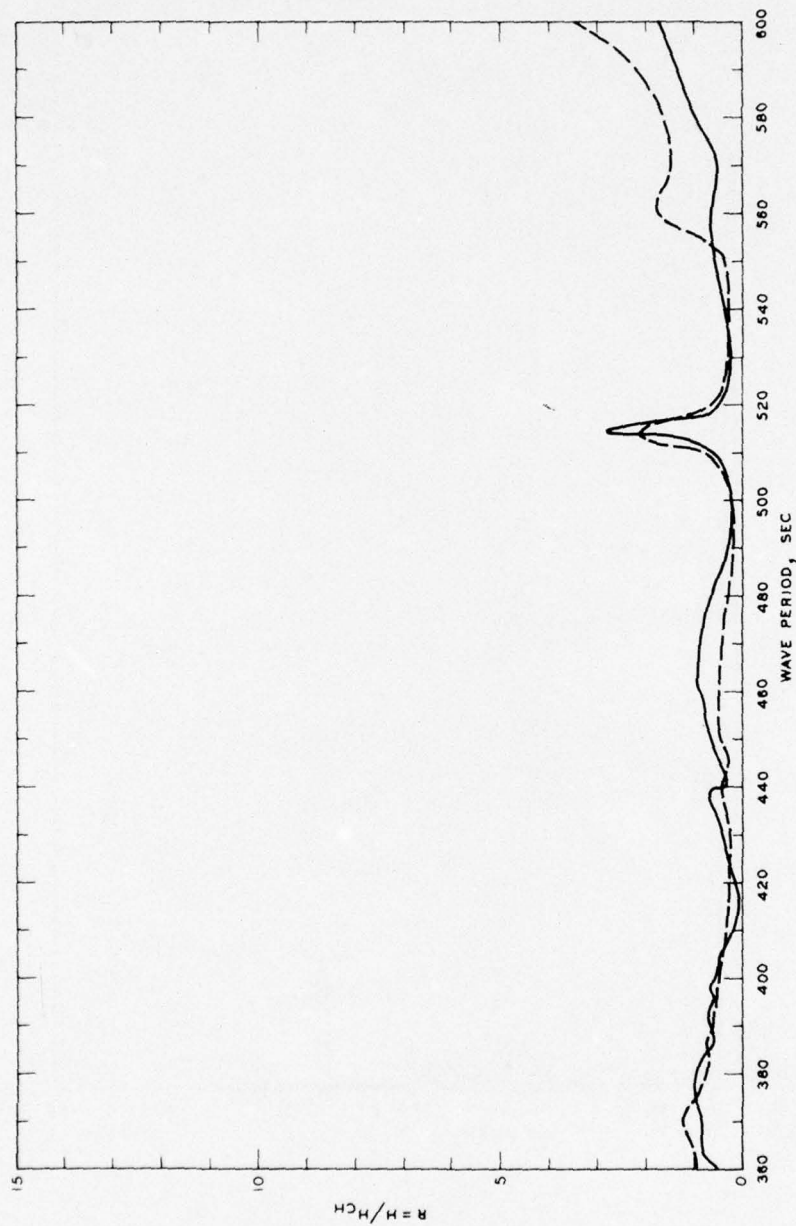
LEGEND

— GRID 4
 --- GRID 4A

NOTE: R = WAVE-HEIGHT AMPLIFICATION FACTOR
 H = WAVE HEIGHT, FT
 H_{CH} = WAVE HEIGHT FOR CLOSED HARBOR, FT

FREQUENCY RESPONSE

WAVE-HEIGHT AMPLIFICATION FACTOR
 STA LB-2, GRIDS 4 AND 4A

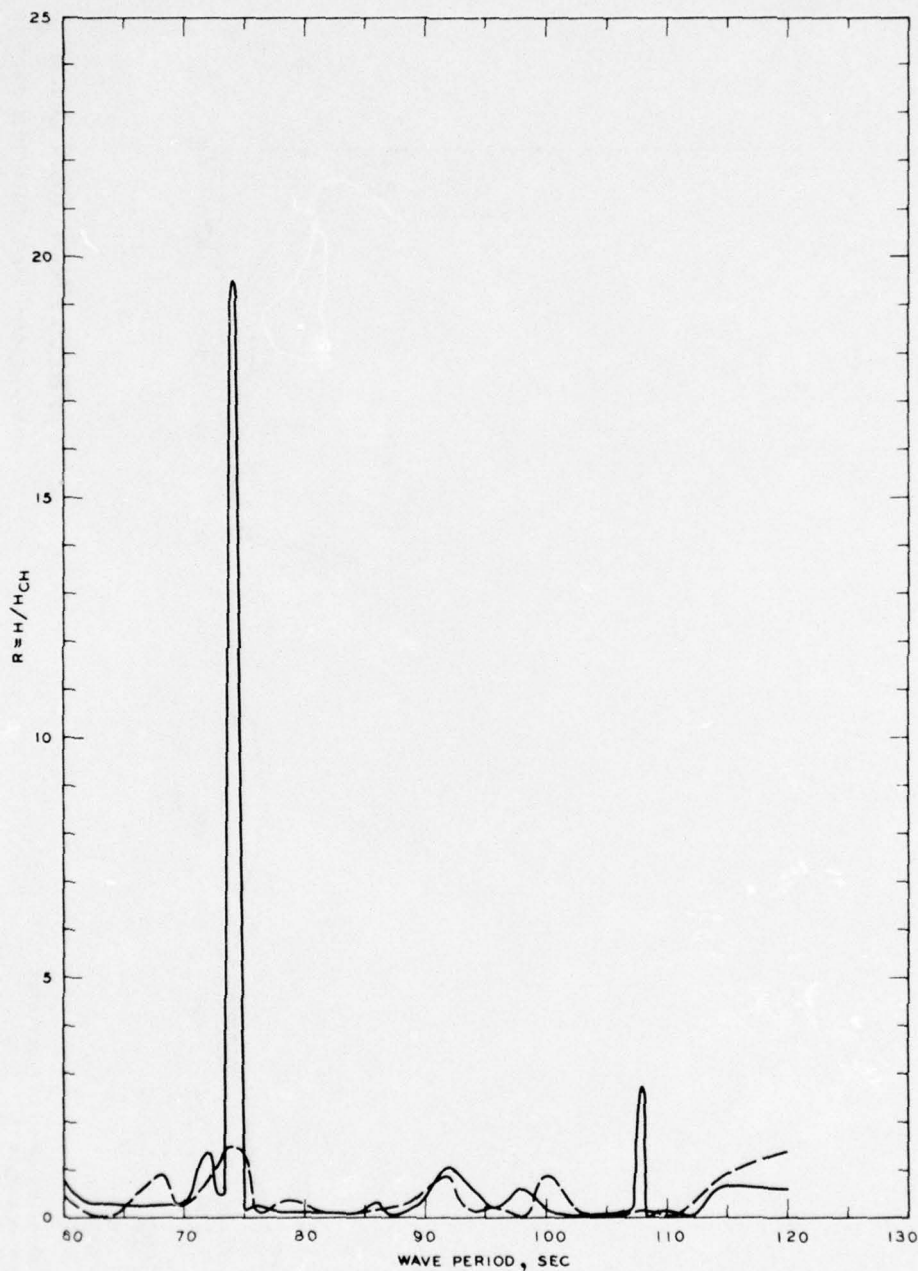


LEGEND

— GRID 5
 --- GRID 5A

NOTE: R = WAVE-HEIGHT AMPLIFICATION FACTOR
 H = WAVE HEIGHT, FT
 H_{CH} = WAVE HEIGHT FOR CLOSED HARBOR, FT

FREQUENCY RESPONSE
 WAVE-HEIGHT AMPLIFICATION FACTOR
 STA LB-2, GRIDS 5 AND 5A

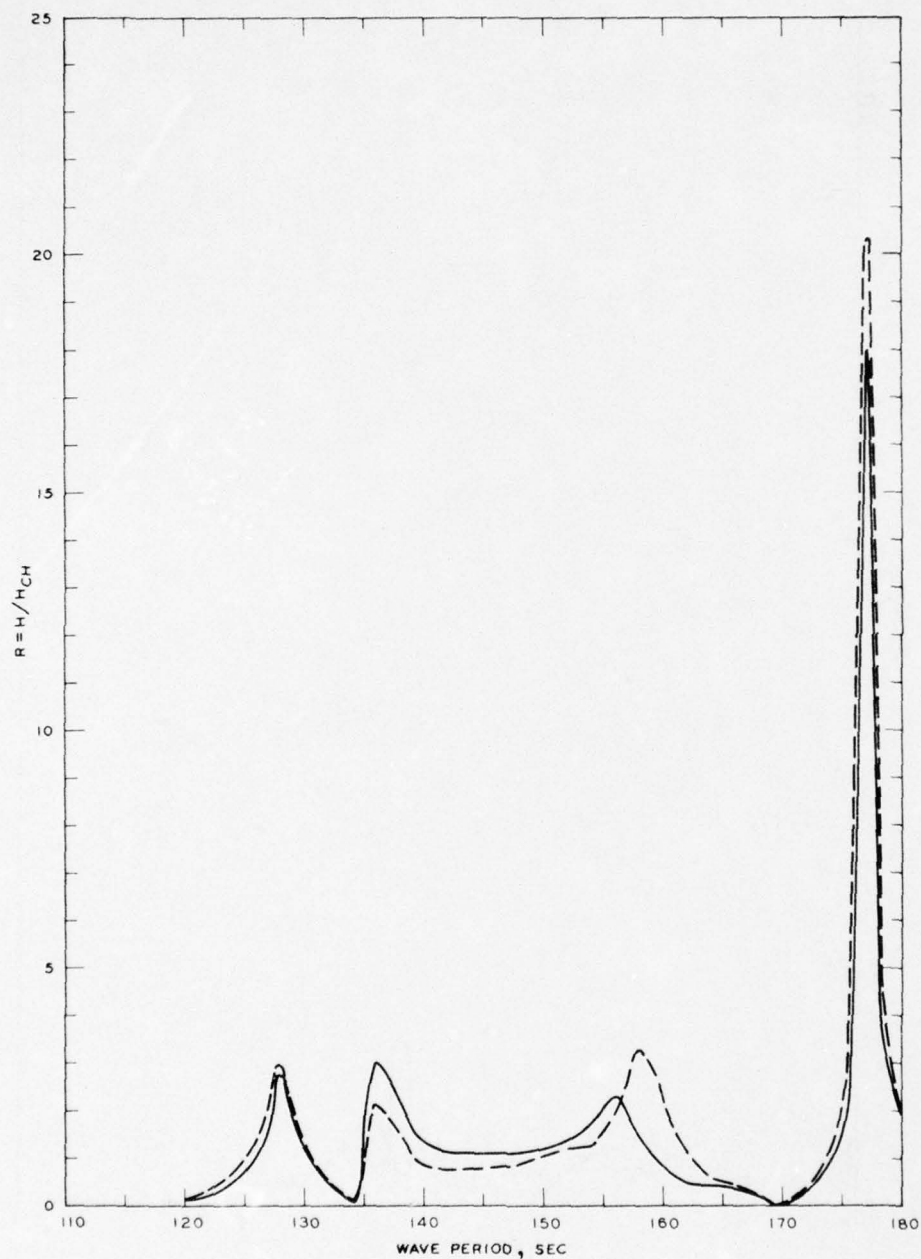


LEGEND

— GRID 1
 - - - GRID 1A

NOTE R = WAVE-HEIGHT AMPLIFICATION FACTOR
 H = WAVE HEIGHT, FT
 H_{CH} = WAVE HEIGHT FOR CLOSED HARBOR, FT

FREQUENCY RESPONSE
 WAVE-HEIGHT AMPLIFICATION FACTOR
 STA LB-3, GRIDS 1 AND 1A

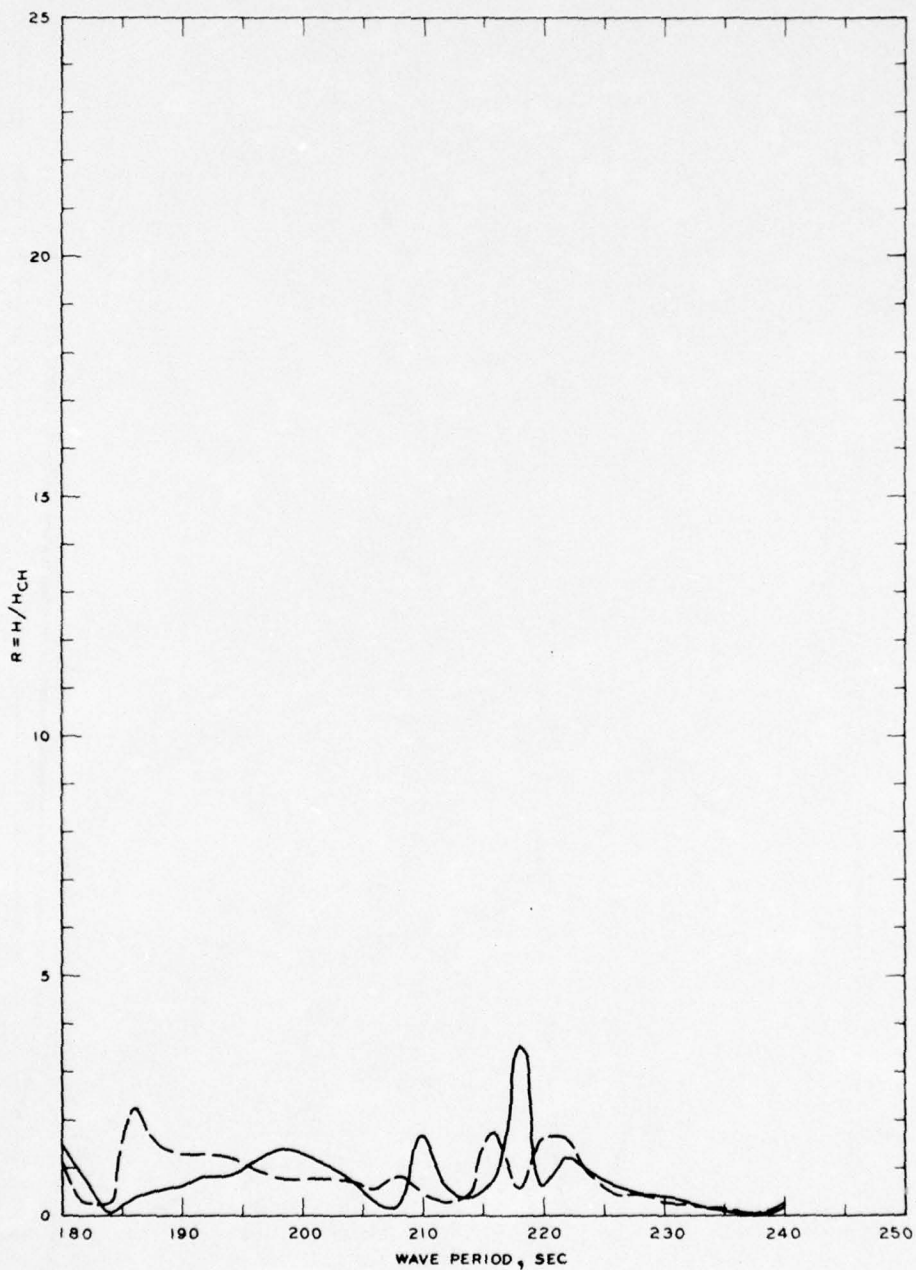


LEGEND

— GRID 2
 - - - GRID 2A

NOTE R = WAVE-HEIGHT AMPLIFICATION FACTOR
 H = WAVE HEIGHT, FT
 H_{CH} = WAVE HEIGHT FOR CLOSED HARBOR, FT

FREQUENCY RESPONSE
 WAVE-HEIGHT AMPLIFICATION FACTOR
 STA LB-3, GRIDS 2 AND 2A

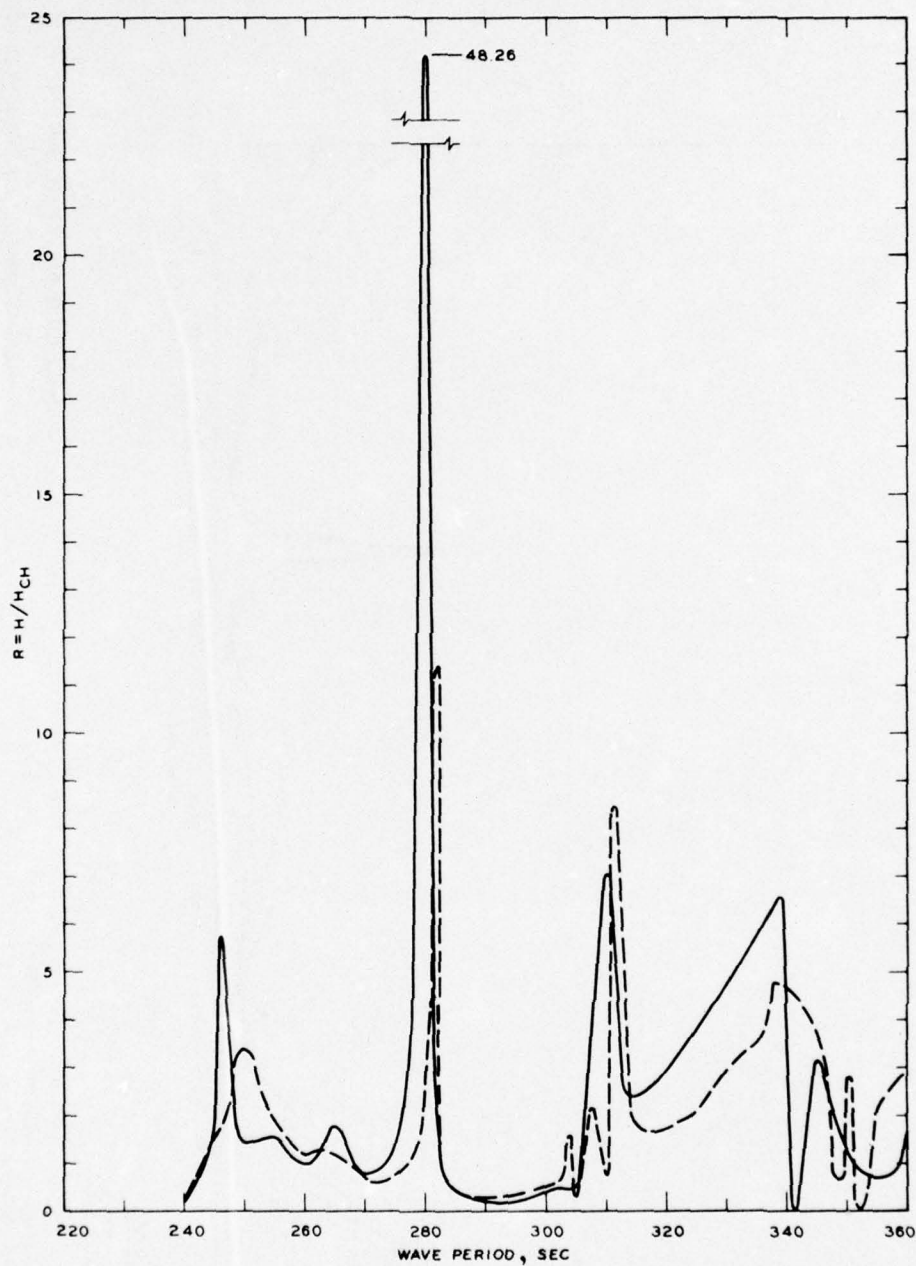


LEGEND

— GRID 3
 - - - GRID 3A

NOTE: R = WAVE-HEIGHT AMPLIFICATION FACTOR
 H = WAVE HEIGHT, FT
 H_{CH} = WAVE HEIGHT FOR CLOSED HARBOR, FT

FREQUENCY RESPONSE
 WAVE-HEIGHT AMPLIFICATION FACTOR
 STA LB-3, GRIDS 3 AND 3A

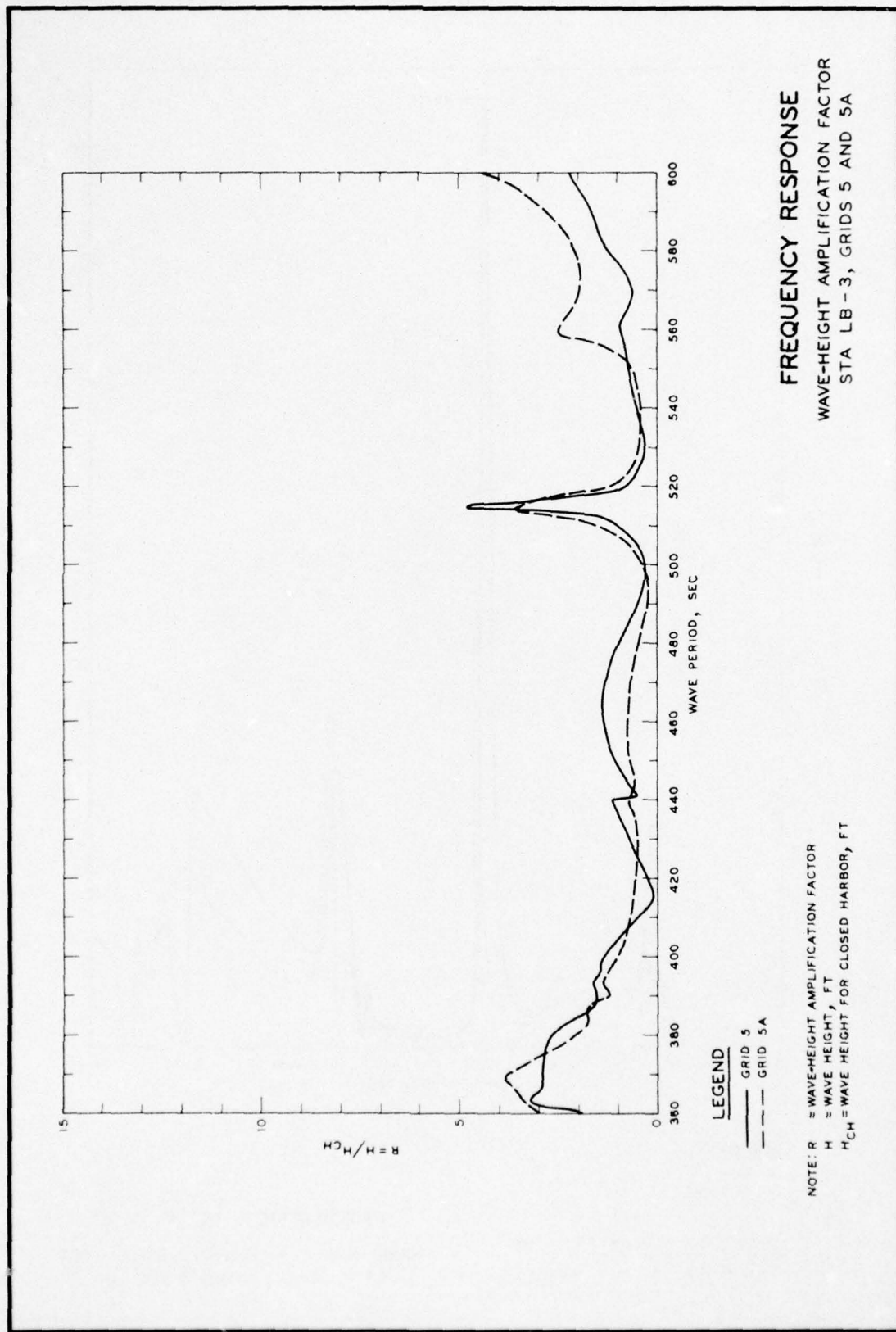


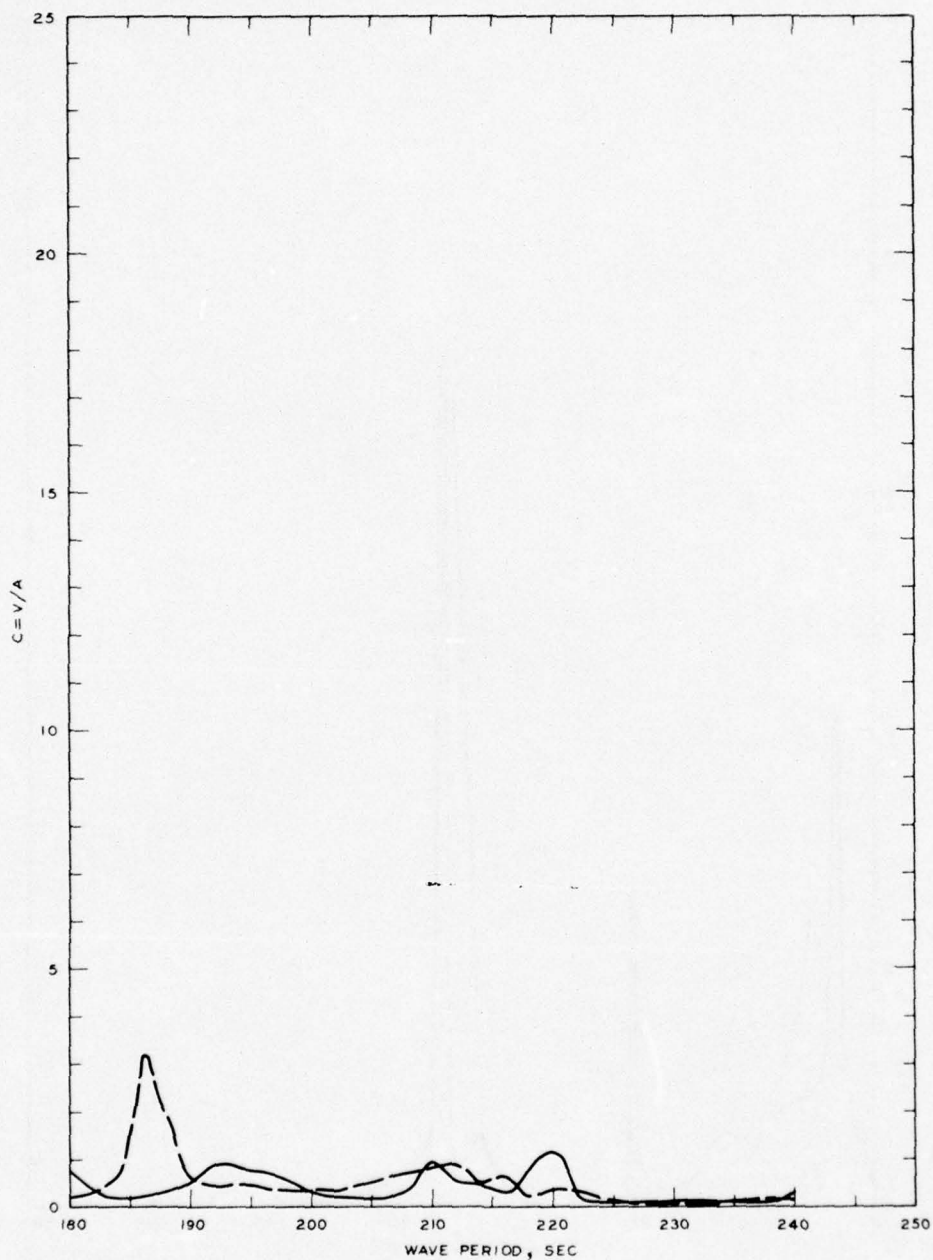
LEGEND

— GRID 4
 - - - GRID 4A

NOTE R = WAVE-HEIGHT AMPLIFICATION FACTOR
 H = WAVE HEIGHT, FT
 H_{CH} = WAVE HEIGHT FOR CLOSED HARBOR, FT

FREQUENCY RESPONSE
 WAVE-HEIGHT AMPLIFICATION FACTOR
 STA LB-3, GRIDS 4 AND 4A





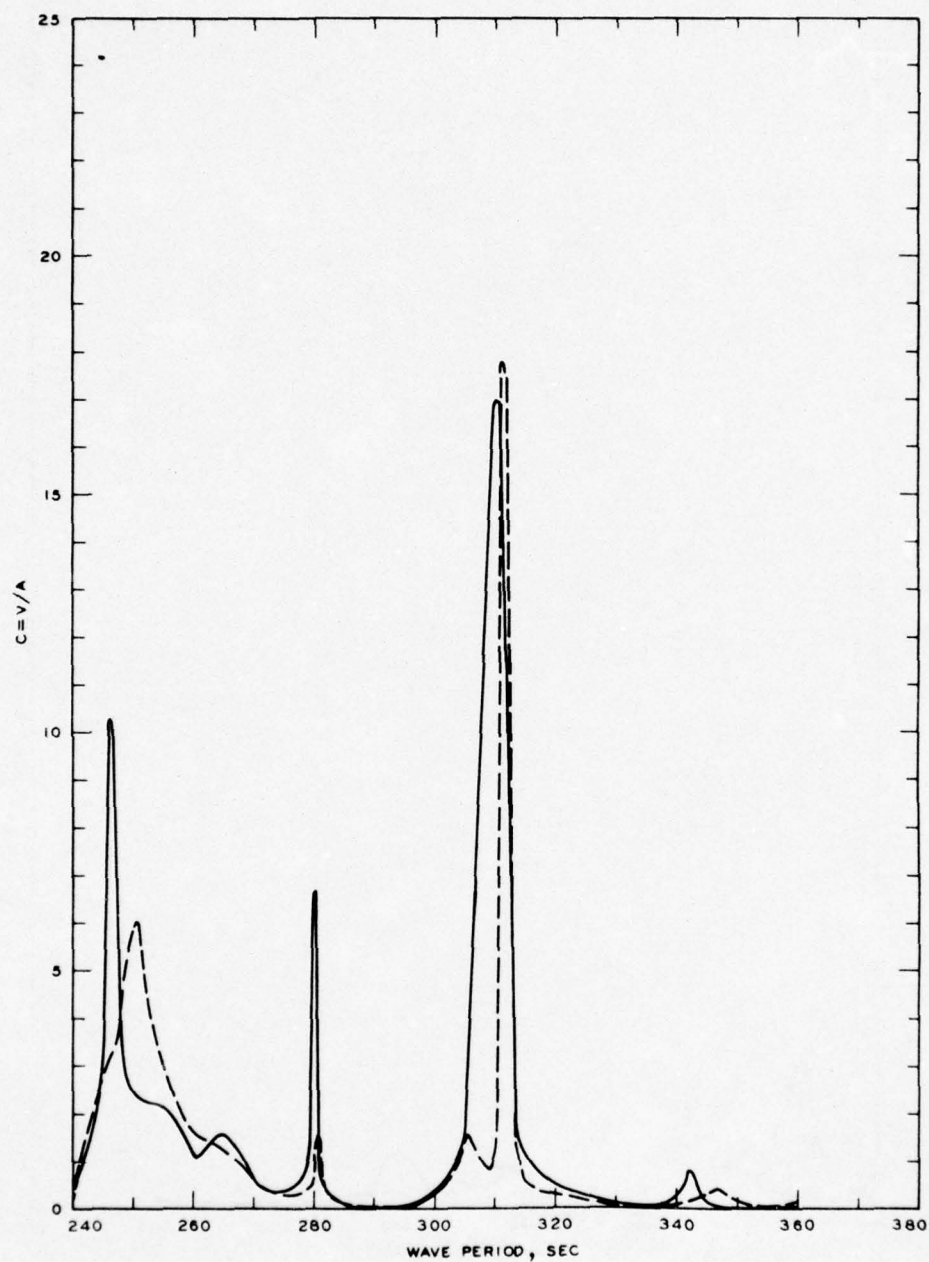
LEGEND

— GRID 3
 --- GRID 3A

NOTE: C = NORMALIZED MAXIMUM CURRENT VELOCITY
 V = CURRENT VELOCITY, FT/SEC
 A = INCIDENT WAVE AMPLITUDE

FREQUENCY RESPONSE

NORMALIZED MAXIMUM CURRENT VELOCITY
 STA LB-1, GRIDS 3 AND 3A

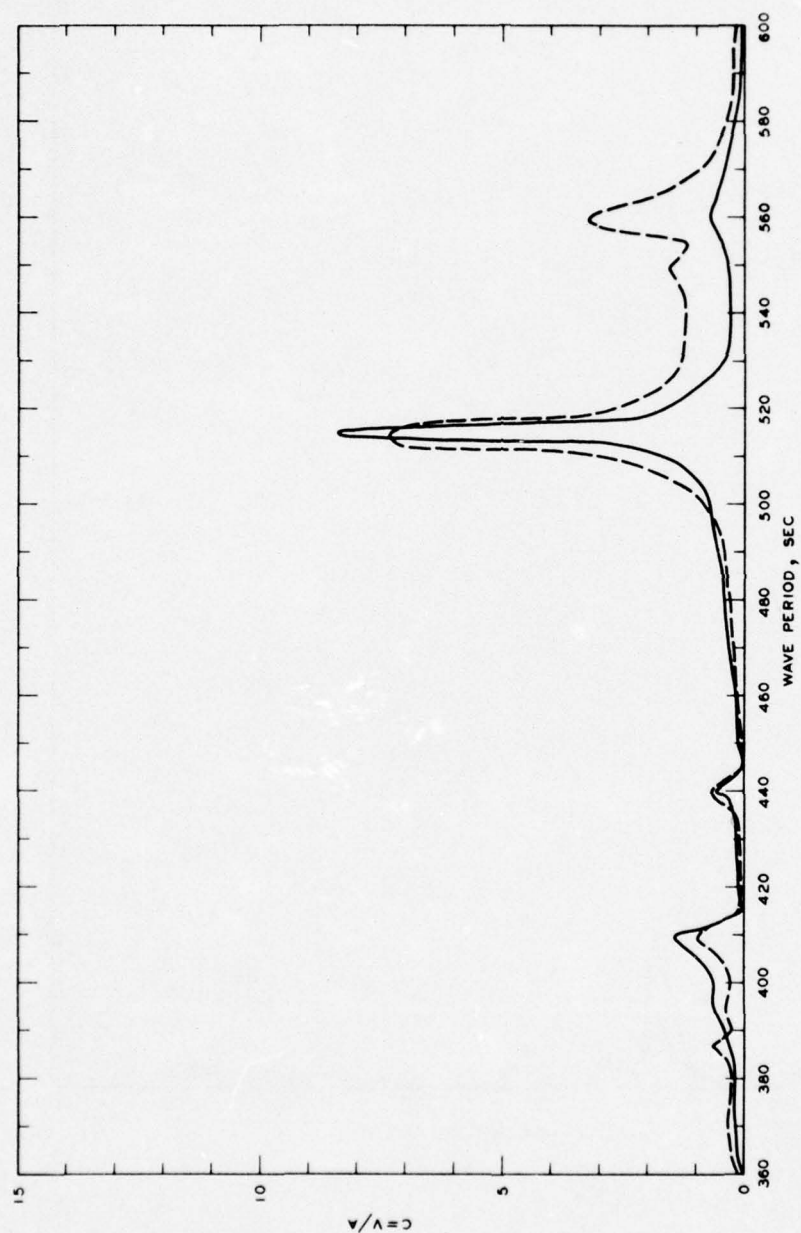


LEGEND

— GRID 4
 - - - GRID 4 A

NOTE: C = NORMALIZED MAXIMUM CURRENT VELOCITY
 V = CURRENT VELOCITY, FT/SEC
 A = INCIDENT WAVE AMPLITUDE

FREQUENCY RESPONSE
 NORMALIZED MAXIMUM CURRENT VELOCITY
 STA LB - 1, GRIDS 4 AND 4A

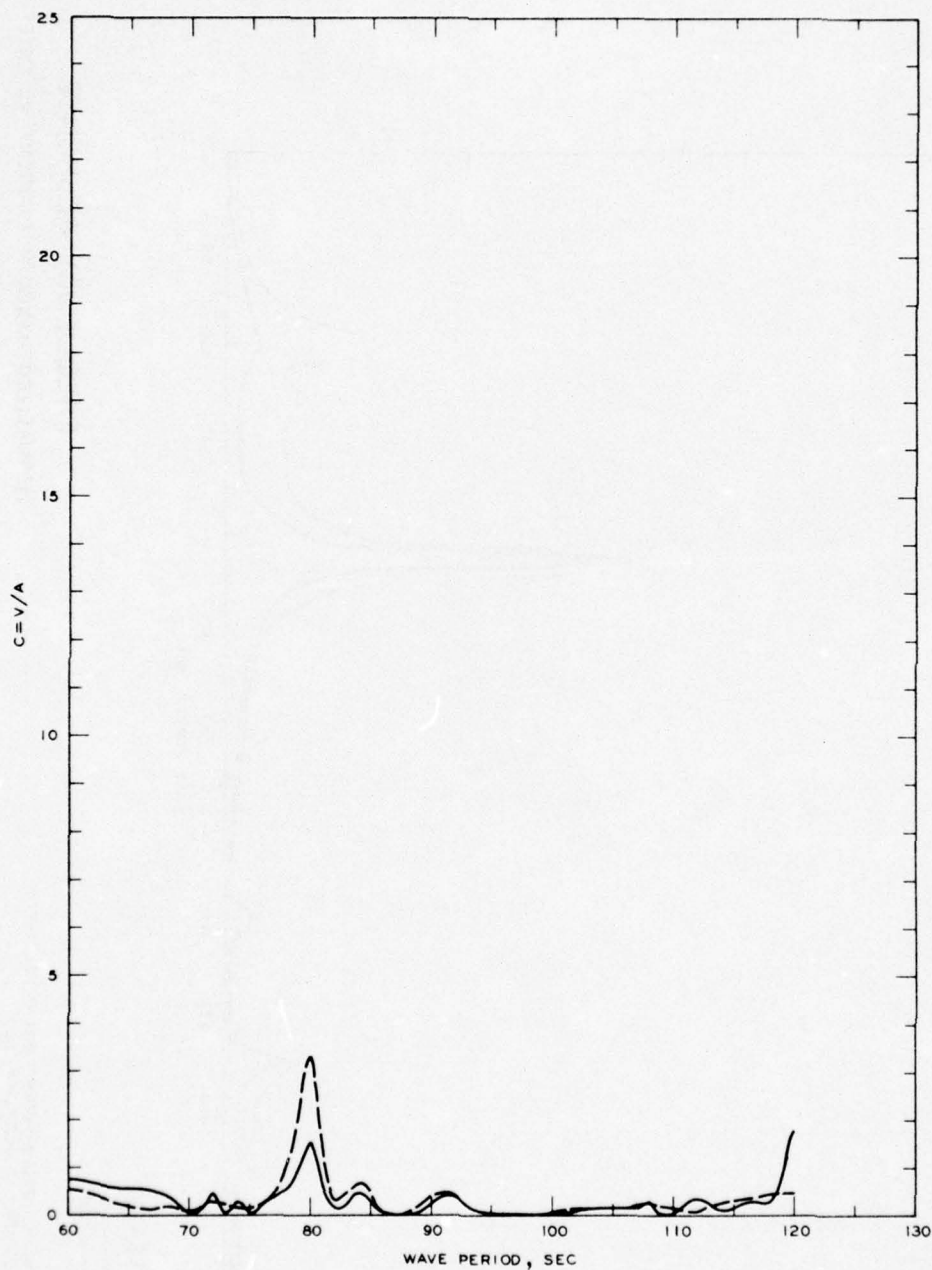


LEGEND

— GRID 5
 --- GRID 5 A

NOTE: C = NORMALIZED MAXIMUM CURRENT VELOCITY
 V = CURRENT VELOCITY, FT/SEC
 A = INCIDENT WAVE AMPLITUDE

FREQUENCY RESPONSE
 NORMALIZED MAXIMUM CURRENT VELOCITY
 STA LB-1, GRIDS 5 AND 5 A



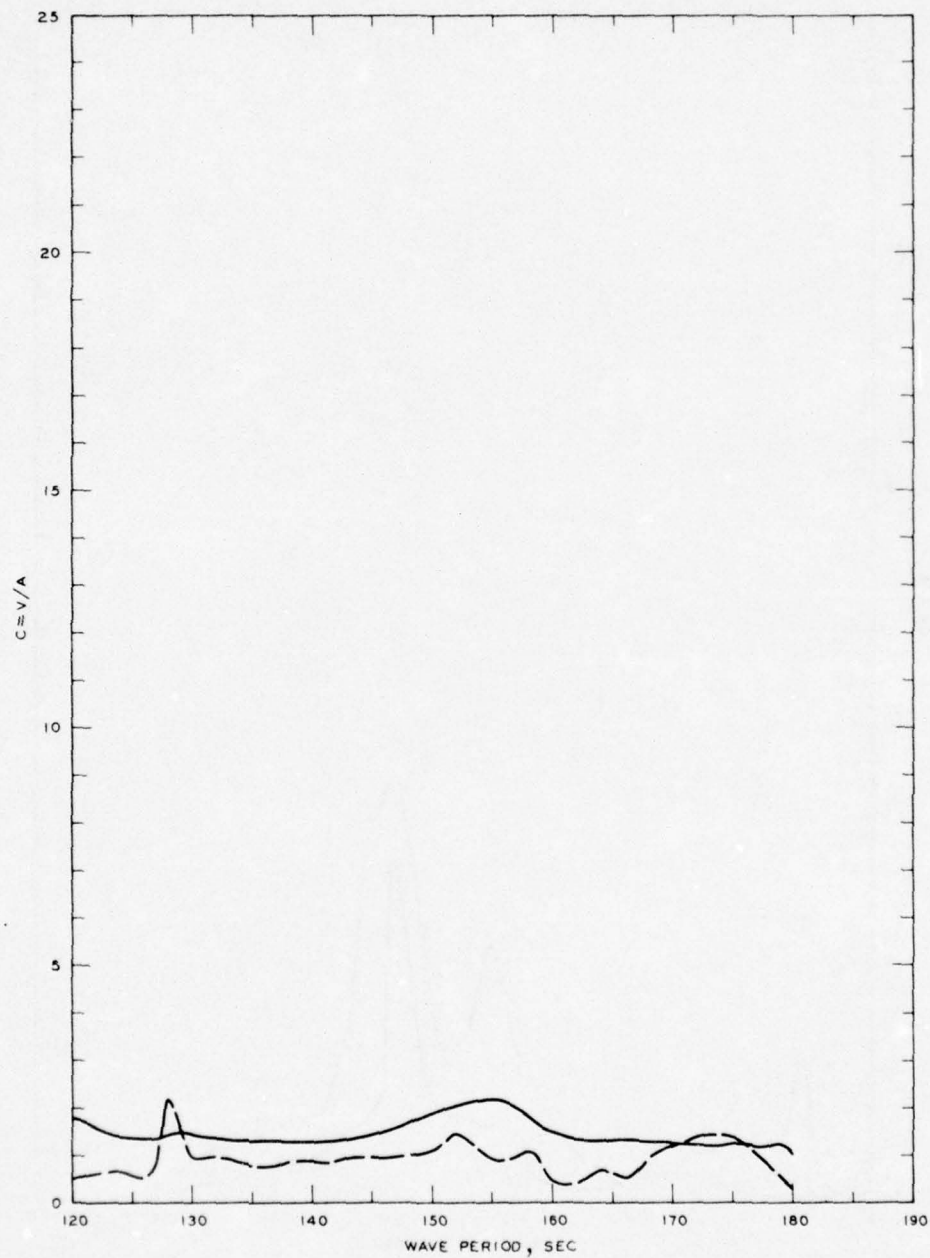
LEGEND

— GRID 1
 - - - GRID 1A

NOTE: C = NORMALIZED MAXIMUM CURRENT VELOCITY
 V = CURRENT VELOCITY, FT/SEC
 A = INCIDENT WAVE AMPLITUDE

FREQUENCY RESPONSE

NORMALIZED MAXIMUM CURRENT VELOCITY
 STA LB-2, GRIDS 1 AND 1A

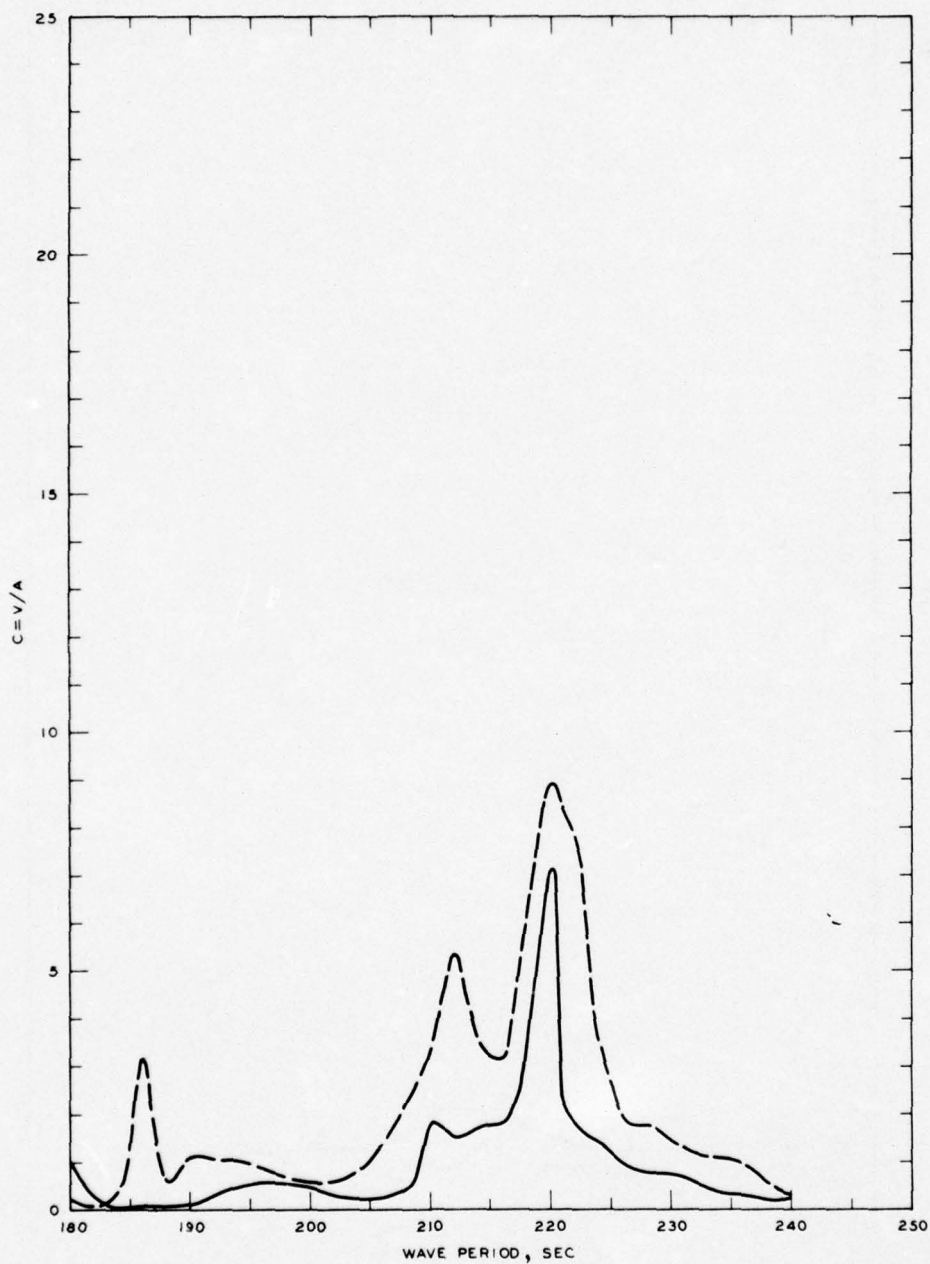


LEGEND

— GRID 2
 - - - GRID 2A

NOTE: C = NORMALIZED MAXIMUM CURRENT VELOCITY
 V = CURRENT VELOCITY, FT/SEC
 A = INCIDENT WAVE AMPLITUDE

FREQUENCY RESPONSE
 NORMALIZED MAXIMUM CURRENT VELOCITY
 STA LB-2, GRIDS 2 AND 2A



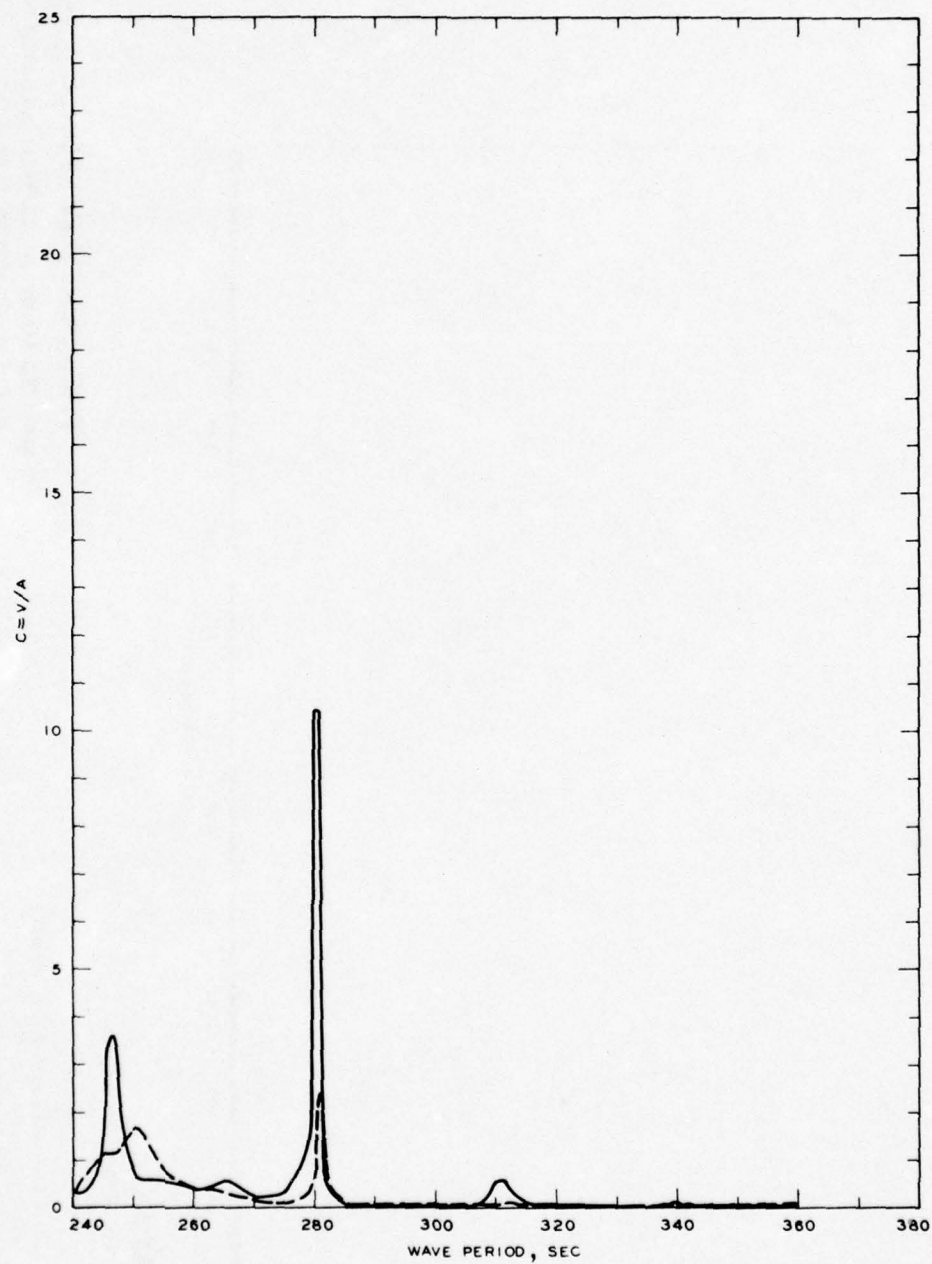
LEGEND

— GRID 3
 - - - GRID 3A

NOTE: C = NORMALIZED MAXIMUM CURRENT
 VELOCITY
 V = CURRENT VELOCITY, FT/SEC
 A = INCIDENT WAVE AMPLITUDE

FREQUENCY RESPONSE

NORMALIZED MAXIMUM CURRENT VELOCITY
 STA LB-2, GRIDS 3 AND 3A

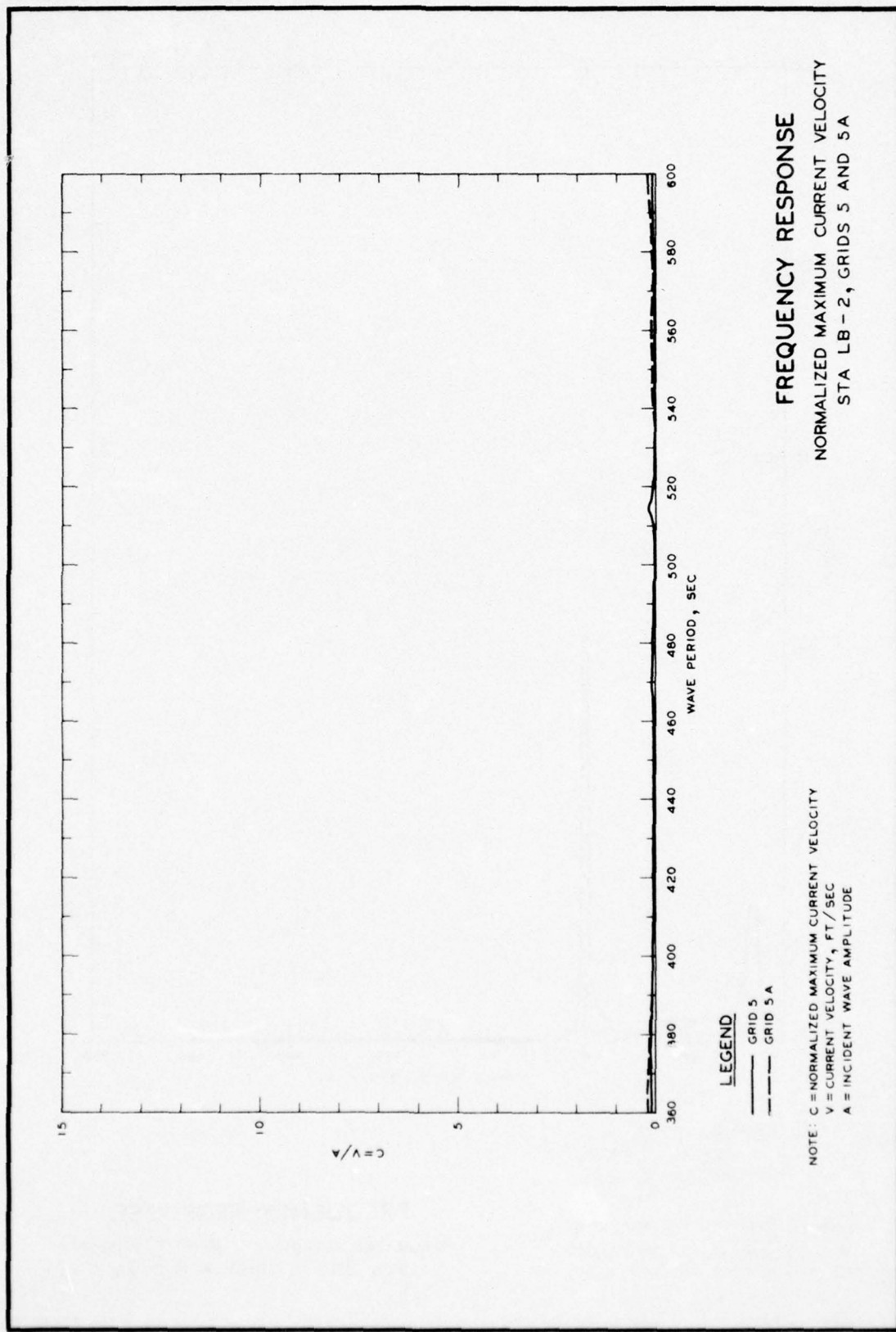


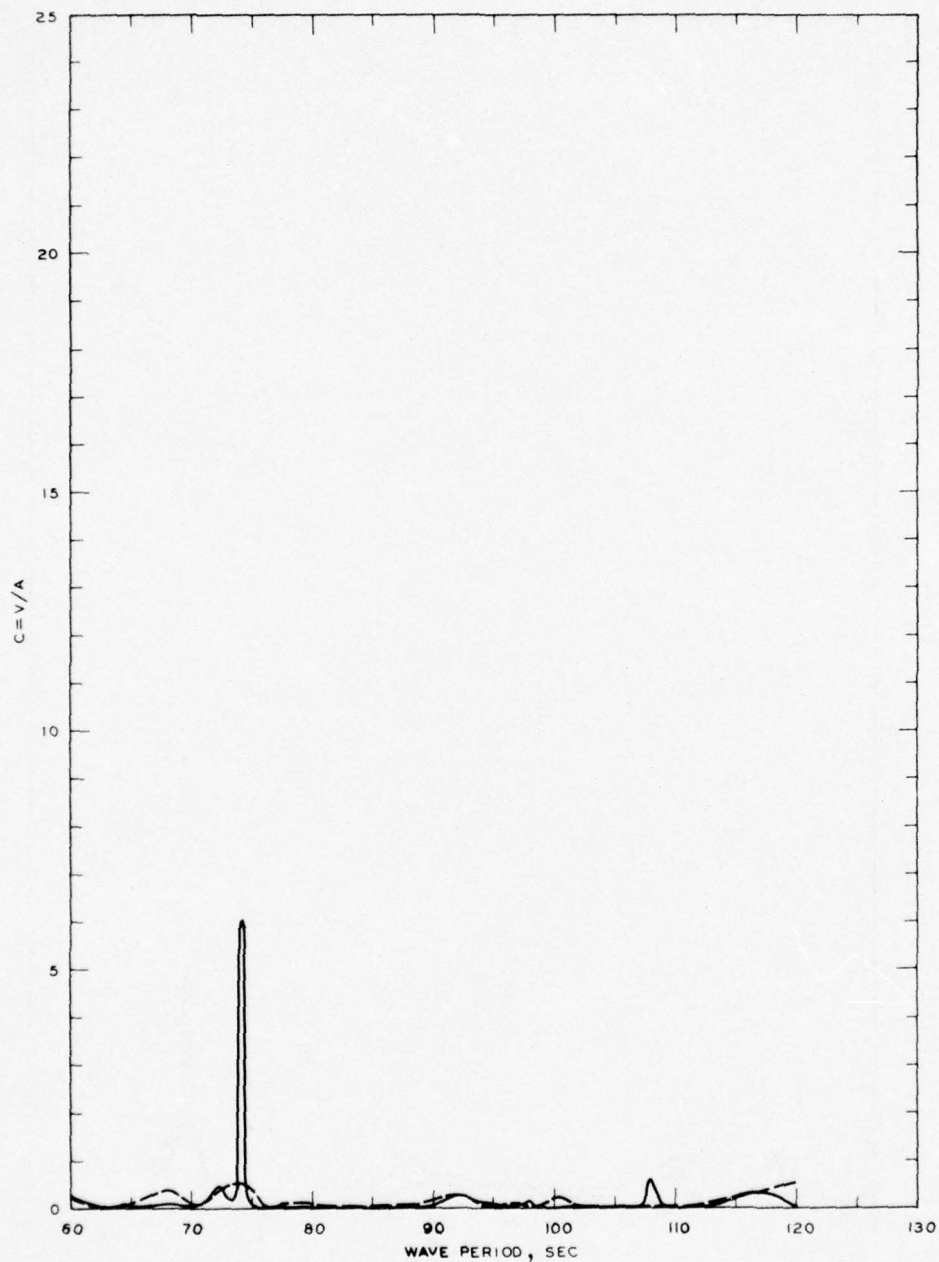
LEGEND

— GRID 4
 - - - GRID 4A

NOTE: C = NORMALIZED MAXIMUM CURRENT VELOCITY
 V = CURRENT VELOCITY, FT/SEC
 A = INCIDENT WAVE AMPLITUDE

FREQUENCY RESPONSE
 NORMALIZED MAXIMUM CURRENT VELOCITY
 STA LB - 2, GRIDS 4 AND 4A





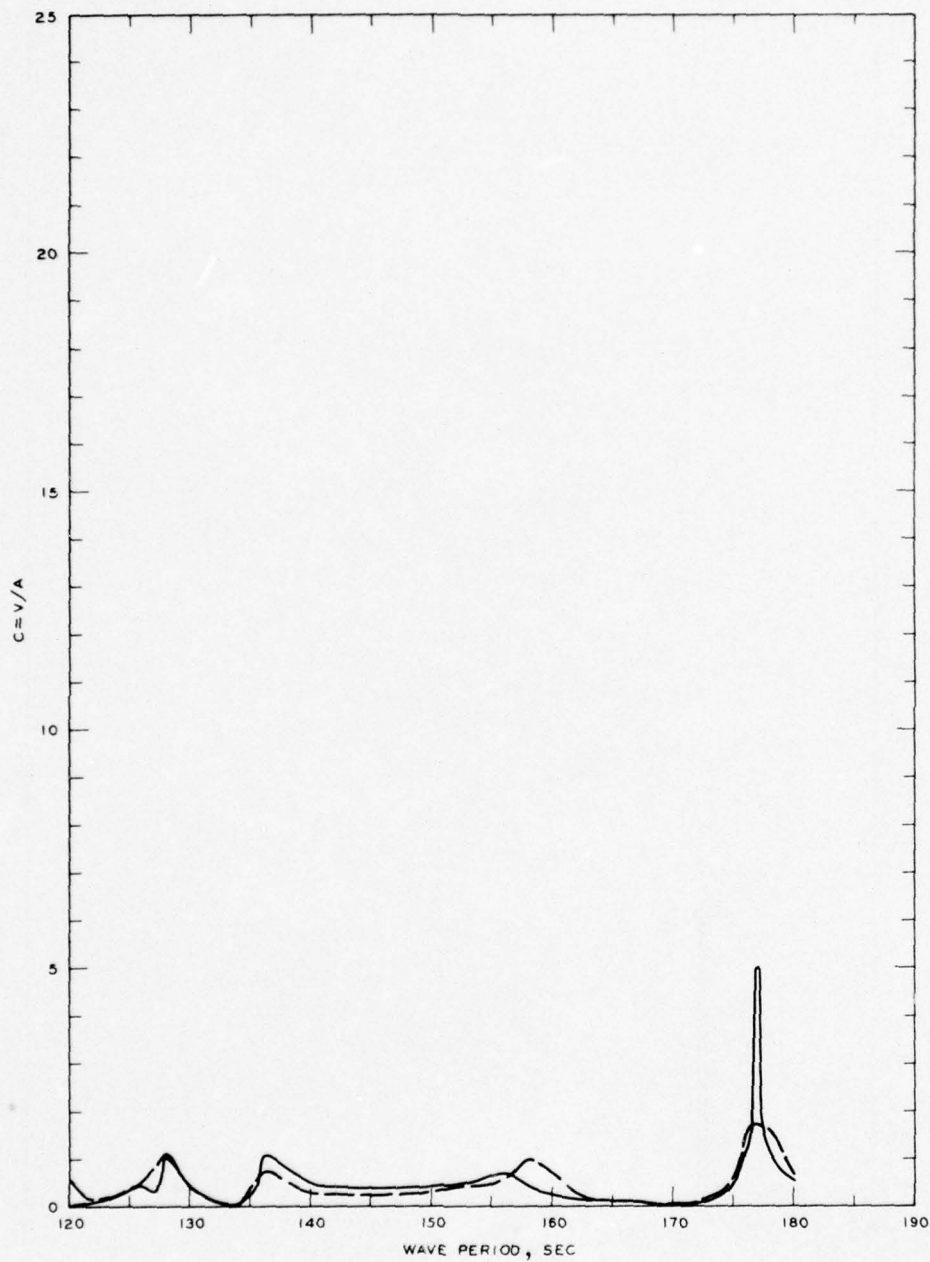
LEGEND

— GRID 1
 - - - GRID 1A

NOTE: C = NORMALIZED MAXIMUM CURRENT
 VELOCITY
 V = CURRENT VELOCITY, FT/SEC
 A = INCIDENT WAVE AMPLITUDE

FREQUENCY RESPONSE

NORMALIZED MAXIMUM CURRENT VELOCITY
 STA LB-3, GRIDS 1 AND 1A



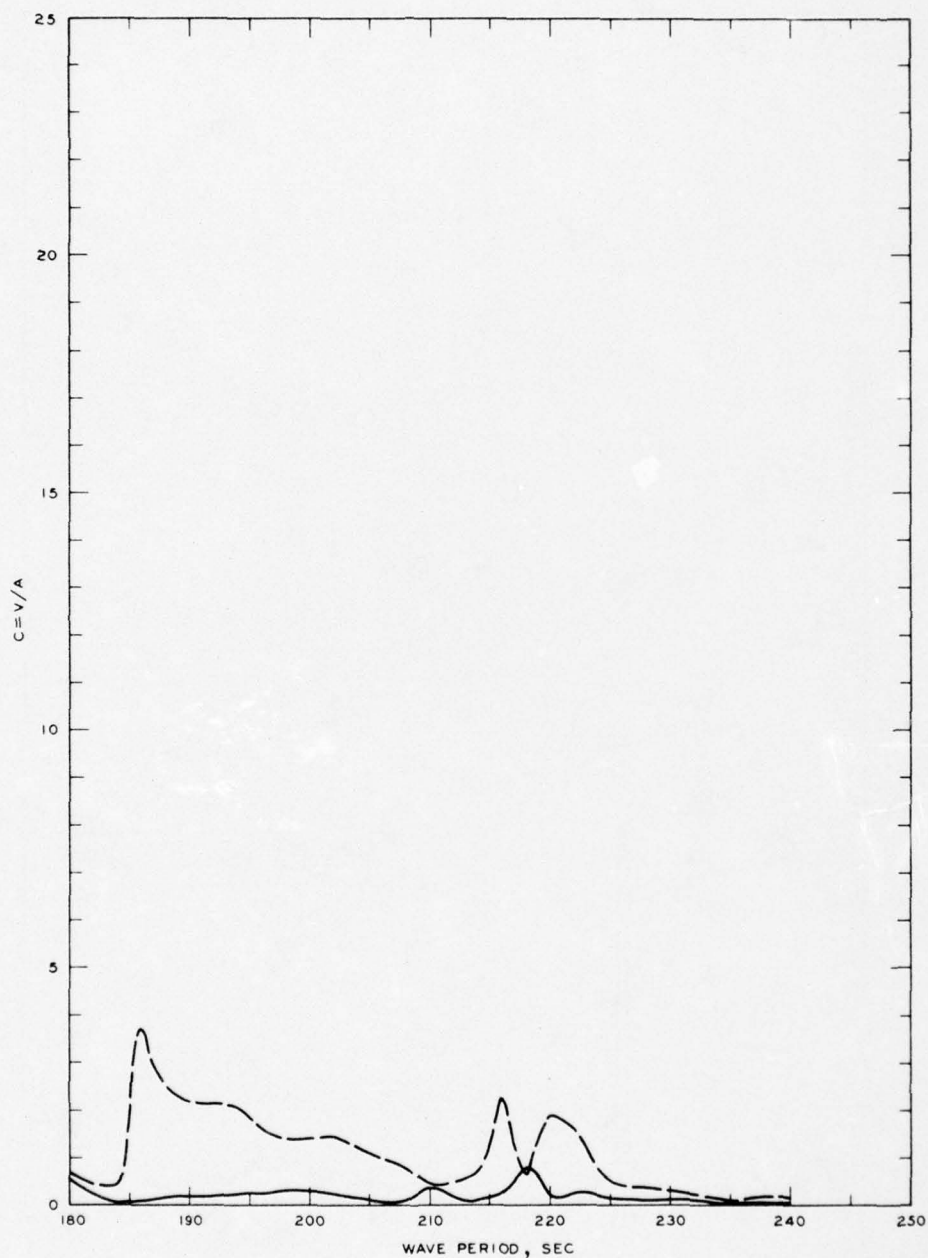
LEGEND

— GRID 2
 - - - GRID 2A

NOTE: C = NORMALIZED MAXIMUM CURRENT
 VELOCITY
 V = CURRENT VELOCITY, FT/SEC
 A = INCIDENT WAVE AMPLITUDE

FREQUENCY RESPONSE

NORMALIZED MAXIMUM CURRENT VELOCITY
 STA LB-3, GRIDS 2 AND 2A

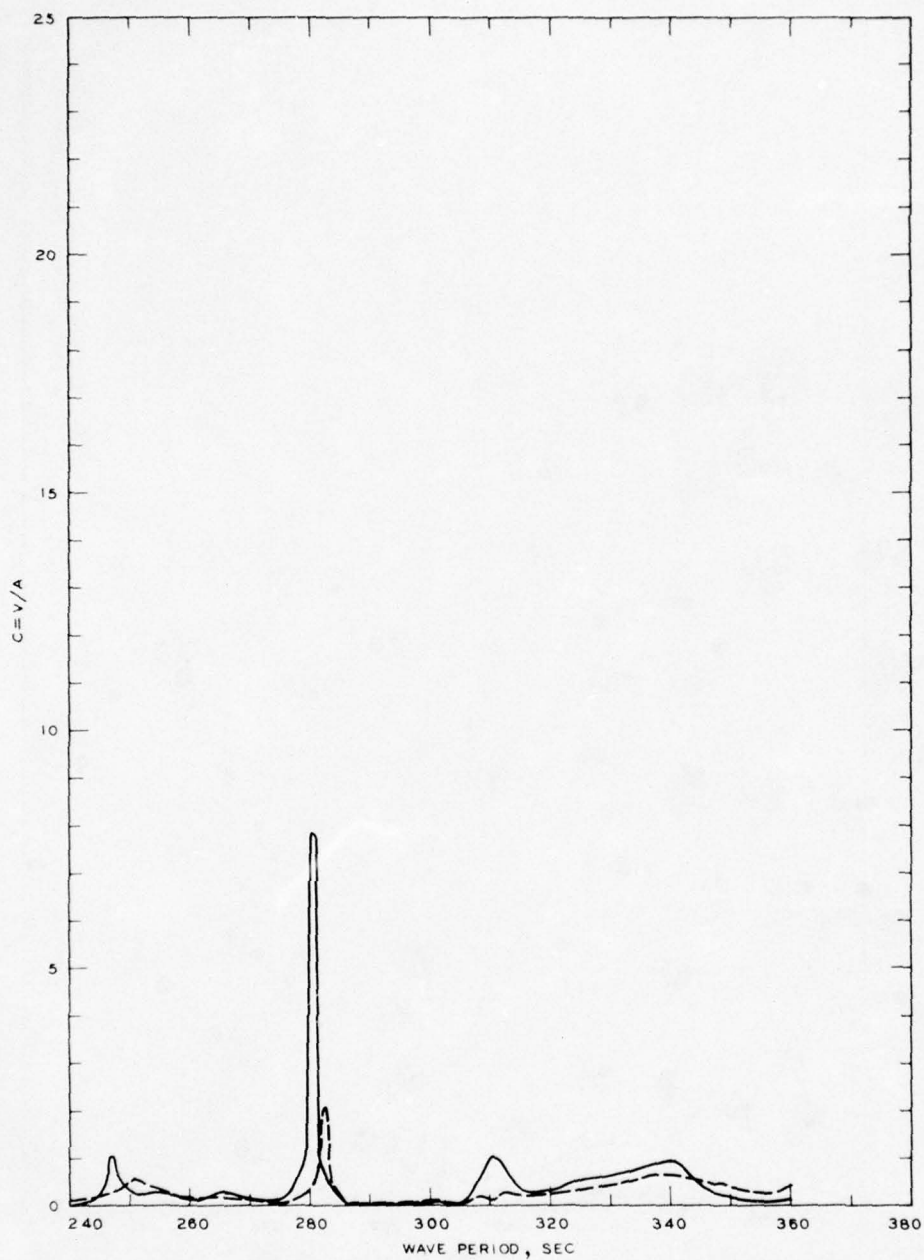


LEGEND

— GRID 3
 - - - GRID 3A

NOTE: C = NORMALIZED MAXIMUM CURRENT VELOCITY
 V = CURRENT VELOCITY, FT/SEC
 A = INCIDENT WAVE AMPLITUDE

FREQUENCY RESPONSE
 NORMALIZED MAXIMUM CURRENT VELOCITY
 STA LB-3, GRIDS 3 AND 3A

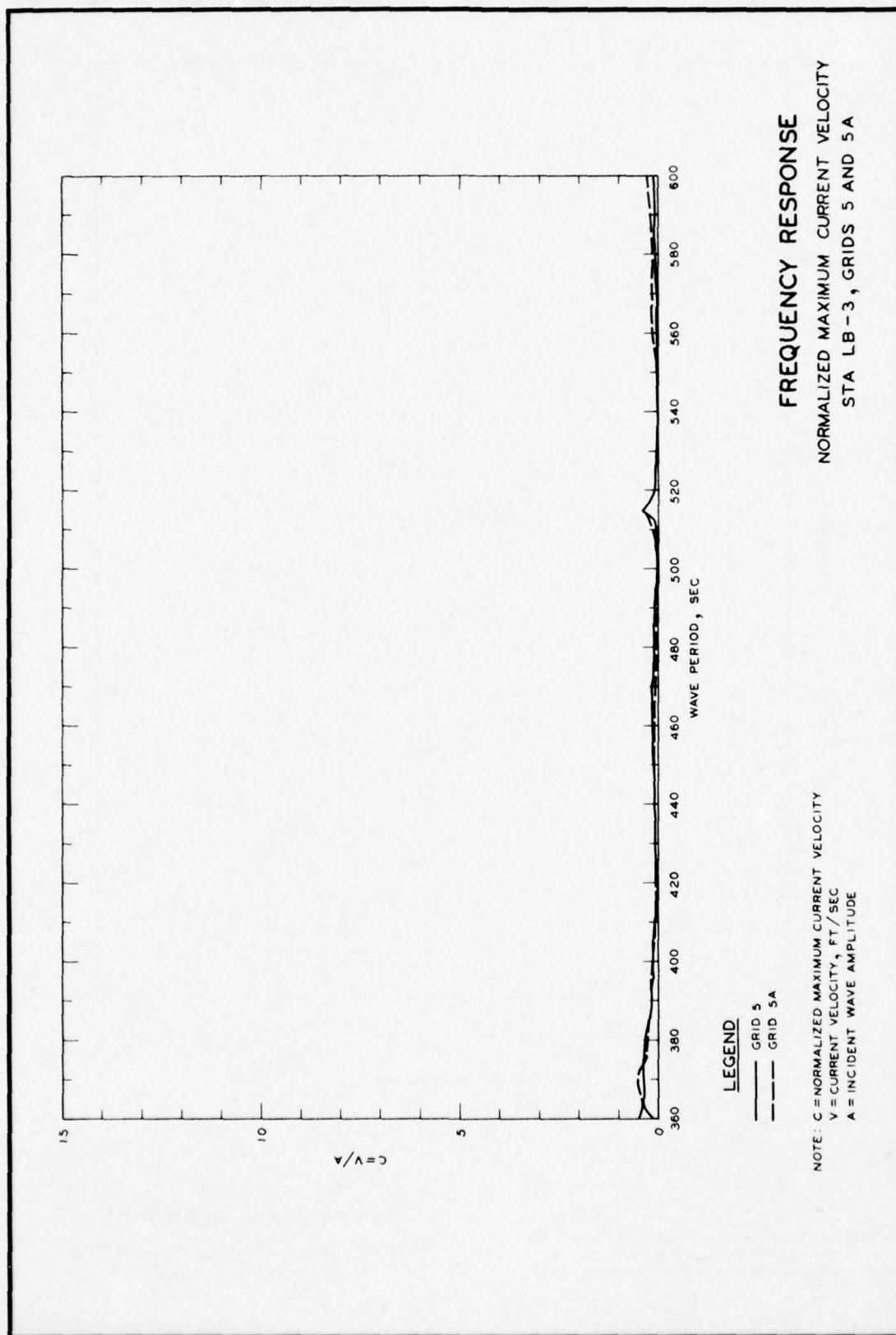


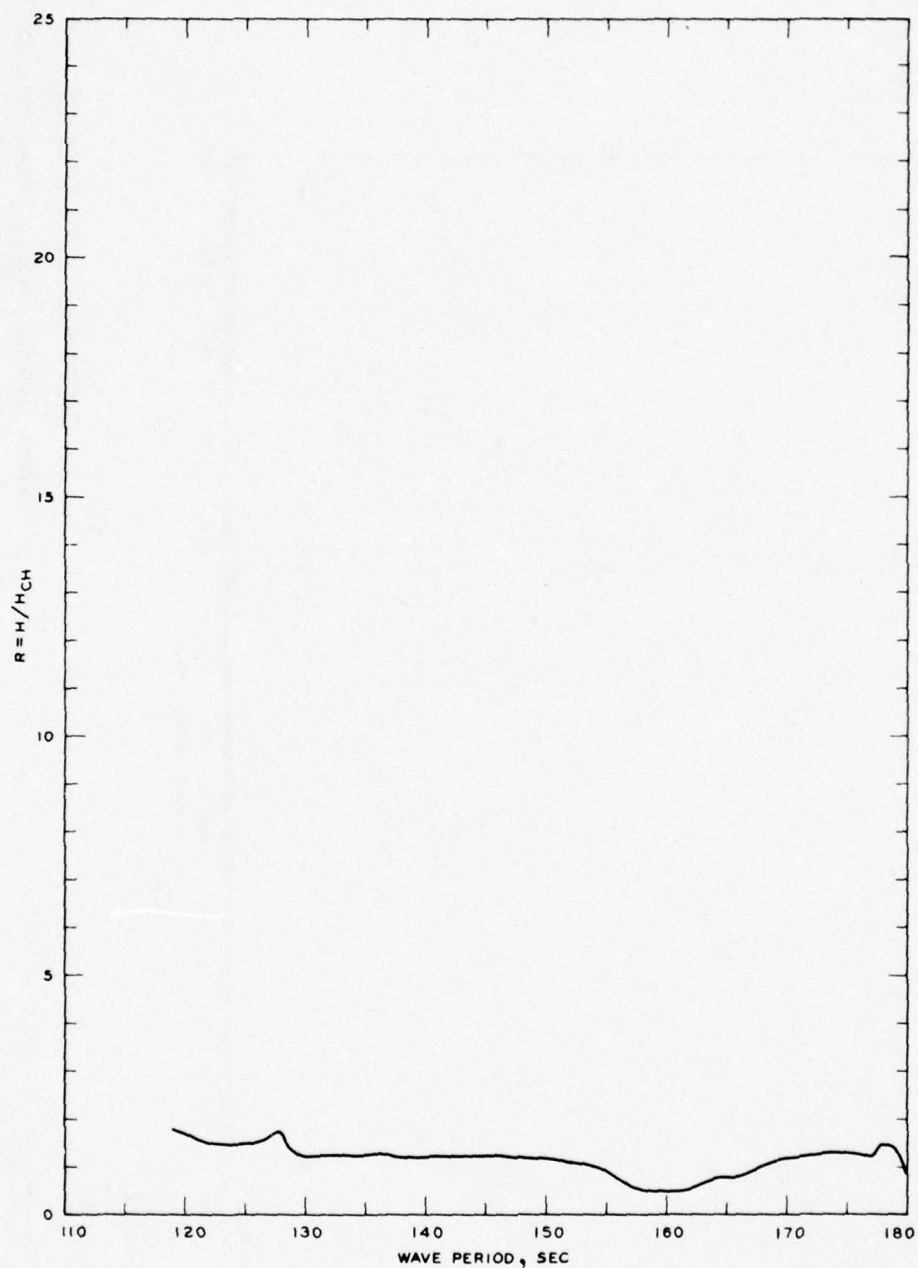
LEGEND

— GRID 4
 - - - GRID 4A

NOTE: C = NORMALIZED MAXIMUM CURRENT
 VELOCITY
 V = CURRENT VELOCITY, FT/SEC
 A = INCIDENT WAVE AMPLITUDE

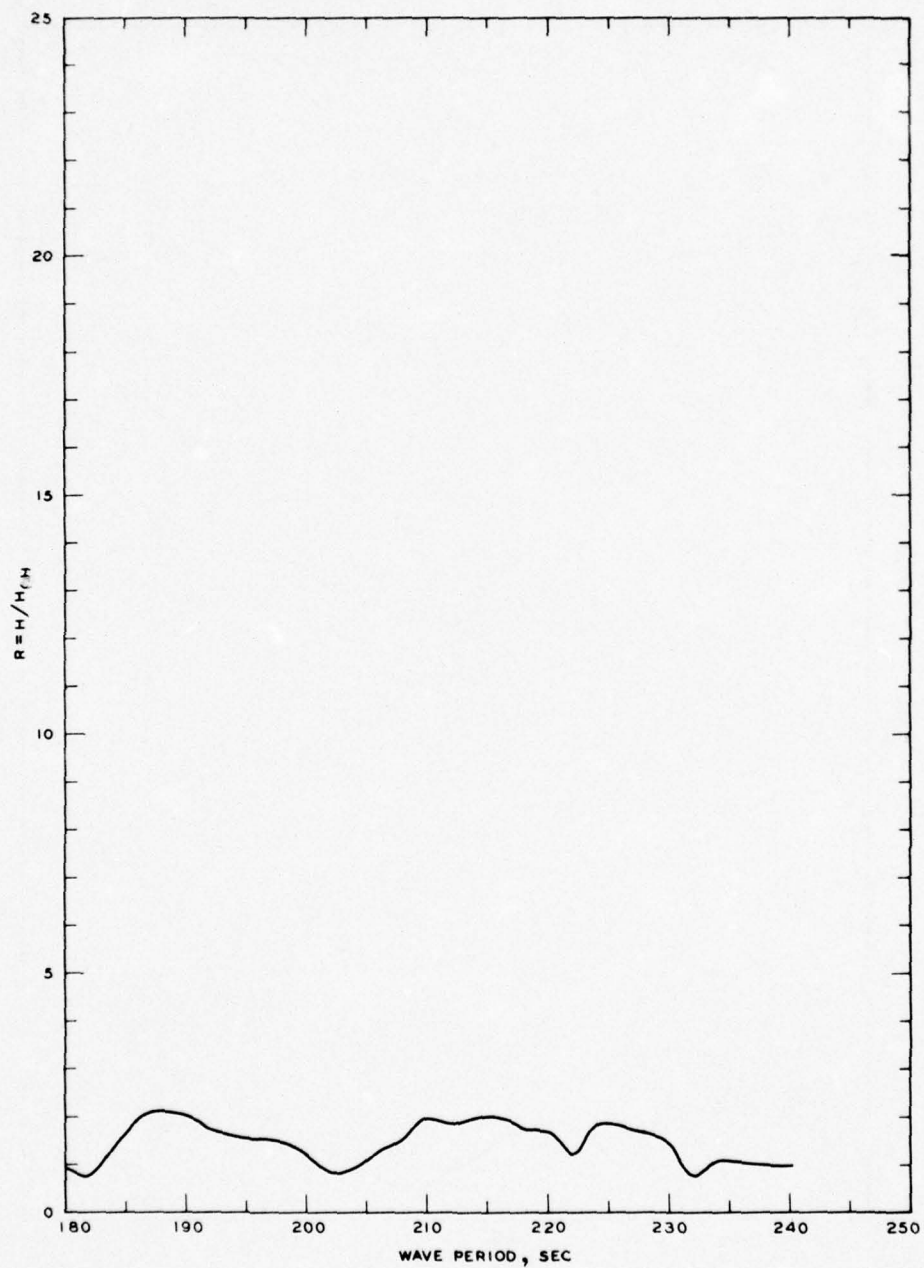
FREQUENCY RESPONSE
 NORMALIZED MAXIMUM CURRENT VELOCITY
 STA LB-3, GRIDS 4 AND 4A





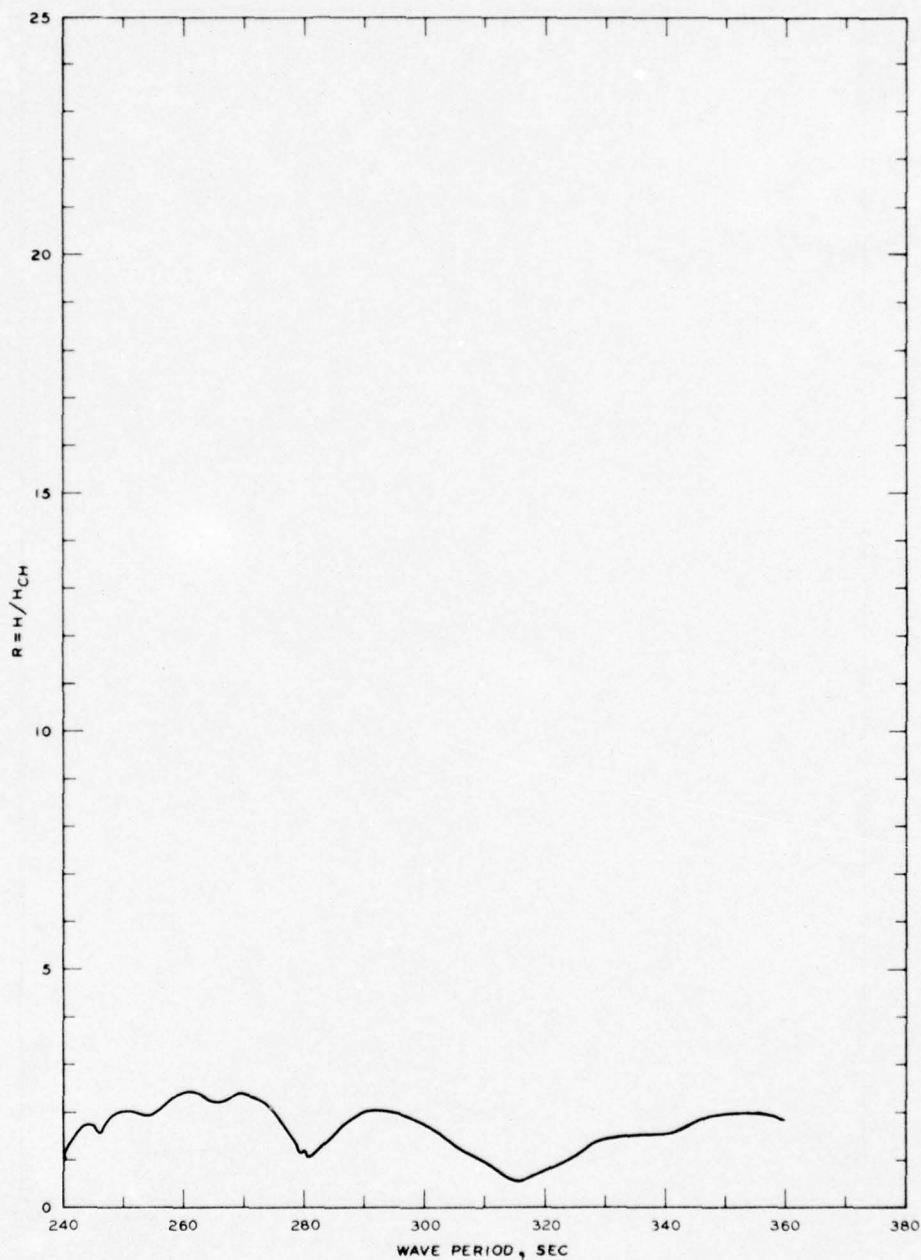
NOTE R = WAVE-HEIGHT AMPLIFICATION FACTOR
 H = WAVE HEIGHT, FT
 H_{CH} = WAVE HEIGHT FOR CLOSED HARBOR, FT

FREQUENCY RESPONSE
 WAVE-HEIGHT AMPLIFICATION FACTOR
 STA LB-4, GRID 2



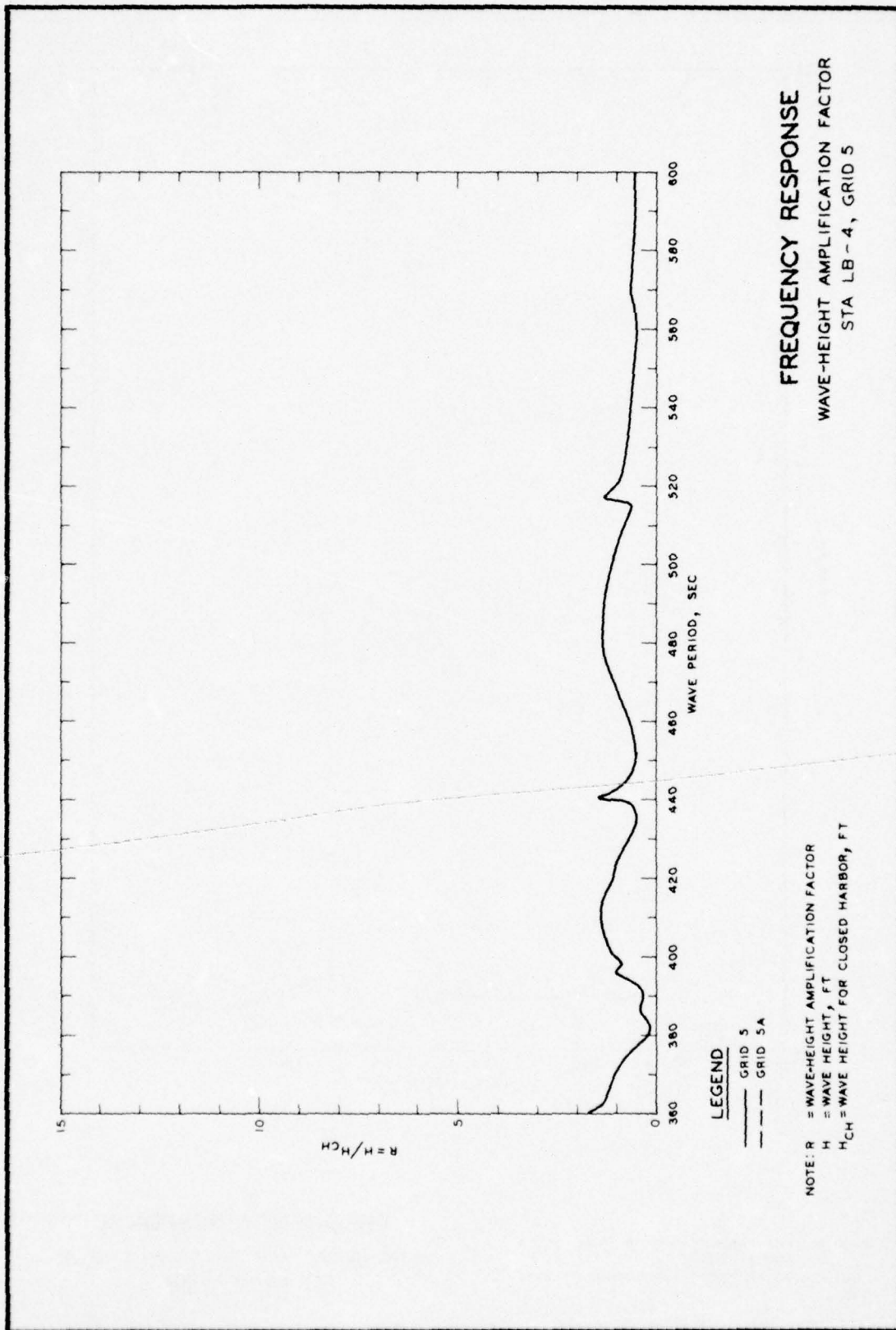
NOTE: R = WAVE-HEIGHT AMPLIFICATION FACTOR
 H = WAVE HEIGHT, FT
 H_{CH} = WAVE HEIGHT FOR CLOSED HARBOR, FT

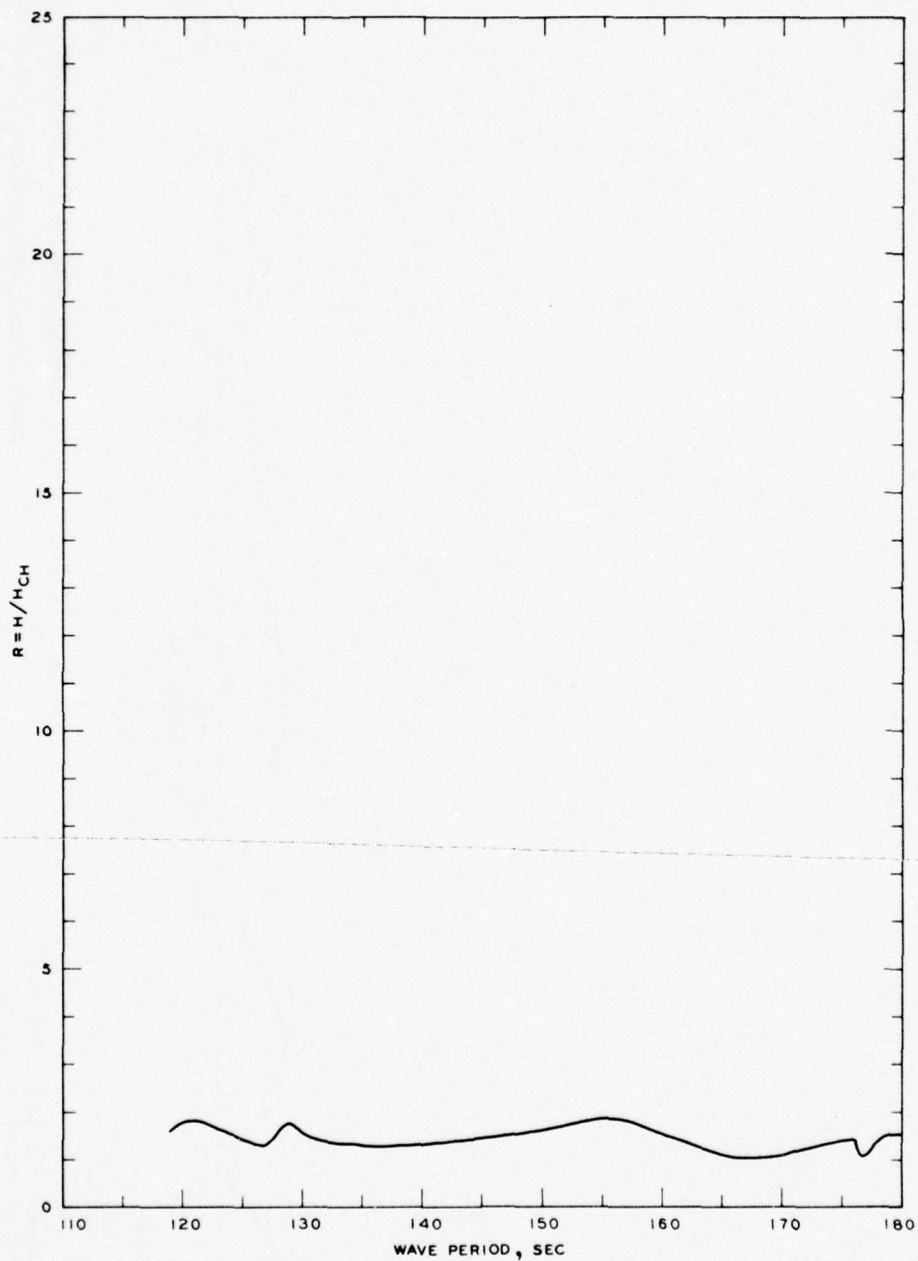
FREQUENCY RESPONSE
 WAVE-HEIGHT AMPLIFICATION FACTOR
 STA LB - 4, GRID 3



NOTE R = WAVE-HEIGHT AMPLIFICATION FACTOR
 H = WAVE HEIGHT, FT
 H_{CH} = WAVE HEIGHT FOR CLOSED HARBOR, FT

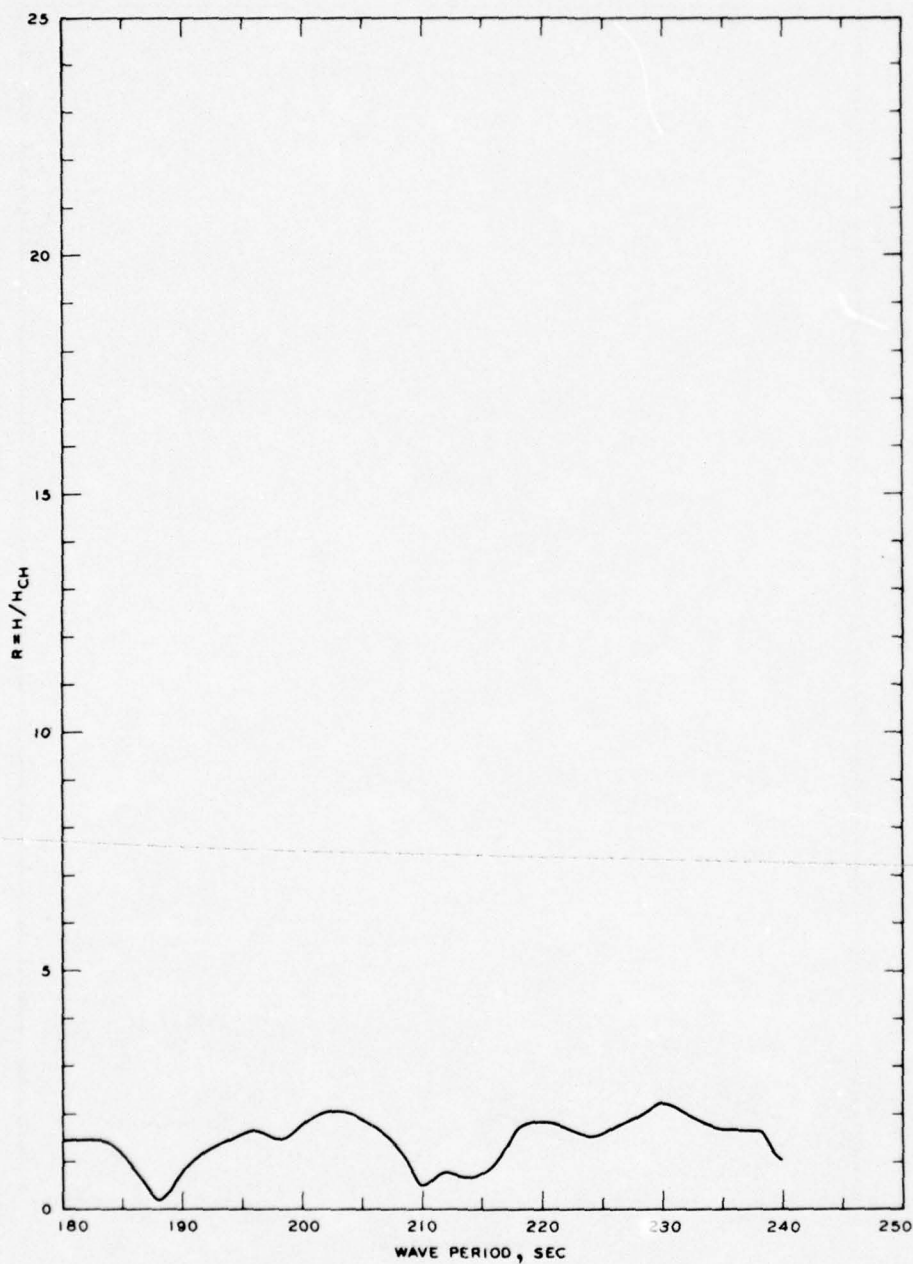
FREQUENCY RESPONSE
 WAVE-HEIGHT AMPLIFICATION FACTOR
 STA LB-4, GRID 4





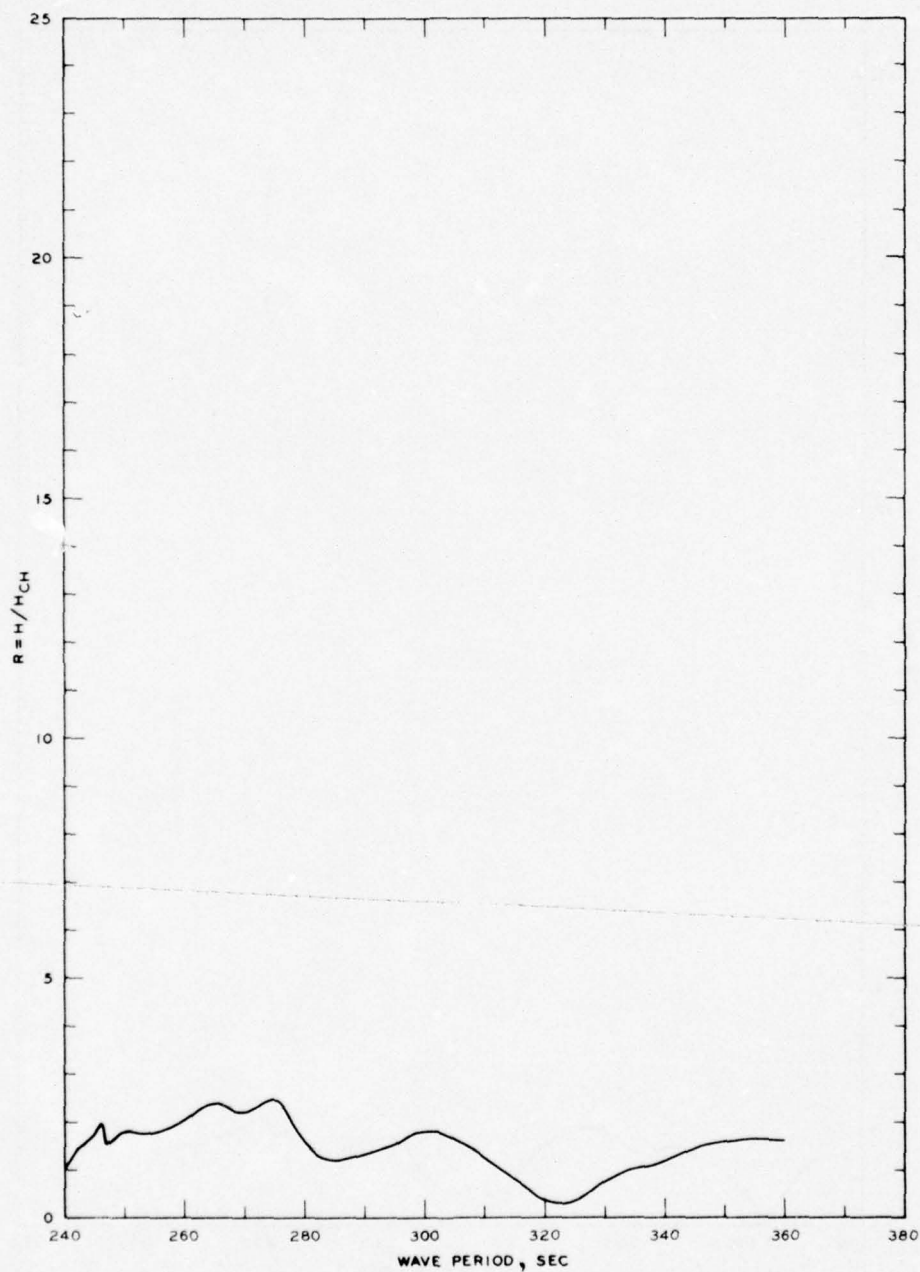
NOTE: R = WAVE-HEIGHT AMPLIFICATION FACTOR
 H = WAVE HEIGHT, FT
 H_{CH} = WAVE HEIGHT FOR CLOSED HARBOR, FT

FREQUENCY RESPONSE
WAVE-HEIGHT AMPLIFICATION FACTOR
STA LB-5, GRID 2



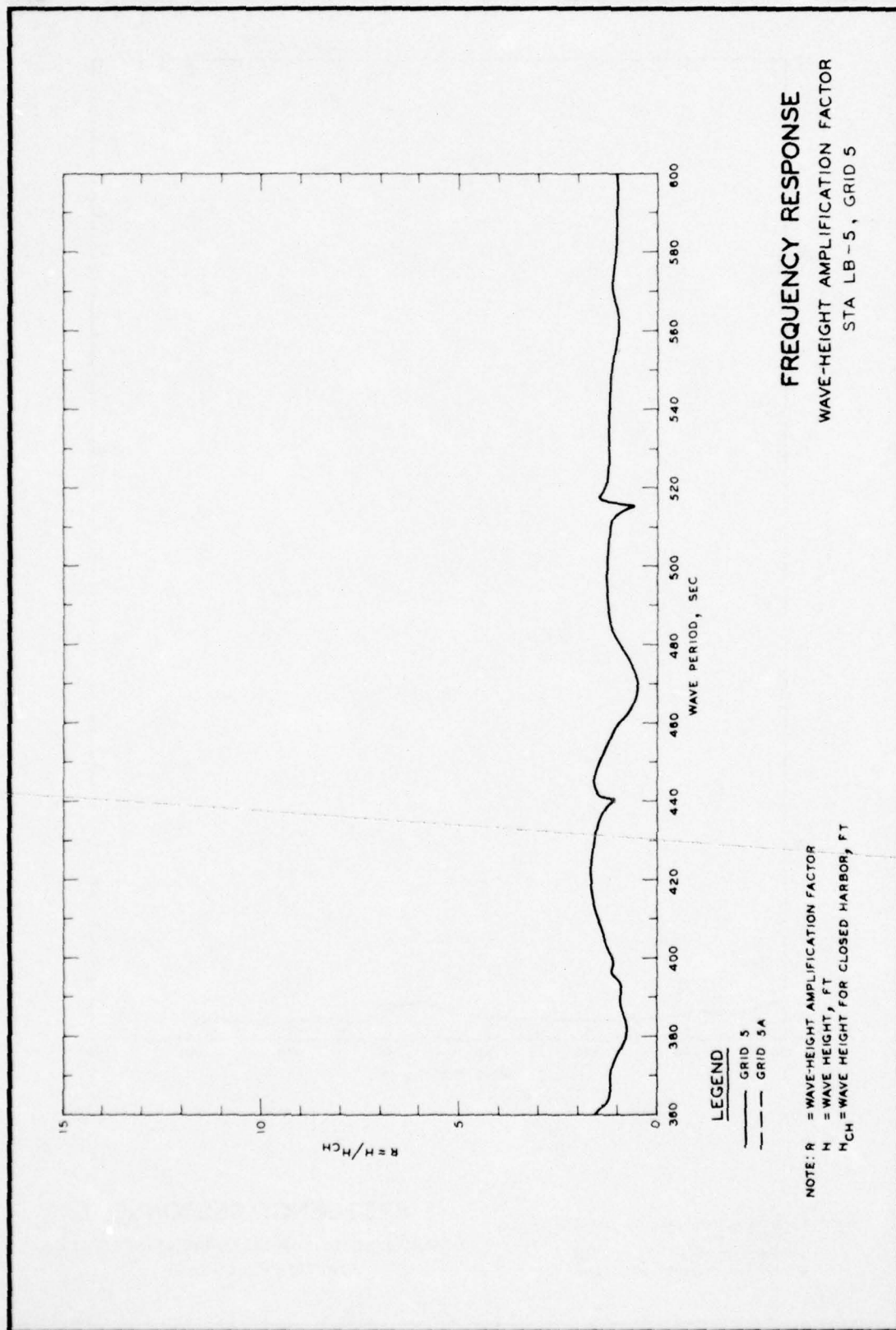
NOTE R = WAVE-HEIGHT AMPLIFICATION FACTOR
H = WAVE HEIGHT, FT
H_{CH} = WAVE HEIGHT FOR CLOSED HARBOR, FT

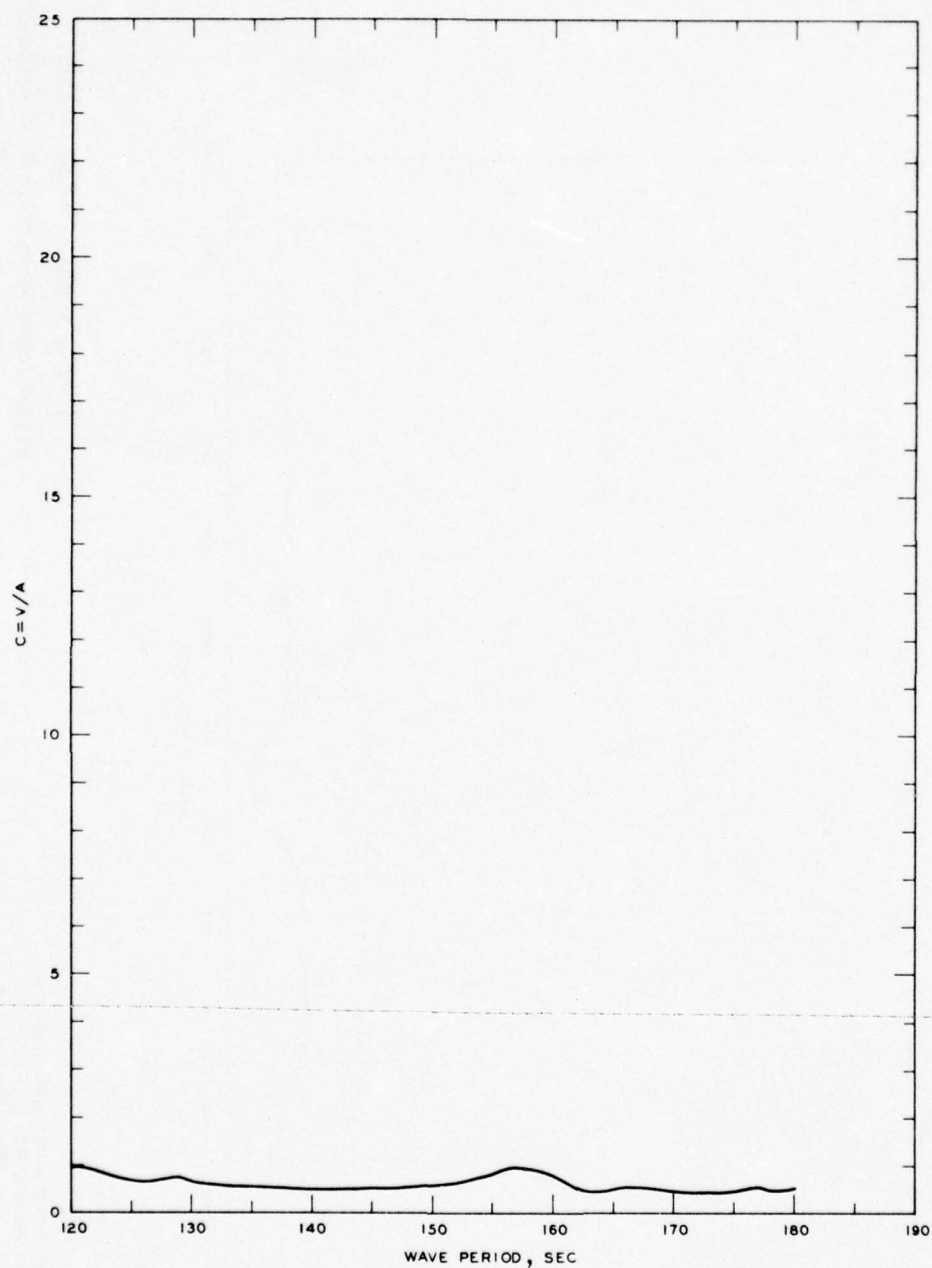
FREQUENCY RESPONSE
WAVE-HEIGHT AMPLIFICATION FACTOR
STA LB-5, GRID 3



NOTE R = WAVE-HEIGHT AMPLIFICATION FACTOR
H = WAVE HEIGHT, FT
H_{CH} = WAVE HEIGHT FOR CLOSED HARBOR, FT

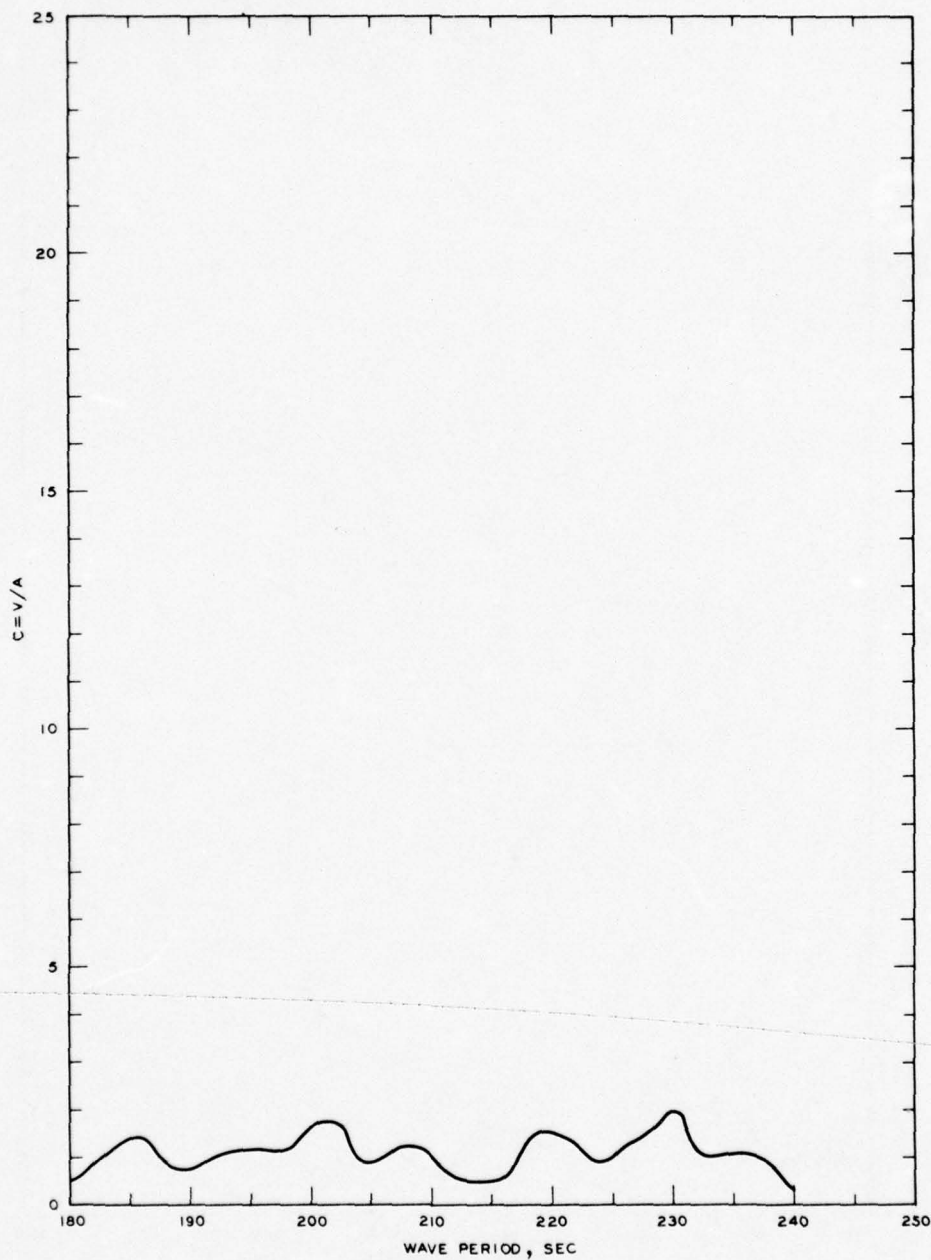
FREQUENCY RESPONSE
WAVE-HEIGHT AMPLIFICATION FACTOR
STA LB-5, GRID 4





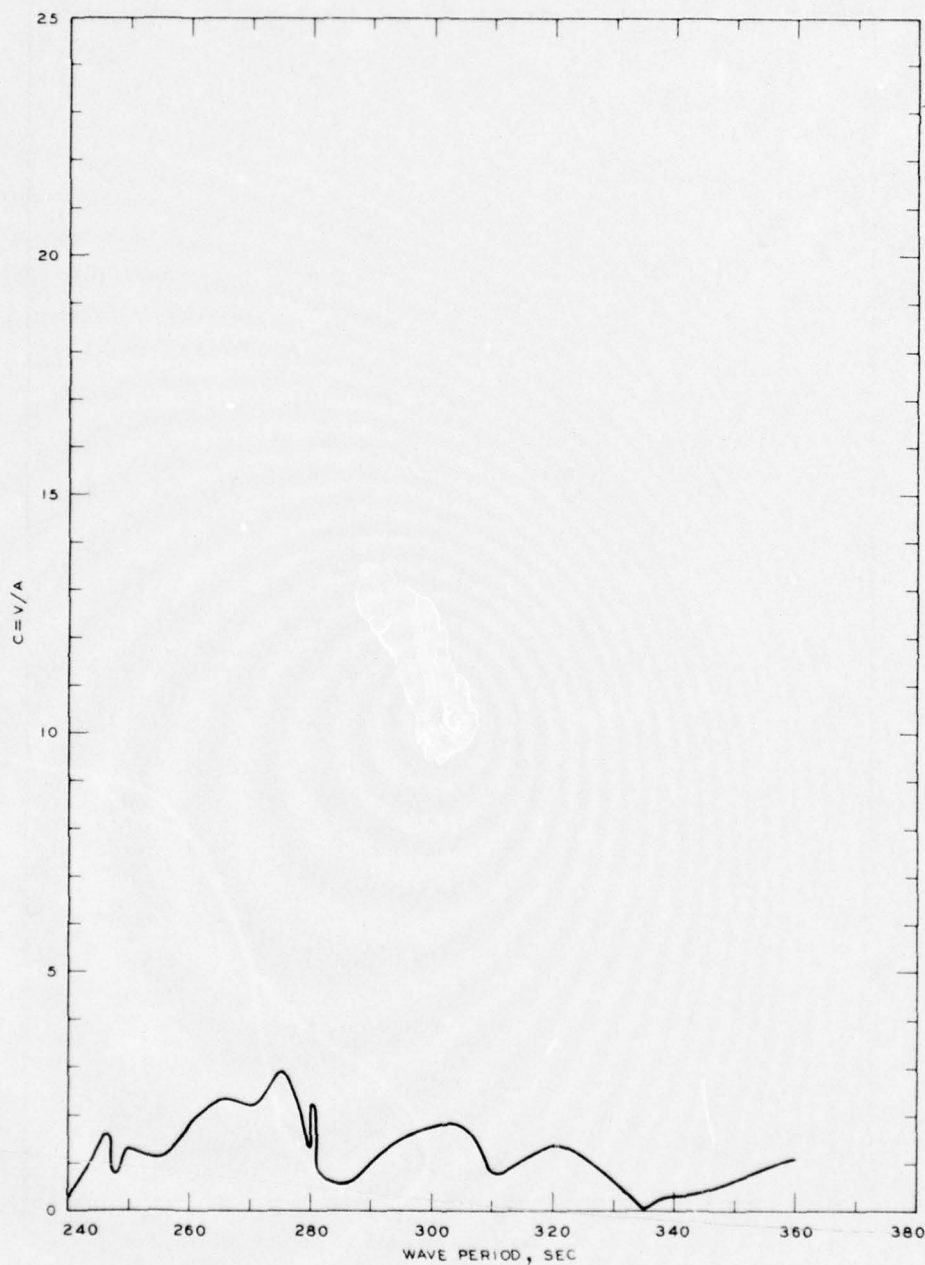
NOTE: C = NORMALIZED MAXIMUM CURRENT
VELOCITY
V = CURRENT VELOCITY, FT/SEC
A = INCIDENT WAVE AMPLITUDE

FREQUENCY RESPONSE
NORMALIZED MAXIMUM CURRENT VELOCITY
STA LB-4, GRID 2



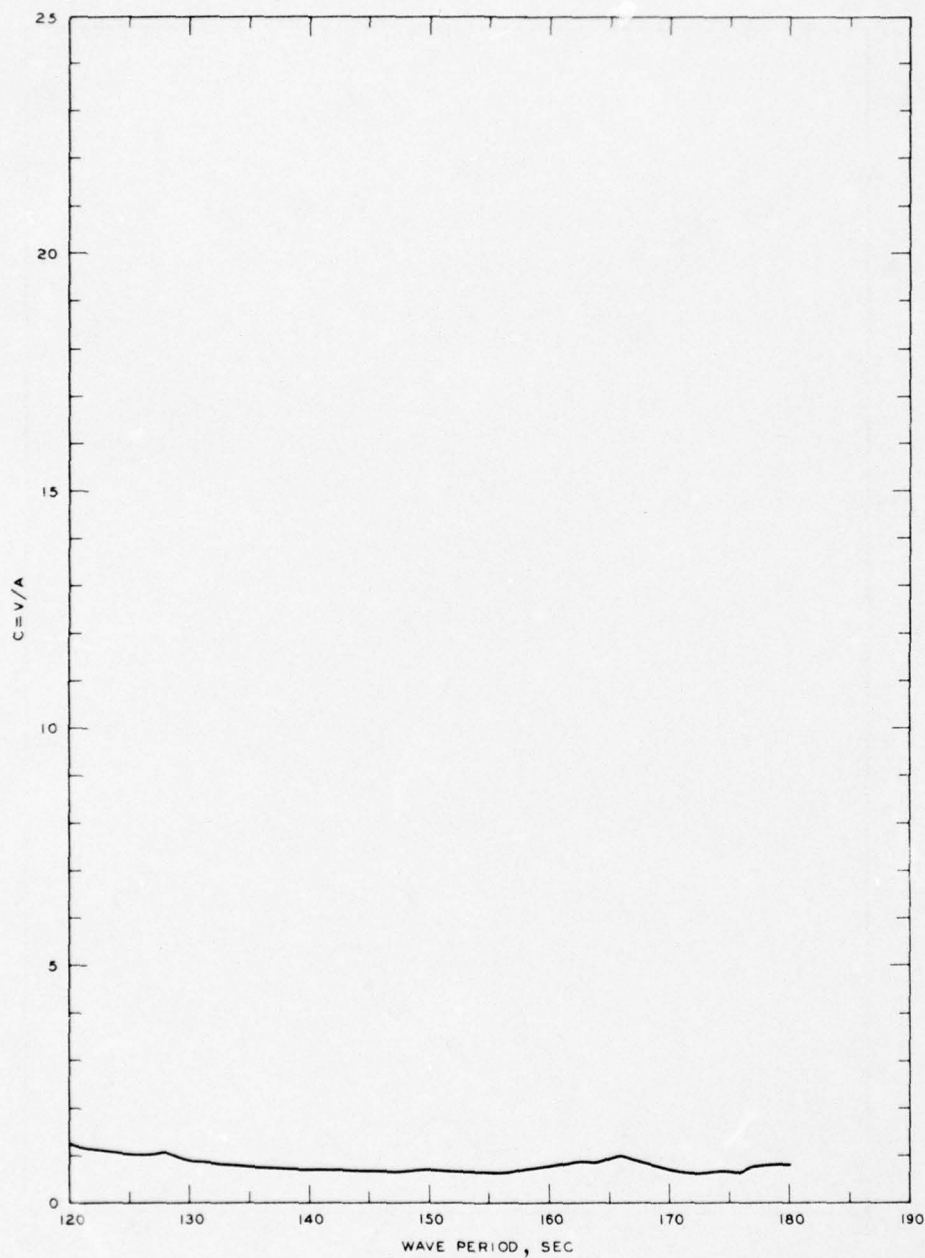
NOTE: C = NORMALIZED MAXIMUM CURRENT
VELOCITY
V = CURRENT VELOCITY, FT/SEC
A = INCIDENT WAVE AMPLITUDE

FREQUENCY RESPONSE
NORMALIZED MAXIMUM CURRENT VELOCITY
STA LB-4, GRID 3



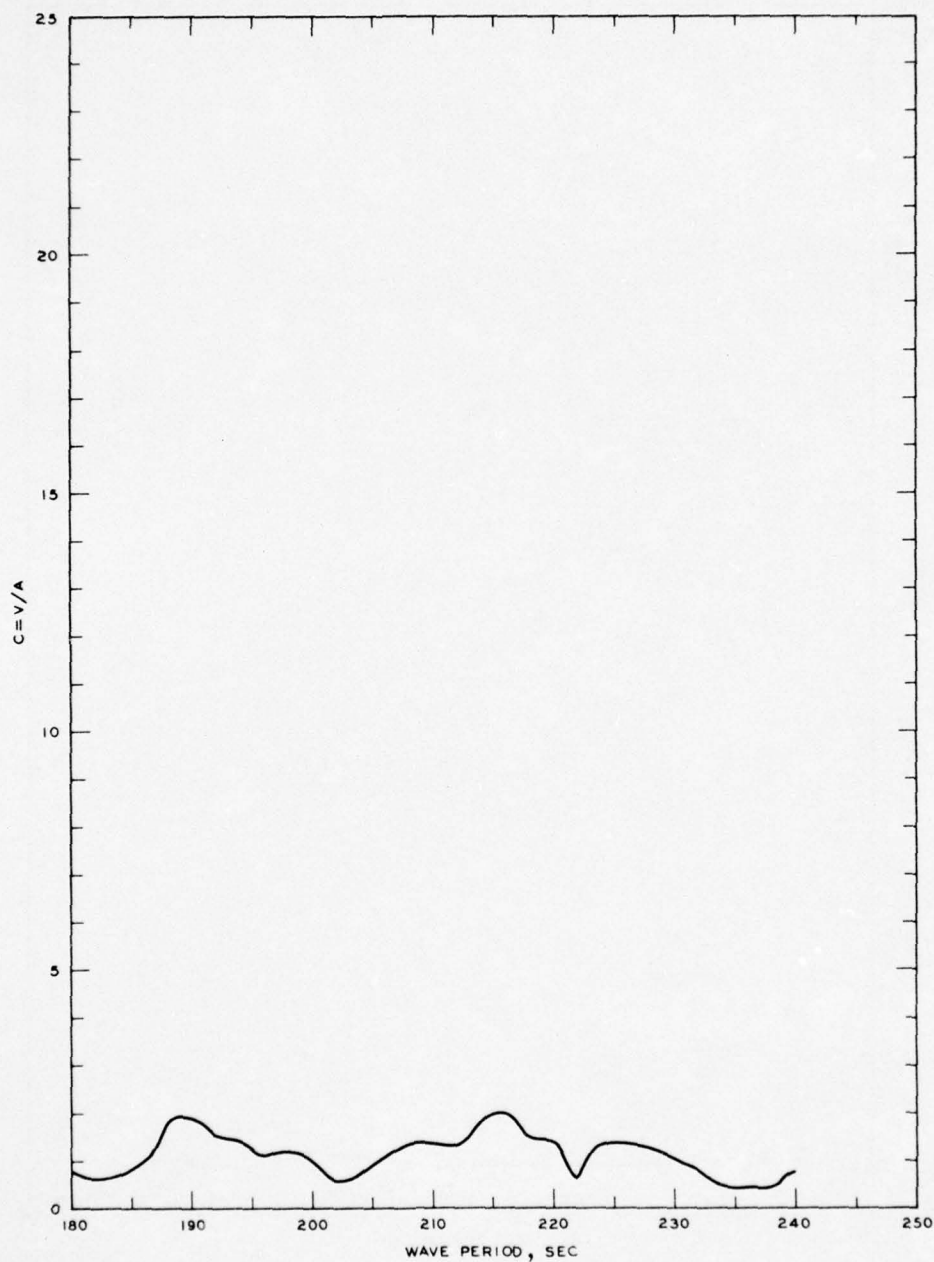
NOTE: C = NORMALIZED MAXIMUM CURRENT
VELOCITY
V = CURRENT VELOCITY, FT/SEC
A = INCIDENT WAVE AMPLITUDE

FREQUENCY RESPONSE
NORMALIZED MAXIMUM CURRENT VELOCITY
STA LB-4, GRID 4



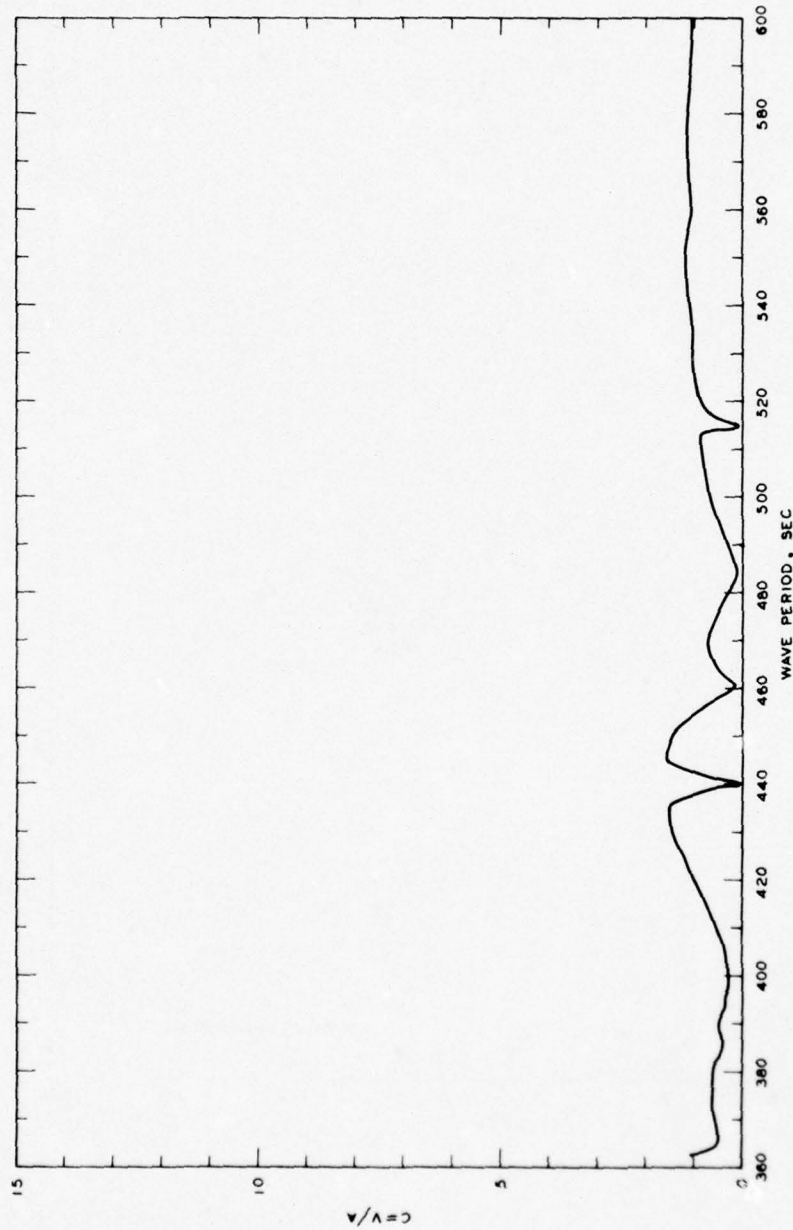
NOTE: C = NORMALIZED MAXIMUM CURRENT
VELOCITY
V = CURRENT VELOCITY, FT/SEC
A = INCIDENT WAVE AMPLITUDE

FREQUENCY RESPONSE
NORMALIZED MAXIMUM CURRENT VELOCITY
STA LB-5, GRID 2



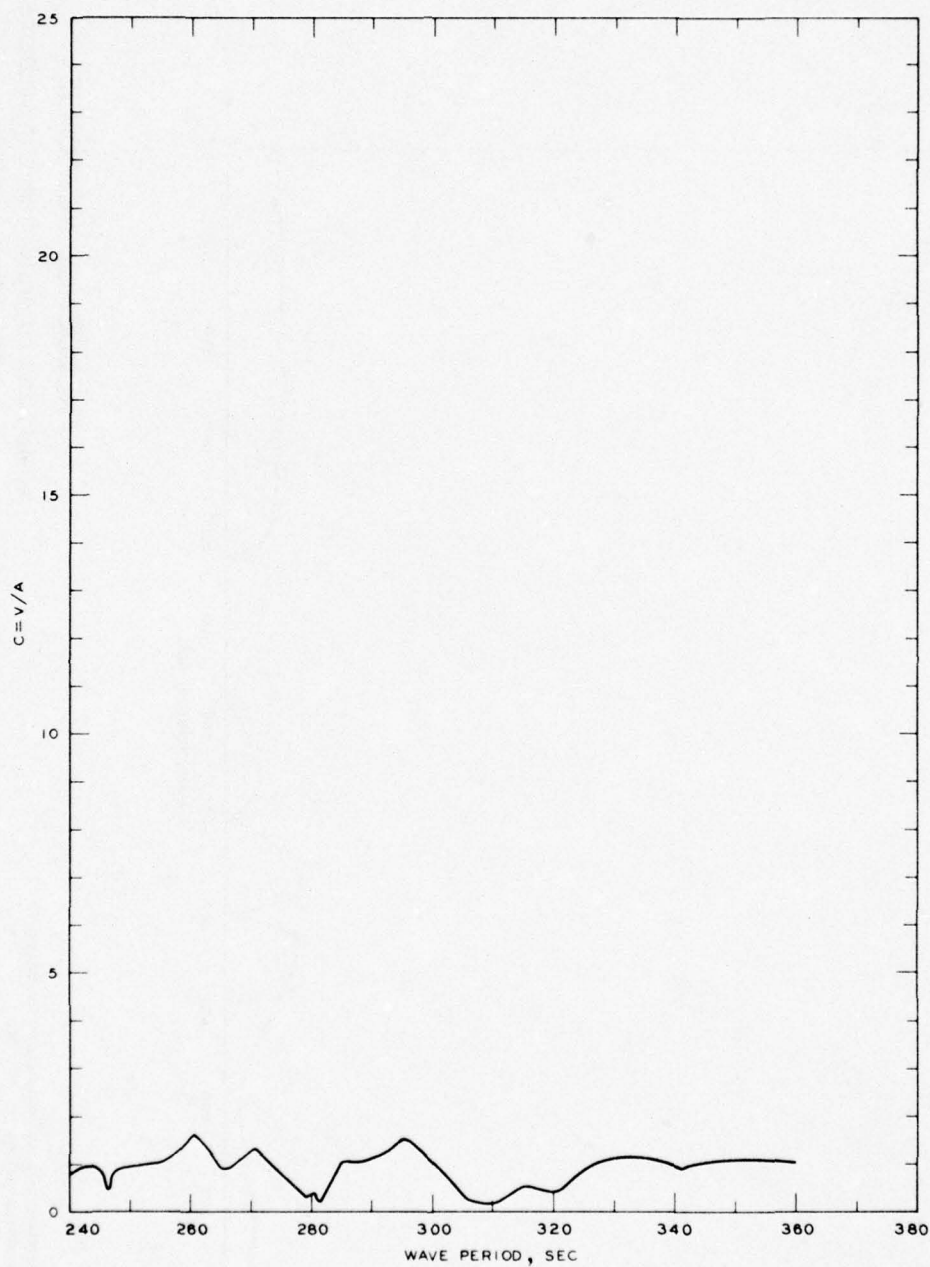
NOTE: C = NORMALIZED MAXIMUM CURRENT
VELOCITY
V = CURRENT VELOCITY, FT/SEC
A = INCIDENT WAVE AMPLITUDE

FREQUENCY RESPONSE
NORMALIZED MAXIMUM CURRENT VELOCITY
STA LB-5, GRID 3



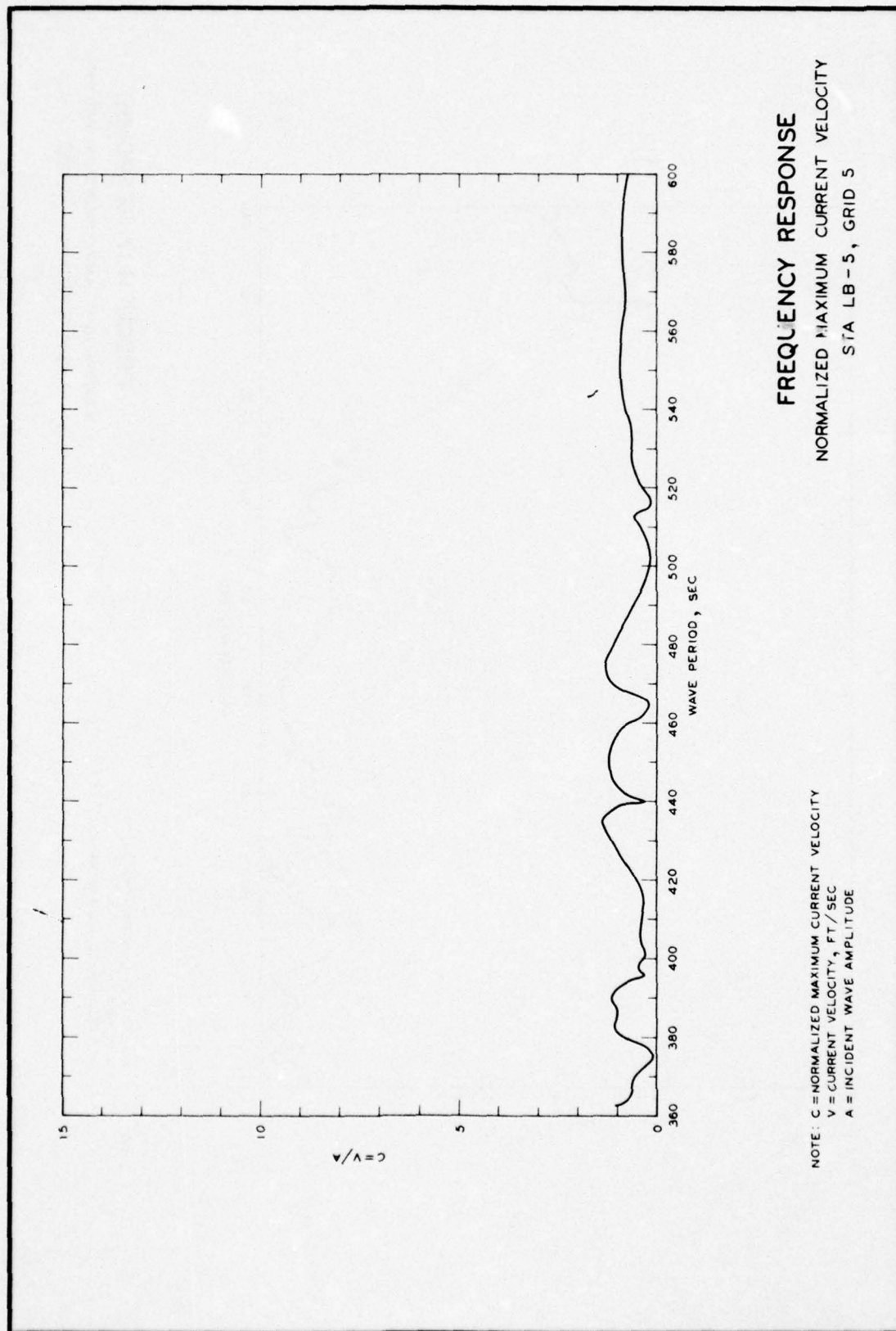
FREQUENCY RESPONSE NORMALIZED MAXIMUM CURRENT VELOCITY STA LB-4, GRID 5

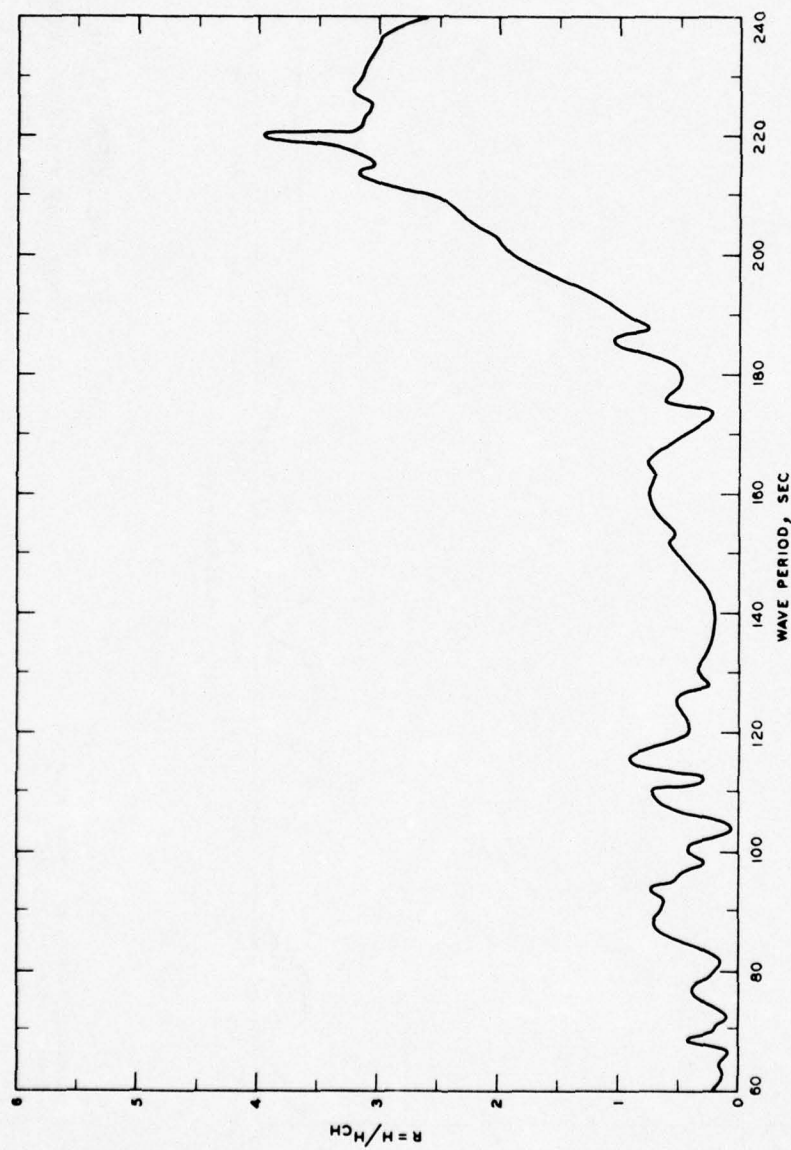
NOTE: C = NORMALIZED MAXIMUM CURRENT VELOCITY
 V = CURRENT VELOCITY, FT/SEC
 A = INCIDENT WAVE AMPLITUDE



NOTE: C = NORMALIZED MAXIMUM CURRENT
VELOCITY
V = CURRENT VELOCITY, FT/SEC
A = INCIDENT WAVE AMPLITUDE

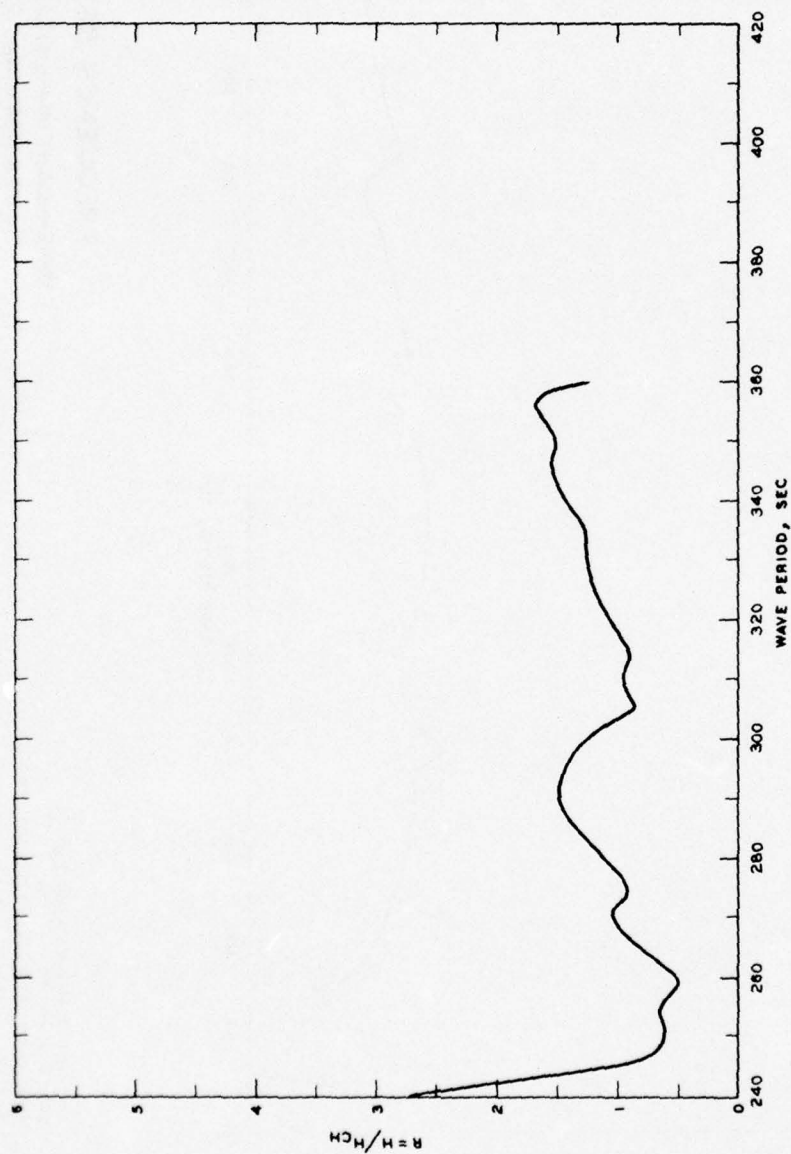
FREQUENCY RESPONSE
NORMALIZED MAXIMUM CURRENT VELOCITY
STA LB-5, GRID 4





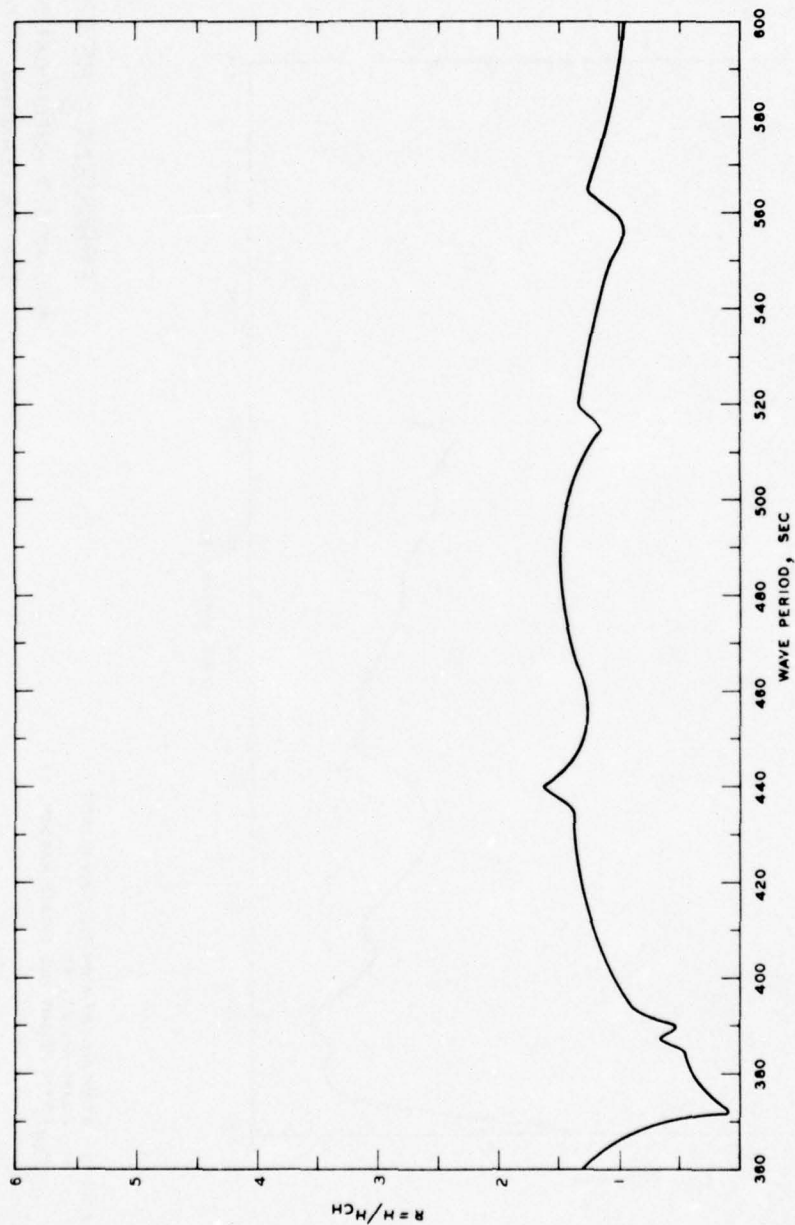
FREQUENCY RESPONSE WAVE-HEIGHT AMPLIFICATION FACTOR TANKER TERMINAL 1, GRIDS 1A-3A

NOTE: R = WAVE-HEIGHT AMPLIFICATION FACTOR
 H = WAVE HEIGHT, FT
 H_{CH} = WAVE HEIGHT FOR CLOSED HARBOR, FT



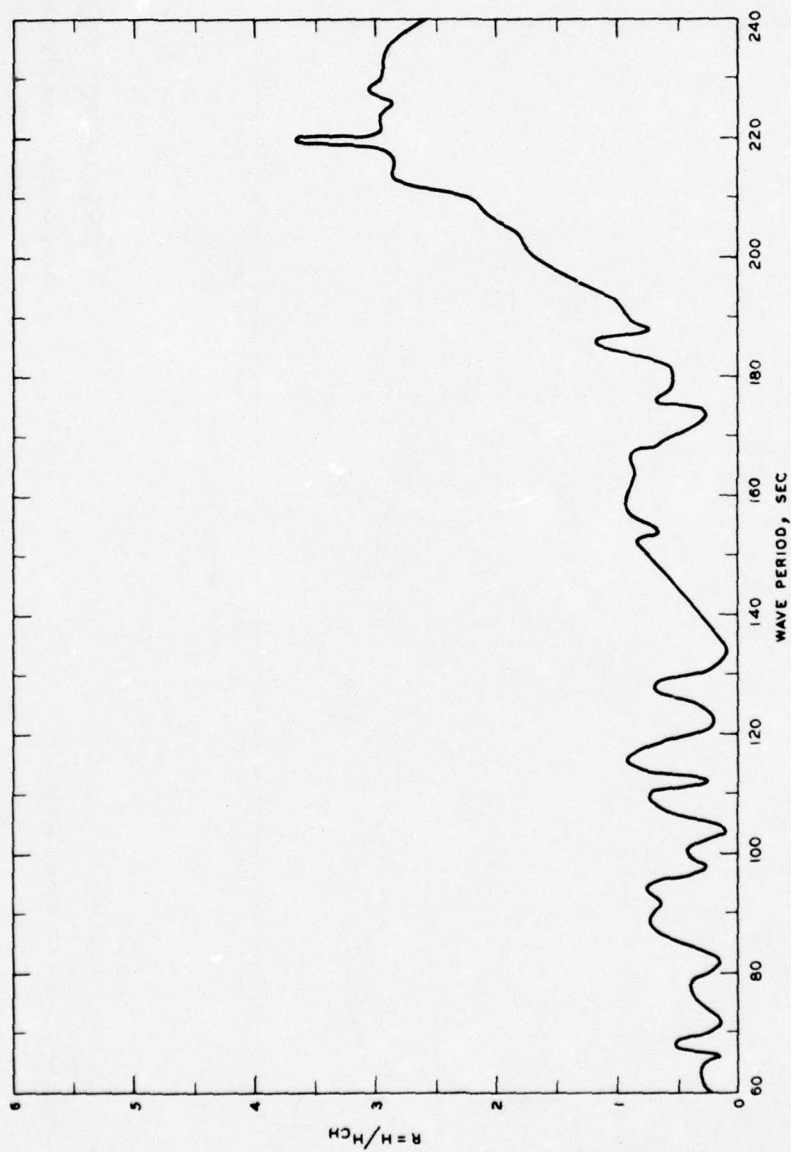
FREQUENCY RESPONSE
WAVE-HEIGHT AMPLIFICATION FACTOR
TANKER TERMINAL 1, GRID 4A

NOTE: R = WAVE-HEIGHT AMPLIFICATION FACTOR
 H = WAVE HEIGHT, FT
 H_{CH} = WAVE HEIGHT FOR CLOSED HARBOR, FT



FREQUENCY RESPONSE WAVE-HEIGHT AMPLIFICATION FACTOR TANKER TERMINAL 1, GRID 5A

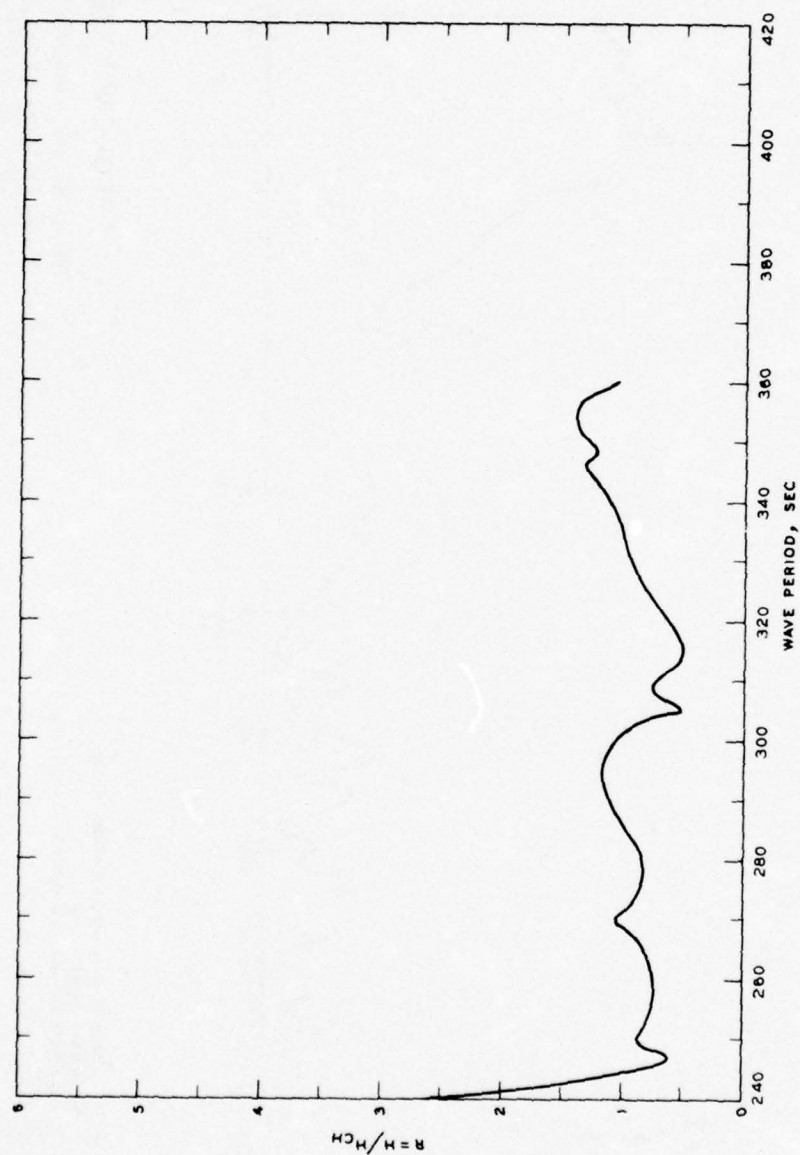
NOTE: R = WAVE-HEIGHT AMPLIFICATION FACTOR
 H = WAVE HEIGHT, FT
 H_{CH} = WAVE HEIGHT FOR CLOSED HARBOR, FT



FREQUENCY RESPONSE

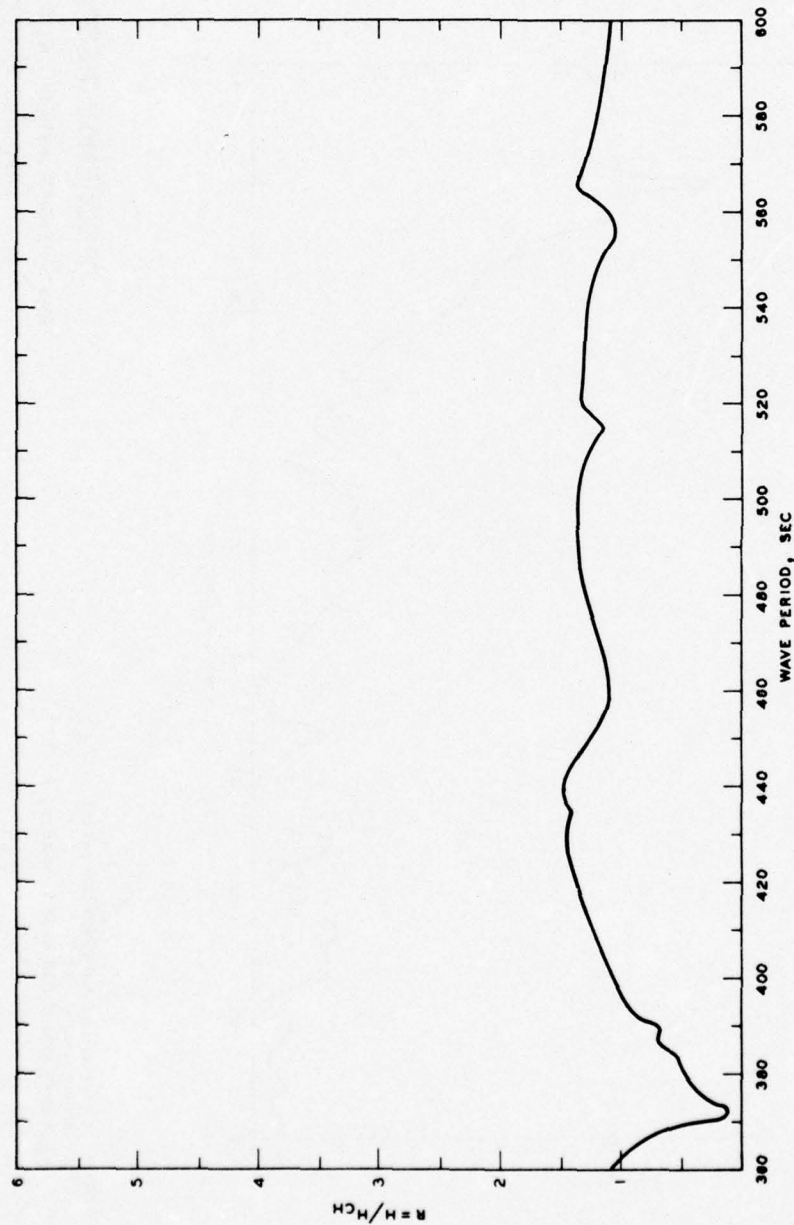
WAVE-HEIGHT AMPLIFICATION FACTOR
TANKER TERMINAL 2, GRIDS 1A-3A

NOTE: R = WAVE-HEIGHT AMPLIFICATION FACTOR
H = WAVE HEIGHT, FT
H_{CH} = WAVE HEIGHT FOR CLOSED HARBOR, FT



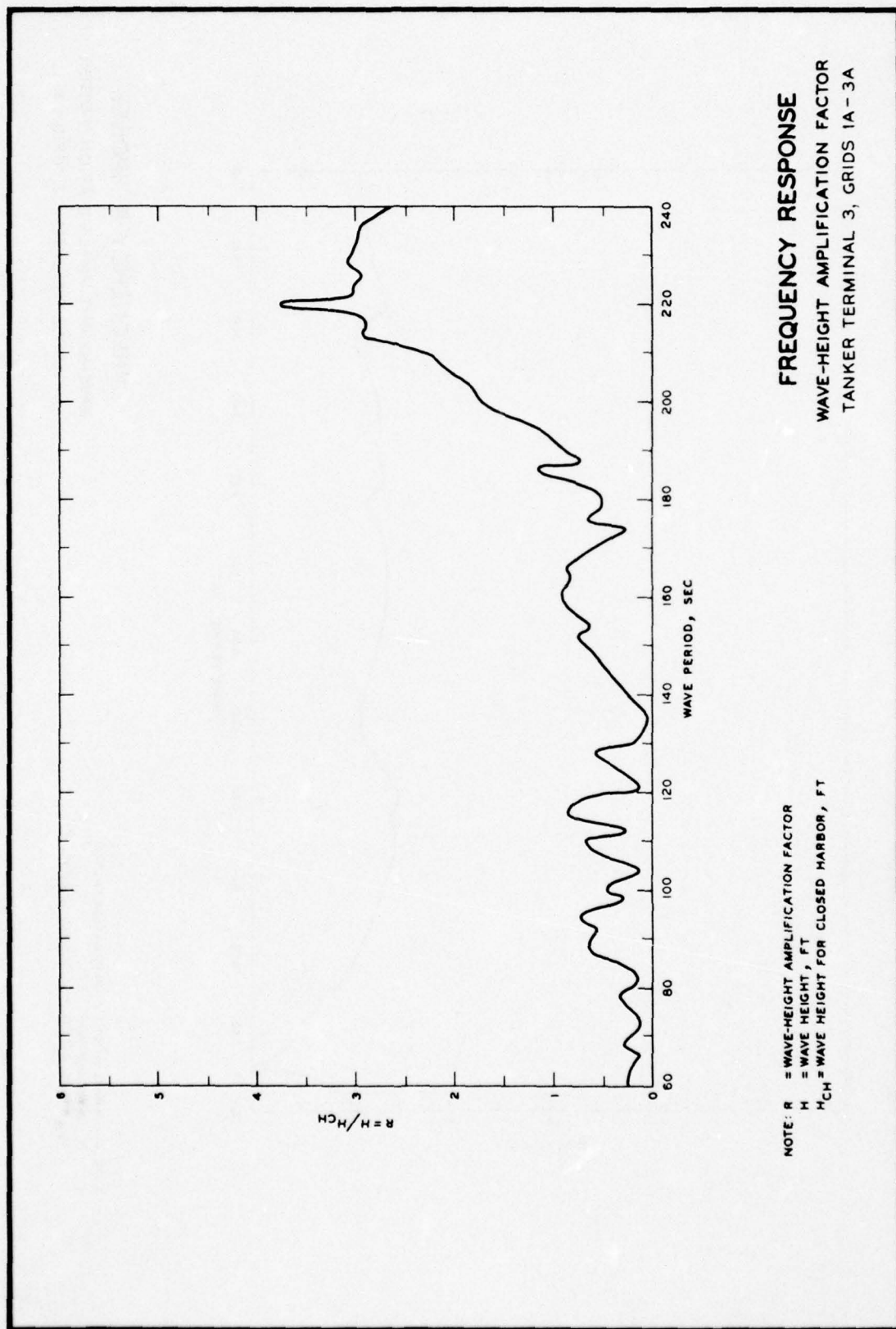
NOTE: R = WAVE-HEIGHT AMPLIFICATION FACTOR
H = WAVE HEIGHT, FT
H_{CH} = WAVE HEIGHT FOR CLOSED HARBOR, FT

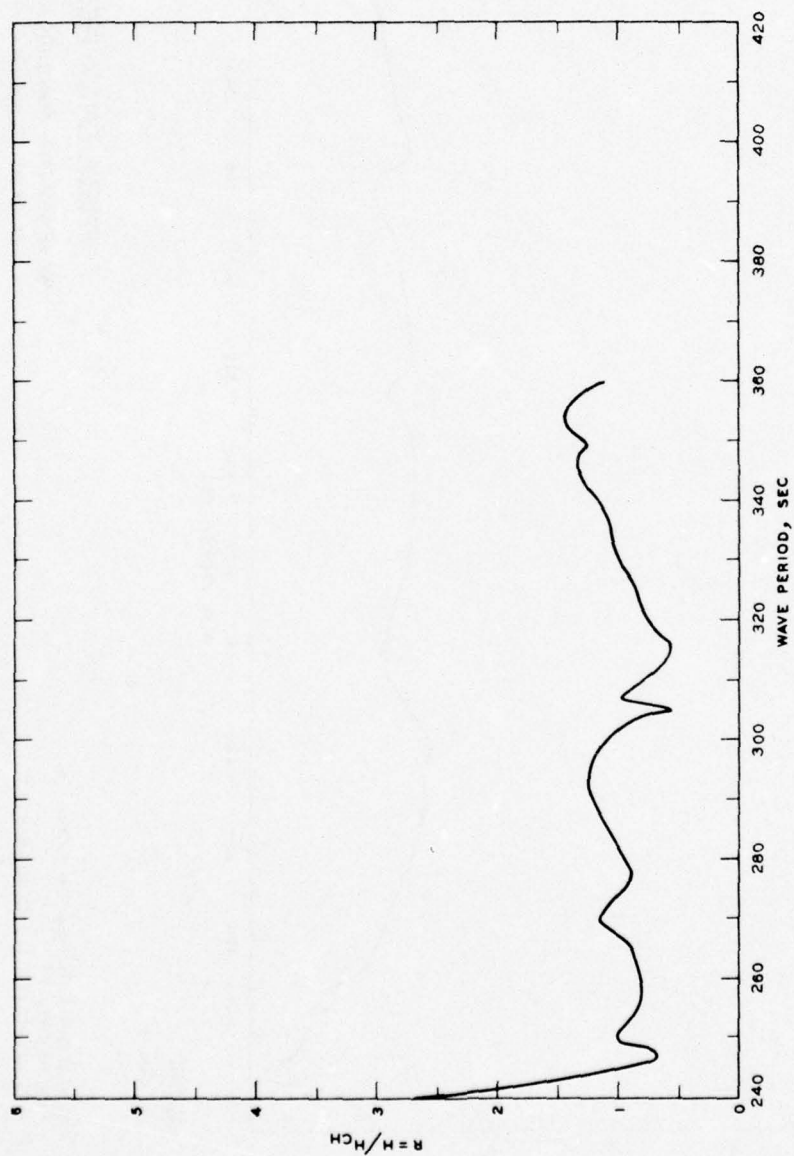
FREQUENCY RESPONSE WAVE-HEIGHT AMPLIFICATION FACTOR TANKER TERMINAL 2, GRID 4A



FREQUENCY RESPONSE **WAVE-HEIGHT AMPLIFICATION FACTOR** **TANKER TERMINAL 2, GRID 5A**

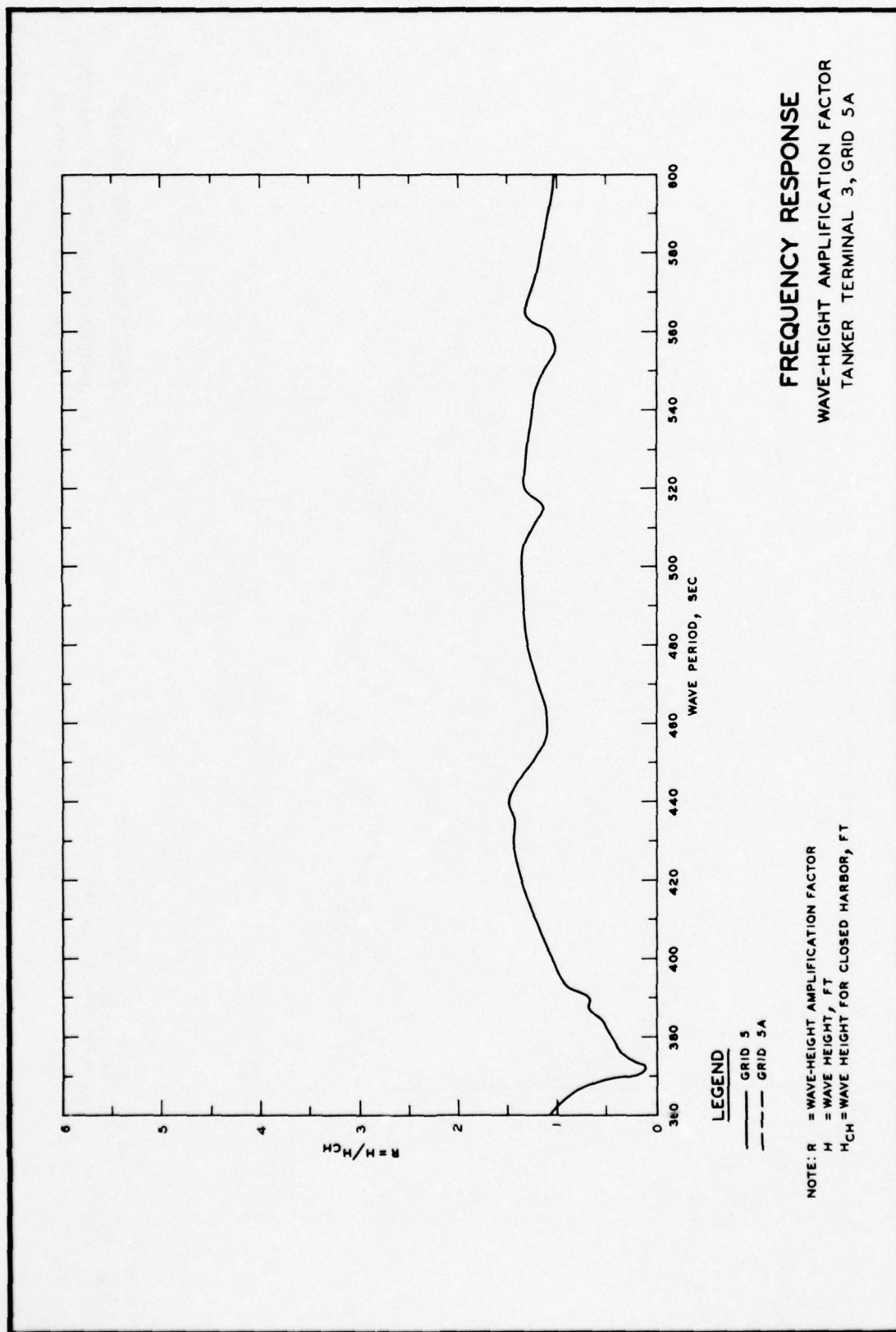
NOTE: R = WAVE-HEIGHT AMPLIFICATION FACTOR
H = WAVE HEIGHT, FT
H_{CH} = WAVE HEIGHT FOR CLOSED HARBOR, FT

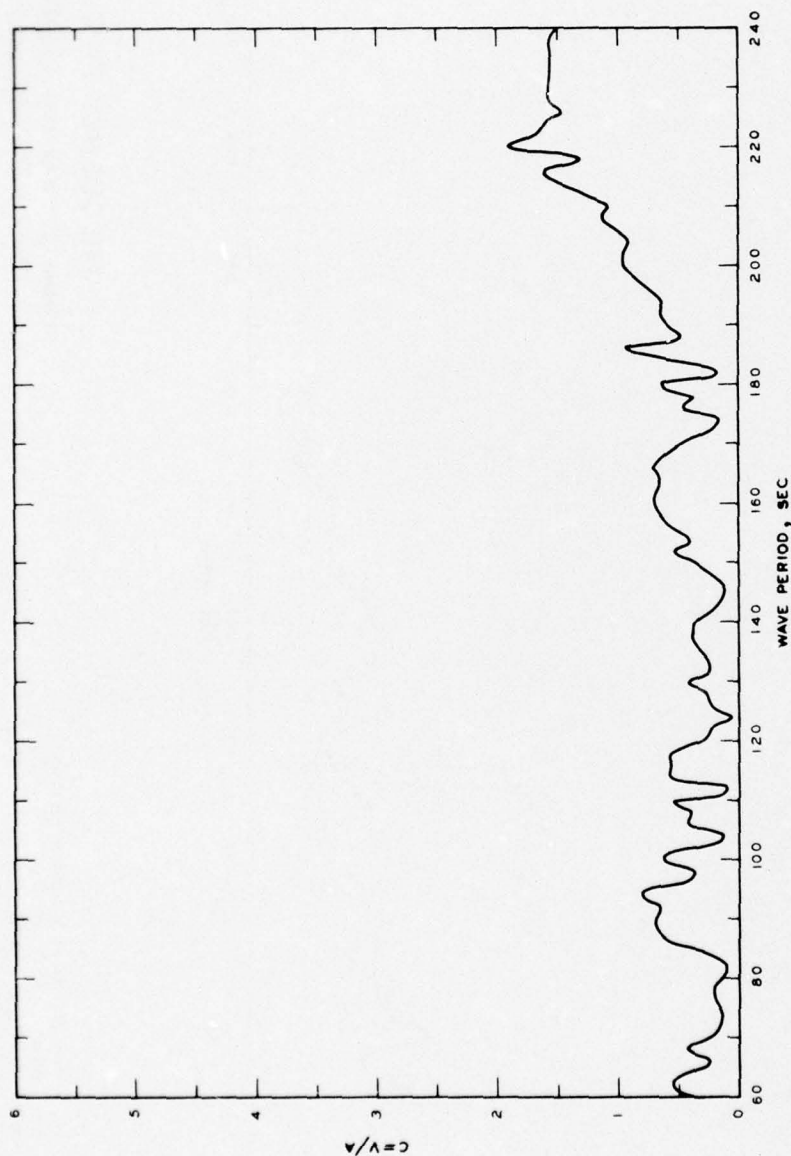




FREQUENCY RESPONSE WAVE-HEIGHT AMPLIFICATION FACTOR TANKER TERMINAL 3, GRID 4A

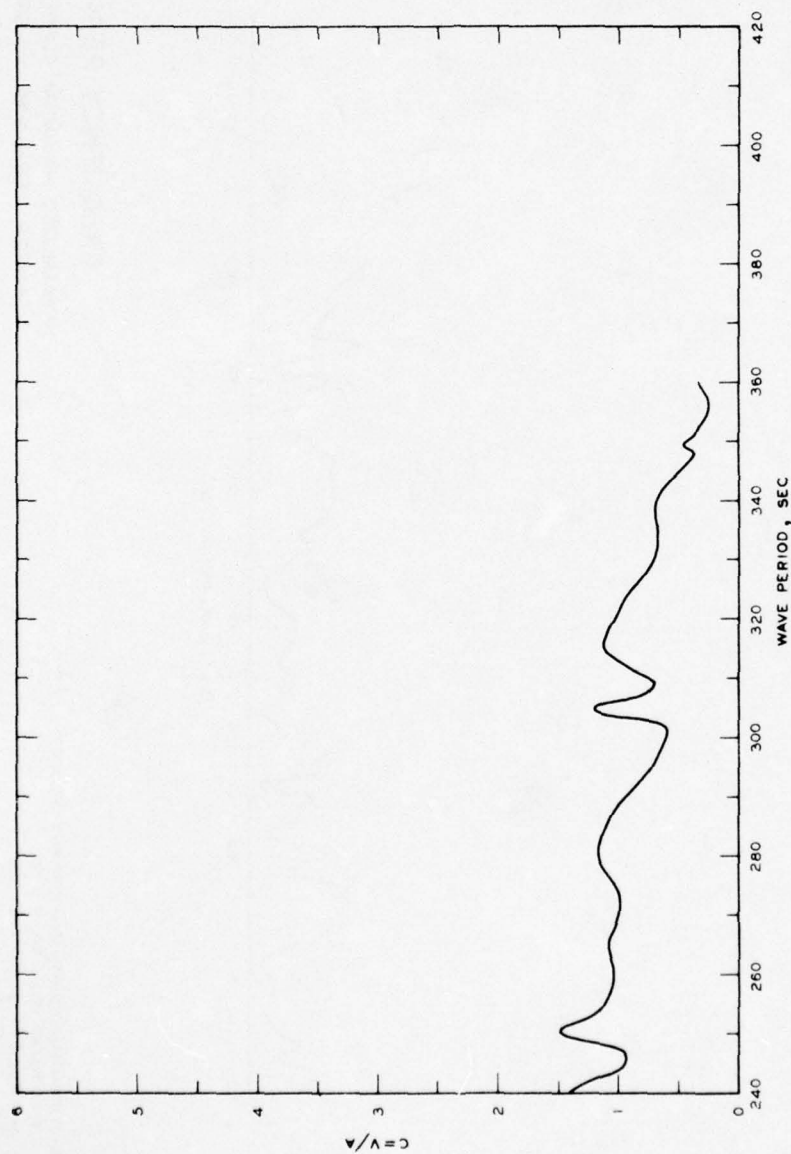
NOTE: R = WAVE-HEIGHT AMPLIFICATION FACTOR
 H = WAVE HEIGHT, FT
 H_{CH} = WAVE HEIGHT FOR CLOSED HARBOR, FT





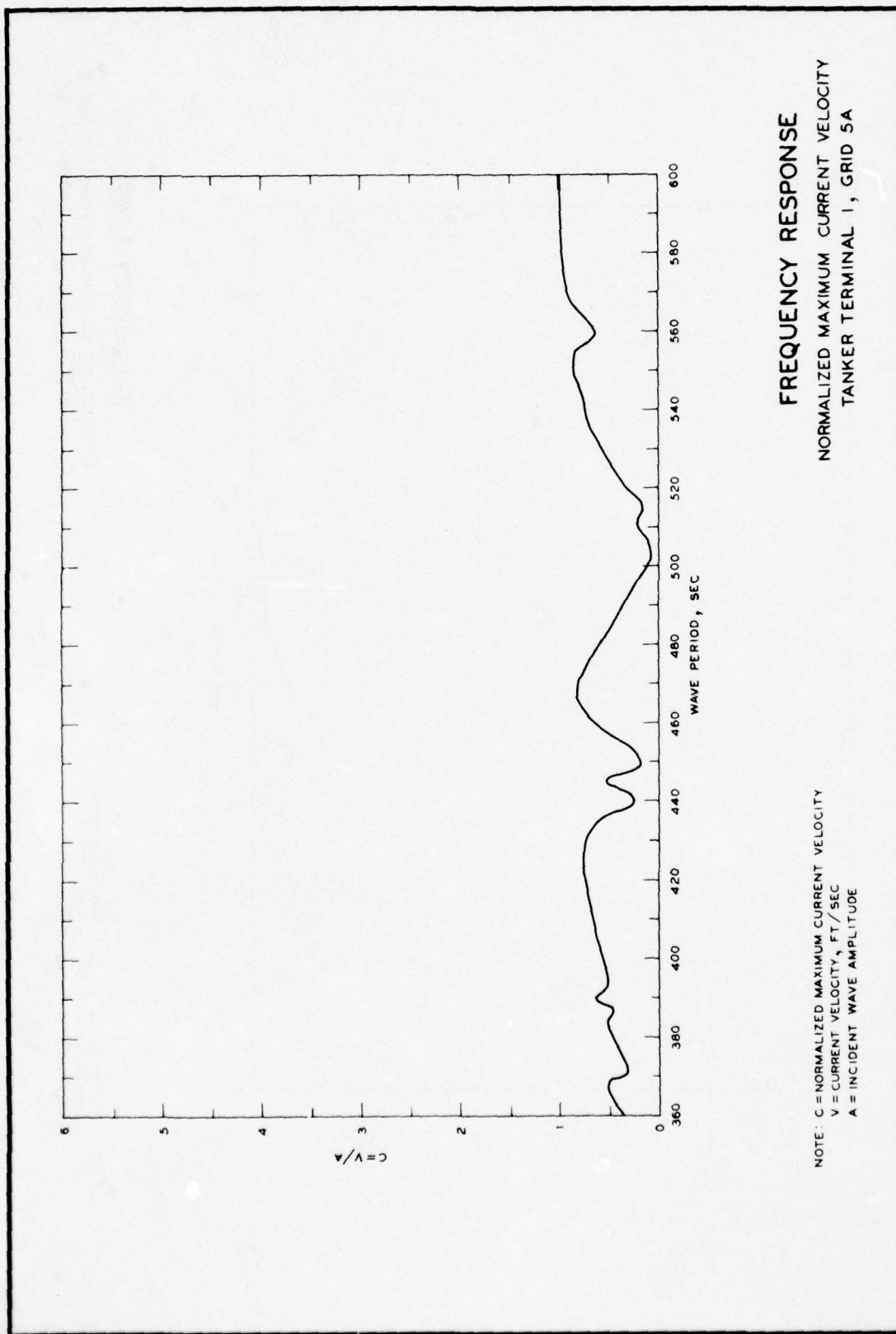
FREQUENCY RESPONSE NORMALIZED MAXIMUM CURRENT VELOCITY TANKER TERMINAL 1, GRIDS 1A-3A

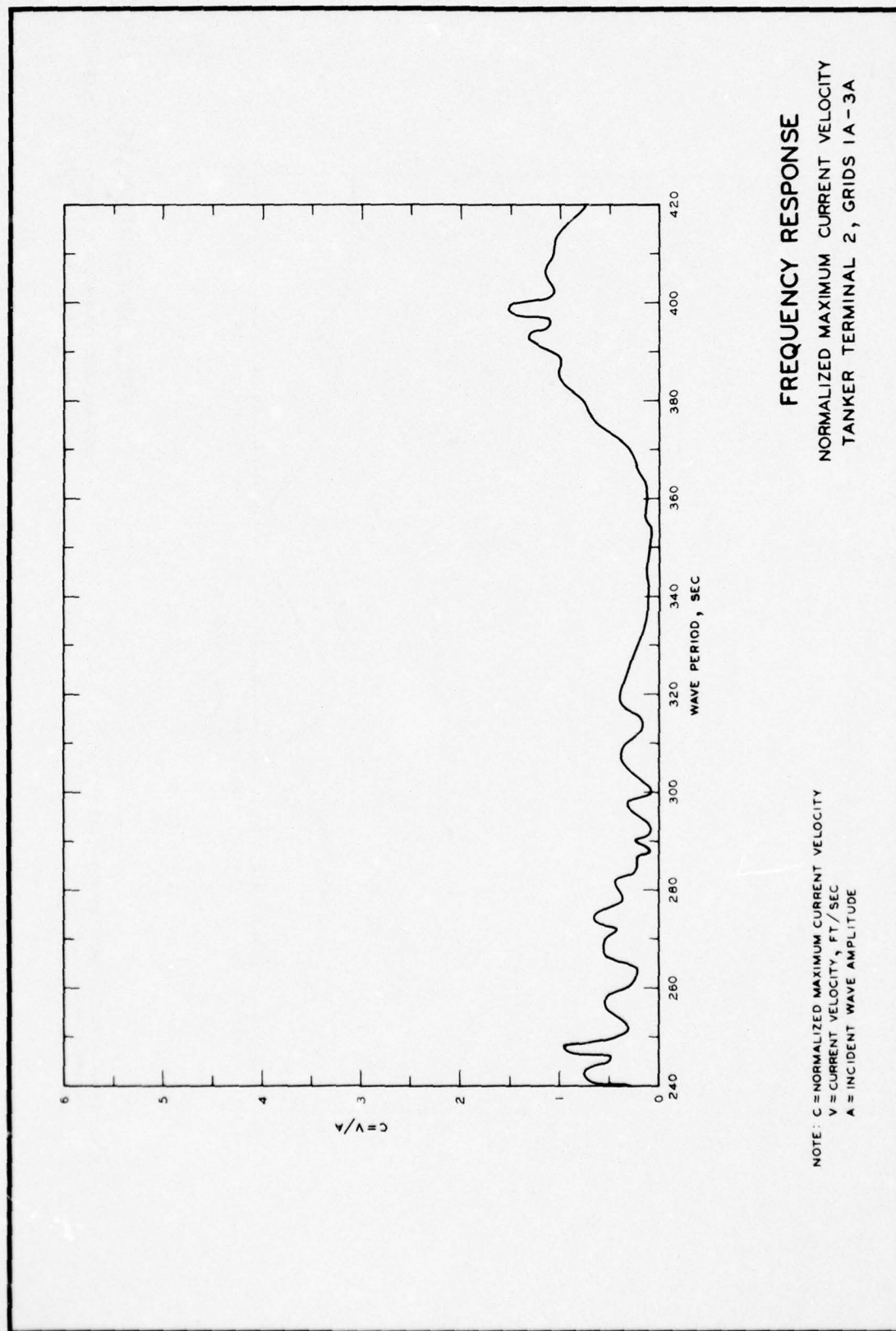
NOTE: C = NORMALIZED MAXIMUM CURRENT VELOCITY
 V = CURRENT VELOCITY, FT/SEC
 A = INCIDENT WAVE AMPLITUDE

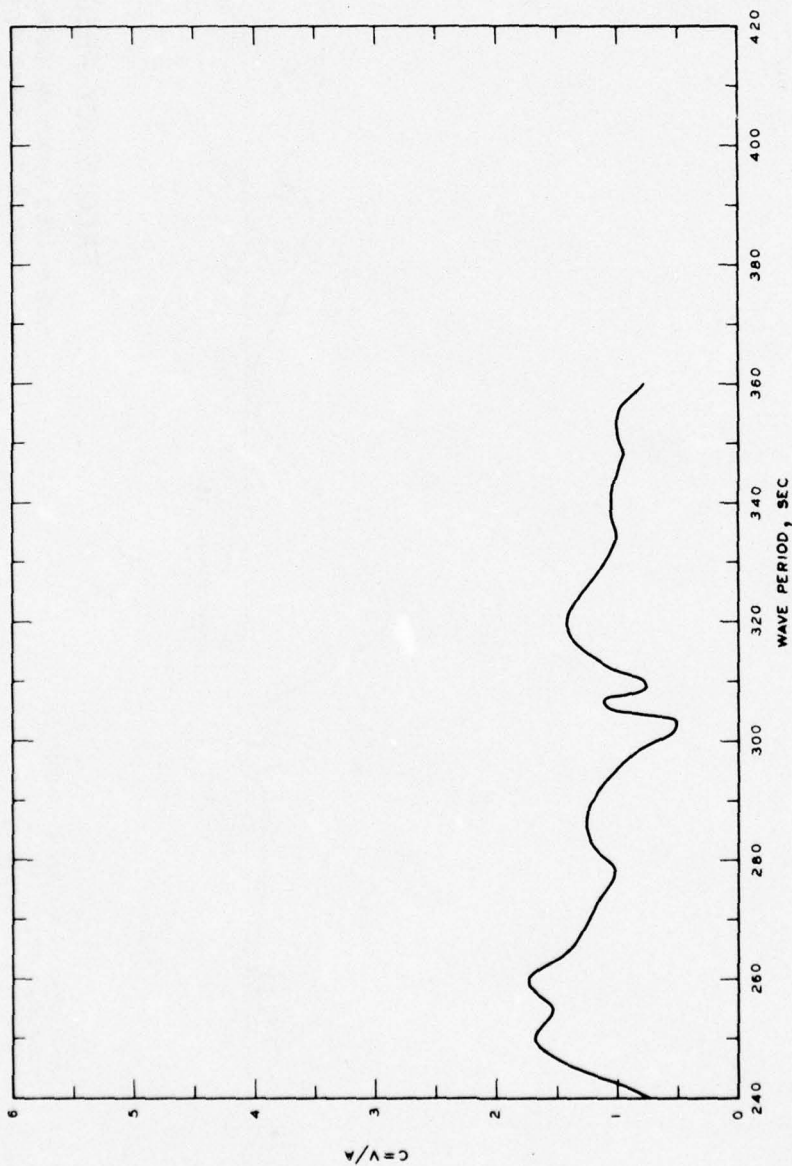


FREQUENCY RESPONSE NORMALIZED MAXIMUM CURRENT VELOCITY TANKER TERMINAL 1, GRID 4A

NOTE: C = NORMALIZED MAXIMUM CURRENT VELOCITY
 V = CURRENT VELOCITY, FT / SEC
 A = INCIDENT WAVE AMPLITUDE

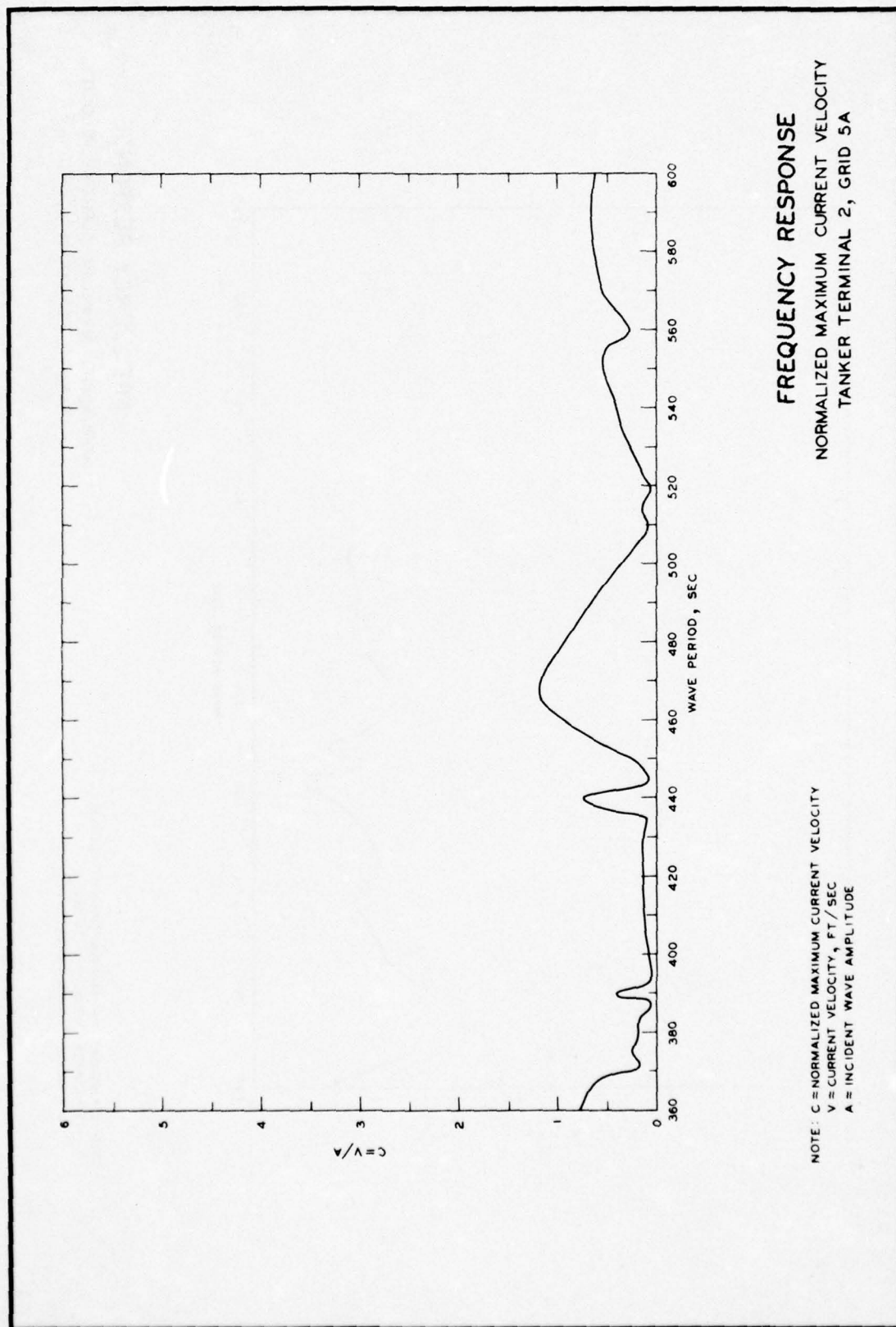


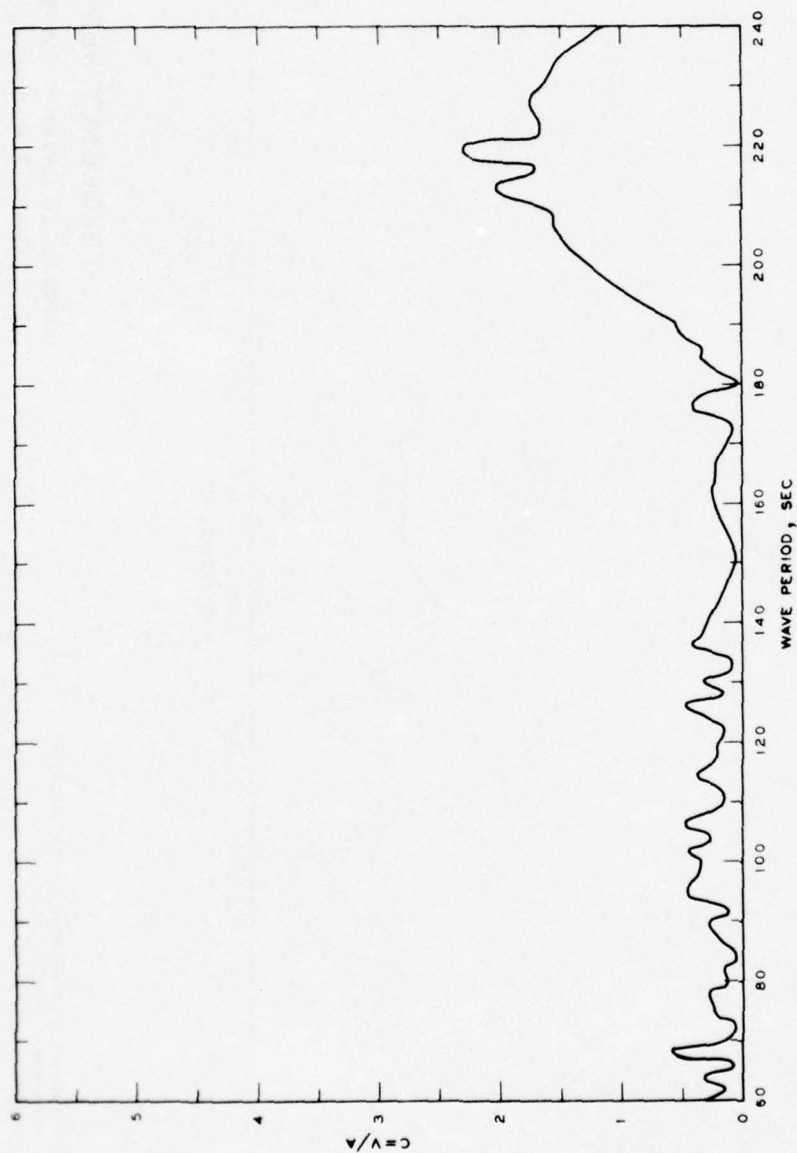




FREQUENCY RESPONSE **NORMALIZED MAXIMUM CURRENT VELOCITY** **TANKER TERMINAL 2, GRID 4A**

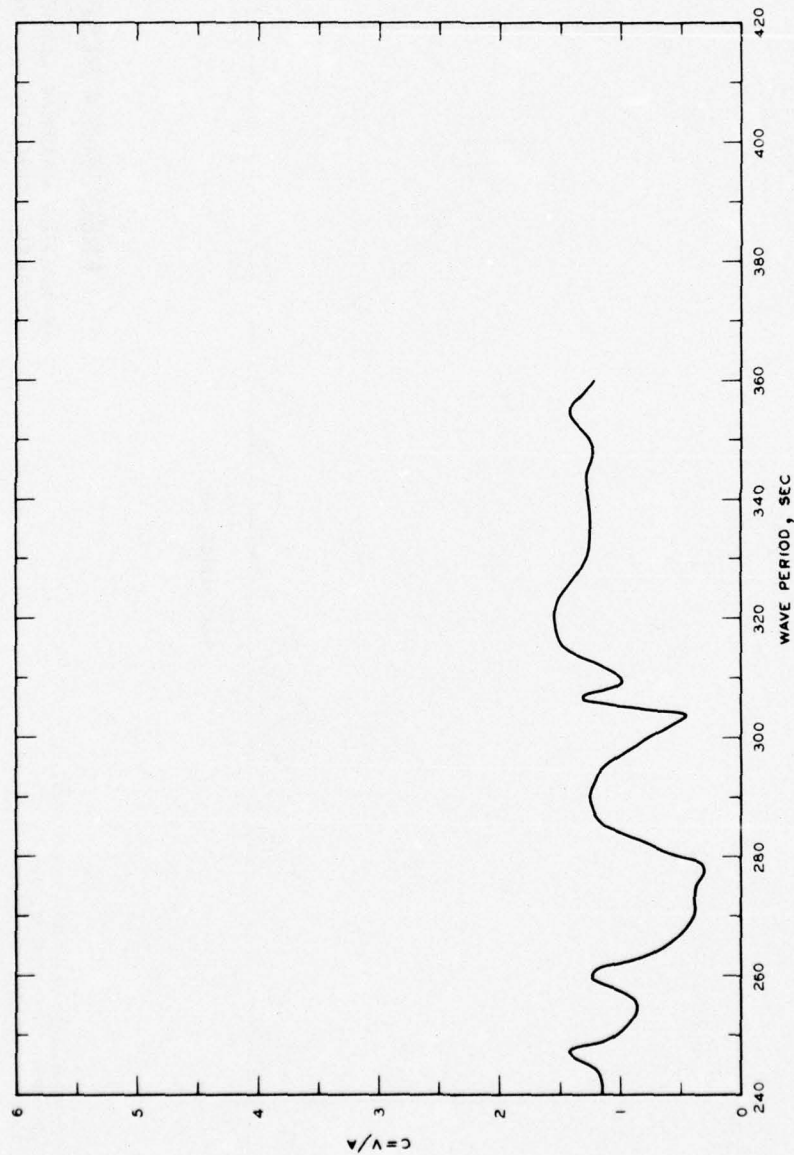
NOTE: C = NORMALIZED MAXIMUM CURRENT VELOCITY
 V = CURRENT VELOCITY, FT/SEC
 A = INCIDENT WAVE AMPLITUDE





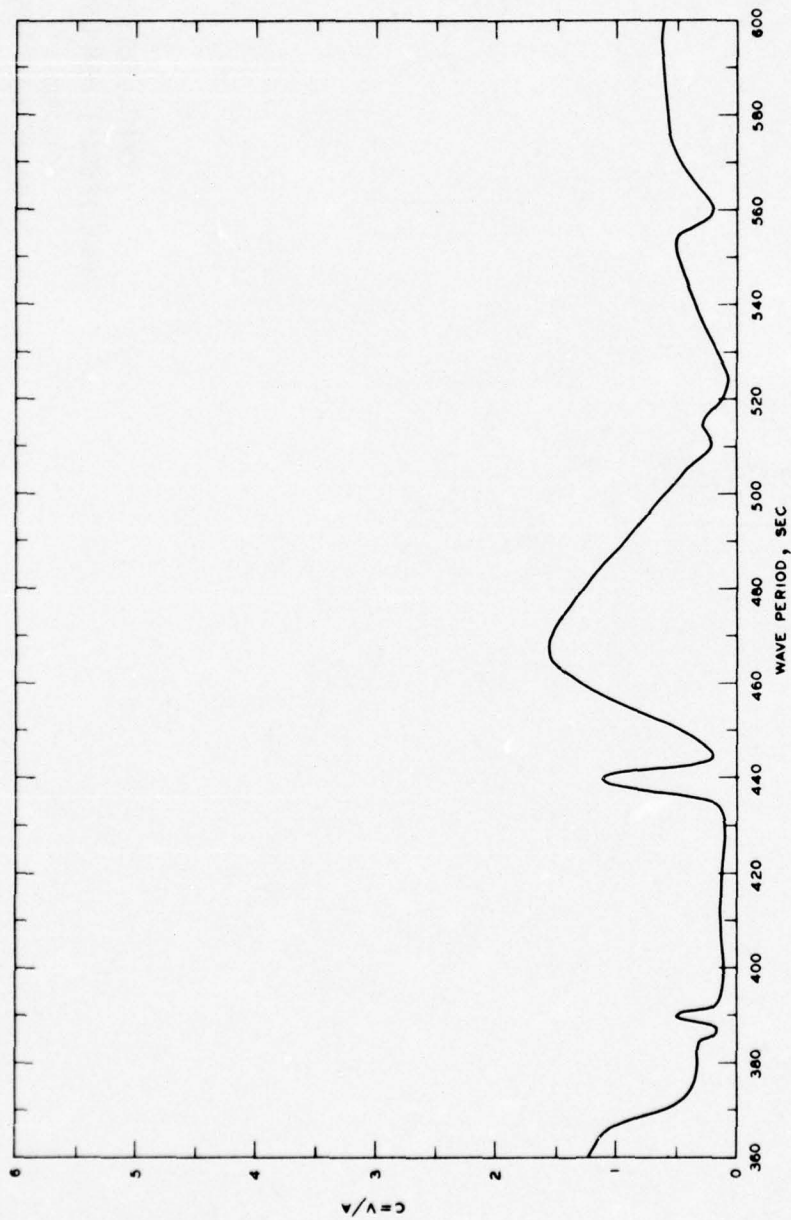
FREQUENCY RESPONSE
 NORMALIZED MAXIMUM CURRENT VELOCITY
 TANKER TERMINAL 3, GRIDS 1A-3A

NOTE: C = NORMALIZED MAXIMUM CURRENT VELOCITY
 V = CURRENT VELOCITY, FT/SEC
 A = INCIDENT WAVE AMPLITUDE



FREQUENCY RESPONSE NORMALIZED MAXIMUM CURRENT VELOCITY TANKER TERMINAL 3, GRID 4A

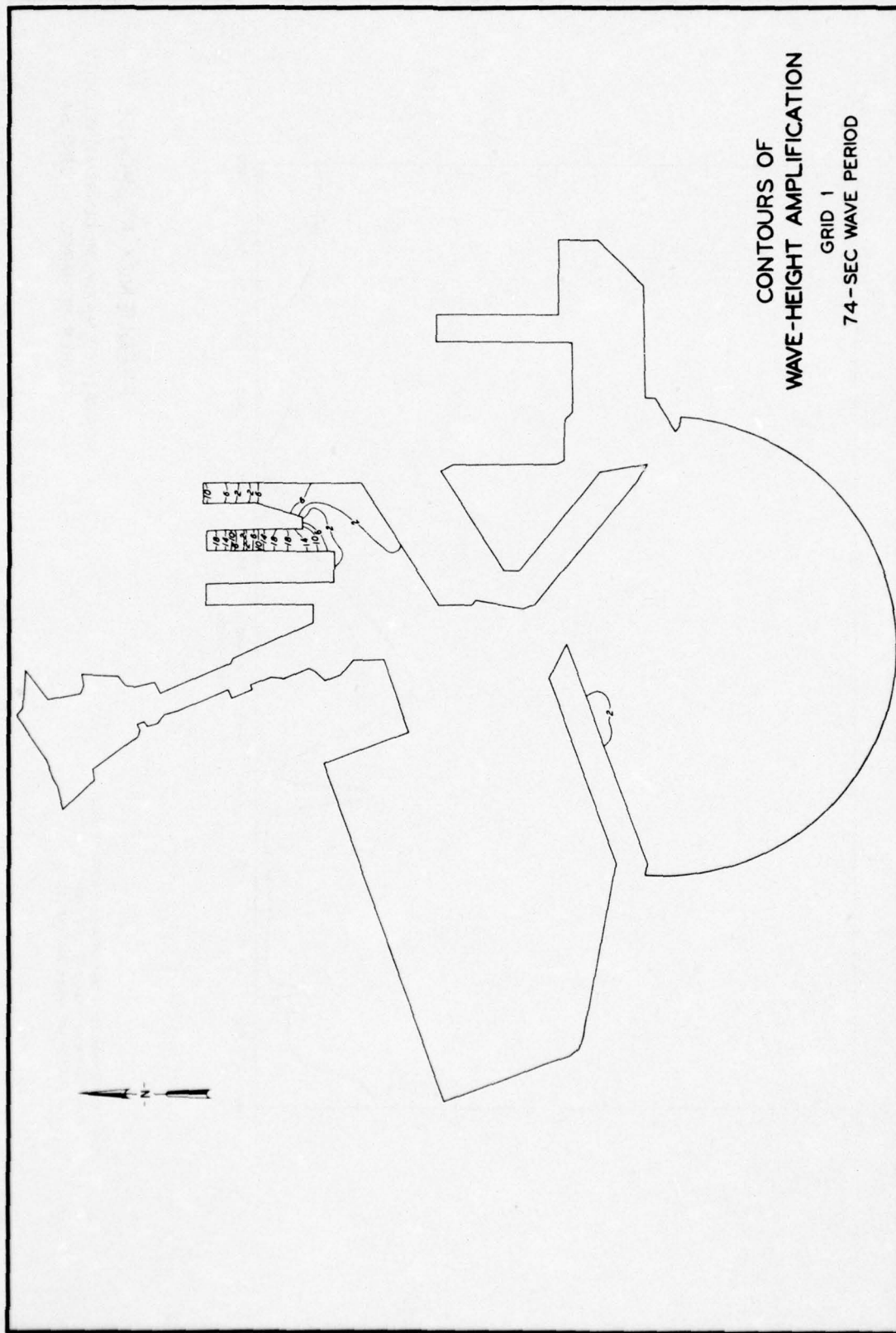
NOTE C = NORMALIZED MAXIMUM CURRENT VELOCITY
 V = CURRENT VELOCITY, FT/SEC
 A = INCIDENT WAVE AMPLITUDE

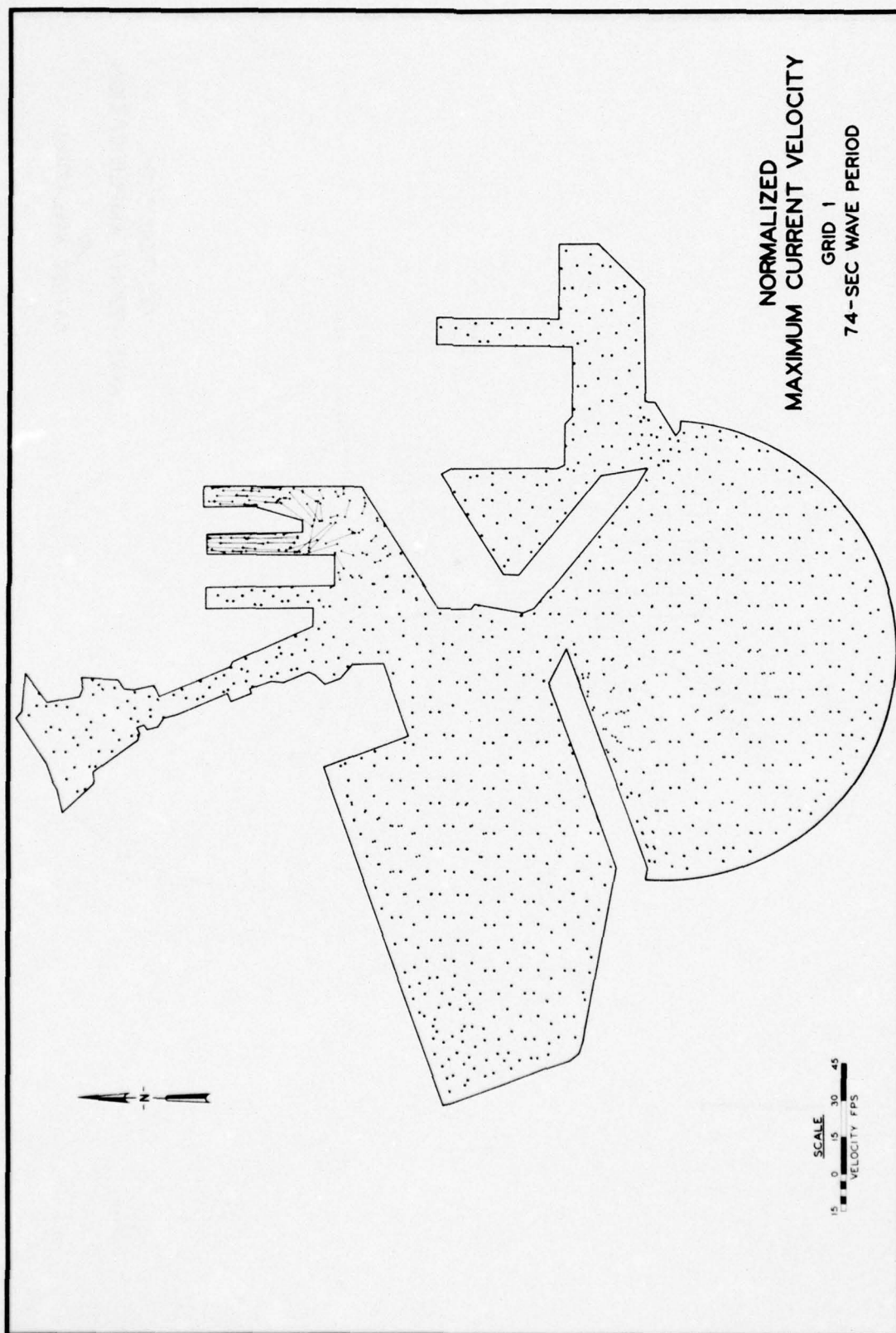


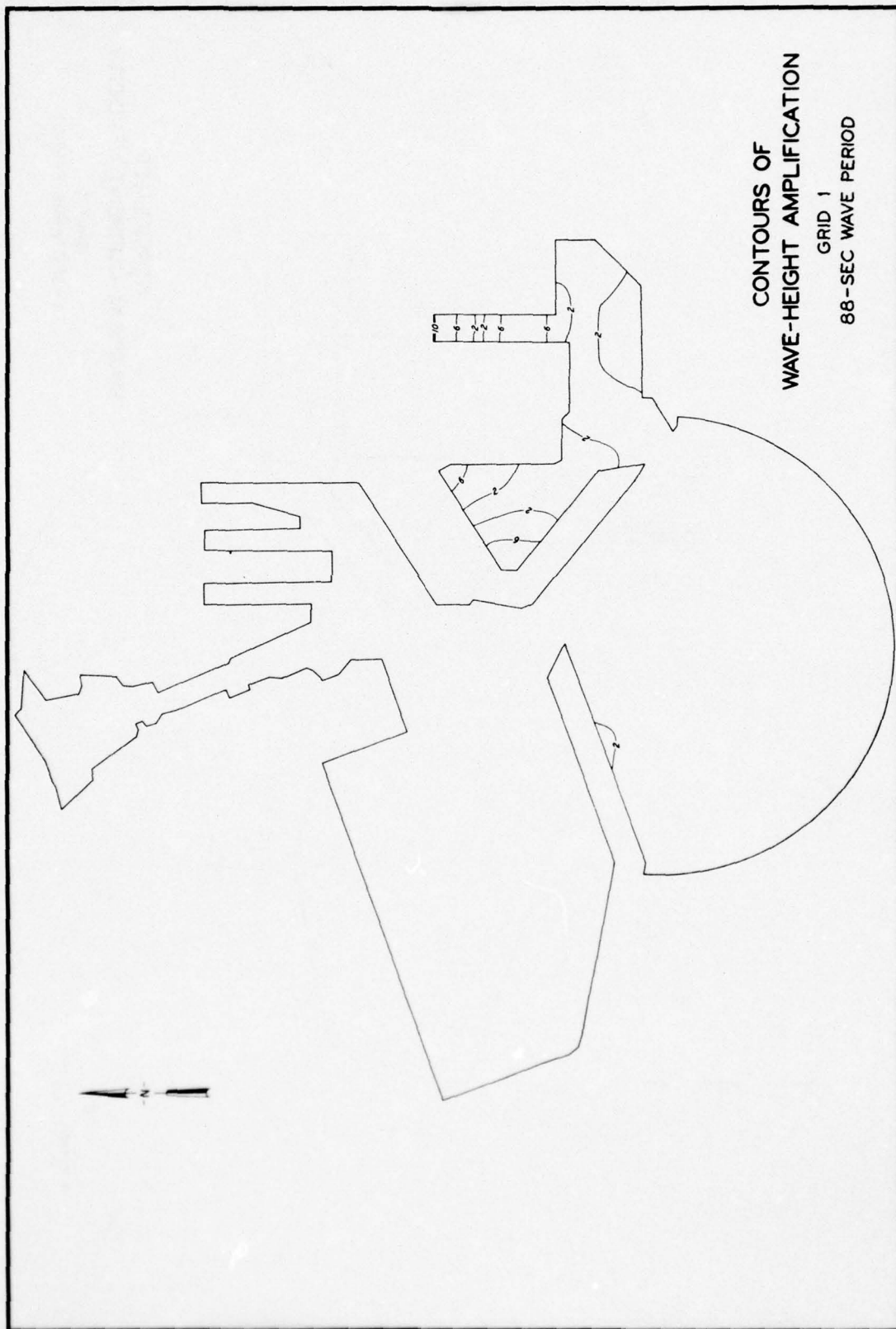
FREQUENCY RESPONSE

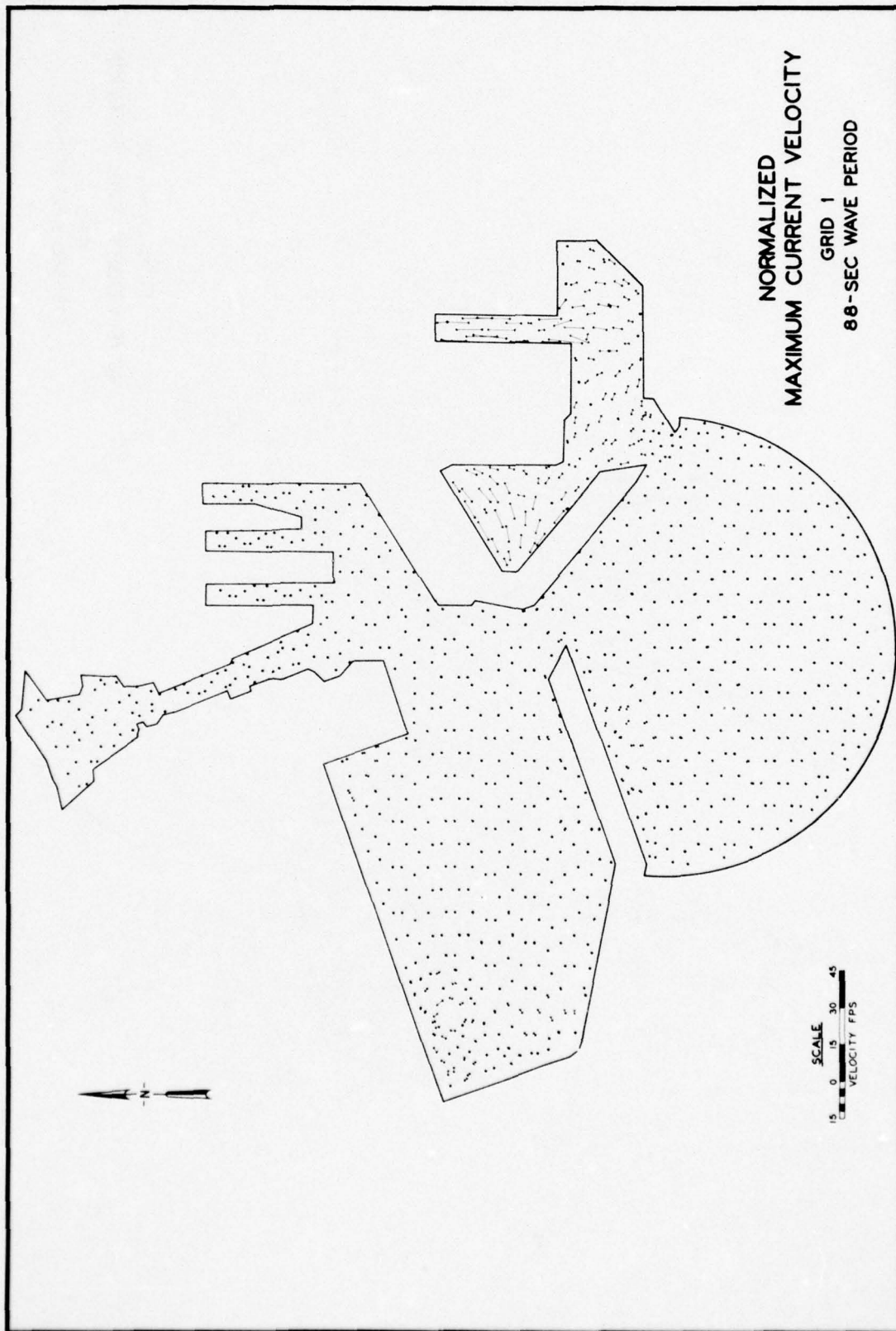
NORMALIZED MAXIMUM CURRENT VELOCITY
TANKER TERMINAL 3, GRID 5A

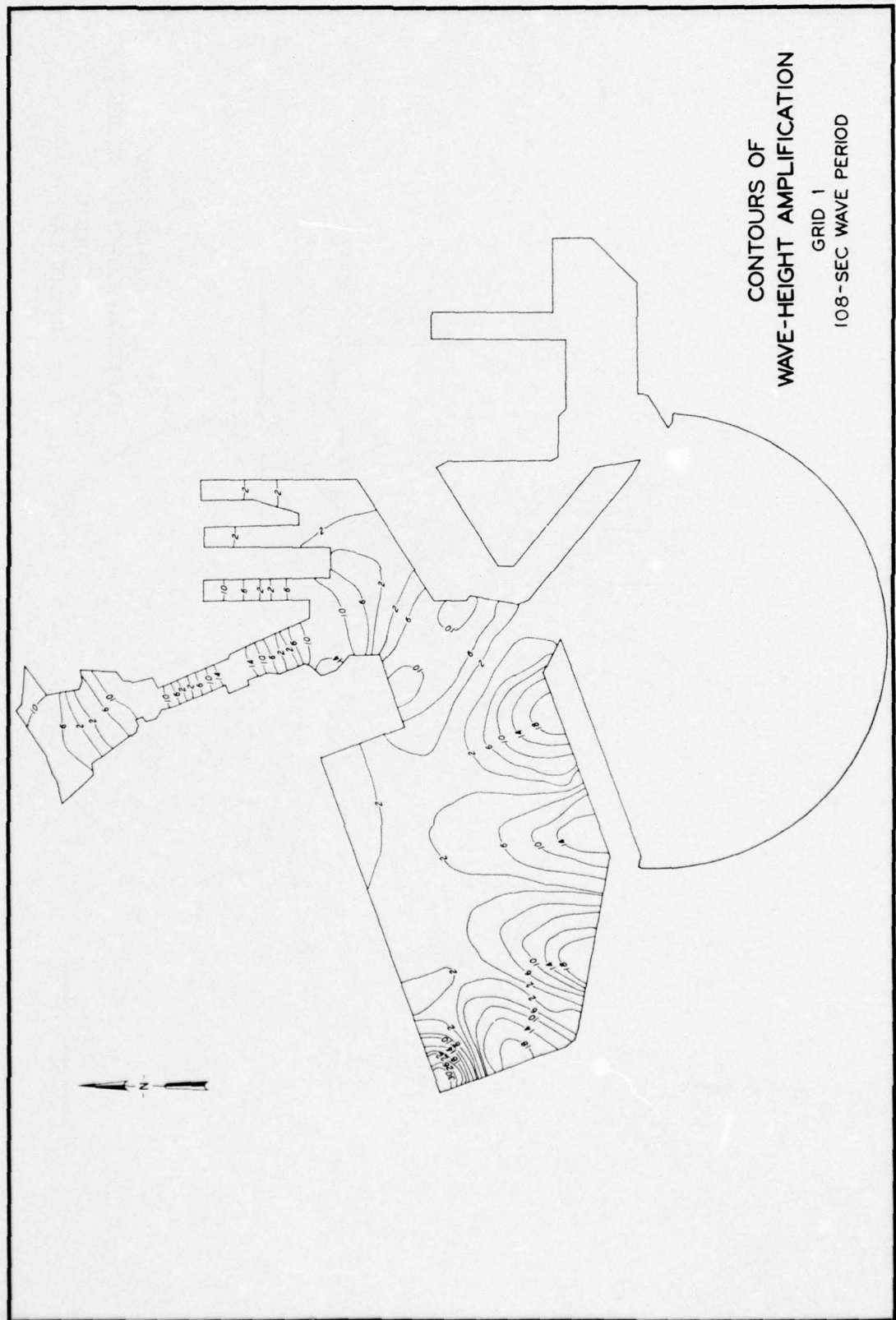
NOTE: C = NORMALIZED MAXIMUM CURRENT VELOCITY
V = CURRENT VELOCITY, FT/SEC
A = INCIDENT WAVE AMPLITUDE

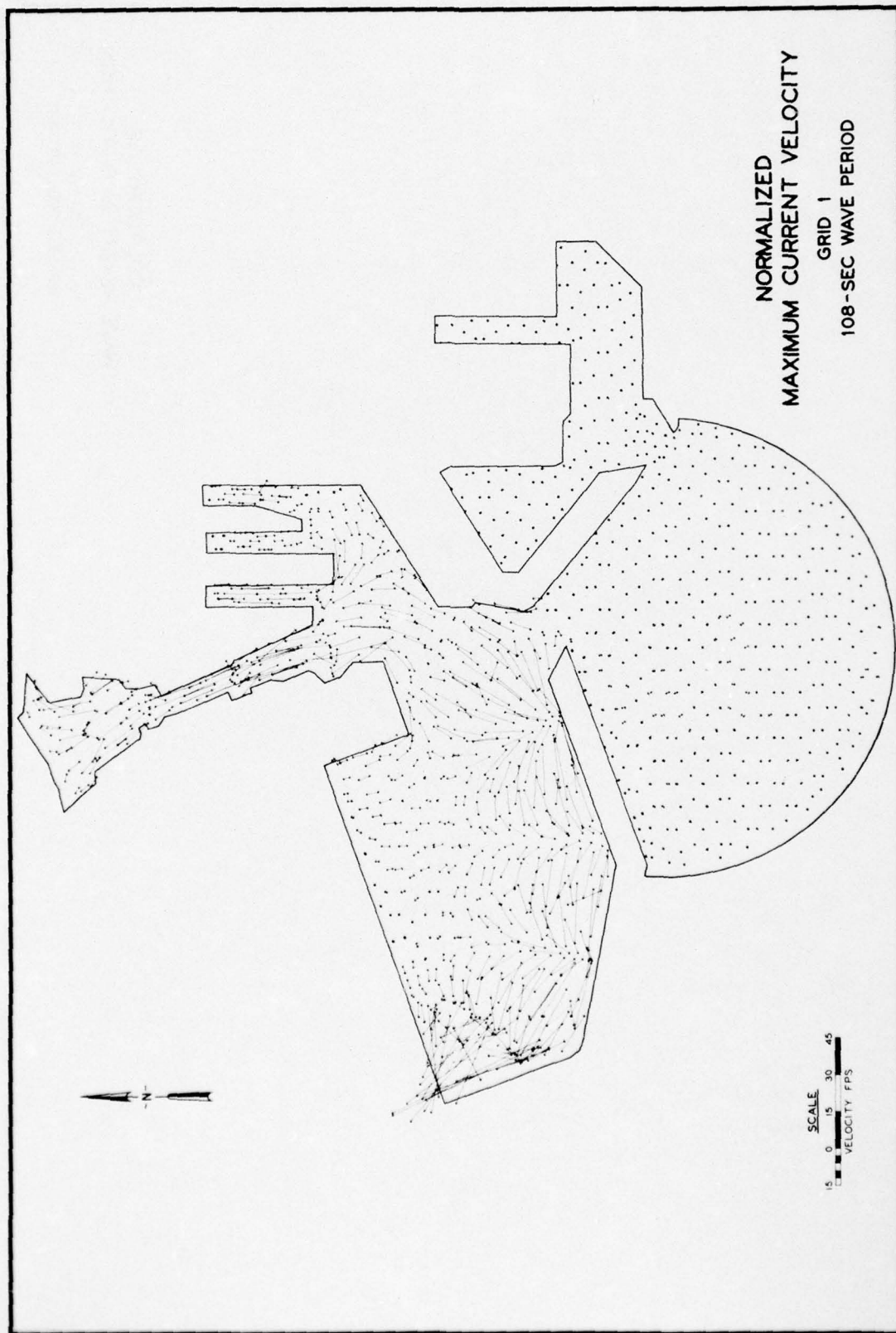




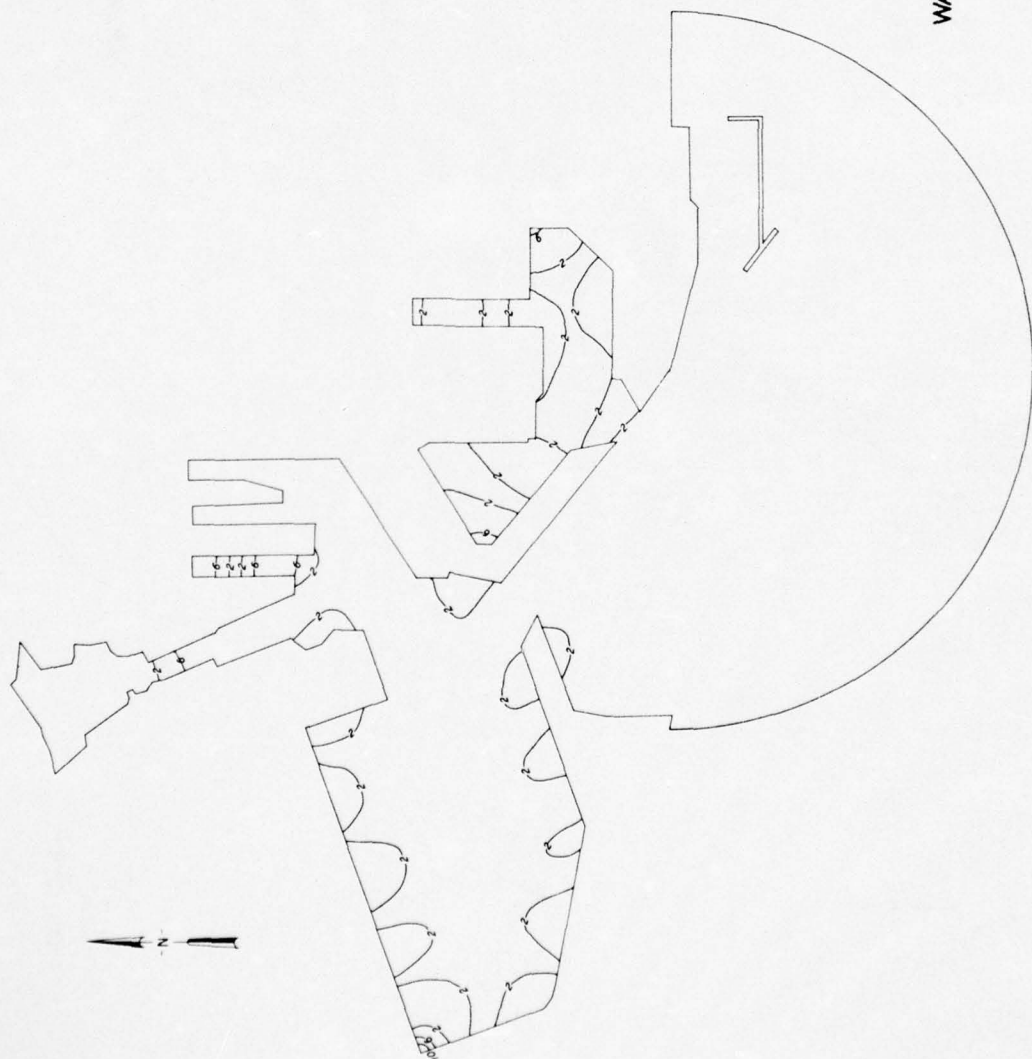


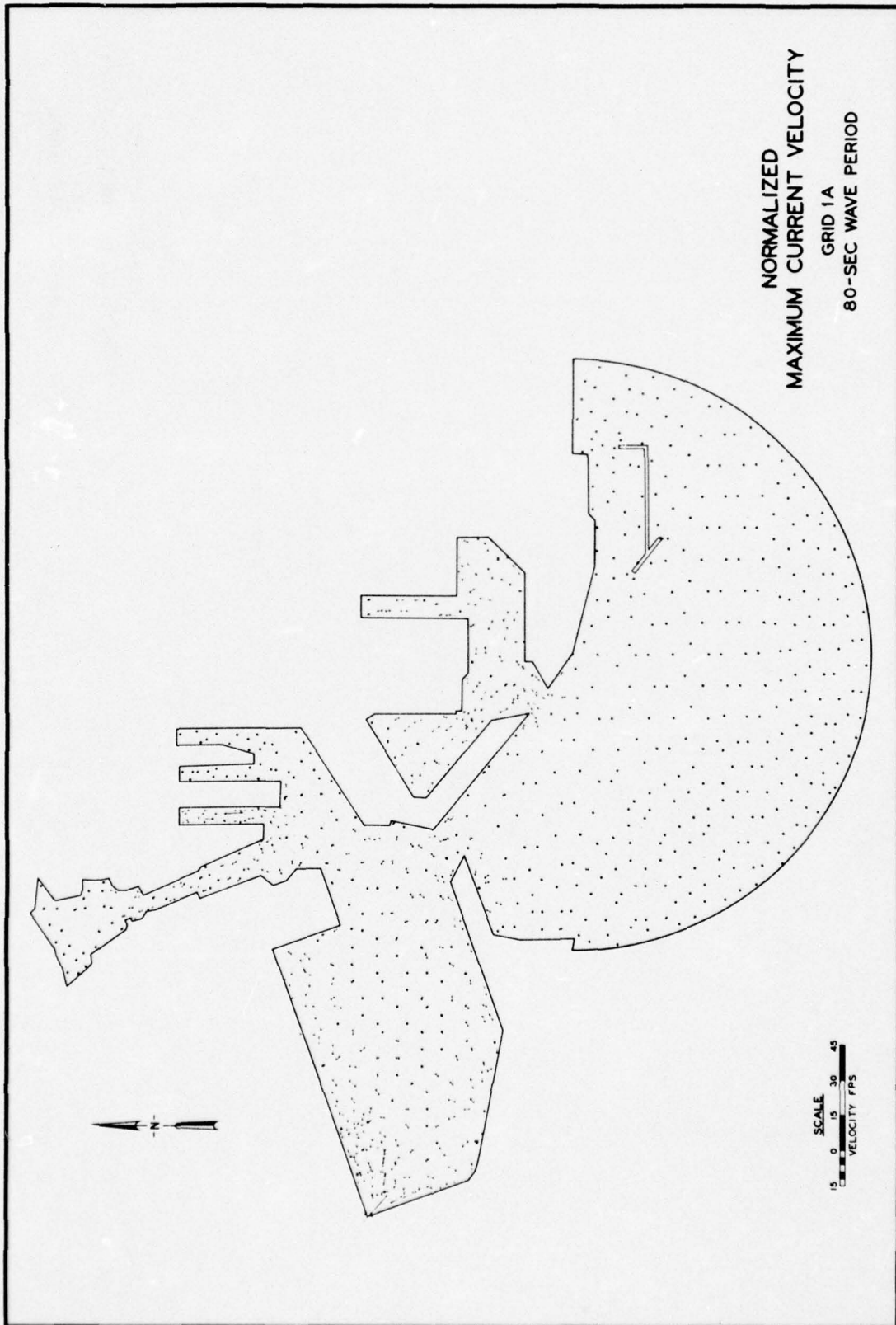






CONTOURS OF
WAVE-HEIGHT AMPLIFICATION
GRID 1 A
80-SEC WAVE PERIOD





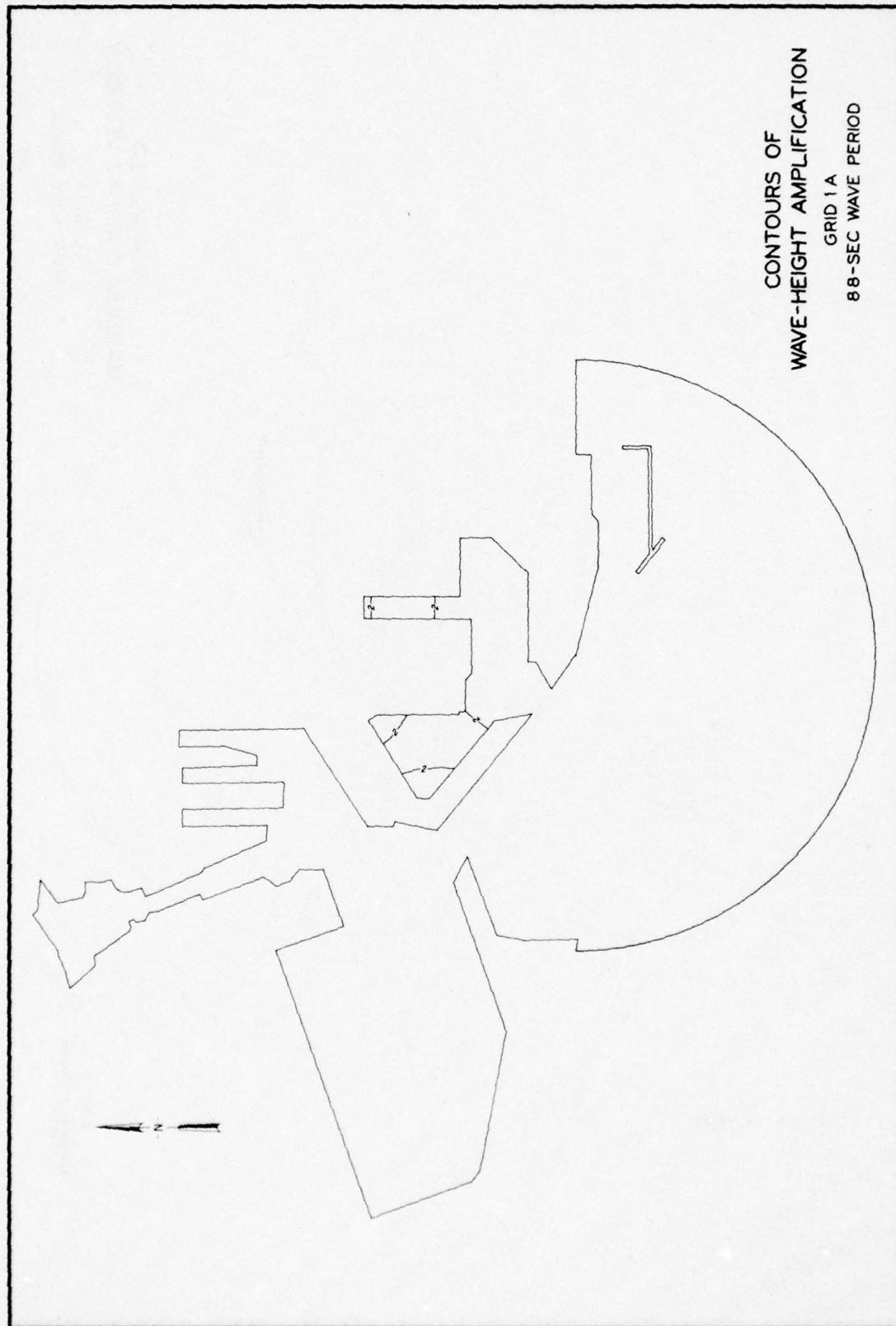
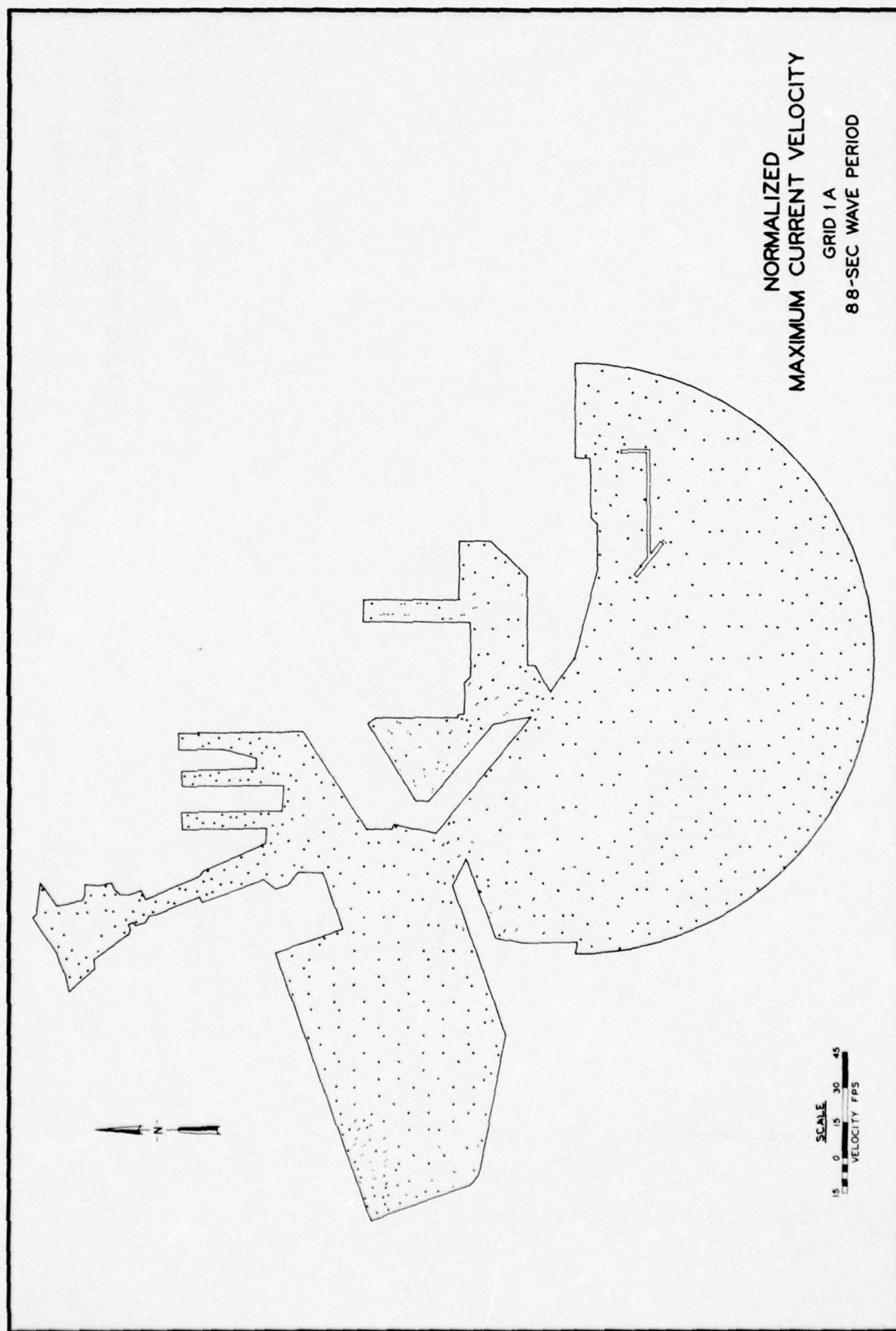


PLATE 132



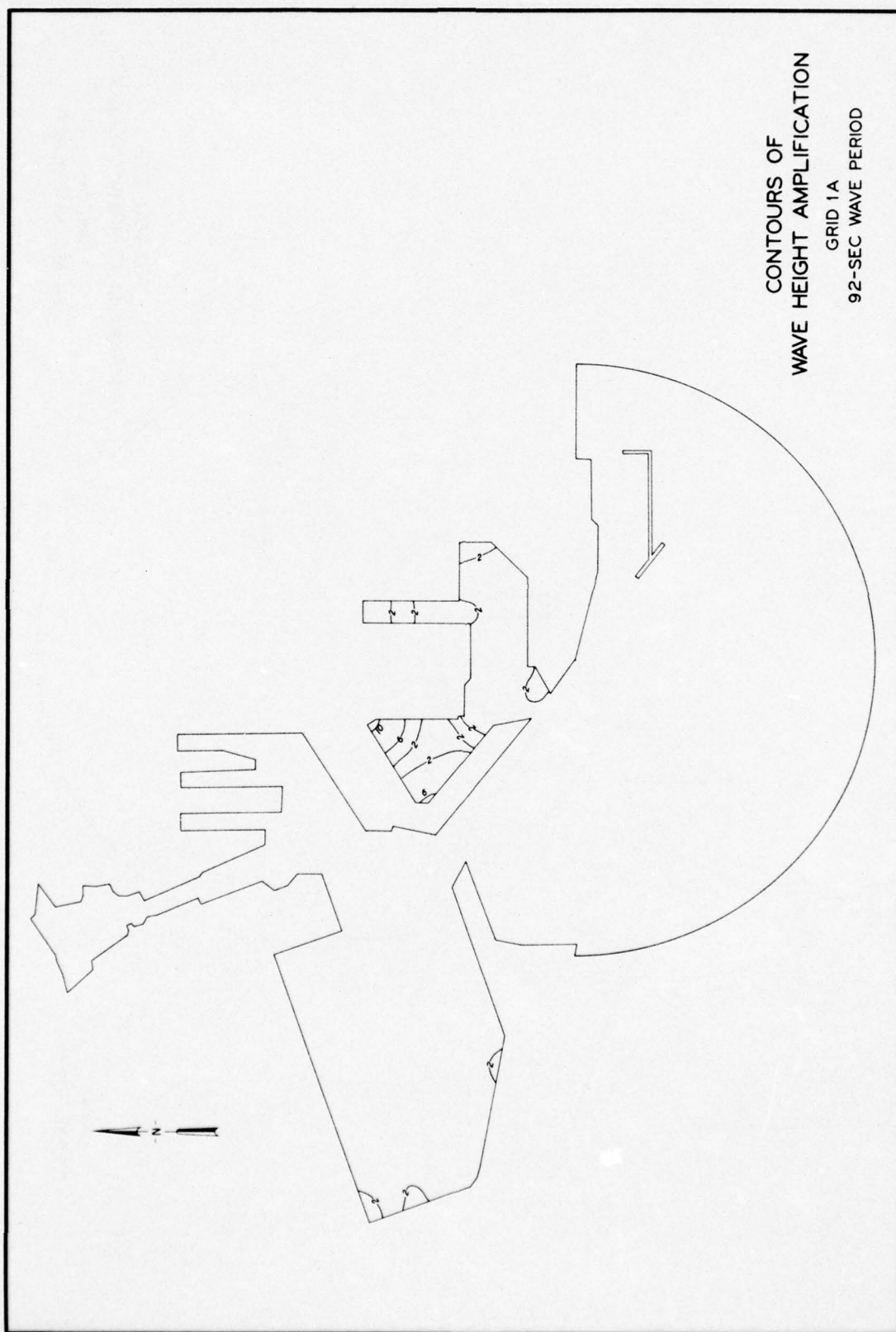
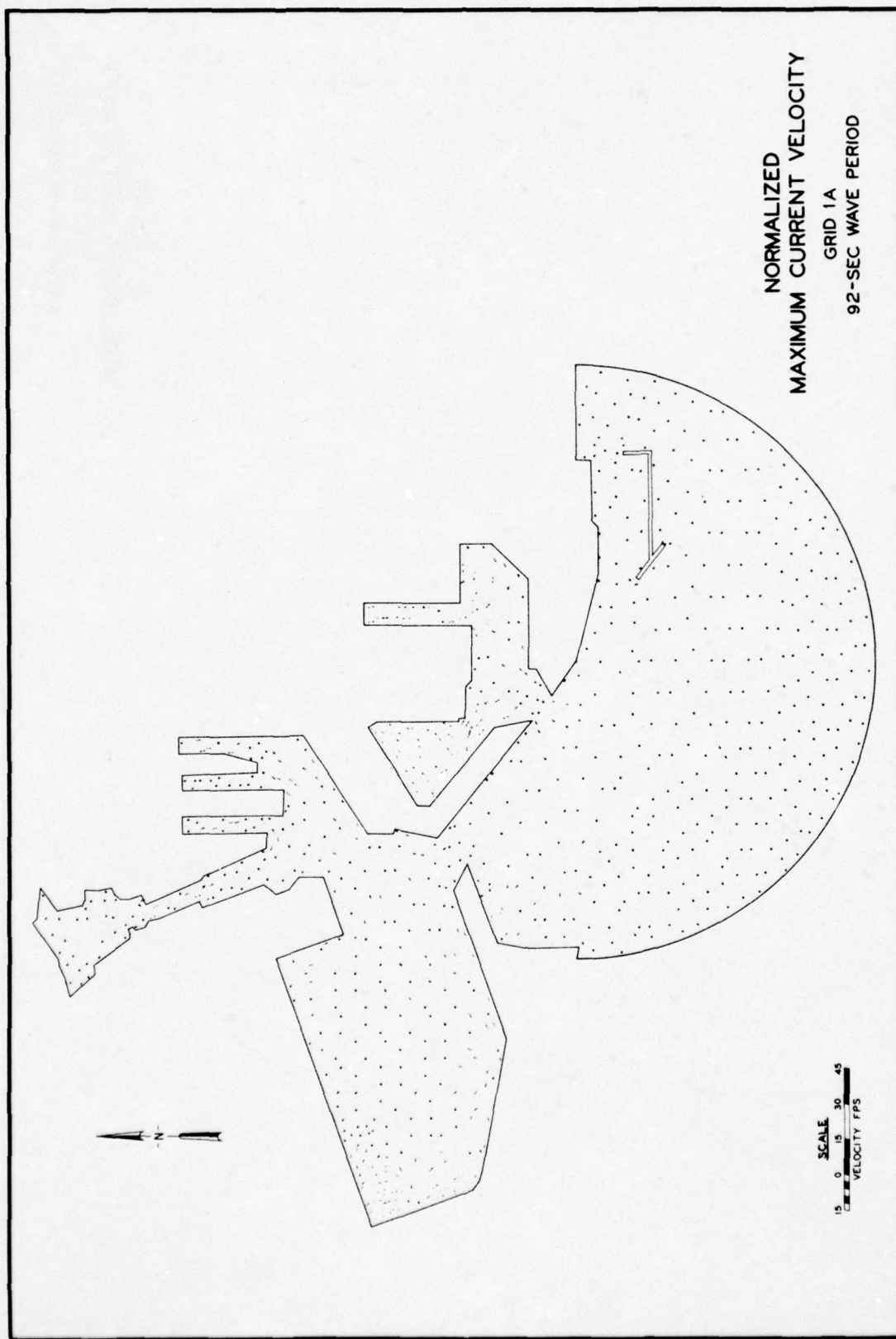
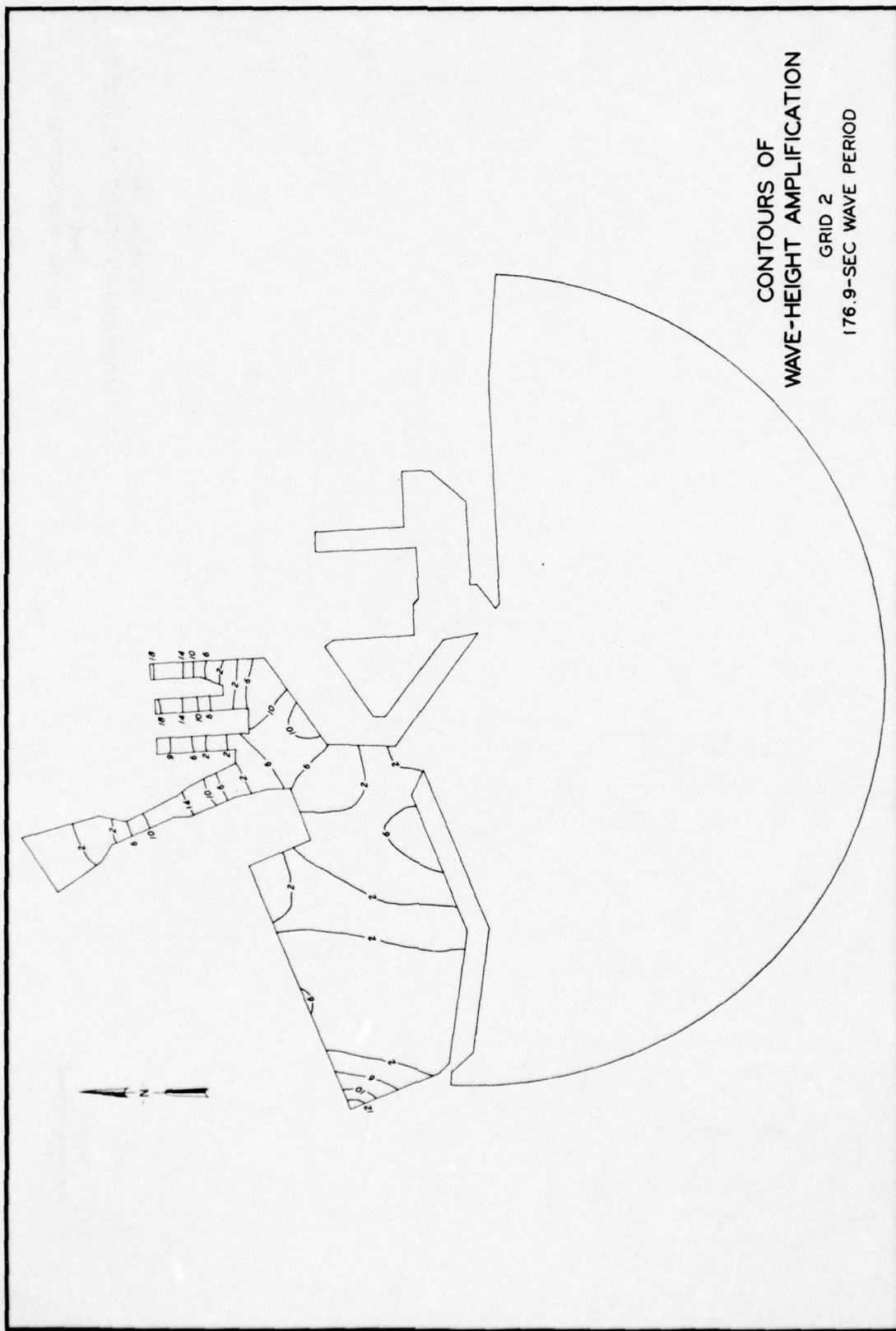
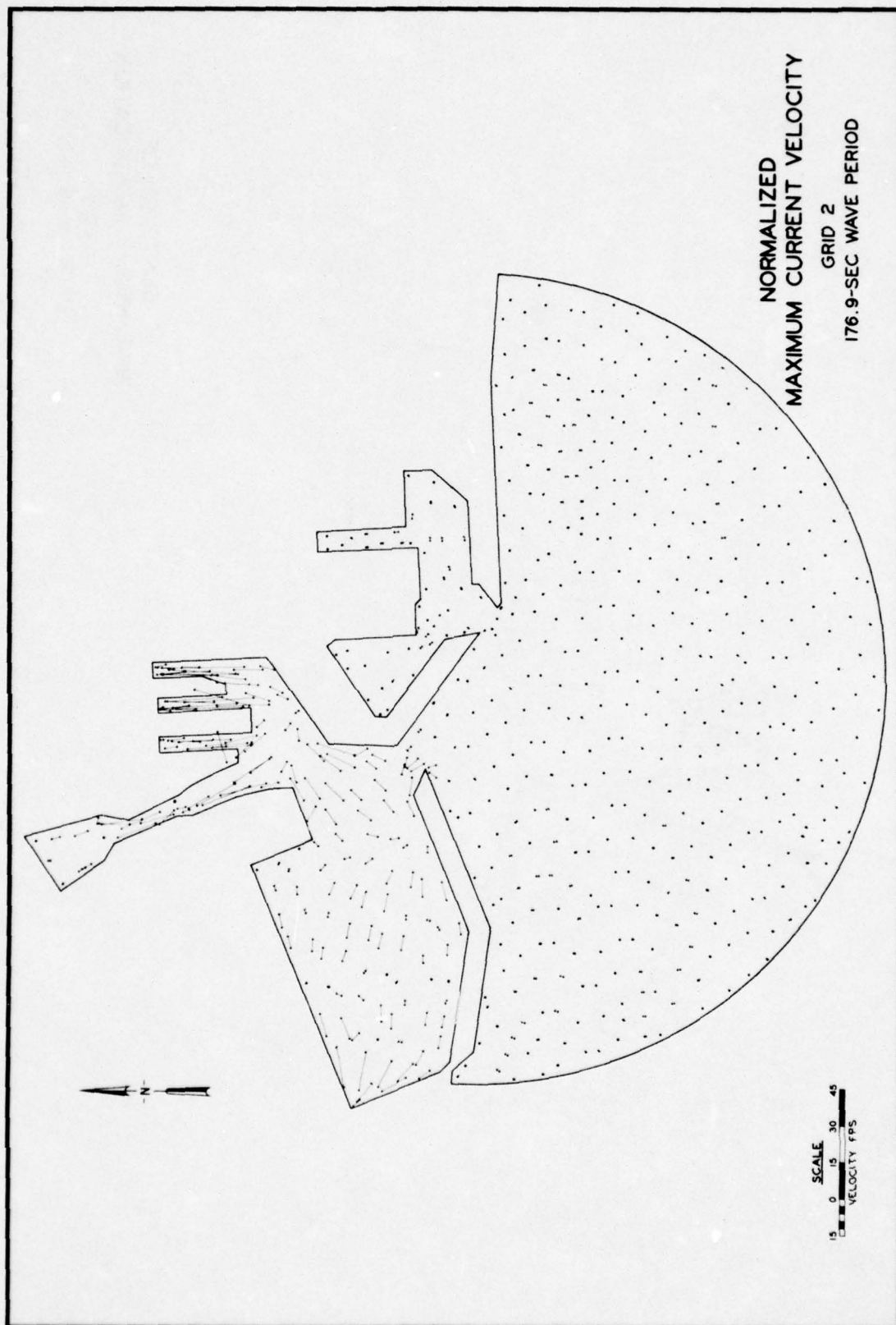


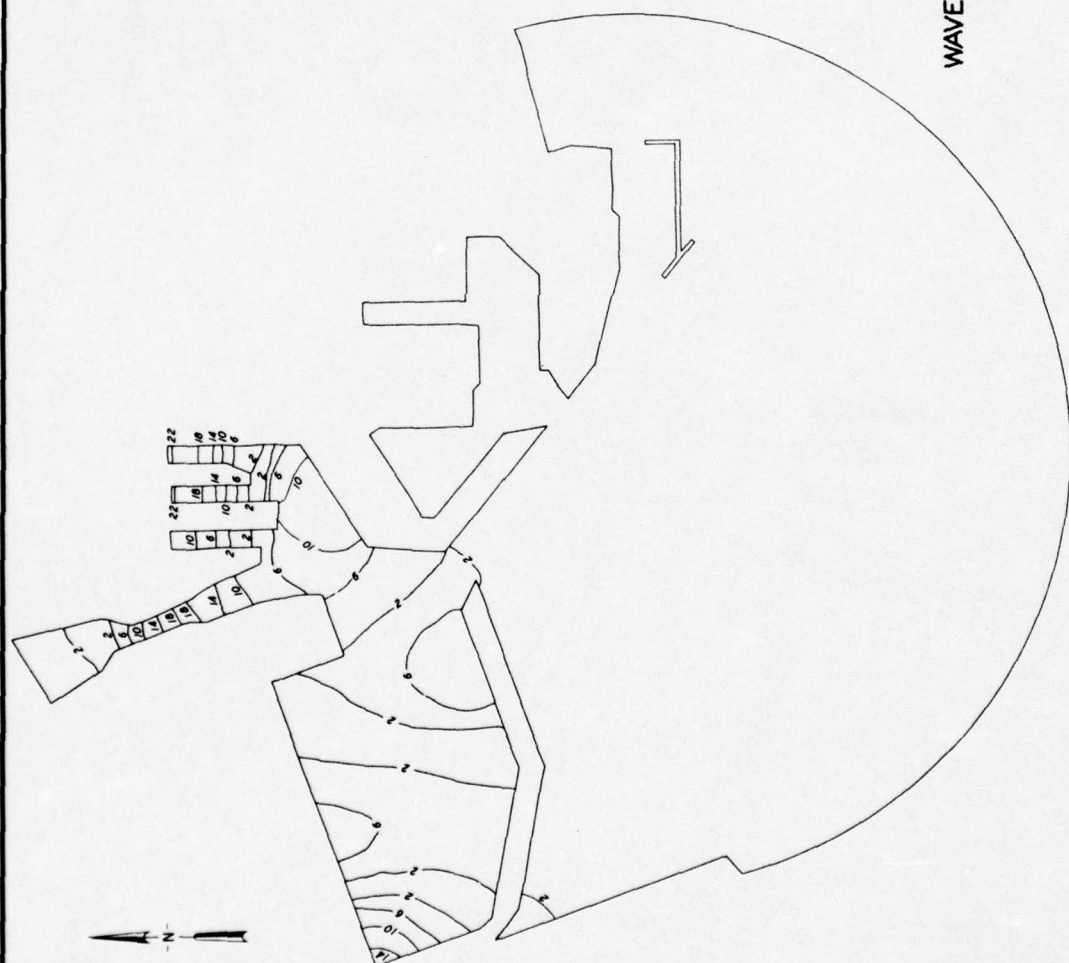
PLATE 134

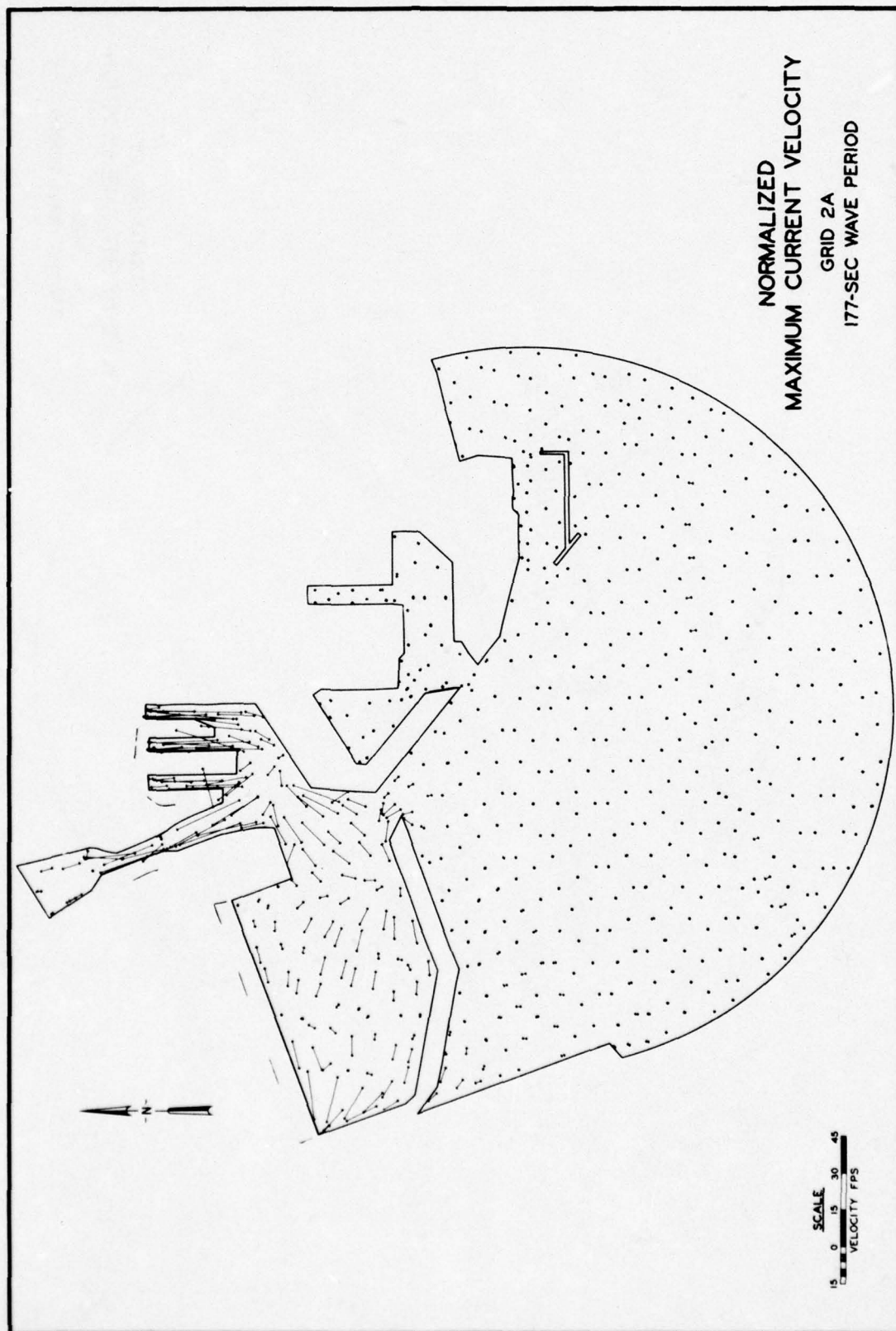


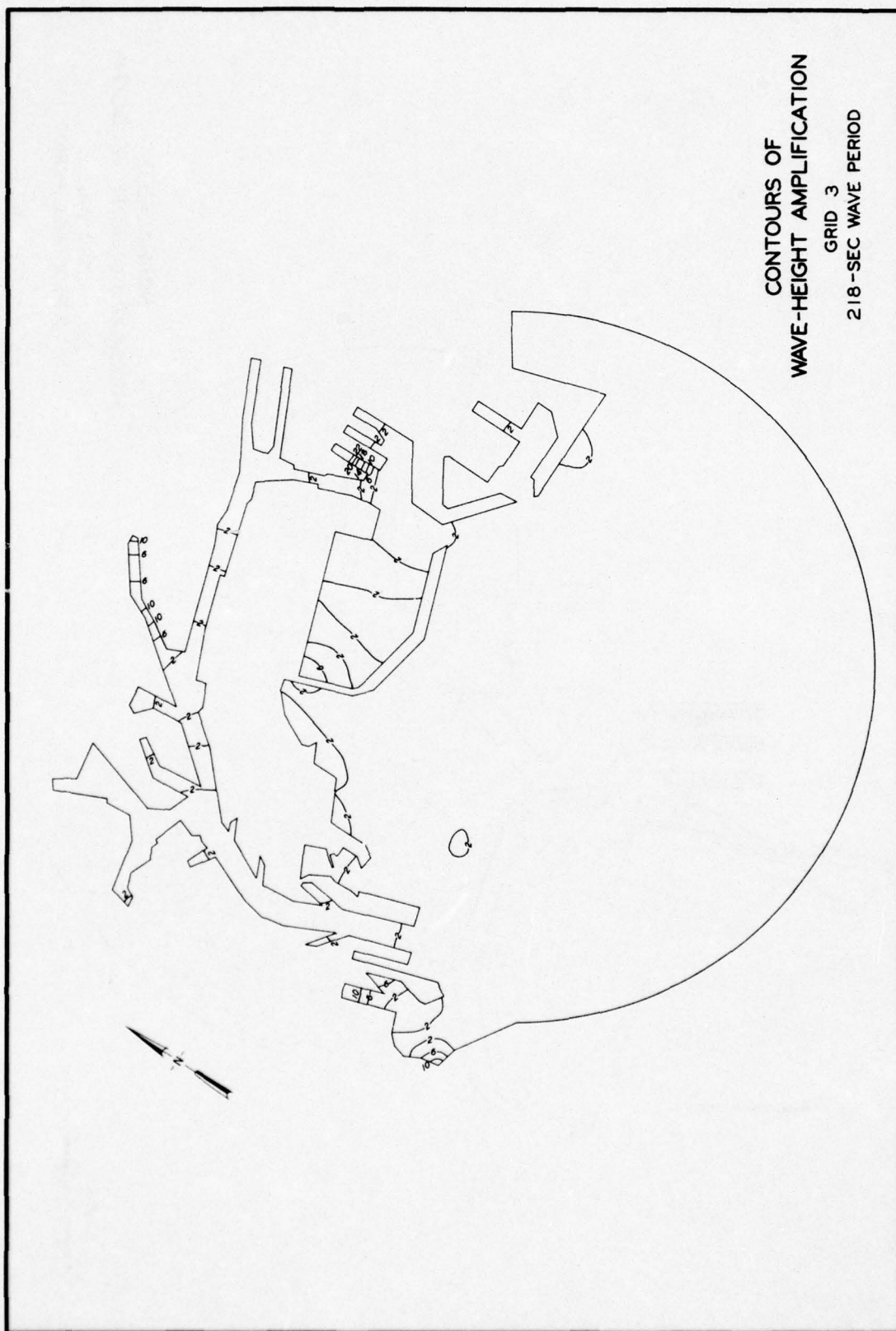


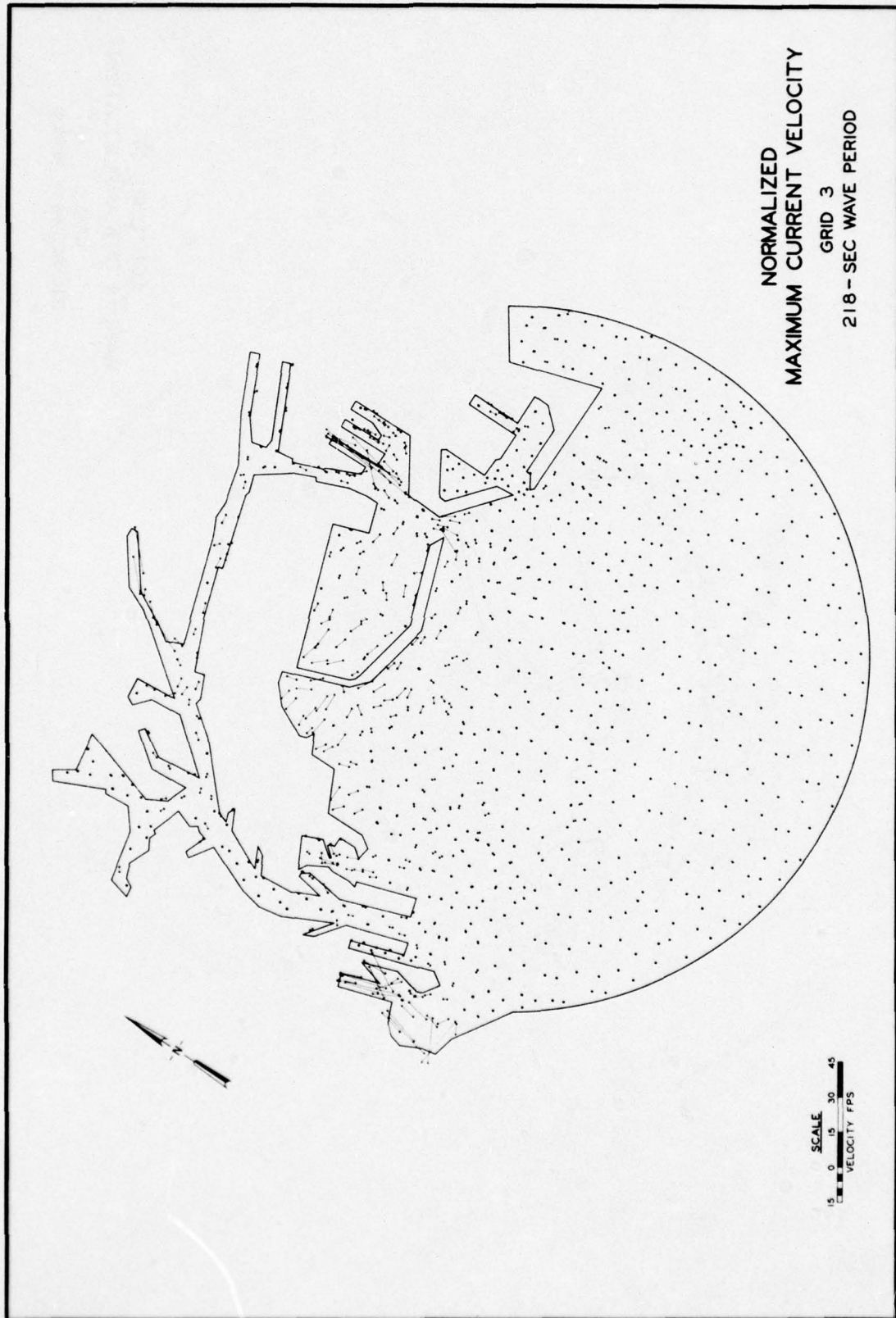


CONTOURS OF
WAVE-HEIGHT AMPLIFICATION
GRID 2A
177-SEC WAVE PERIOD

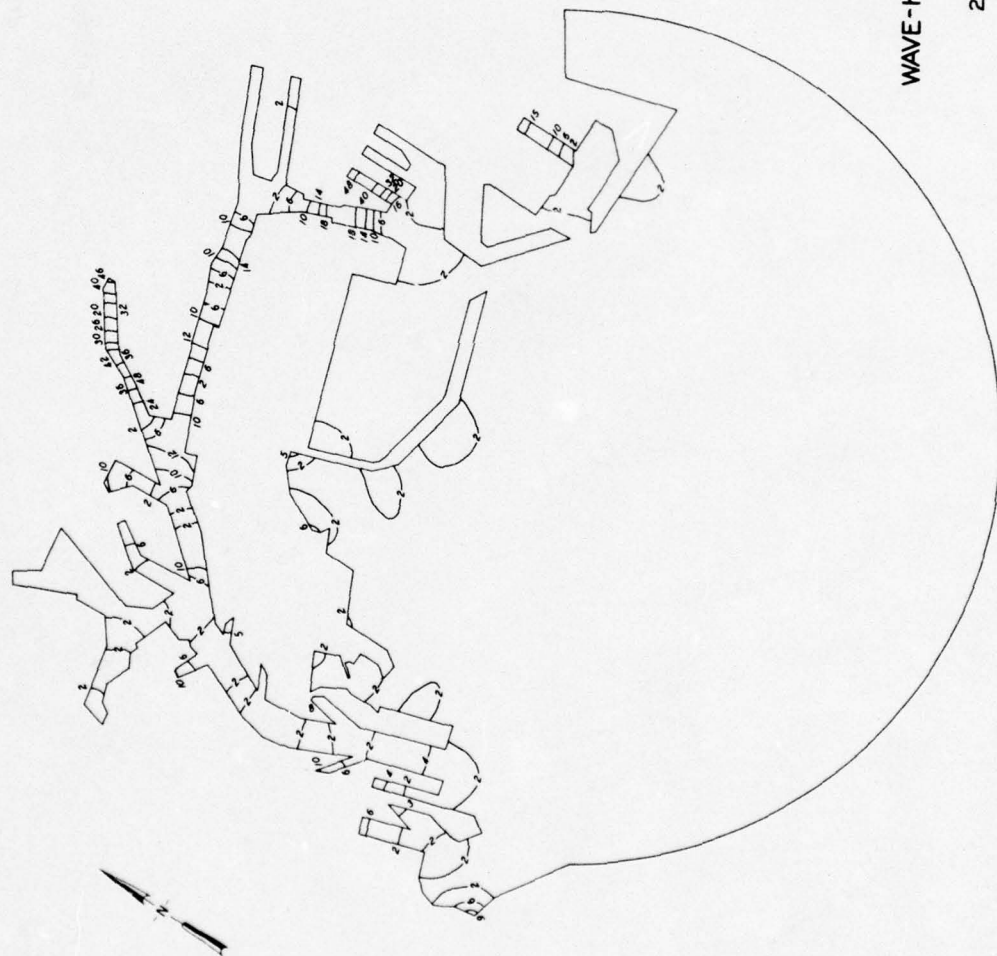




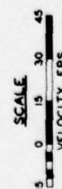
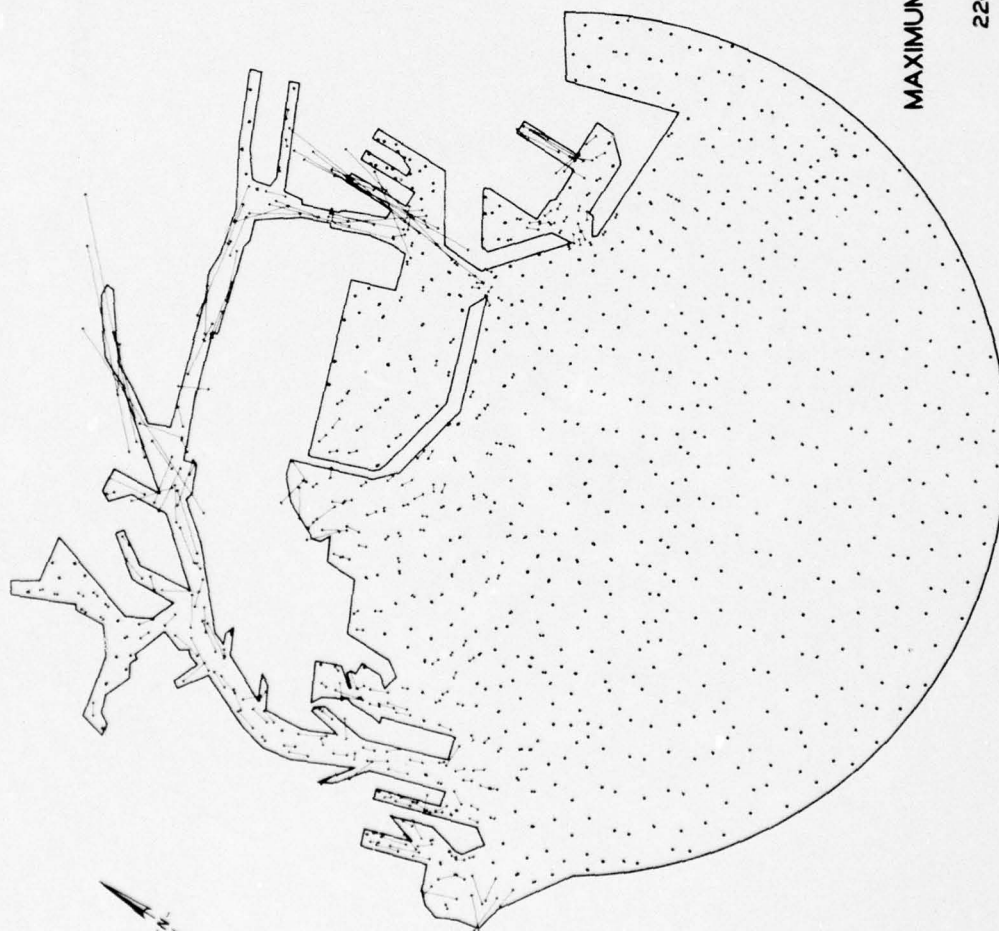




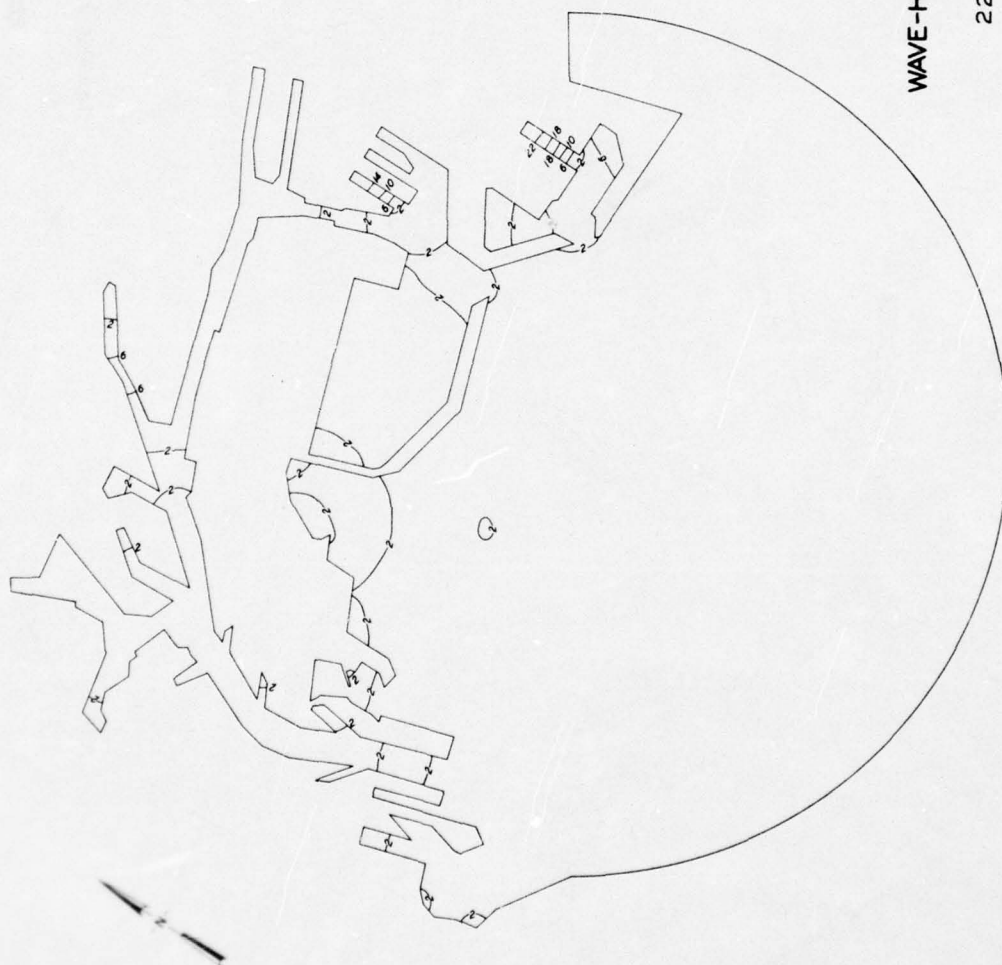
CONTOURS OF
WAVE-HEIGHT AMPLIFICATION
GRID 3
220-SEC WAVE PERIOD

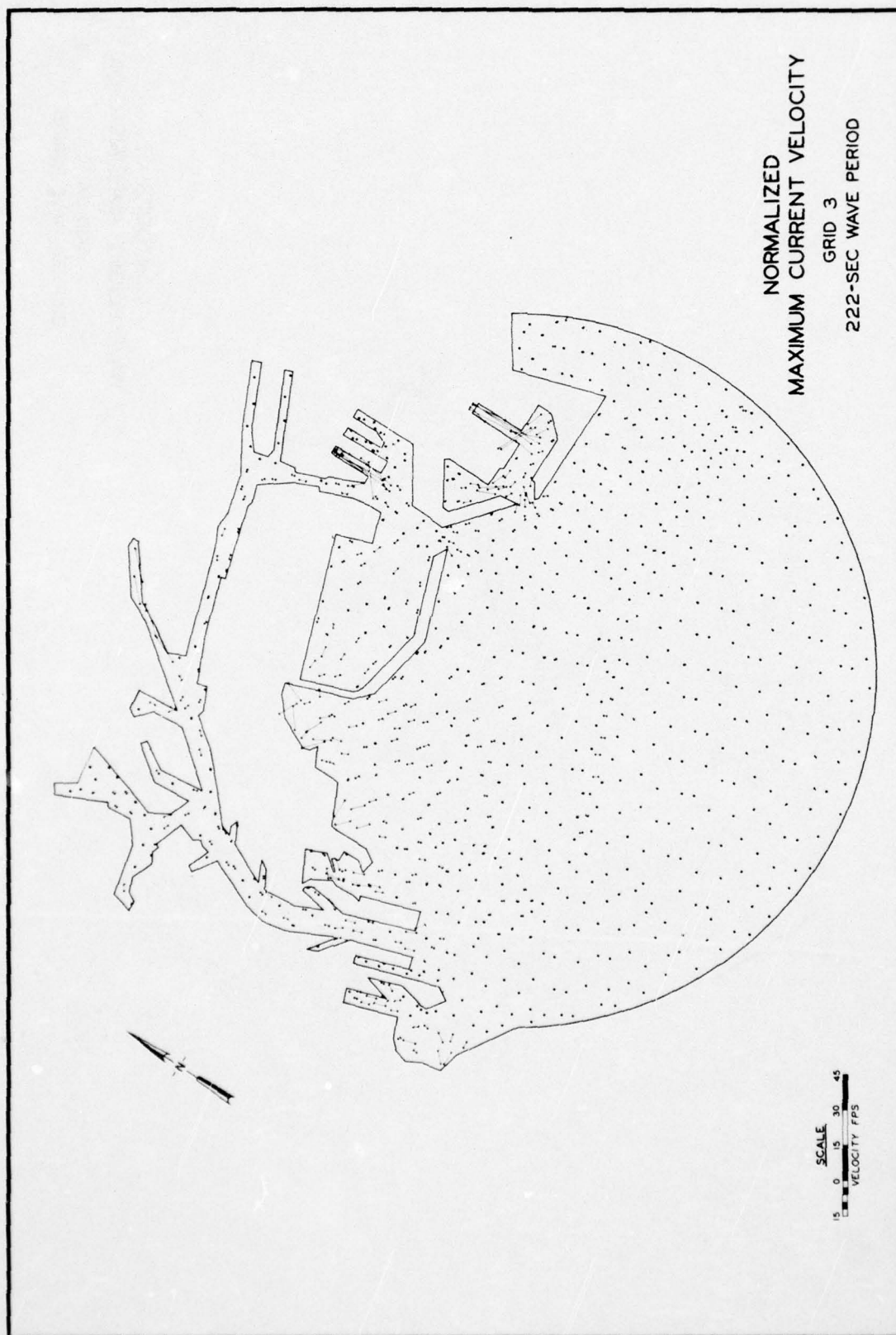


NORMALIZED
MAXIMUM CURRENT VELOCITY
GRID 3
220-SEC WAVE PERIOD

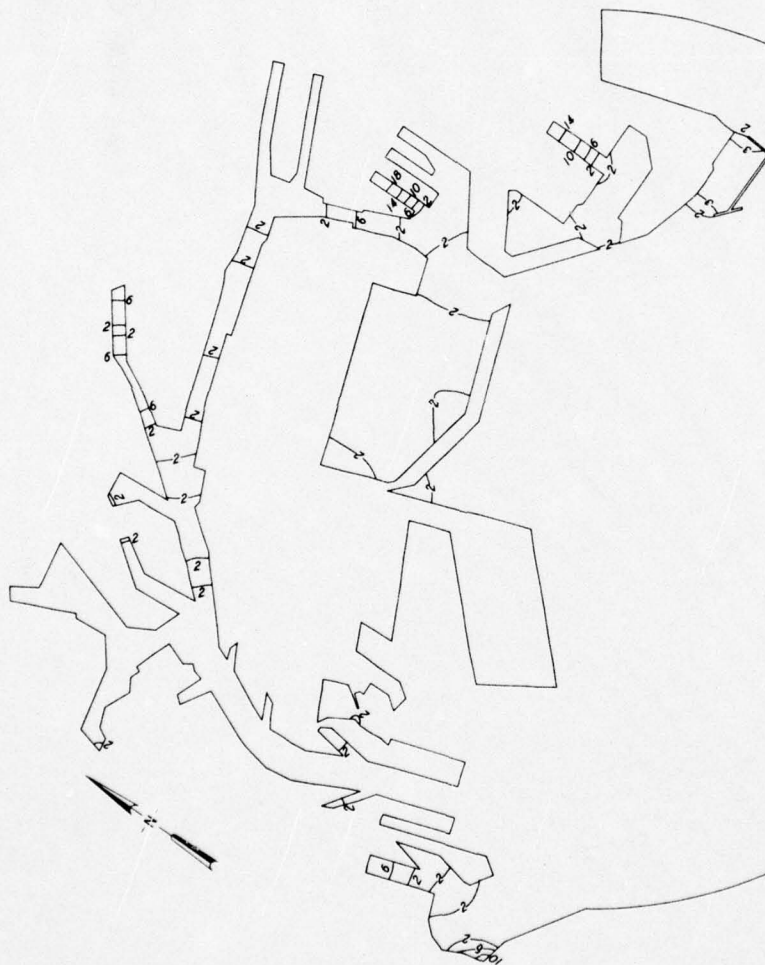


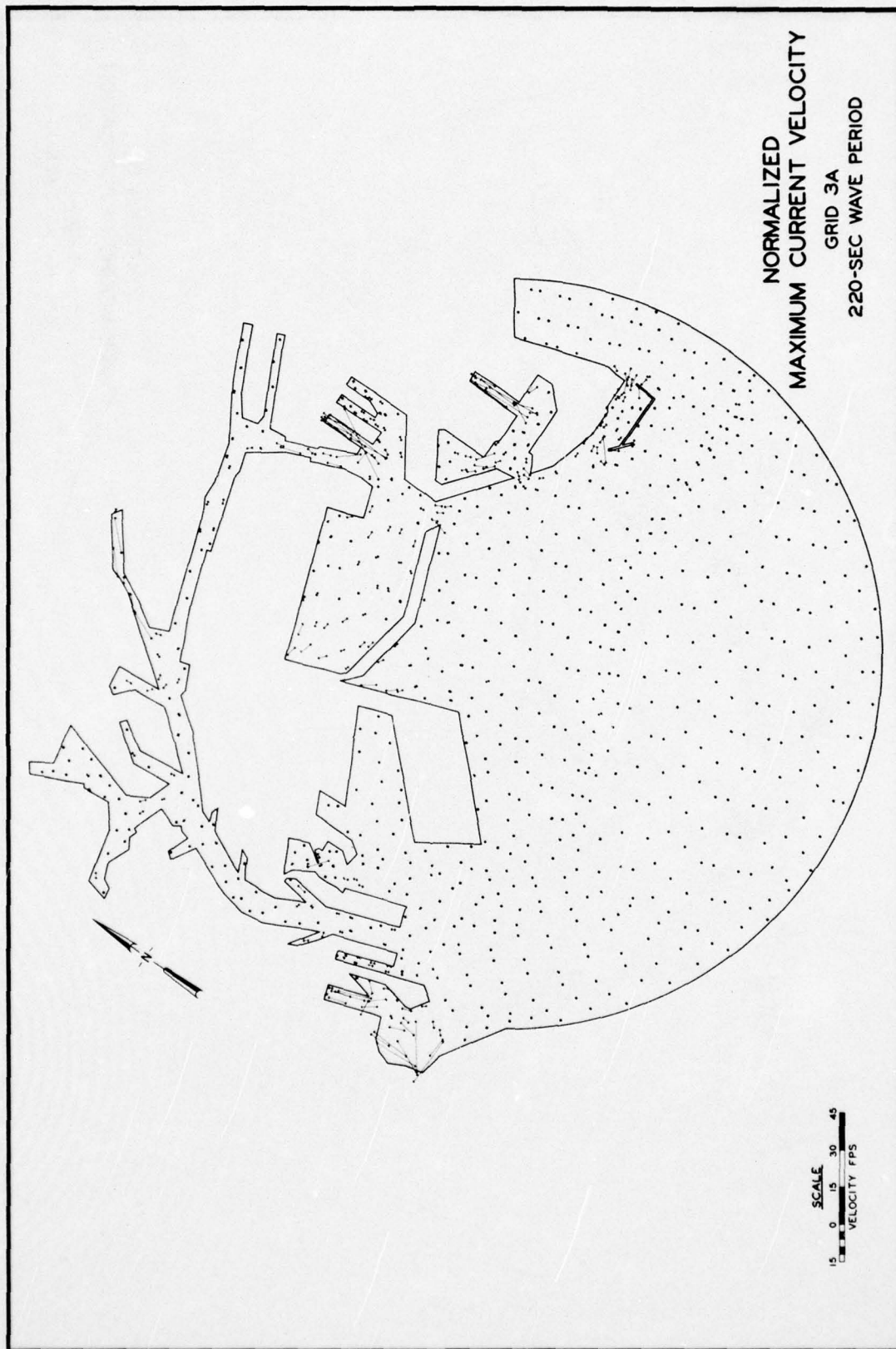
CONTOURS OF
WAVE-HEIGHT AMPLIFICATION
GRID 3
222-SEC WAVE PERIOD

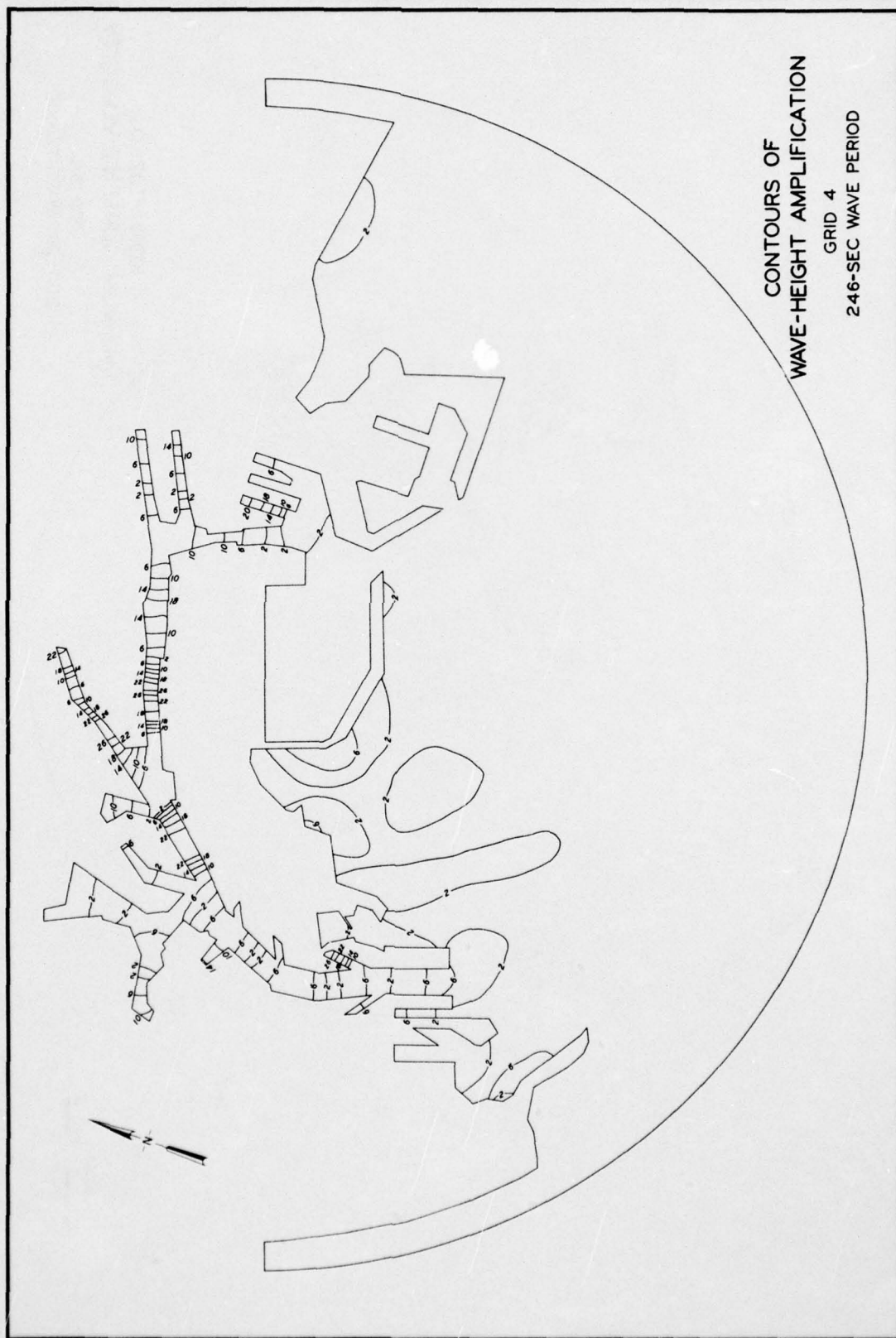




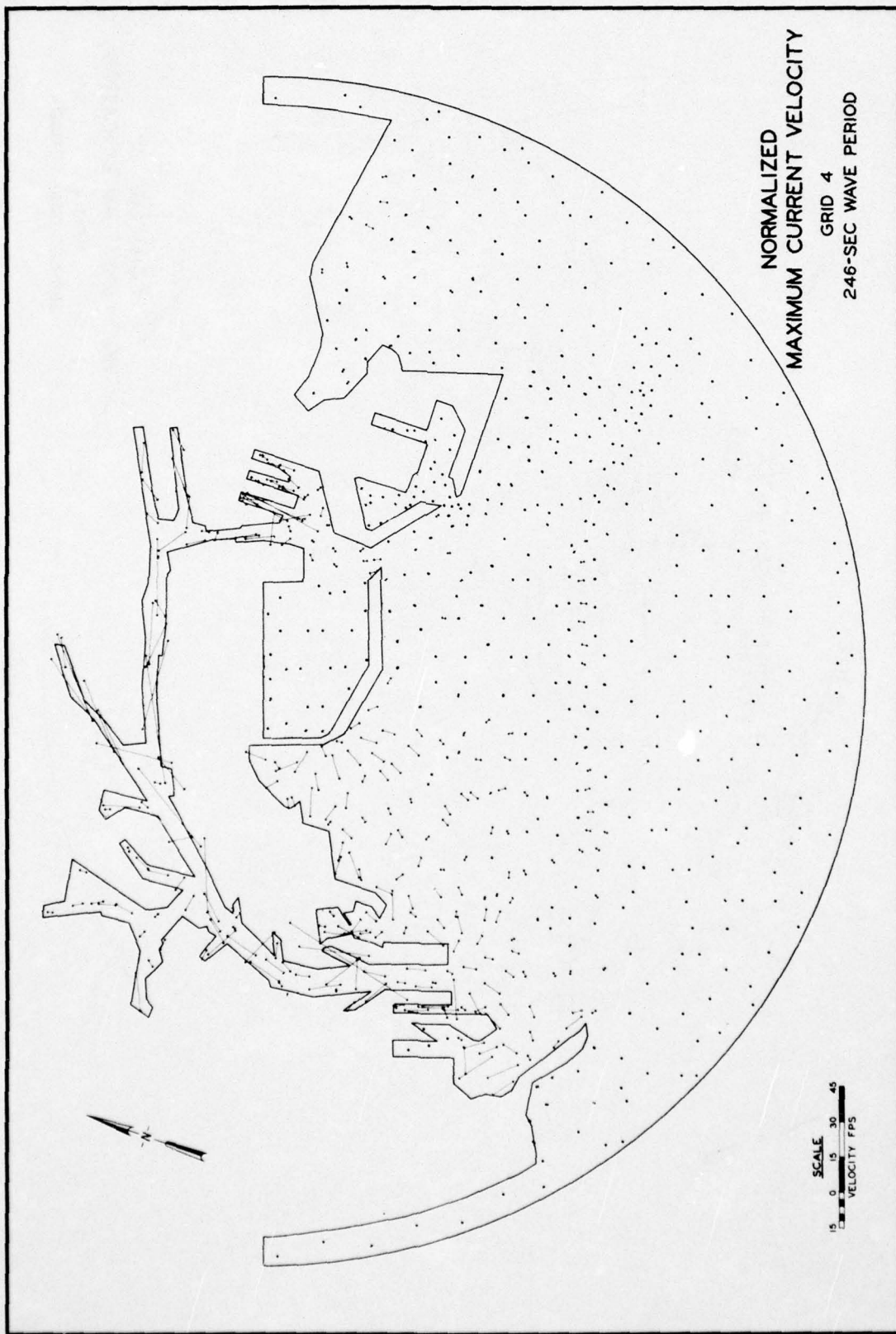
CONTOURS OF
WAVE-HEIGHT AMPLIFICATION
GRID 3A
220-SEC WAVE PERIOD

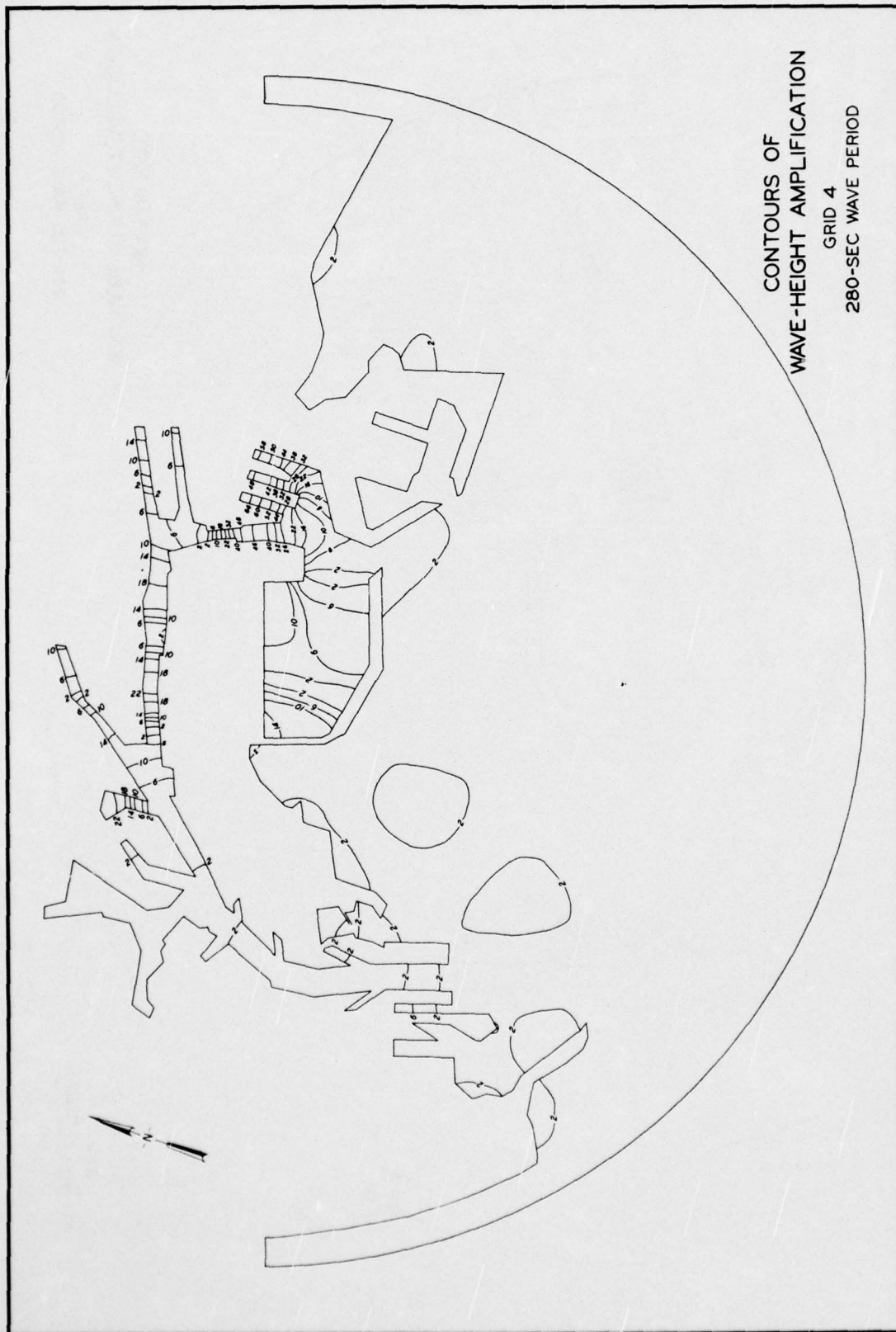


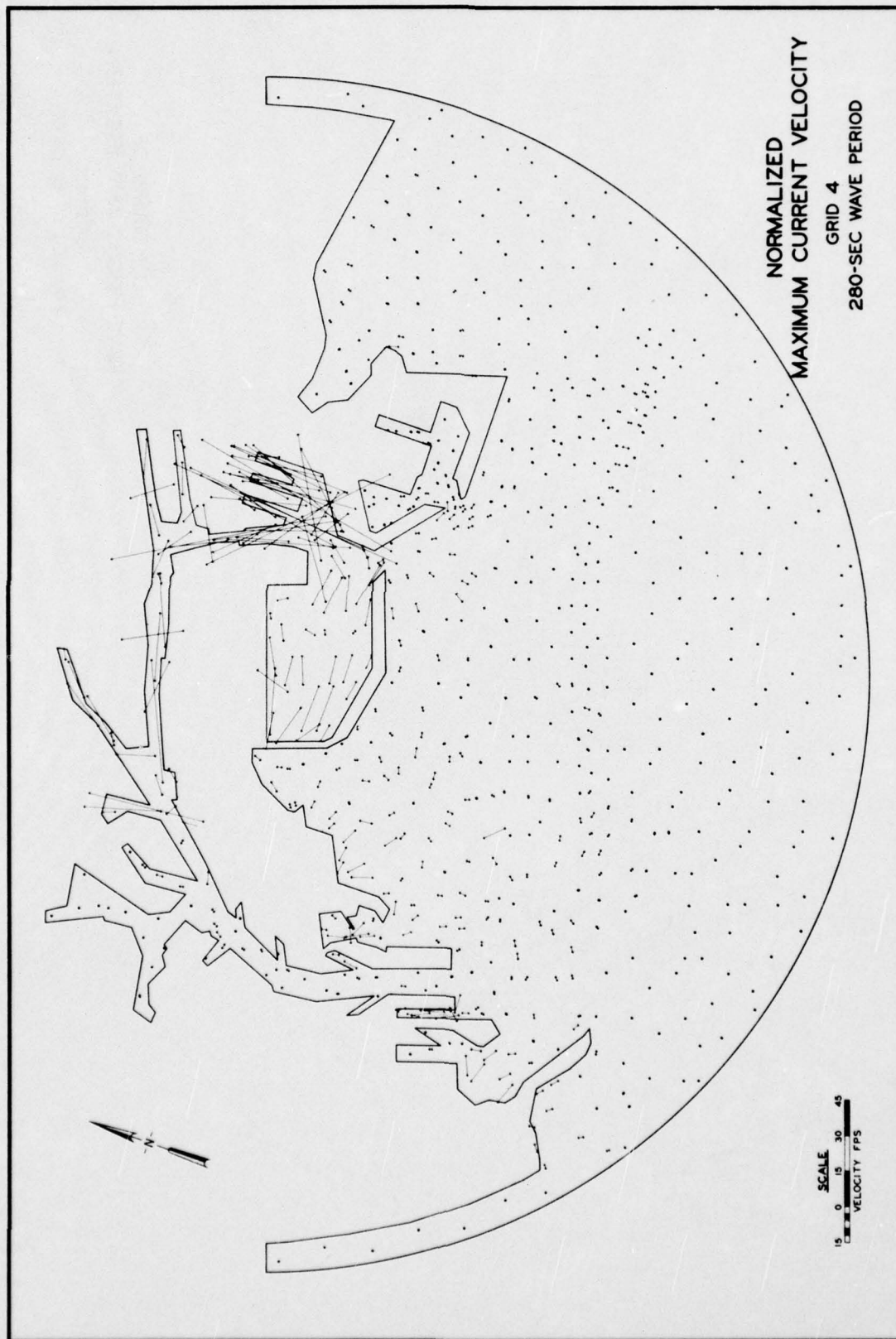


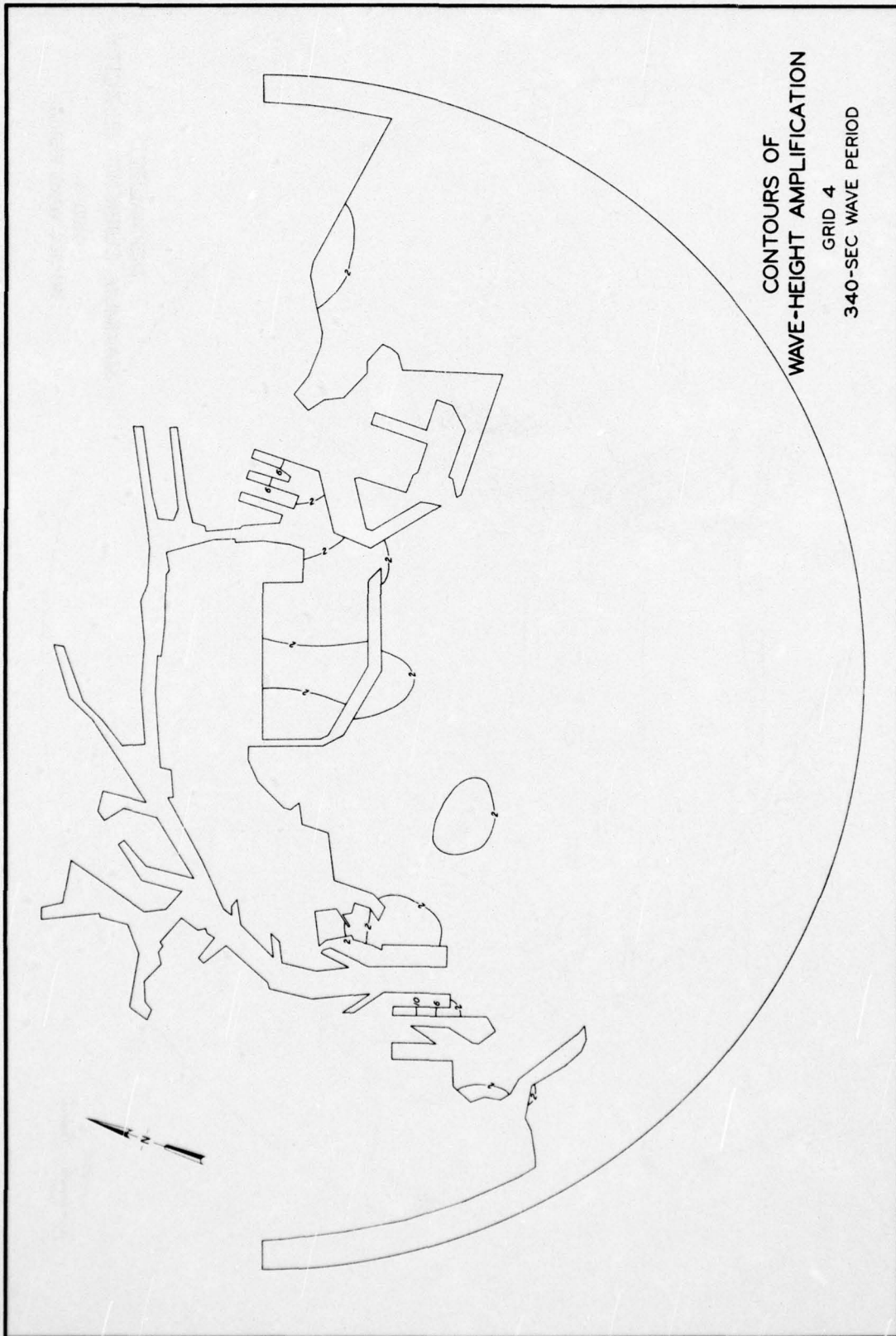


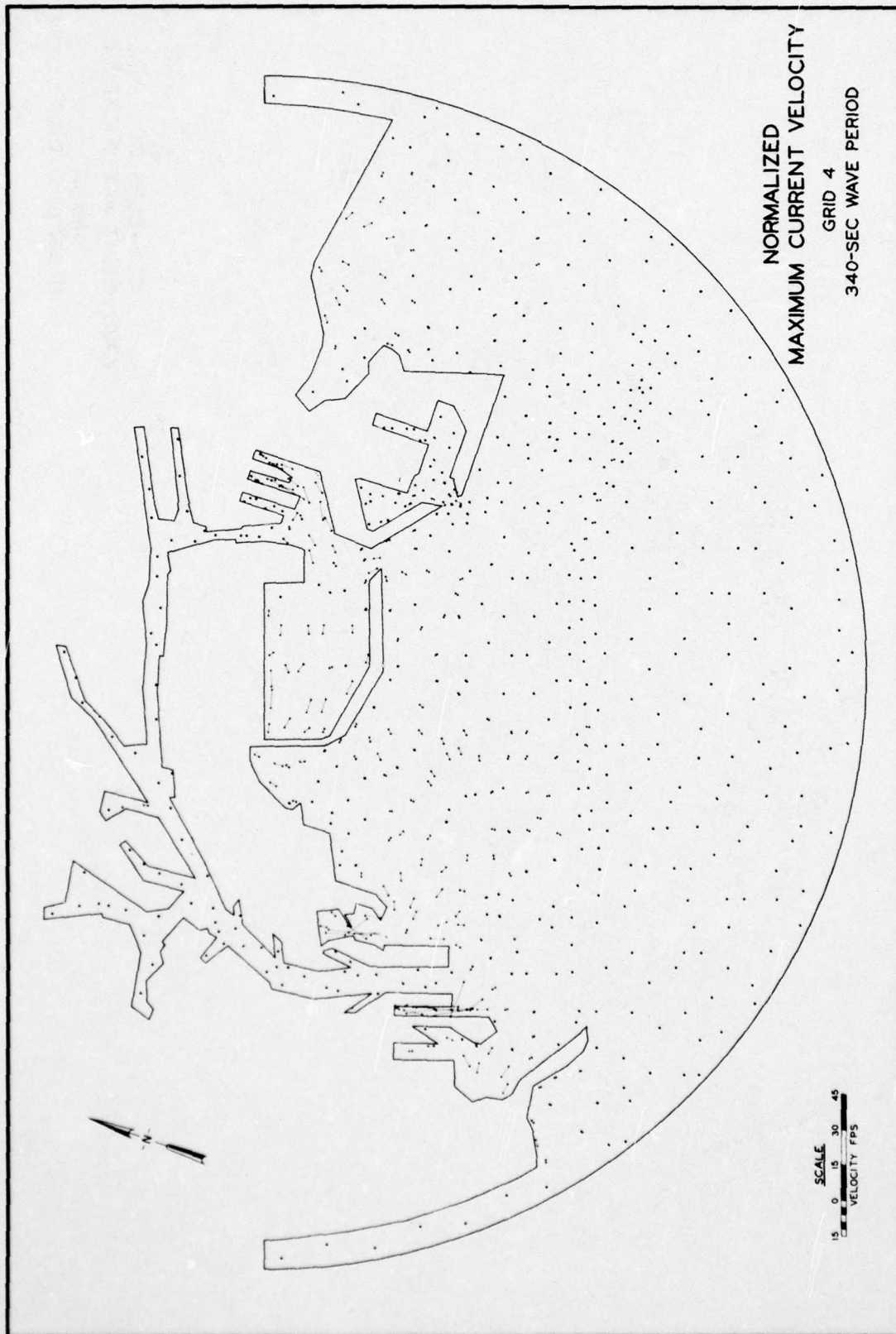
CONTOURS OF
WAVE-HEIGHT AMPLIFICATION
GRID 4
246-SEC WAVE PERIOD

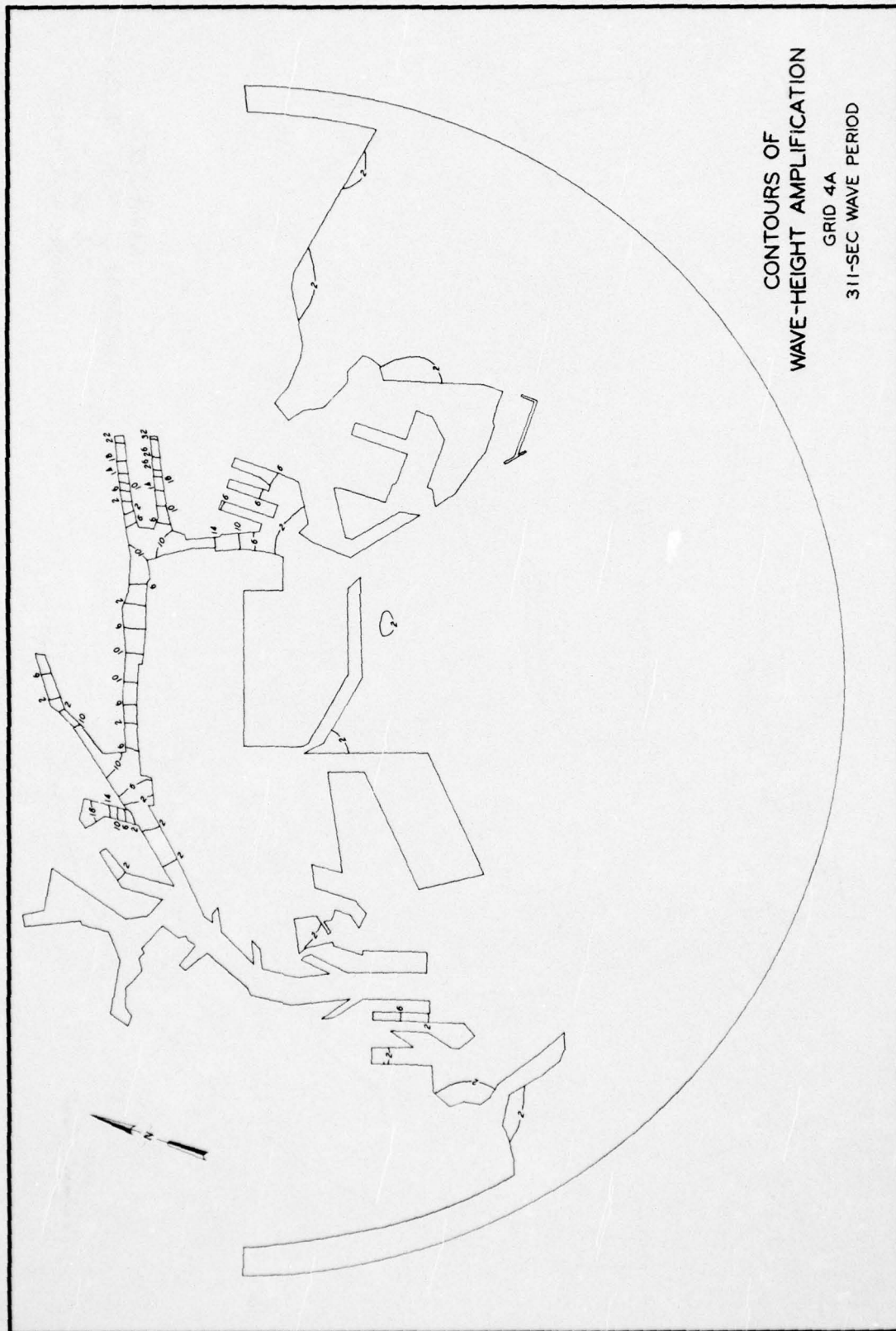


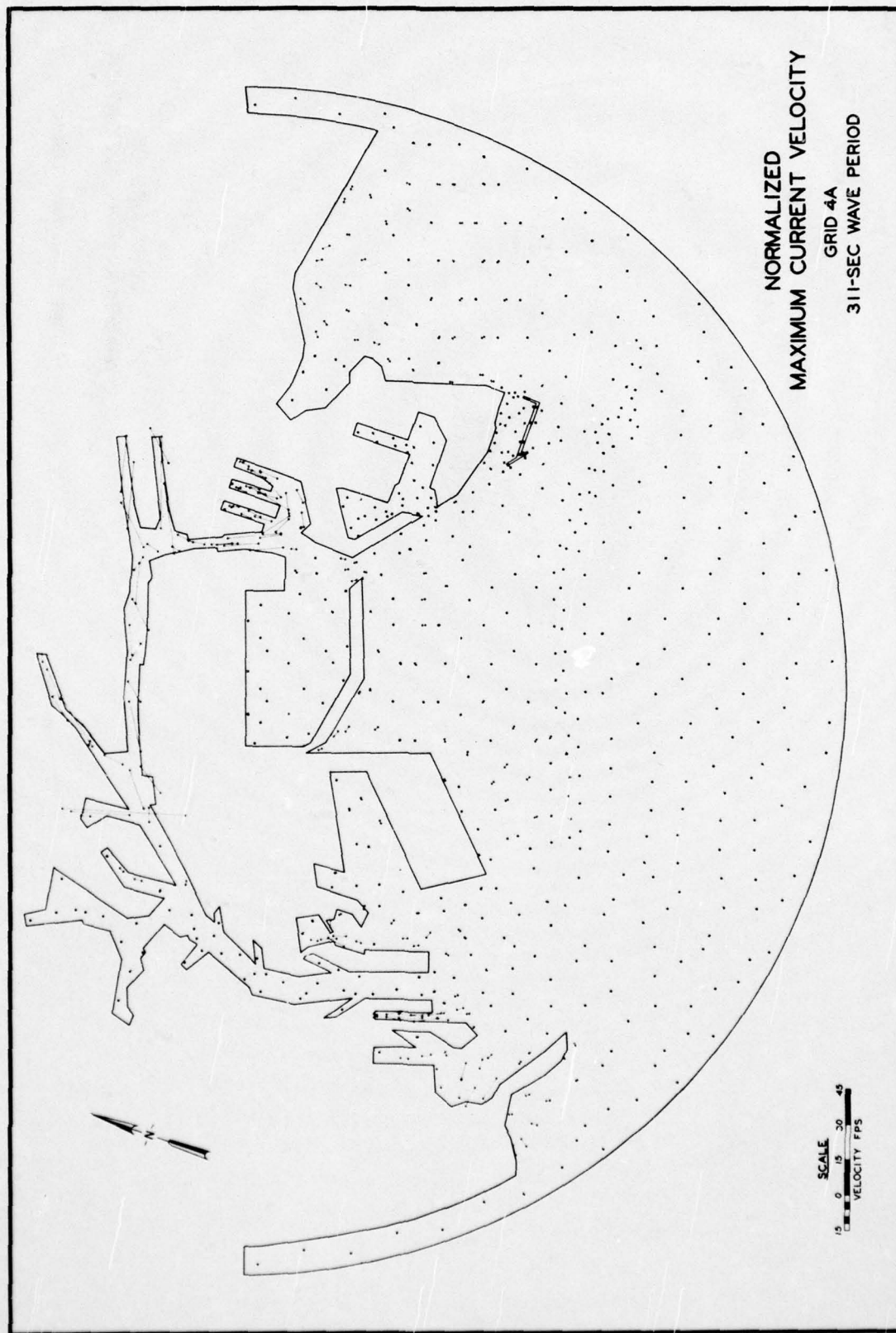


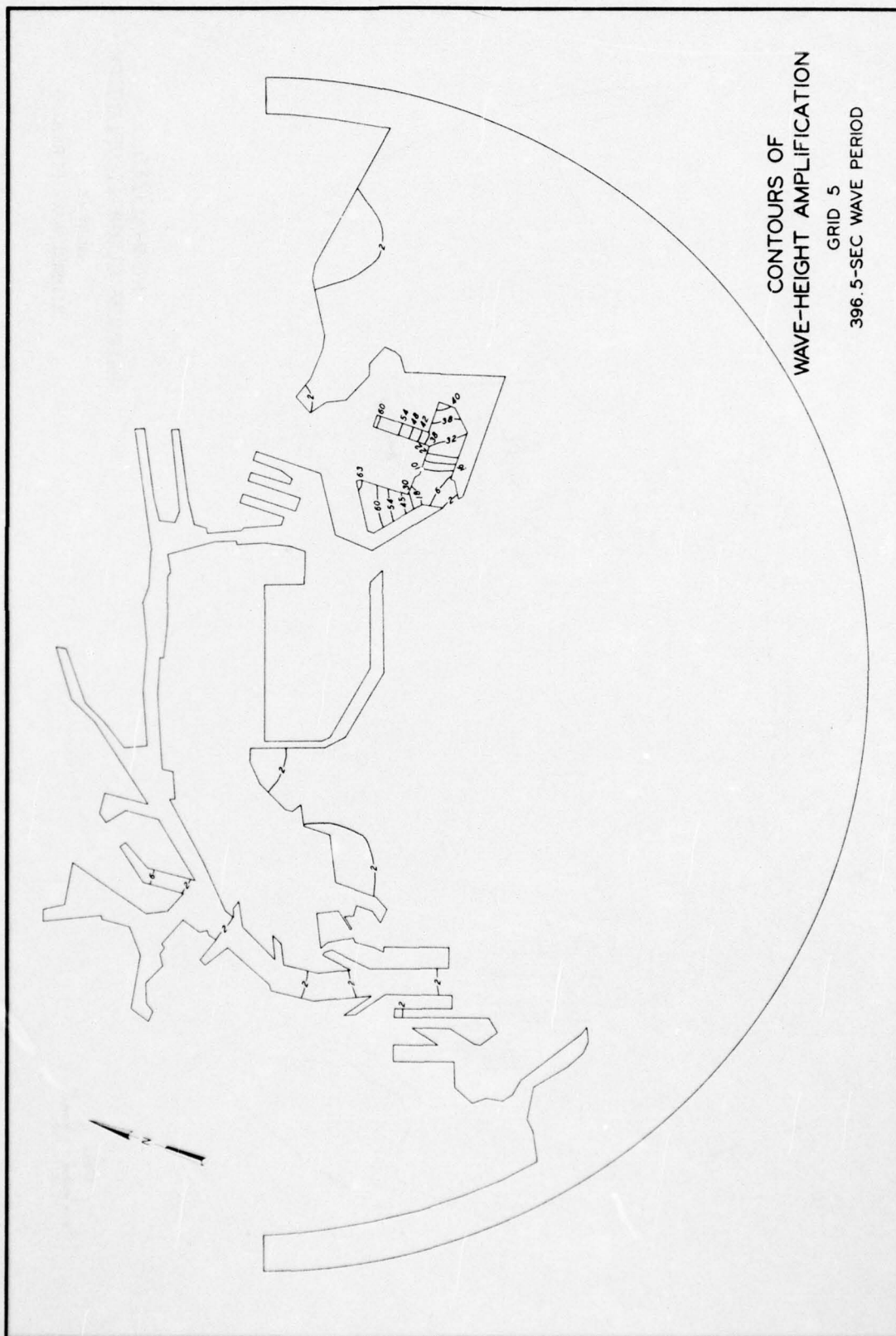


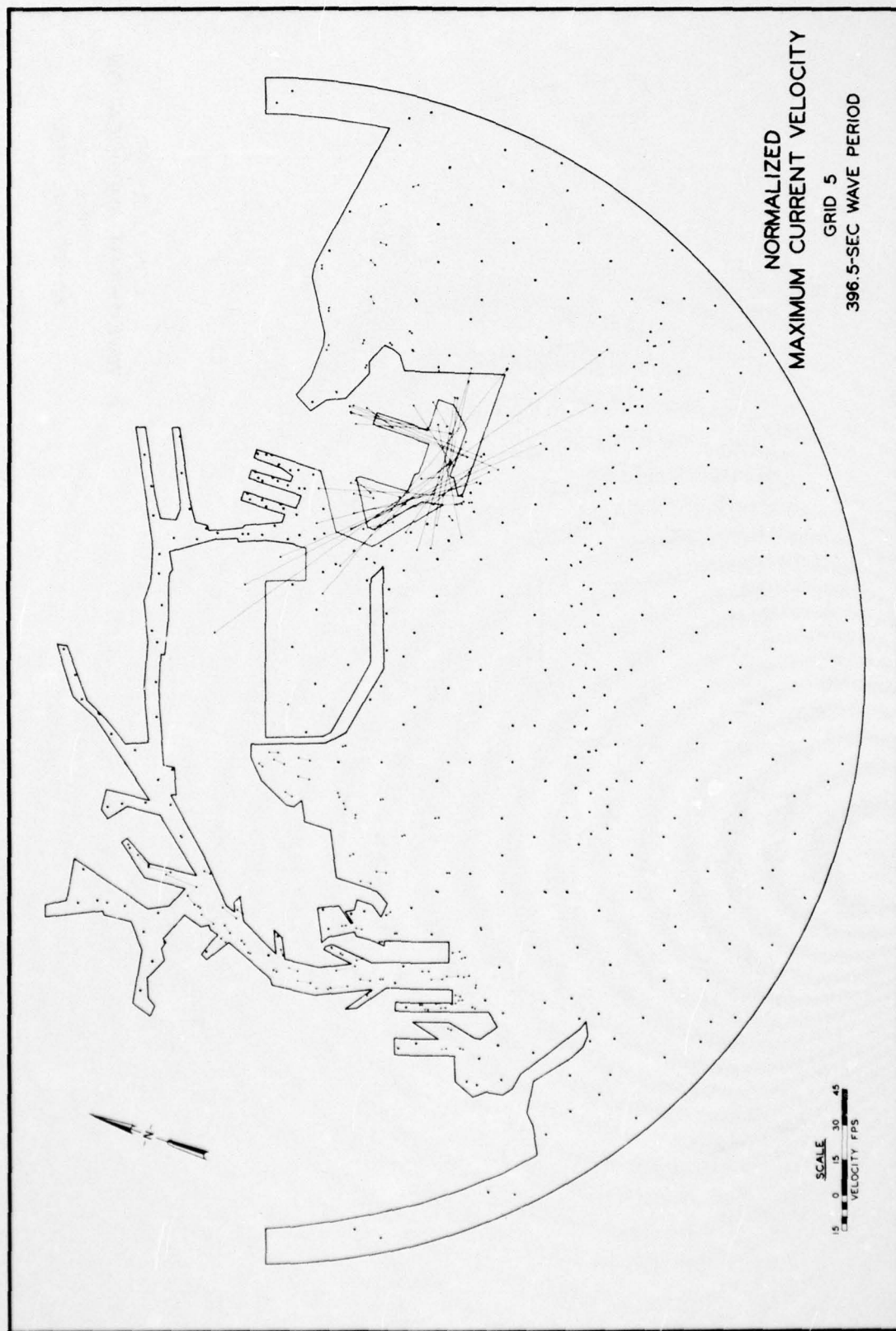












AD-A031 171

ARMY ENGINEER WATERWAYS EXPERIMENT STATION VICKSBURG MISS F/G 8/3
LONG BEACH HARBOR NUMERICAL ANALYSIS OF HARBOR OSCILLATIONS. RE--ETC(U)
SEP 76 J R HOUSTON

UNCLASSIFIED

WES-MP-H-76-20-1

NL

3 OF 3

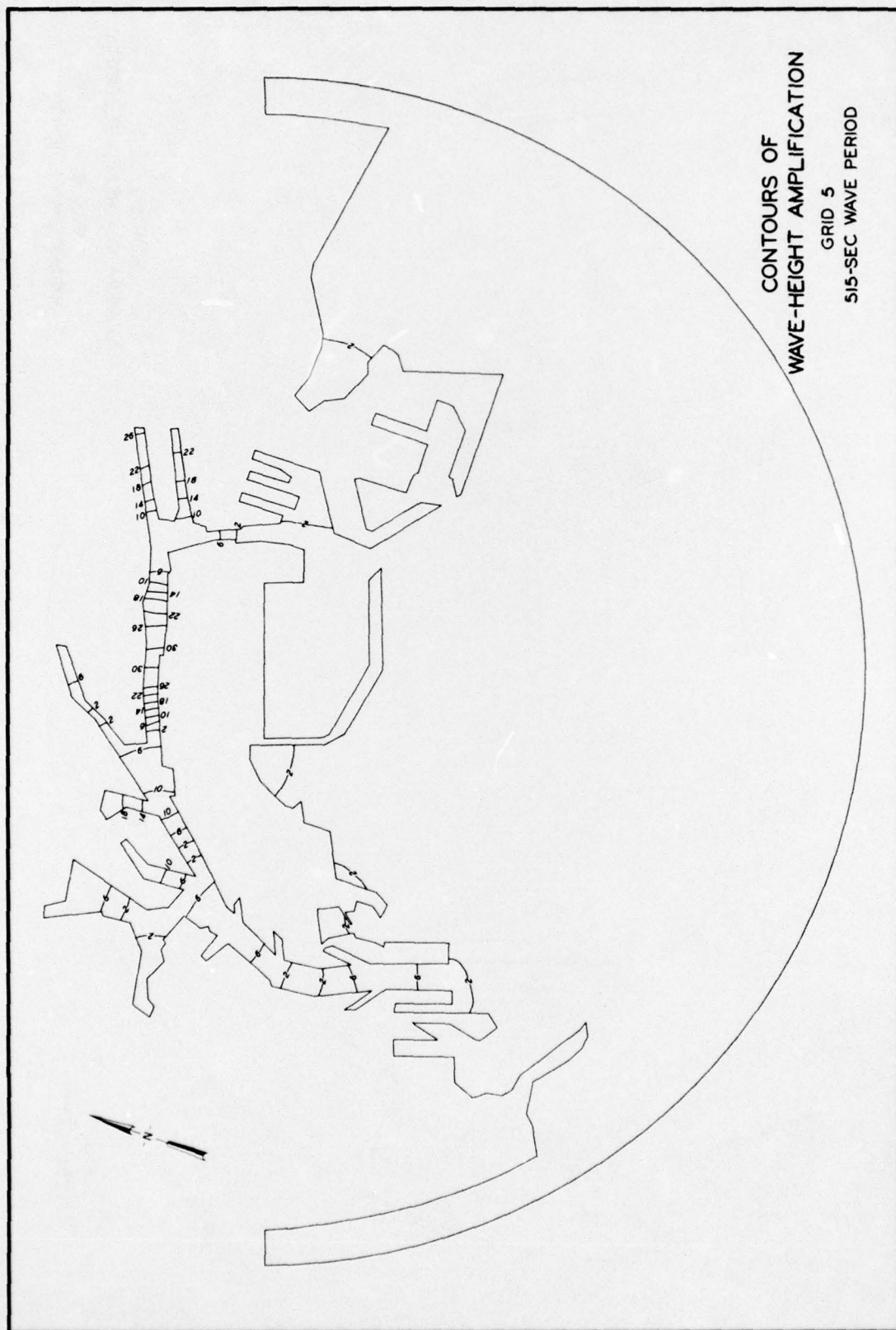
AD
A031171

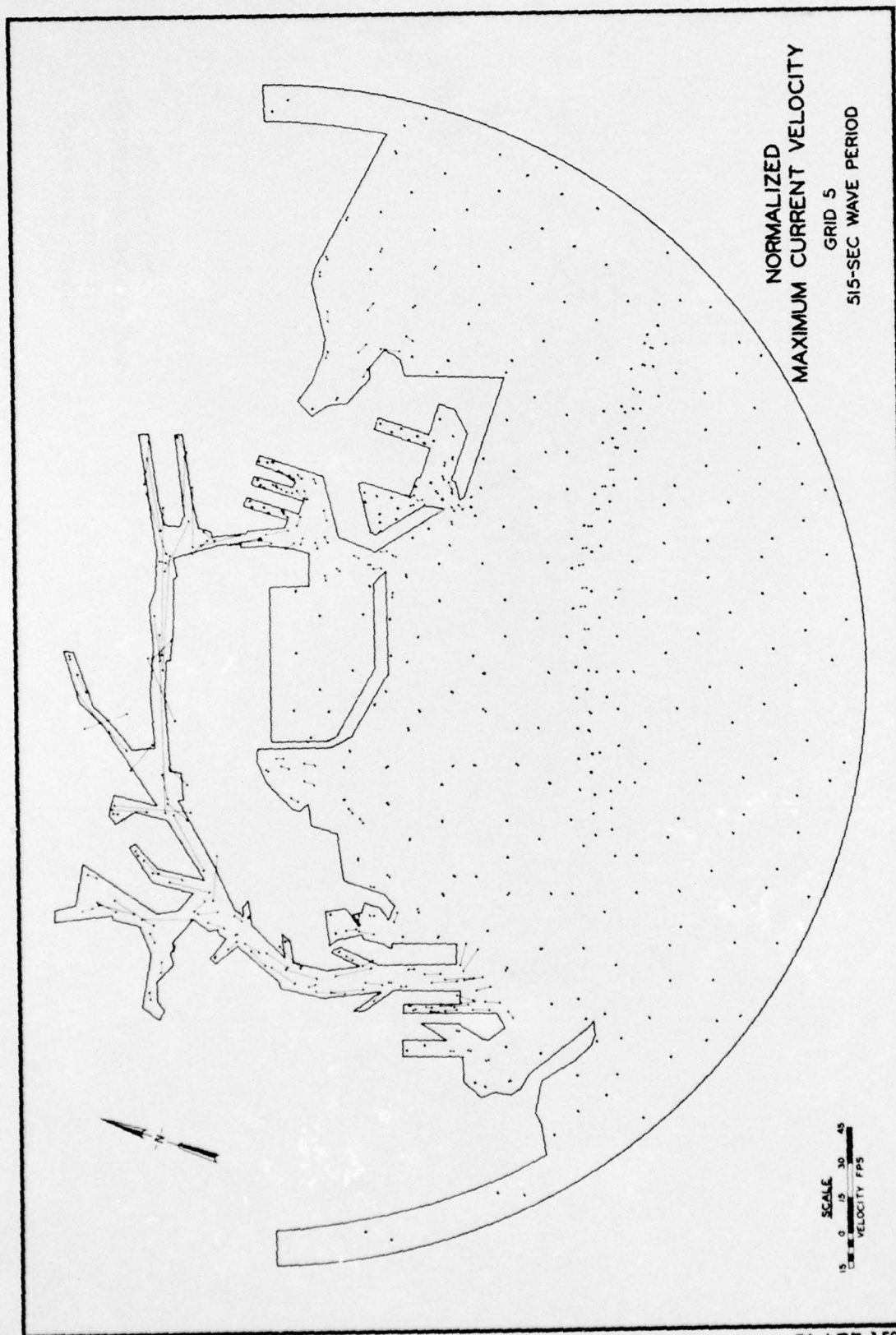


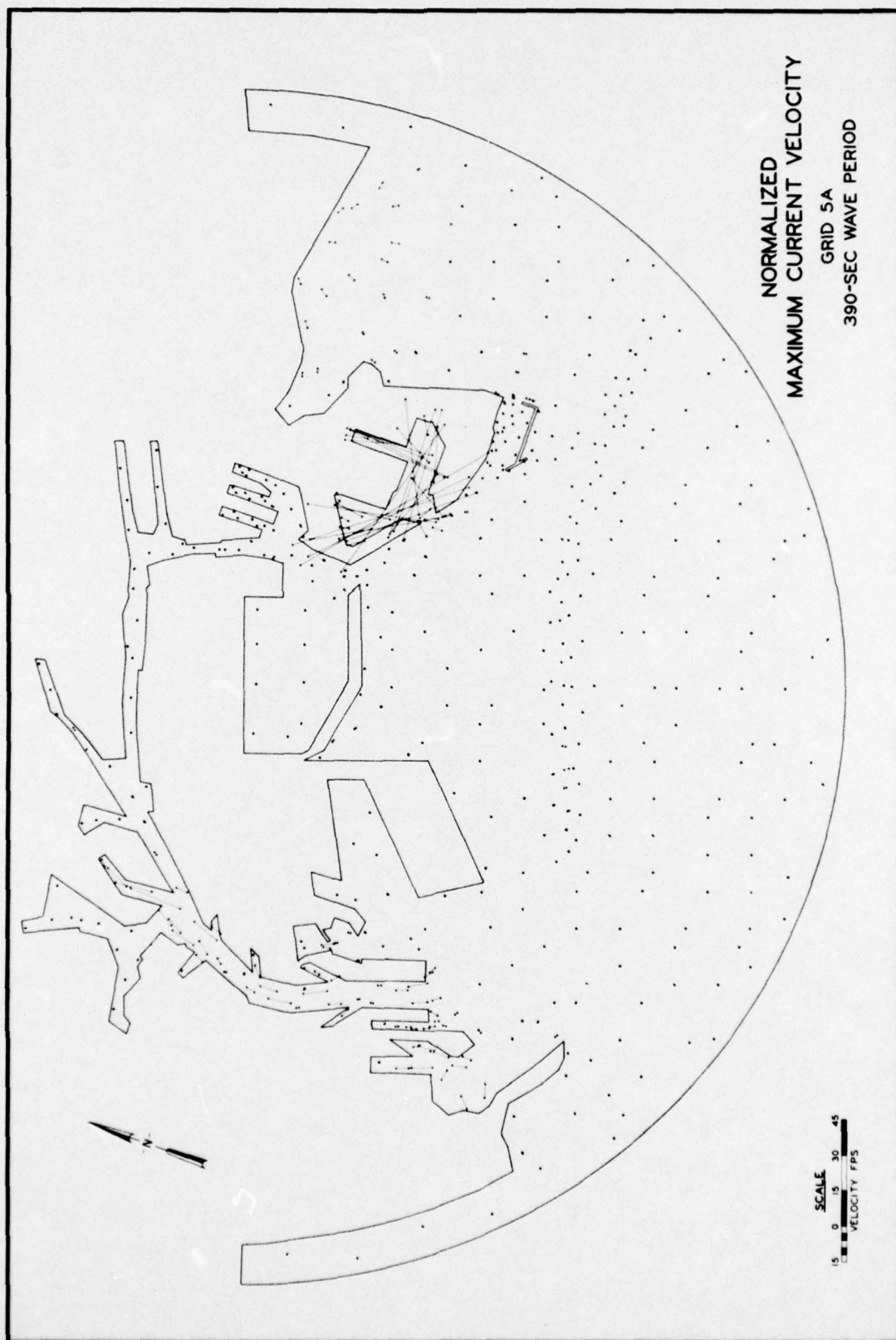
END

DATE
FILMED

11 - 76







APPENDIX A: NOTATION

a	Boundary of region
a_i	Amplitude of incident wave
a_t	Amplitude of transmitted wave
A	Region inside harbor
b(w)	Amplitude of frequency component w
b_o	Incident wave amplitude
d	Average rock diameter
g	Acceleration due to gravity, 32.2 ft/sec ²
G	Element slope matrix
h	Water depth, ft
H_n	Hankel function of the first kind of order n
i	Imaginary number
k	Wave number
n	Integer
N	Interpolation function
n_a	Unit normal vector outward from region A
r	Spherical coordinate, ft
R_e	Real number
t	Time, sec
T	Wave period
u	Velocity in x-direction, ft/sec
U	Total horizontal velocity, ft/sec
v	Velocity in y-direction, ft/sec
w	Angular frequency, radians/sec
x	Cartesian coordinate, ft
y	Cartesian coordinate, ft
α_n	Unknown coefficient
γ	Coefficient
Δ	Area of element
∇	Gradient operator, ft ⁻¹
θ	Spherical coordinate, radians
λ	Wavelength of incident waves

ξ Response of harbor
 ϕ Total velocity potential, ft^2/sec
 ϕ_a Total velocity potential evaluated on boundary a , ft^2/sec
 ϕ_I Velocity potential of incident wave, ft^2/sec
 ϕ_R Far field velocity potential, ft^2/sec
 ϕ_S Scattered wave velocity potential, ft^2/sec

In accordance with ER 70-2-3, paragraph 6c(1)(b), dated 15 February 1973, a facsimile catalog card in Library of Congress format is reproduced below.

Houston, James R

Long Beach Harbor numerical analysis of harbor oscillations; Report 1: Existing conditions and proposed improvements, by James R. Houston. Vicksburg, U. S. Army Engineer Waterways Experiment Station, 1976.

1 v. (various pagings) illus. 27 cm. (U. S. Waterways Experiment Station. Miscellaneous paper H-76-20, Report 1)

Prepared for Port of Long Beach, Long Beach, California. Includes bibliography.

1. Finite element method. 2. Harbor oscillations. 3. Long Beach Harbor. 4. Numerical analysis. I. Port of Long Beach. (Series: U. S. Waterways Experiment Station, Vicksburg, Miss. Miscellaneous paper H-76-20, Report 1)
TA7.W34m no.H-76-20 Report 1